Targeting DNA Damage, Apoptosis, and the Cell Cycle for the Radiosensitization of Aggressive Forms of Breast Cancer

by

Andrea Michelle Pesch

A dissertation submitted in partial fulfillment
of the requirements for the degree of
Doctor of Philosophy
(Pharmacology)
in the University of Michigan
2022

Doctoral Committee:

Associate Professor James Rae, Co-Chair
Associate Professor Corey Speers, Co-Chair
Associate Professor Christine Canman
Assistant Professor Matthew Soellner

Andrea M. Pesch

ampesch@umich.edu

ORCID iD: 0000-0003-0228-8792

Dedication

To Mary Jane Pesch, who taught us all how to live life to the fullest and how to embrace our innate ability to be kind, benevolent, and resilient.

Acknowledgements

I am eternally grateful to my mentors, Dr. Corey Speers and Dr. James Rae, for their phenomenal scientific training and for having full confidence in me and my scientific abilities even before I had that confidence in myself. Jimmy, you (and Christina!) took a chance on me as an 18-year-old University of Michigan freshman with no formal science or research experience and helped teach me how to ask important research questions while always stressing the importance of both doing good science and being a good person; I can't imagine a better place to have started my research career. Thank you for leading by example at how to be a "PhD among MDs" and for showing me how to speak both the languages of basic science and clinical medicine simultaneously. I wouldn't have considered going to graduate school if it wasn't for your support and, as it turns out, your recommendation to do an "easy" first graduate school rotation with Corey was one of the best pieces of advice you ever gave me.

To Corey, there is no world in which I could "design" a better mentor for my PhD. Thank you for your trust in giving me the confidence, freedom, and drive to lead my own projects, and for the constant encouragement you provided when I needed it (and, wow, did I need it sometimes…). You refused to let me dwell on my failures, *never* missed an opportunity to brag (and tweet!) about my achievements, nominate me for an award, or do something that you knew would help me build my career as a scientist. Thank you for always being supportive of my goals

– whether it was pursuing a non-academic science career or opening a French patisserie – and for putting so much of your own energy into helping me reach them. Despite all of the experiments that failed and the 12-hour time points I begrudgingly came in to lab for, I've truly enjoyed being part of your lab over these last four years, the countless "Ice Cream Monday" walks to Michigan Creamery, the lab group messages with endless gifs, and the gift of working on some really cool science with you. I may have already handed in my resignation from the lab party planning committee and I may not have a lab bench anymore, but I will always be a member of the Speers' lab at heart.

It truly takes an army to do great science, and I have been extremely fortunate to be mentored by a number of brilliant and accomplished scientists and clinicians. To Dr. Lori Pierce and Dr. Ted Lawrence, thank you for taking the time out of your busy schedules to hear about my ongoing projects in the lab and for actively investing in my future as a scientist; I am grateful for your time, energy, and expertise, and I am honored to have had the privilege to work with you both. To Dr. Dan Hayes and Dr. Erin Cobain and the rest of the breast oncology team at Michigan, thank you for helping me learn how to contextualize my work in the breast cancer field and for helping me solidify the connections between my basic science training and my desire to do impactful, translational work. In addition, I would like to thank the rest of my thesis committee (Drs. Chris Canman and Matthew Soellner) for their feedback and active participation in my thesis committee meetings to help me overcome obstacles in the lab and make progress quickly toward my degree.

The “Speers Squad” would crumble without the support of our brilliant, patient, and down-to-earth lab manager Kari. Thanks for all of your expertise in leading the xenograft studies, for keeping me updated on Loomi doughnut flavors on Sundays, and for letting me bother you whenever I’m trying to avoid my other responsibilities at work. To Ben Chandler, thanks for teaching me how to “believe in myself”, helping me become an independent and efficient scientist, and for your heartfelt enthusiasm for a night out at Ricks’. To Kassidy and Charlie, thank you for all of the fun lab memories despite the unusual COVID-style lab setup – I can’t wait to see what you accomplish during your PhDs. To Meilan and Bryan, thank you for making lab a fun and welcoming place to work and for being willing to lend a hand on my projects when I needed help. I also want to thank all of the lab members from other groups (especially the Rae lab, the Wahl lab, and the Lawrence lab) that have helped me find reagents, troubleshoot my experiments, and find success in the lab.

One of the best parts about graduate school has been mentoring undergraduate students and helping them become part of our team. Nicole Hirsh, your passion for science is infectious and it has been an absolute privilege to be your mentor. Thank you for always deciphering my chicken scratch instructions for cell culture experiments, for going above and beyond in any task I ever asked of you, and for being my “partner in crisis” while we both work toward the next milestones of our careers. Cassandra Ritter, I will always be impressed by all the things you’ve been able to accomplish – both inside and outside of lab – and I have no doubt you will make the best future doctor. Lynn Lerner, thank you for your love of running qPCR plates, your trivia skills, your endless sense of humor, and for being an integral, youthful, and vibrant part of the

Speers Squad during my last year. To the other students that I've worked with along the way (especially Eric Olsen, Tanner Ward, Connor Ward, Marlie Androsiglio, Amanda Zhang, Meleah Cameron, Yashmeet Kaur, Maria Fields, and Caroline Bishop) thank you for jumping in and helping out with so many different projects; I hope you enjoyed our time together as much as I did, and I hope you learned a few things along the way.

To my best friends and bridesmaids: you are the most incredible group of women, and I am grateful for the time I've gotten to spend with each one of you. To Anna, my organizational partner in crime, the other half of the "A Team", and my "co-graduate chief resident" – you have made the past 5 years in lab unforgettable, and I cannot express how much I will miss your leadership, your friendship, and your scientific insight. I remember being adamant as a first-year graduate student that I wanted to be the only new student joining a lab, but I am humble enough to admit to everyone that I was totally, completely, utterly wrong about that. To Julie, ma meilleure amie, our standing Friday night dinners and game nights were the single greatest part of the last five years and I had so much fun acting as co-chairs and co-directors of every project, departmental committee, and outreach organization we led over the years. You are the epitome of hardworking, and being my best friend is the greatest service you have ever provided to me. Most importantly, I can always count on your honesty and that you will always have my back when I need you.

To Rebecca, who had already started planning my future wedding when we were on the soccer field back in the third grade, I am grateful for your encouragement, baked goods, and kindness over nearly two decades of friendship. I had no doubt that you would continue to be

exceptional in college, medical school, and as a new mom, but you continue to shine beyond everyone's wildest expectations. To Alexandra, you are smart and strong and you never back down from a challenge. You rise to any obstacle and always know how to make me feel good about myself – and I love being crazy cat moms together. (Also, a special shout out to Rylan, Ankur, and Curtis for being the best double-date partners we could ever ask for!) Finally, to Solana, thank you for loving me even when we cut our own bangs, wore Hollister t-shirts to middle school, or watched exclusively horror movies. Thank you for putting up with two years of being my roommate and for being the cool, independent, strong, successful woman we all strive to be someday.

I want to thank the pharmacology community for being a vibrant community in which to learn and grow. I think I have been part of a project, committee, course, or seminar with nearly every one of the Pharmacology faculty and I've really enjoyed getting to know many of you beyond your research projects. Thank you for engaging actively with my thesis work and for making this department feel like home for the last five years. I have met so many wonderful people here – but I especially want to thank Anthony and Gwen for being there to celebrate my victories, for commiserating and complaining together when I'm stressed, and for helping me get through this arduous journey – especially during the prelim process. Finally, a special thank you to Liz Oxford for always giving students a voice in the department, helping me enact some of my craziest ideas, for putting up with everyone's complaints, and for being someone that students can turn to when they need someone to listen.

I am grateful to a number of other groups at Michigan for their financial support of my work, including the Center for the Education of Women (Irma M. Wyman Fellowship), the Program in Biomedical Sciences (Benard Maas Fellowship), and Rackham Graduate School (Margaret Ayers Host Award, Graduate Student Research Grants, Graduate Student Travel Grants) for helping to fund my work over the years. My work has also been supported by the Pharmacological Sciences Training Program (T32-GM007767) and a Ruth L. Kirschstein National Research Service Award (NRSA) Individual Predoctoral Fellowship (F31-CA254138) through the National Institutes of Health. As a trainee in oncology, I would also like to thank the American Association for Radiation Oncology (ASTRO) and the American Association for Cancer Research (AACR) for awarding me multiple conference travel grants, oral presentations, and the 2021 Women in Cancer Research (WICR) award. I would also like to thank the Breast Cancer Research Foundation / the Susan G. Komen Foundation for supporting our lab's research during my time as a graduate student. Finally, a huge thank you to all of my mentors who wrote numerous letters of recommendation to support me in seeking out these opportunities.

My wonderful parents have never wavered in providing their love, support, and encouragement throughout not only my PhD, but for any goals that I've chased after in life. The memories we've made during my time in grad school are some of my absolute favorites, and I wouldn't trade that time for anything in the world. Thank you for always doing your best to make my life easier – no matter if I'm 13 miles away or 1300 miles away – and being not only the best parents, but the best friends I could ask for. I am immeasurably grateful for all of the sacrifices you have made for my education, my well-being, and my happiness over the years; part of this

PhD has always been for you both. To my husband, my partner, and my co-cat parent Nicholas – you are a constant force that keeps me grounded no matter what. Thank you for loving and accepting me as I am, despite my flaws, and for always looking for opportunities to make me smile. Thank you for calling me out when I deserve it, listening to my rants, and for being the "real adult" that keeps our apartment running when I don't want to. I'm so grateful that our paths crossed eight years ago at Mary Markley, and I'm so incredibly blessed that I get to be on this adventure called life with you – even if we don't always have an itinerary to know exactly what comes next.

Table of Contents

List of Tables

List of Figures

Abstract

Breast cancer is the most common invasive cancer diagnosed in women, and there is a critical need to identify novel treatment strategies. To that end, therapies designed to target molecular drivers specific to individual breast cancer subtypes have the potential to improve locoregional disease control, decrease rates of metastasis, and increase overall survival in patients with breast cancer. Thus, we sought to nominate and validate strategies for the radiosensitization of aggressive breast tumors in a subtype-specific manner. By focusing on clinical-grade pharmacological inhibitors of proteins involved in apoptosis, DNA repair, and the cell cycle, we proposed multiple novel preclinical combination therapies for inflammatory breast cancer (IBC), triple negative breast cancer (TNBC) and estrogen receptor positive (ER+) breast cancers. First, we demonstrated that pharmacological PARP1 inhibition using velparib or olaparib radiosensitized IBC models both *in vitro* and *in vivo* through the potentiation of DNA strand breaks and a delay in overall DNA repair capacity with the combination treatment. Next, we asked if the use of CDK4/6 inhibitors – which are currently only approved for the treatment of metastatic, ER+ breast cancer – would affect the radiation response when administered concurrently with radiation treatment. We demonstrated that repair of RT-induced DNA damage was suppressed with CDK4/6 inhibition and that radiosensitization occurred in a cell cycle-independent manner with palbociclib, ribociclib, or abemaciclib. In both ER+ and TNBC,

efficacy of the combination therapy was predicted by the presence or absence of the retinoblastoma tumor suppressor (RB). Genetic or pharmacologic knockout of *RB1* abrogated CDK4/6 inhibitor-mediated radiosensitization, but re-expression of RB in ER+ and TNBC models was sufficient to restore the radiosensitization phenotype. Combined RT and CDK4/6 inhibition caused clinically relevant levels of radiosensitization *in vivo* and led to the development of multiple clinical trials (Phase I/II) to test the safety, tolerability, and efficacy of this combination therapy in patients with ER+, RB-intact breast cancer. Finally, because there are very few targeted therapies available for the treatment of TNBC, we sought to nominate additional subtype-specific targets for radiosensitization in radioresistant models of TNBC. In this study, we demonstrated that Bcl-xL inhibition led to radiosensitization in TNBC cell lines with low Mcl-1 expression. While transient Mcl-1 knockdown was sufficient to sensitize radioresistant cell lines to Bcl-xL-mediated radiosensitization, overexpression of Mcl-1 or CRISPR-mediated knockout of the *PTEN* tumor suppressor induced radioresistance. Together, this data suggests that subtype-specific approaches for the radiosensitization of breast cancer can be an effective way to increase the efficacy of current treatment options for breast cancer patients. In addition, the use of multiple FDA-approved compounds has allowed a number of these approaches to move into early clinical trials for patients with breast cancer, increasing the translational relevance of these findings.

Chapter 1 : Modulating the Radiation Response for Improved Outcomes in Breast Cancer[1]

Abstract

Radiation (RT) therapy is critical for the management and local control of breast cancers to prevent the development of distant metastases and to improve overall survival rates in certain groups of patients. While the clinical utility of radiation therapy has been consistently demonstrated, the development and optimization of combination therapies with RT continues to be of great clinical interest. Preclinical and clinical studies have demonstrated that the effects of radiation can be enhanced when used in combination with therapies that cause additional suppression of DNA damage response, apoptosis, and hormone receptor signaling pathways, among others. In addition, it has become increasingly important to understand the underlying biological differences between the various breast cancer subtypes, as this may contribute to differential responses to radiation and

[1] This chapter was published in *JCO: Precision Oncology* in January 2021.

to radiosensitizing therapies. This review will focus on the preclinical and early clinical use of small molecules and antibodies that increase the efficacy of radiation therapy, specifically in the context of breast cancer.

Introduction

Radiation (RT) is an effective therapeutic modality in breast cancer used as part of the standard of care to prevent locoregional recurrences and distant metastases. Conventionally, fractionated RT is thought to affect multiple aspects of tumor cell physiology, including the four R's of radiobiology: repair of DNA damage, redistribution of cells in the cell cycle, repopulation, and reoxygenation. Beyond the 4 R's, genetic variation, tumor heterogeneity, and the tumor microenvironment can also contribute to radiosensitivity in breast cancer[1]. While breast cancer patients are almost always treated with a multimodal approach, the co-administration of available therapies with RT can have a large impact on tumor response by changing the sensitivity of cancer cells to RT and sparing normal tissue. For the treatment of breast cancer in particular, combining RT with other cytotoxic or targeted therapies has led to improvements in recurrence-free and disease-free survival rates. There are several preclinical and clinical approaches to the radiosensitization of aggressive breast cancers, which have an impact both on current treatment strategies and potential changes to the standard of care.

Cytotoxic Chemotherapies

Treatment of breast cancer in patients without metastatic spread of disease has always included surgical removal of the tumor. Although surgical resection remains part of the modern treatment paradigm, chemo- and radiation therapies have been added to the standard of care in certain patients based on the results of multiple phase III randomized trials demonstrating improved disease-free and overall survival[2,3]. Since then, the benefits of chemotherapy in breast cancer have become well established, and many studies have sought to determine the most effective agents and sequence to use in both the neoadjuvant and the adjuvant setting[4]. Many of

these agents work by introducing or potentiating DNA damage, and combination therapy with RT has shown synergy with several chemotherapeutic agents.

Many chemotherapy agents used for the treatment of breast cancer work by inhibiting the synthesis of DNA or its precursors, including fluorinated pyrimidine analogs such as gemcitabine and 5-fluorouracil or the purine nucleoside antimetabolite cordycepin[5]. Preclinical studies with gemcitabine showed efficacy as a radiosensitizer in both wild type and p53 mutant MCF-7 cells[6] (though initial results from others were mixed[7]), and has led to clinical trials with gemcitabine[8] and capecitabine[9,10] (NCT03958721) in combination with RT. These pivotal studies were some of the first to demonstrate the value of combination chemotherapy and RT in breast cancer, which has led to an increased interest in the potential use of other chemotherapeutic agents with concurrent RT. A similar mechamism occurs with 5-fluoruracil, the active component of the prodrug capecitabine, which leads to G_1/S cell cycle resassorment and increased tumor regression when administered to patients with neoadjuvant chemotherapy-refractory, inoperable, advanced breast cancer[11]. By interfering with DNA synthesis and DNA repair, nucleoside and nucleotide analogs increase the ability of RT to cause lethal double strand DNA (dsDNA) breaks in breast cancer cells[5-7].

Other antineoplastic drug classes that regulate the epigenetic addition or removal of bulky groups from the DNA backbone are also commonly used in the treatment of breast cancer and have recently been shown to influence radiation sensitivity. For example, the enzyme DNA methyltransferase, which adds regulatory methyl groups to DNA, can be inhibited at high concentrations with the DNA methylase inhibitor 5-aza-2'-deoxycytidine to radiosensitize triple negative breast cancer (TNBC) cells by inducing G_2/M arrest and stalling DNA repair[12]. On the

other hand, alyklating agents such as cisplatin bind to purine nucleotides in DNA including guanine and cross-link DNA to prevent proper strand separation necessary for DNA replication.

The safety of cisplatin and RT is being explored in patients with Stage II or III TNBC (NCT01674842), but in patients with inflammatory breast cancer, 5-fluorouracil and cisplatin given concurrently with a total dose of 65 Gy fractionated RT has already demonstrated an increase in overall and disease-free survival with minimal associated toxicities compared to convential radiotherapy[13]. Clinical use of akylating agents can result in dose-limiting skin toxicities, but a recent phase I/II clinical trial with cyclophosphamide and the anthracycline doxorubicin (NCT00278109) with partial breast irradiation reported minimal toxicities[14]. More targeted studies are also underway to determine the effects of combination therapy specifically for patients with breast cancer brain metastases with RT and temozolomide (NCT00875355, NCT02133677).

Taxanes, including paclitaxel, work by stabilizing microtubule assembly and are widely used as part of neoadjuvant treatment of breast cancer to shrink tumors before surgical resection; they also remain a backbone of standard adjuvant therapy for node-positive or advanced stage breast cancer. Combination therapy with microtubule-stabilizing agents and RT has been reported to be safe across many different cancer types, and there have been multiple phase II clinical studies in breast cancer that have reported combinations of either docetaxel[15], paclitaxel[16] (NCT00006256, NCT00003050), or ixabepilone (NCT01818999) with concurrent RT. Although our understanding of the interactions between cytotoxic chemotherapies and RT are increasing, further studies are needed to pinpoint optimal treatment paradigms and understand the incidence and severity of potential side effects.

Nuclear Hormone Receptors

Breast cancers are molecularly categorized by the presence of nuclear hormone receptors including the estrogen receptor (ER), progesterone receptor, and – more recently – the androgen receptor (AR), because these molecular differences lead to large differences in the effectiveness of targeted and non-targeted treatments. The first "molecularly targeted" therapy to be approved for breast cancer was tamoxifen, in the 1970s, which acts as a selective estrogen receptor modulator (SERM) to antagonize ER signaling in breast tissue. While effective as a monotherapy, inhibition of nuclear hormone receptor signaling is of increasing interest as a modulator of radiosensitivity in breast cancer[17].

Although previously recognized as a therapeutic approach in prostate cancer[18,19], pharmacological inhibition of AR has been shown to radiosensitize AR+ breast cancer cells[20,21]. Mechanistic studies have suggested a role for the androgen receptor in DNAPK signaling and the non-homologous end joining (NHEJ) response to double strand DNA (dsDNA) breaks[20], though at present the androgen receptor's transcriptional ability cannot be excluded as a potential mechanism of radiosensitivity. In addition, inhibition of HSP90, a protein chaperone that interacts with both the androgen and estrogen receptors, can also modify radiosensitivity of breast cancer cells[22]. This may suggest that modulation of multiple types of hormone receptor signaling pathways may be able to affect the cellular response to RT, though HSP90 client proteins are diverse, including other mediators of radiosensitivity including the DNA damage response protein ATR[23].

ER, most commonly exploited with targeted anti-estrogen therapies such as tamoxifen in the treatment of estrogen receptor positive (ER+) breast cancers, is less understood in terms of its role in the radiation response. Since the approval of the first anti-estrogen therapies, the question

of whether or not to administer hormone therapy concurrently with RT has remained an important clinical question[17]. There is preclinical evidence to suggest that ER itself may be a modulator of radiosensitivity, and that its absence may directly contribute to the intrinsic radioresistance of TNBC cells that do not express ER, PR, or HER2[24]. This is also consistent with the clinical observation by Kyndi et al. in 2008 that HER2+ and TNBC have higher rates of locoregional recurrence after RT than ER+ patients[25]. Further, knockdown or loss of ER expression in ER+ breast cancer cell lines has been associated with radioresistance[26].

It is known that the response of ER+, estrogen-dependent breast cancer cell lines to therapies such as tamoxifen and RT is highly dependent on many factors, including the availability of estrogens and the size of the tumor (or spheroid)[27]. The historical perception of this proposed combination therapy was based on the hypothesis that by stopping or slowing the growth of rapidly proliferating ER+ breast cancer cells with anti-ER therapies, RT would be less effective, as RT is most effective in rapidly cycling cells. Additionally, cells would arrest in G_0/G_1, the least radiosensitive phase of the cell cycle. Indeed, initial studies with tamoxifen showed that radiosensitivity is influenced by the overall availability of estrogens, suggesting that tamoxifen slightly radioprotects ER+ breast cancer cells[28]. Exogenous 17-β-estradiol can be used to blunt this effect[27,28], suggesting that this is a direct effect of estrogenic signaling pathways.

Although these studies suggested some antagonism between inhibition of estrogen receptor signaling and RT therapy in breast cancer cells, more recent preclinical studies hint that this interaction might be slightly more synergistic than previously thought. Wang *et al.* showed that pretreatment of MCF-7 cells with fulvestrant leads to decreased cell survival in combination with RT through suppression of DNA damage response pathways and G_1 cell cycle arrest[29]. In line with these findings, tamoxifen treatment of mammary tumors in female Sprague Dawley rats

exposed to 1-methyl-1-nitrosourea decreases both the size and metastatic dissemination of tumor cells to a greater degree than either tamoxifen or RT alone[30].

These types of translational questions become even more complicated beyond the confines of a controlled, experimental setting, and there is currently no consensus as to the most effective sequence of tamoxifen and RT therapy. Some studies have reported no sequence dependence in preventing locoregional recurrence when combining tamoxifen and RT[31,32], while others have suggested a potential benefit of concurrent tamoxifen and RT[33-35]. To that end, there are multiple ongoing phase 3 clinical trials that seek to optimize the timing of endocrine therapies such as tamoxifen (CONSET, NCT00896155) or the aromatase inhibitor anastrozole (STARS, NCT00887380) and RT. More comprehensive phase 4 clinical trials such as REaCT-RETT (NCT03948568) are also underway to provide a more complete understanding of additional toxicities or side effects that may result from combination treatment with RT and endocrine therapies.

HER2 and EGFR

Along with the presence of nuclear hormone receptors, breast cancers are stratified based on amplification of HER2, which is part of the epidermal growth factor receptor (EGFR) family of receptor tyrosine kinases. HER2 signaling drives growth and proliferation in HER2-amplified breast cancers, but overexpression of the HER2 protein has also been correlated with radioresistance [36,37]. With the use of genetic HER2 knockdown[37,38] or silica nanoparticles expressing anti-HER2 antibodies[39] in HER2-expressing cell lines, this radioresistance phenotype can be reversed. It is also known that HER2-overexpressing breast cancer stem cells express

higher levels of aldehyde dehydrogenase and are more radioresistant than their HER2-negative counterparts[38], suggesting that this aggressive and radioresistant subpopulation of cells can contribute to disease relapse or metastasis.

Clinically, HER2 inhibition is an effective monotherapy for patients with HER2-amplified tumors. The monoclonal antibody trastuzumab (Herceptin) was approved in 1998 for patients with HER+ breast cancer as the first FDA-approved monoclonal antibody for a solid tumor. Mechanistically, trastuzumab works by binding to the extracellular portion of HER2 to block HER2-mediated signaling. When trastuzumab is administered with RT, breast cancer cell lines display decreased Akt and MAPK/ERK phosphorylation and increased apoptosis compared to treatment with trastuzumab alone[40,41]. There is also some evidence to suggest that trastuzumab may affect the efficiency of DNA repair pathways and the cell cycle[42], which may contribute to radiosensitization. As a result, the combination of trastuzumab and external beam radiation therapy has been evaluated in multiple trials for patients with HER2 overexpressing breast cancer (NCT00943410)[43], as well as in patients with HER2+ ductal carcinoma in situ (DCIS) to improve the efficacy of therapy (NCT00769379).

In the years following, the small molecule dual tyrosine kinase inhibitor lapatinib was approved for the treatment of HER2+ breast cancers that progressed after adjuvant chemotherapy or treatment failure with trastuzumab. Unlike trastuzumab, lapatinib binds intracellularly to prohibit HER2 autophosphorylation and dimerization, but the radiosensitizing effects of HER2 inhibition appear to be comparable with both drugs. Preclinical studies with lapatinib have demonstrated similar suppression of AKT/ERK signaling[44-46] and decreased phosphorylation of DNA-dependent protein kinase (DNAPK), a crucial mediator of non-homologous end joining (NHEJ) [44]. In addition to unresolved dsDNA breaks, increased senescence and apoptosis leads to

increased cell death in breast cancer cells as a result of lapatinib and RT[44]. Since its approval, lapatinib has also been used clinically (NCT00379509, NCT01868503)[43] in combination with RT to radiosensitize HER2+ breast cancers. In addition, targeted clinical trials have been developed to explore whole-brain radiation therapy or stereotactic radiosurgery with lapatinib for patients with brain metastases (NCT01622868). Other related anti-HER2 targeting therapies such as pertuzumab and trastuzumab emtansine (TDM-1) are routinely used in the treatment of HER2+ breast cancers, but their utility as radiosensitization agents has not been directly studied.

The observation that RT induces phosphorylation of epidermal growth factor receptor (EGFR) family members in breast cancer cell lines – beyond just HER2 – was one of the first indications that EGFR signaling may influence the radiation response in breast cancers[47,48]. In models of breast cancer with acquired resistance to radiation, ER+ breast cancer cell lines including MCF-7 and ZR-751s lose expression of the estrogen receptor and gain expression of HER2/EGFR signaling[26,48], suggesting that these compensatory growth signaling pathways may be important in the radiation response. Recently published data also suggest that EGFR signaling activity may influence early local recurrences after radiation, further supporting a role for the EGFR signaling pathway in radiation resistance[49].

Many of the targeted HER2/EGFR inhibitors have some activity across the EGFR family of proteins. However, as EGFR inhibition has become a more relevant treatment strategy in other cancers, newer and more specific EGFR inhibitors such as cetuximab, canertinib, panitumumab, and nimotuzumab have become available, with similar preclinical radiosensitizing effects in breast cancer[89-92]. Consistent with existing data for HER2 and EGFR signaling, EGFR3-mediated signaling is radioprotective in breast cancer cells[93,94], but because of the overlap between EGFR signaling pathway signaling, further comparative studies are needed to make

direct conclusions comparing the efficacy of specific inhibition of each of the EGFR family members. Furthermore, overexpression of the dominant-negative, truncated EGFR-CD533 protein leads to radiosensitization of breast cancer cells after repeated doses of radiation[95,96] while overexpression of TOB1, a negative regulator of HER2 activity, is radiosensitizing.

While current clinical trials utilize FDA-approved agents (**Figure 1.1**), additional preclinical strategies with novel agents for EGFR/HER2-mediated radiosensitization are also being explored in breast cancer[97-99]. Novel inhibitors with activity against insulin-like growth factor receptors have shown efficacy by decreasing pERK signaling in addition to a decrease in p-EGFR[100,101], consistent with the clinical observation the IGFR overexpression after radiation treatment is associated with early local recurrence[102]. Additional work has explored the role of small oligonucleotides, including miR-200c[103] and miR-7[104], that deactivate EGFR and upregulate DNA damage signaling pathways, resulting in an increase in γH2AX foci formation and persistence of DNA damage in triple negative MDA-MB-468 cells. In addition to more effective ways to target HER2/EGFR proteins, HER2-mediated radioresistance can be overcome by targeting compensatory signaling pathways using the small molecular FAK inhibitor PF-562281[37] or inhibition of downstream NF-κB or pro-apoptotic signaling[36,105]. While it is clear that modulation of HER2/EGFR signaling is an attractive radiosensitization strategy in breast cancer, the extensive repertoire of compounds and strategies available to manipulate this system – including additional EGFR family members and novel compounds that lead to co-suppression of multiple signaling pathways – creates many opportunities to determine the optimal clinical approach.

PI3K and mTOR Signaling

Numerous studies have elucidated the far-reaching effects of PIK3CA inhibition, some of which play a role in the radiation response in breast cancer. After exposure to ionizing RT, the resulting activation of *PIK3CA*/Akt signaling leads to growth-stimulatory effects that are radioprotective, and these effects can be reversed with the addition of specific PIK3CA or mTOR pathway inhibitors[50,51]. In addition to mutations, overexpression, and amplification of the PIK3CA family proteins that are common in breast cancer, co-suppression of PIK3CA signaling and other pathways that drive proliferation can lead to synergistic responses. In the context of EGFR/HER2-mediated radioresistance, the addition of PI3K inhibition to either EGFR[52] or HER2 inhibition[53] can lead to synergistic responses that increase cell death through changes in cell cycle distribution or an increase in apoptosis. Pharmacological *PIK3CA* inhibition in combination with RT influences the expression of other pathways, including NF-κB signaling[54] or ERK/MEK signaling[40,46,55] that increase the efficacy of radiation treatment[56], but perhaps the most common co-targeted pathway with *PIK3CA* inhibition is the mTOR signaling pathway.

The *PIK3CA* pathway signaling influences a variety of widespread and interconnected signaling pathways. The PI3K/mTOR signaling pathway is activated by extracellular receptor tyrosine kinase activity and external signals of cellular stress, included those induced by RT. In the context of breast cancer, the expansion of radioresistant breast cancer stem cell populations and their self-renewal has been attributed to PI3K/mTOR signaling and can be repressed with the combination of radiation and dual mTOR/PI3K signaling[106]. Dual strategies that target both pathways – or novel compounds such as the novel PI3K/mTOR inhibitor NVP-BEZ235 that block both pathways – have been successful in radiosensitizing breast cancer through suppression of HIF-1α signaling as well as increased autophagy and apoptosis[107]. Response to

RT therapy is also influenced by intact PTEN signaling[108,109], the presence of constitutively active Ras protein[50,110], or modulation of the downstream RAC1 GTPase involved ERK1/2-mediated G_2/M checkpoint activation[111].

Many signaling pathways involved in metabolic stress are coordinated through the activation of the mammalian target of rapamycin (mTOR) and are closely linked to both the cellular control of autophagy and the radiation response[51,112]. While there are conflicting reports on the ability of the mTORC1 inhibitor rapamycin to radiosensitize breast cancer cell lines cells[51,106,113], there are a number of studies that demonstrate radiosensitivity through modulation of mTOR pathway members. For example, pharmacologic[114,115] or genetic inhibition[116] of SIRT1, a negative regulator of mTOR1 function, increases radiosensitivity of breast cancer cells and suppress tumor growth in an IL-6-dependent manner. Taken together, these studies indicate a strong potential for PIK3CA/mTOR family inhibitors, either alone or in combination, to serve as effective radiosenstization agents in the treatment of breast cancer.

PARP Inhibition

In contrast to the use of targeted therapies that are unique to the underlying physiology of breast cancer, other radiosensitization strategies are effective across a range of cancer types. Pharmacological inhibition of polyadenosine ribosome polymerase (PARP), first approved for ovarian cancer, is now being used as both as a monotherapy and in combination with RT for the treatment of inflammatory[57,58] (NCT03598257) breast cancer and TNBC[59] (NCT03109080). Although generally well tolerated during treatment, long term follow-up revealed significant long-term toxicities that were not initially apparent in preclinical and early clinical data. Despite

this, similar studies are underway with newer PARP inhibitors including rucaparib (NCT03542175), and niraparib[60,61] (NCT03945721).

PARP1 inhibition in combination with RT is thought to increase breast cancer cell death by broadly suppressing DNA repair and increasing the number of dsDNA breaks[57,59,62]. The PARP protein catalyzes the polymerization of ADP-ribose groups to sites of DNA damage, using ADP donated from a required NAD+ cofactor. Because the nicotinamide precursor needed for PARP1-mediated ribosylation is an endogenous inhibitor of PARP1, NAD+ itself also has the ability to radiosensitize breast cancer cell lines in a PARP-dependent manner[63]. The addition of these polymerized groups recruits necessary protein machinery for single strand DNA repair processes including base excision repair, nucleotide excision repair, and mismatch repair, as well as dsDNA repair pathways such as homologous recombination (HR) and NHEJ. In breast cancers with existing deficits in DNA repair capacity – including *BRCA1/2* mutations – the addition of a PARP inhibitor leads to suppression of DNA repair and leads to synthetic lethality[57,59].

DNA Damage Response

Although PARP inhibitors often take advantage of existing DNA repair deficits, there are numerous ways to suppress DNA repair capacity in breast cancer. Ionizing radiation induces predominantly single strand breaks in DNA, and it has been shown that mutations in single strand repair pathways (including the mismatch repair genes *MSH2* and *MSH3*) may confer radiosensitivity to breast tumors[64]. However, it is the failure of DNA repair and the introduction of dsDNA breaks that are eventually lethal to the cell. Unsurprisingly, pre-existing mutations in *BRCA1* and *ATM* have been shown to strongly enhance the response of cells to ionizing

radiation[65]. Accordingly, selective pharmacological inhibition of double strand break repair pathways has been explored as an effective way to enhance the response of breast cancer cells to RT.

Breast cancer cells can repair dsDNA breaks with HR, which is mediated through the actions of proteins such as ATR, ATM, and RAD51. The CHK1/2 inhibitor AZD7762 inhibits the ability of cells to undergo HR and – in combination with RT – radiosensitizes breast cancer cell lines[66,67] in a p53-dependent manner[66]. Similar results are seen with MK8776 and KU-55933, which target CHK1 and ATM, respectively[68,69]. Direct inhibition of the downstream mediator RAD51 with miR-155[70] or RAD51 siRNA can also achieve similar results, suggesting that HR can be manipulated in a variety of ways to achieve a radiosensitization phenotype.

When cells lack a template chromosome for HR, or if HR is suppressed, dsDNA breaks must be repaired with NHEJ. NHEJ is the most basic form of dsDNA repair, and inhibition of NHEJ can significantly delay or prevent repair of dsDNA breaks. During NHEJ, DNA protein kinase (DNAPK) activation at sites of dsDNA breaks leads to the recruitment of accessory proteins such as Ku70/80 that are necessary for active repair. Because NHEJ does not rely on the availability of template DNA for repair, the resulting repair is more error prone. Thus, small molecule DNAPK inhibitors such as NU7761 and AZD7648 sensitize breast cancer cell lines to the toxic effects of RT through the buildup of unresolved dsDNA breaks[69,71,72]. Many nonspecific inhibitors of the PI3K family, including NU7761 or the novel compound PI-103[73], not only inhibit cellular proliferation through inhibition of PI3K, but also retain high affinity for the conserved active site of the PI3K-related kinases DNAPK, ATM, and/or ATR that leads to radiosensitization.

Although many of these preclinical agents are not candidates for further clinical development, inhibition of ATR, which is required for HR initiation, has shown success in the radiosensitization of TNBC cells in the preclinical[23,74] and clinical settings. This has led to initial phase I studies to determine the safety of combination therapy with the ATR kinase inhibitor berzosertib (M6620) for TNBC or ER+/HER2- breast cancers (NCT04052555). Berzosertib is also being studied in multiple solid tumor types with pre-existing deficits in DNA damage repair (NCT04266912) in combination with RT and the DNAPK inhibitor nedisertib (M3814)[75], which has entered early phase I and II clinical trials for the treatment of multiple solid tumor types in combination with RT both with and without the immunomodulatory agent avelumab (NCT04266912, NCT02516813, NCT03724890, NCT04068194).

The ability of cells to repair damaged DNA is linked inextricably to the control of cell cycle checkpoints designed to prevent cells from dividing in the presence of DNA damage. While there are multiple different types of DNA repair, the availability of specific repair proteins and template DNA varies throughout the cell cycle. For example, HR-mediated DNA repair is restricted to the S and G_2 phases after DNA has undergone duplication and a sister chromatid is available. Thus, because DNA synthesis and repair are essential to cellular homeostasis and regulated cell division, kinases involved in cell cycle checkpoints are uniquely positioned to affect the RT response in breast cancer.

Cell Cycle

Cyclin proteins interact with cyclin-dependent kinases (CDKs) in order to initiate a series of phosphorylation events that drive cells through specific cell cycle phases and checkpoints. However, pharmacological inhibition of CDKs can prevent the formation of these critical

complexes. Pan-CDK inhibitors such as roscovitine have limited use as monotherapies in breast cancer because of dose-limiting toxicities, but roscovitine in combination with RT may be able to radiosensitize breast cancer cell lines through a suppression of the DNA damage response in p53 mutant cell lines[117,118]. With the introduction of more specific CDK inhibitors, more targeted radiosensitization has become possible. The CDK12/13-specific compound SR-4835 radiosensitizes TNBC through a novel mechanism related to the induction of intronic polyadenylation cleavage sites[119], while CDK4/6 inhibitors radiosensitive ER+ breast cancers through HR suppression[120].

Cell cycle progression is also influenced by tumor suppressor proteins such as p53 and RB1 that are often mutated in breast cancer, leading to unchecked cell cycle progression and variable response to RT. In TNBC cells where the RB protein is frequently mutated or lost, RB-null cells are more sensitive to γ-irradiation than RB-intact cell lines[121]. Failure to progress through the G_1/S cell cycle checkpoint is also complicated by impaired p53 signaling[62,66,122,123] or alternations in the p53-specific E3 ubiquitin ligase MDM2 that lead to loss of MDM2-mediated p53 suppression. In HER2-overexpressing breast cancer cell lines, for example, the radiation response is correlated with decreased MDM2 expression[42], consistent with other studies that have reported radiosensitizing effects of anti-MDM2 oligonucleotides[124,125], though this effect occurred regardless of p53 status. Additional tumor suppressor proteins such as BTG1 and BTG2 can also influence breast cancer cell radiosensitivity through pleiotropic effects on cell cycle progression, DNA damage, and apoptosis[126,127].

In addition, the actions of other cell cycle kinases can influence the response to radiation. Though the effects of single agent inhibition of the cell cycle kinase MELK on the proliferation of breast cancer cells is debated, it is known that the increase of MELK expression in G_2/M is

radioprotective in triple negative breast cancer cells[128]. The G_2 checkpoint kinase WEE1, which phosphorylates many CDKs necessary for G_2 checkpoint progression, can be effectively inhibited with MK-1775 (adavosertib), which is effective as both a single agent and a radiosensitizer in p53-defective models of breast cancer[129]. Alternatively, during S phase, the S-phase kinase-associated protein 2 (SKP2) has been suggested to radiosensitize breast cancer through suppression of PDCD4 ubiquitination with either SKP2 knockdown or use of the small molecule SKP2 inhibitor SMIP004[130].

When cells undergo mitosis, proteins of the spindle assembly complex are required for proper cell division and the prevention of aberrant chromosome segregation. This spindle assembly can be targeted directly through MiR-27a-based suppression of CDC27 activity that leads to radiosensitivity[131], or through the inhibition of protein kinases necessary for activation of the spindle assembly complex or anaphase promoting complex. For example, inhibition of TTK (MPS1) sensitizes TNBC cell lines through inhibition of homologous recombination[132]. Similarly, modulation of PP2A, the phosphatase involved in inactivation of TTK, can also influence the response of ER+ breast cancer cells to ionizing radiation[133]. Polo-like kinase 1, essential for phosphorylation and activation of the APC, suppresses cell cycle progression and the 53BP1-mediated DNA damage response in homologous recombination[134], leading to increased breast cancer cell death when combined with ionizing radiation[135]. By targeting breast cancer cells in a radiosensitive phase of the cell cycle (predominately G_2/M), these strategies lead to more effective tumor cell death in combination with RT.

Immunotherapy

Immunotherapy plays an increasingly important role in the treatment of advanced, metastatic breast cancer and is likely to have an expanded role in the treatment of patients without metastatic disease, particularly in the case of TNBC[76]. While many studies have examined the addition of immunotherapies to the current standard of care, the novelty of these therapies limits our knowledge of how these novel immune checkpoint inhibitors may influence the response of breast tumors to ionizing radiation. RT is thought to enhance the response of tumors to immunotherapy at least in part through the actions of tumor-associated T cells, such as induction of the DNA exonuclease Trex1[77] that modulates radiation-induced T cell regulation in combination with immune checkpoint inhibition.

However, the immunotherapy agents that have shown the most promise in breast cancer so far are undoubtedly the targeted PD-1/PD-L1 therapies. In breast cancer cell lines, RT synergizes with anti-PD-1/PD-L1 therapy and enhances tumor kill when given in combination with α-CD137 and α-PD-1 monoclonal antibodies[78]. This combination therapy also increases the number of tumor-specific effector immune cells present in the tumors[79], which is thought to contribute to the curative responses seen *in vivo*. The addition of therapies that block PD-1/PD-L1 signaling has even been shown to overcome acquired resistance to fractionated RT in TNBC and other solid tumors[80]. Ongoing clinical trials with RT and PD-1/PD-L1 inhibition and are summarized in **Table 1.1**. Direct modulation of the PD-1 and PD-L1 interaction also has implications for cytokine and chemokine signaling pathways that modulate the immune response. To that end, anti TGFβ therapy has been explored both preclinically[81,82] and clinically (NCT01401062, NCT02538471).

Although immunotherapies targeting PD-1/PD-L1 or CLTA4 are the most well-studied, there are several other therapies that seek to utilize the immune system to increase the efficacy of radiation therapy. Therapies targeted against CTLA-4 or toll-like receptors have also shown promise in breast cancer. The abscopal effect has been observed previously in models of breast cancer, and it has been suggested that the immune signaling may be responsible[83]. In TSA breast carcinoma cells, mice treated with the CTLA-4 monoclonal antibody 9H10 and radiation showed a decrease not only in the growth of tumors within the radiation field, but an abscopal effect that decreased metastatic growth and resulted in less overall tumor burden in these mice[84]. As a result, there are multiple trials examining tremelimumab (NCT02563925, NCT01334099) in breast cancer.

Immunotherapies that inhibit toll-like receptor signaling in breast cancer (NCT01421017, NCT03915678) or activate OX40 on the surface of T-cells (NCT01862900) have also been initiated. For breast tumors that do not initially respond to combined immunotherapy and radiation treatment, the addition of Axl inhibition in Axl-expressing tumors increasing the efficacy of combination treatment[85]. Finally, the immunosuppressant agent fingolimod (FTY720), a sphingosine analog, increases radiosensitivity of breast cancer cells *in vitro* by inhibiting SphK1 and increasing apoptosis and autophagy[86]. In short, immunotherapy will be a prominent feature of current and future radiosensitization studies in breast cancer. Additional detailed descriptions of the immune regulation and infiltration of breast tumors, and the potential side effects and biomarkers for immunotherapy and RT beyond the scope of this paper have recently been reviewed elsewhere[87,88].

Emerging Preclinical Strategies

Although many radiosensitization agents have been clinically utilized for the treatment of breast cancer, there are several radiosensitization strategies that are still under early preclinical investigation (summarized in **Table 1.2**). While many of these strategies target apoptosis[136-148], autophagy[149-156], or metabolic changes[157,158] usually thought to be minor contributing pathways to breast cancer radiosensitization, a number of these approaches likely have mixed mechanisms that lead to broad suppression of the DNA damage response, cell cycle progression, or decreased hypoxia and HIF1a-related signaling[127,159-167]. On-target and off-target effects of compounds designed to affect proliferation or cell-cell communication, such as the suppression of notch signaling[168] through gamma secretase inhibition[169] (NCT01217411), can also be valuable approaches in the radiosensitization of breast cancer. Finally, the radiosensitizing effects of many natural products and dietary supplements are just starting to be realized[118,170-176], and the concomitant use of these compounds during radiation treatment should be advised with caution in the absence of additional information.

Clinical Strategies for Radioprotection

In addition to emerging clinical strategies to re-oxygenate and radiosensitize breast tumors (NCT00083304 with efaproxiral, NCT02757651, NCT03946202 with hydrogen peroxide), there is also an interest in the off-label use of common compounds or pharmaceuticals that may improve the therapeutic index of RT by offering radioprotection of normal tissue. Although terminated, a trial with the popular cholesterol-lowering statin lovastatin was initiated to study the potential of concurrent statin treatment to ameliorate long term effects of radiation therapy (NCT00902668). Even the sleep-aid melatonin, taken primarily to improve duration and

quality of sleep, has mixed effects on radiation sensitivity, and has been proposed as an adjunct therapy to decrease radiation-induced dermatitis in breast cancer (NCT03716583). Topical radioprotection has been explored using curcumin (NCT01042938), the anti-inflammatory compound found in turmeric, or the tricyclic anti-depressant doxepin (NCT02447211) to prevent the formation of skin lesions. Finally, the vasodilatory compound pentoxifylline has also been used clinically and has been shown to prevent radiation-induced fibrosis in breast cancer patients receiving multimodal treatment[177-179]. While still under investigation, strategies to mitigate side effects from radiation or minimize healthy tissue toxicity provide unique insight into the radiation response in both tumor and healthy tissue.

Conclusions

There are numerous biological pathways that can be manipulated to increase the efficacy of targeted RT for the treatment of breast cancer (**Figure 1.2**). While inhibition of hormone receptors, DNA damage repair, and immunomodulatory signaling represent the majority of the approaches to radiosensitization currently being studied in the clinic (**Table 1.1**), there are a number of other emerging preclinical radiosensitization strategies (**Table 1.2**) and radioprotective approaches to minimize normal tissue toxicity. Although not reviewed here, multi-candidate approaches to radiosensitization – including the development of predictive gene signatures – are an important component of future radiosensitization studies because they are able to incorporate gene and protein expression data across multiple pathways alongside data on clinical progression and outcomes. Because many of the signaling pathways involved in the RT response have significant biological overlap, new combination therapies designed for radiosensitization of breast cancer may have the potential to influence the response of the tumor to other modalities used during subsequent treatments. Finally, as novel radiosensitization

strategies make their way into the clinic, trials must be designed with appropriate long term follow up because combination therapies with RT can often lead to delayed toxicities.

Acknowledgements

The authors would like to acknowledge funding support from the NIH Pharmacological Sciences Training Program (T32GM007767 to AP), the National Cancer Institute of the National Institutes of Health (F31CA254138 to AP), and the University of Michigan Center for the Education of Women+ (Irma M. Wyman Fellowship to AP). The authors would also like to thank BioRender for assistance in making all figures.

Figures

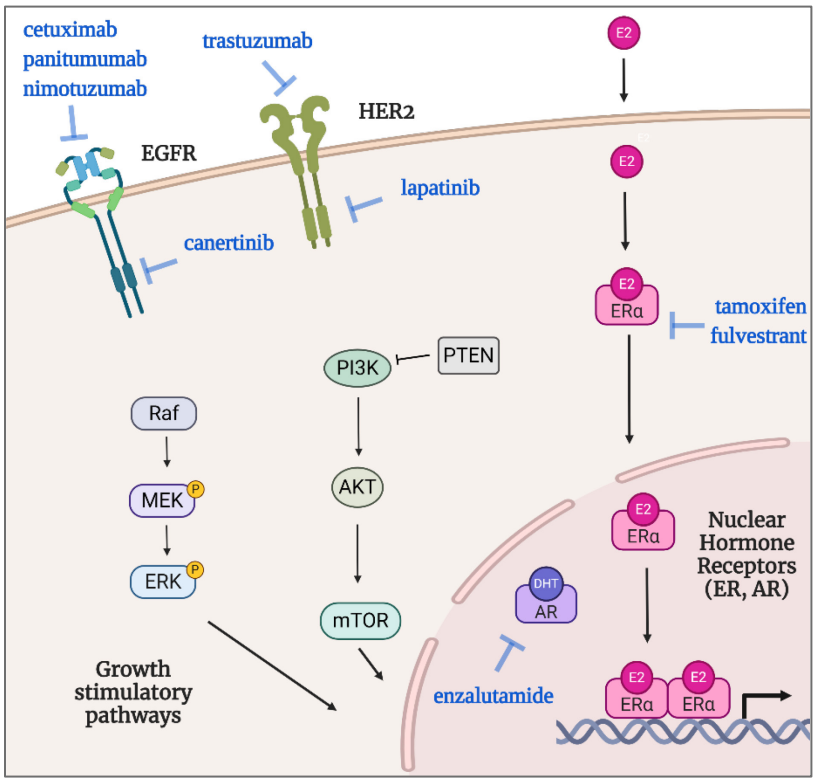

Figure 1.1: Radiosensitization of breast cancer with FDA-approved drugs targeting proliferation.

While hormone receptors and EGFR/HER2 are often targeted as monotherapies in the treatment of breast cancer, these FDA-approved therapies (blue) can be purposed for use as radiosensitization agents in breast cancer. (Abbreviations: EGFR = epidermal growth factor receptor, HER2 = human epidermal growth factor receptor, ER = estrogen receptor, AR = androgen receptor, E2 = estradiol, DHT = dihydrotestosterone)

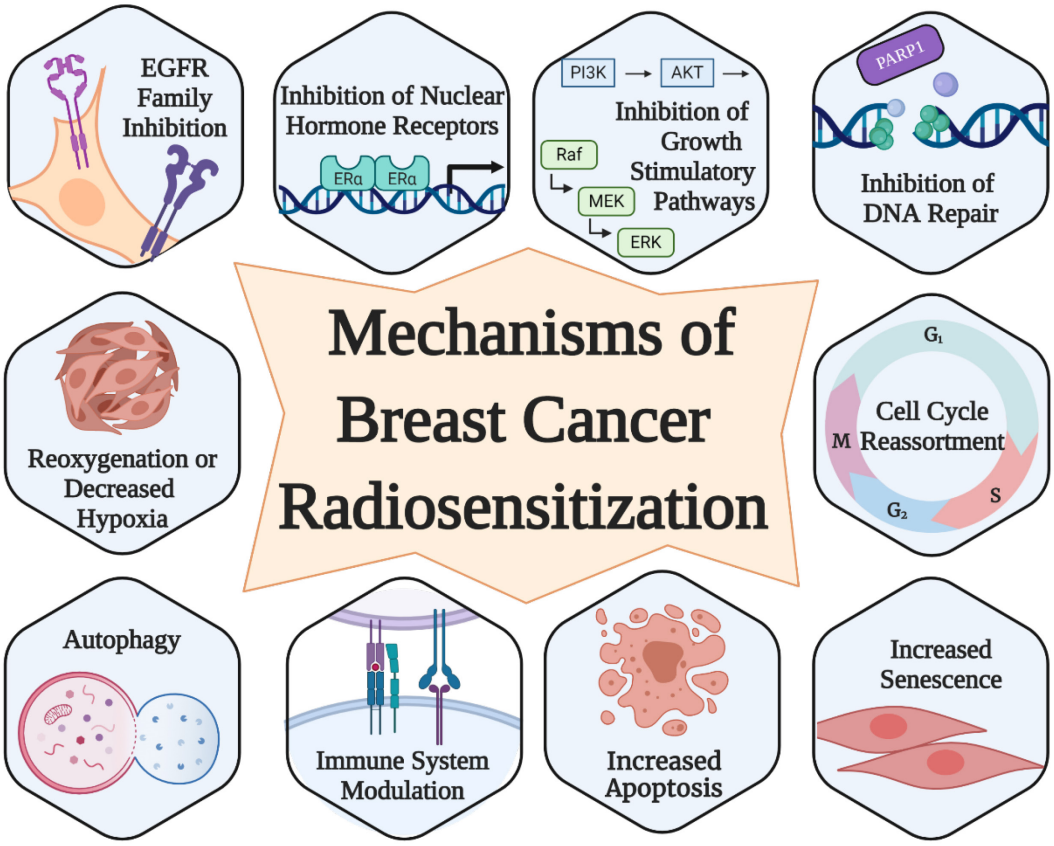

Figure 1.2: Summary of current radiosensitization strategies currently in use or development for the treatment of breast cancer.

While some radiosensitization strategies (including nuclear hormone receptor or HER2 inhibition) are widely recognized in the treatment of breast cancer, there are many novel mechanisms of radiosensitization that are under preclinical or early clinical development.

Tables

ID	Title	Name of Agent(s)	Radiation Treatment	Phase/ Patients	Patient Group
NCT01674842	A Phase I Dose-Escalation Study of Cisplatin and Radiation Therapy for Patients with Triple Negative Breast Cancer	Cisplatin	External beam whole breast RT over 6 weeks	I (55 patients)	TNBC
NCT02422498	A Phase II Trial of Homologous Recombination Repair Status as a Biomarker of Response in Locally Recurrent/Metastatic Triple Negative Breast Cancer Patients Treated with Concurrent Cisplatin and Radiation Therapy	Cisplatin	External beam whole breast RT. 37.5 Gy (15 fractions) for metastatic cases or 50 Gy in 25 fractions (optional 10-14 Gy boost) in locoregionally recurrent cases	II (54 patients)	TNBC
NCT01289353	Phase I-II Study of Concurrent Adjuvant Systemic Therapy and Accelerated Radiotherapy (Over 3 Weeks)	Carboplatin	Whole breast 3D-RT or IMRT (2.7 Gy x 15 fractions =40.50 Gy) and 3 Gy to the tumor bed for 2 fractions (Total = 46.5 Gy)	I/II (39 patients)	Stage I and II TNBC
NCT00006256	Concurrent Taxol (Paclitaxel) and Definitive Breast Radiation Therapy in Early Stage Breast Cancer Following Four Cycles of Adriamycin/Cytoxan Chemotherapy	Paclitaxel with doxorubicin and cyclophosphamide	External beam whole breast RT 5 days a week for approximately 6-7 weeks	II (44 patients)	Invasive Breast Cancer
NCT03948568	A Pragmatic Randomised, Multicentre Trial Evaluating Optimal Timing of Endocrine Therapy and Radiation Therapy in Early-stage Breast Cancer (REaCT-RETT)	Tamoxifen Letrozole Anastrozole Exemestane	External beam whole breast RT	IV (218 patients)	Hormone receptor positive breast cancer
NCT00887380	A Randomised Comparison of Anastrozole Commenced Before and Continued During Adjuvant Radiotherapy for Breast Cancer Versus Anastrozole and Subsequent Anti-oestrogen Therapy Delayed Until After Radiotherapy	Anastrozole	External beam whole breast RT 1 month of randomization	III (2023 patients)	ER+ breast cancer (PR+ or PR-)

NCT00896155	A Randomized Trial of Concurrent Versus Sequential Tamoxifen with Radiotherapy to Assess the Extent of Pulmonary Fibrosis and Disease Related Control and Survival in Breast Cancer Patients	Tamoxifen	Standard RT given either sequentially or consecutively with tamoxifen	III (260 patients)	ER+ or PR+ breast cancer
NCT03691493	A Phase II Multi-Institutional Study of Concurrent Radiotherapy, Palbociclib, and Hormone Therapy for Treatment of Bone Metastasis in Breast Cancer Patients	Letrozole, Anastrozole, Exemestane, Tamoxifen, or Fulvestrant with palbociclib	External beam RT over 5-10 days to metastatic site	II (42 patients)	ER+/HER2- breast cancer with bone metastases
NCT04220476	CIMER: Combined Immunotherapies in Metastatic ER+ Breast Cancer	Letrozole with palbociclib	Immunogenic-SBRT days 1-12, where each oligometastatic lesion is treated every 24-48 hours	II (204 patients)	Metastatic HR+/HER2-
NCT00769379	A Phase III Clinical Trial Comparing Trastuzumab Given Concurrently with Radiation Therapy and Radiation Therapy Alone for Women with HER2-Positive Ductal Carcinoma in Situ Resected by Lumpectomy	Trastuzumab	External beam whole breast RT over 5-6 weeks	III (2000 patients)	HER2+ Ductal Carcinoma in Situ
NCT03109080	A Phase I of Olaparib With Radiation Therapy in Patients with Inflammatory, Loco-regionally Advanced or Metastatic TNBC (Triple Negative Breast Cancer) or Patient with Operated TNBC With Residual Disease	Olaparib	External beam whole breast RT (3D conformal RT or IMRT) with SIB	I (24 patients)	Triple negative, inflammatory, loco-regional advanced/ metastatic
NCT03542175	A Phase I Study of Rucaparib Administered Concurrently with Postoperative Radiotherapy in Patients with Triple Negative Breast Cancer with an Incomplete Pathologic Response Following Neoadjuvant Chemotherapy	Rucaparib	External beam whole breast RT 50 Gy total (2 Gy/fraction) to the breast or chest wall plus a 10 Gy boost to the lumpectomy cavity	I (30 patients)	TNBC

NCT03598257	A Phase II Randomized Trial of Olaparib (NSC-747856) Administered Concurrently with Radiotherapy Versus Radiotherapy Alone for Inflammatory Breast Cancer	Olaparib	External beam whole breast RT (5 days per week for 6 weeks)	II (300 patients)	IBC
NCT03945721	A Phase I Study of Niraparib Administered Concurrently with Postoperative RT in Triple Negative Breast Cancer Patients	Niraparib	External beam whole breast RT administered concurrently with niraparib	I (30 patients)	TNBC
NCT02227082	Olaparib Dose Escalation in Combination with High Dose Radiotherapy to the Breast And regional Lymph Nodes in Patients with Breast Cancer	Olaparib	23 x 2.03 Gy per fraction (total 46.69) to the whole breast/lymph nodes with tumor SIB of 23 x 0.63Gy (Total= 61.18 Gy)	I (7 patients)	Inoperable or/and metastatic BC
NCT04052555	A Phase 1b Study of M6620 in Combination with Radiation Therapy to Overcome Therapeutic Resistance in Chemotherapy Resistant Triple Negative and Estrogen and/or Progesterone Receptor Positive, HER2 Negative Breast Cancer	Berzosertib	External beam whole breast RT 5 days a week for 5-6 weeks depending on the type of surgery	Ib (42 patients)	Non-metastatic TNBC / locally recurrent ER+/ HER2-
NCT03366844	Preoperative Combination of Pembrolizumab and Radiation Therapy in Patients with Operable Breast Cancer	Pembrolizumab	RT Boost upfront (8 Gy for 3 fractions.)	I/II (60 patients)	High-risk, ER+/HER 2- or TNBC
NCT03524170	RACHEL1: A Phase I Radiation and Checkpoint Blockade Trial in Patients with Metastatic Hormone Receptor Positive, HER2 Negative Breast Cancer	anti-PD-L1 / TGFbetaRII fusion protein M7824	Standard RT once a day for 5-10 days, started 3 days after the first day of M7824 administration	I (20 patients)	HR+/ HER2- metastatic breast cancer
NCT02730130	A Multicenter Single Arm Phase II Study to Assess the Efficacy of Pembrolizumab Plus Radiotherapy in Metastatic Triple Negative Breast Cancer Patients	Pembrolizumab	External beam RT: 3000 cGy, delivered in five 600cGy fractions within 5-7 days for palliation	II (17 patients)	Metastatic TNBC

NCT03051 (72	A Phase II Study of Pembrolizumab In Combination with Palliative Radiotherapy for Metastatic Hormone Receptor Positive Breast Cancer	Pembrolizumab	Palliative radiotherapy (5 treatments)	II (8 patients)	Metastatic HR+/HER 2- breast cancer
NCT02977468	Effects of MK-3475 (Pembrolizumab) on the Breast Tumor Microenvironment in Triple Negative Breast Cancer with and Without Intra-operative RT: A Window of Opportunity Study	Pembrolizumab	IORT performed during breast conserving surgery	I (15 patients)	Non-metastatic TNBC
NCT02499367	Adaptive Phase II Randomized Non-Comparative Trial of Nivolumab After Induction Treatment in Triple-negative Breast Cancer (TNBC) Patients: TONIC-trial	Nivolumab	20 Gy to metastatic lesion	II (84 patients)	Metastatic TNBC
NCT03875573	Neo-adjuvant Chemotherapy Combined with Stereotactic Body Radiotherapy to the Primary Tumour +/- Durvalumab, +/- Oleclumab in Luminal B Breast Cancer: a Phase ll Randomised Trial	Durvalumab + Oleclumab with paclitaxel and ddAC	Pre-operative RT (boost dose) 3x8 Gy on the primary tumour at week 5. Given over 3 days in 3 fractions (1X8 Gy daily)	II (147 patients)	Non-metastatic Luminal B BC
NCT03818685	A Multicenter, Randomised, Open-label Phase II Study to Evaluate the Clinical Benefit of a Post-operative Treatment Associating Radiotherapy + Nivolumab + Ipilimumab Versus Radiotherapy + Capecitabine for Triple Negative Breast Cancer Patients with Residual Disease After Neoadjuvant Chemotherapy	Nivolumab and Ipilimumab or Capecitabine	External beam whole breast RT initiated one week before chemotherapy	II (98 patients)	Non-metastatic TNBC with residual disease
NCT03804944	Converting HR+ Breast Cancer into an Individualized Vaccine	Pembrolizumab ± Ftl-3 ligand (CDX-301)	Focal hypo-fractionated RT 8 Gy x 3 fractions, starting day 8, every other day	II (100 patients)	Stage II-III, HR+HER 2- breast cancer
NCT03483012	A Phase II Study of Atezolizumab in Combination with Stereotactic Radiation for Patients with Triple-negative Breast Cancer and Brain Metastasis	Atezolizumab	SRS within 14 days of brain MRI	II (45 patients)	Stage IV TNBC

NCT03915678	Atezolizumab Combined with Intratumoral G100 AnD Immunogenic Radiotherapy in Patients with Advanced Solid Tumors	Atezolizumab and G100 (TLR4 agonist)	Short course irradiation: 2 fractions of 2 Gy for a total dose of 4 Gy, High dose irradiation: 3 to 5 fractions for a total of 27 – 60 Gy. RT starts one week after the first administration of atezolizumab.	II (247 patients)	TNBC (and other solid tumors)
NCT03430479	Phase Ib/II Study to Assess Efficacy, Safety & Immunological Biomarker of Anti PD-1 Antibody with Radiation Therapy in Patients with HER2-negative Metastatic Breast Cancer	Nivolumab with hormone therapy	Standard radiotherapy	Ib/II (32 patients)	ER+, HER2-metastatic breast cancer
NCT03872505	A Randomized Phase II Study Evaluating Pathologic Response Rates Following Pre-operAtive Non-Anthracycline Chemotherapy, Durvalumab (MEDI4736) +/- RAdiation Therapy (RT) in Triple Negative Breast Cancer (TNBC): The PANDoRA Study.	Durvalumab with carboplatin and paclitaxel	The second dose of durvalumab will be given in conjunction with an RT boost, consisting of 8 Gy in 3 fractions for a total of 24 Gy.	II (140 patients)	Invasive TNBC
NCT03946202	Randomised Phase II Trial Testing Efficacy of Intra-tumoural Hydrogen Peroxide as a Radiation Sensitiser in Patients with Locally Advanced/Recurrent Breast Cancer	Hydrogen Peroxide	3 weeks of standard radiotherapy	II (184 patients)	Primary locally advanced BC / locally recurrent BC

Table 1.1: Current clinical trials assessing the safety and/or efficacy of combination therapies with radiation in women with breast cancer.

(Abbreviations: BC = breast cancer, RT = radiation, TNBC = triple negative breast cancer, IMRT = Intensity-modulated radiotherapy, SBRT = stereotactic body radiation therapy, SIB = simultaneous integrated boost, IORT = Intraoperative radiation therapy, SRS = stereotactic radiosurgery, WBRT = whole brain radiation therapy).

Primary Mechanism	Compound / Approach	Effects / Mechanism of Radiosensitization	Model Type	Reference(s)
Apoptosis	ABT-737 (BCL-2 family inhibitor)	Increased apoptosis with downregulation of BCL-2 and Bcl-xL	TNBC	Li et al 2012[137]
Apoptosis	Genetic knockdown of COX2	Increased apoptosis with decreased Bcl-2/Bcl-XL expression and increased BAK expression	TNBC	Lin et al. 2013[139]
Apoptosis / Cell Cycle	AMD3100 (SDF-1 receptor antagonist)	Increased apoptosis, increased Bax and reduced Bcl-2 expression with G_2/M arrest	TNBC	Zhou et al. 2018[138]
Apoptosis / Cell Cycle	2-deoxy-D-glucose and MLN4924 (inhibitor of SCF E3 ligase)	Increased apoptosis through G_2/M arrest and increased caspase 3 production	ER+ and HER2+	Oladghaffari et al. 2017 and Yang et al. 2012[140,141]
Apoptosis	SM-164 (SMAC inhibitor)	Increased apoptosis through degradation of cIAP-1 and activation of caspases 3, 8, and 9	Multiple subtypes	Yang et al 2011[142]
Apoptosis	Akt inhibition (MK-2206)	Decreased Akt1 levels and increased apoptosis	TNBC	Johnson et al 2020[148]
Apoptosis / Cell Cycle	Naphthazarin (anti-inflammatory)	Cell cycle arrest and increased apoptosis	ER+	Kim et al 2015[176]
Apoptosis / DNA Damage	Enterolactone (phytoestrogen) [172] [179] [180] [180] [179] [177]	Decreased G_2/M arrest, increased chromosomal damage and apoptosis	ER+ and TNBC	Bigdeli et al. 2016[172]
Apoptosis / DNA Damage	Genetic knockdown of CAV-1	G_2/M arrest, failure to repair DNA damage, and a resulting increase in apoptosis	TNBC, HER2+	Zou et al 2017[146]
Apoptosis / DNA Damage	H-87, H-89 (PKA inhibitor)	Inhibition of DNAPK with decreased RAD51 and Bcl-2 expression	ER+	Chin et al. 2005[150]
Apoptosis / DNA Damage	Mebendazole	G_2/M arrest, increased dsDNA damage and apoptosis	TNBC	Zhang et al. 2018[147]
Apoptosis / DNA Damage	Equol	increased radiation-induced apoptosis and increased radiation-induced dsDNA damage	ER+ and TNBC	Taghizadeh et al 2015[171]
Autophagy	3-methyladenine, chloroquine	Increased LC3-II positive vacuole production abolished by inhibition of autophagy	TNBC	Chaachouay et al. 2011[149]
Autophagy	Genetic knockdown of ATG family genes	Diminished accumulation of autophagosomes and decreased autophagy	TNBC	Apel et al. 2008 [151]
Autophagy	Tunicamycin	Increased autophagy mediated by eIF2α kinase in caspase 3/7 deficient cells	ER+	Kim et al 2010[152]

Autophagy	SP600125 (JNK inhibitor)	Inhibition of autophagy and increased apoptosis	ER+ and TNBC	Li et al. 2016[153]
Autophagy	5Z-7-oxozeaenol (TAK1 inhibition)	Reduction in radiation induced TAK1 phosphorylation and increased autophagy	TNBC	Han et al. 2014[154]
Cell Cycle	Knockdown of TRIB3	G_0/G_1 arrest and decreased Notch1 signaling	TNBC	Lee et al 2019[168]
Cell Cycle / DNA Damage	Genetic knockdown of the lncRNA HOTAIR	Increased DNA damage, apoptosis, and cell cycle arrest resulting upregulation of miR-218	ER+ and HER2+	Hu et al. 2019[143]
Cell Cycle / DNA Damage	Genistein (soy isoflavone)	G_2/M arrest and HR suppression, increased DNA damage, and increased apoptosis	Multiple subtypes	Lin et al 2013[118]
Cell Cycle / DNA Damage	Huaier (herbal medicine)	Increased G_0/G_1 arrest, persistence of yH2AX foci, and suppression of RAD51-mediated HR	ER+ and TNBC	Ding et al 2016[173]
Cell Cycle / DNA Damage	N-butylidenephthalide	Increased dsDNA breaks, suppression of HR repair, G_2/M arrest and increased apoptosis	ER+ and TNBC	Su et al. 2018[174]
Cell Cycle / DNA Damage	Berberine	G_2/M cell cycle arrest and suppression of HR activity through downregulation of RAD51	ER+ and TNBC	Wang et al 2012[175]
DNA Damage	Optically Activated Gold Nanoshells	Increase in ALDH+ radioresistant TNBC stem cells	TNBC	Atkinson et al 2010[165]
DNA Damage	LJI308 (S6 kinase inhibitor)	Decreased dsDNA repair	Multiple	Lettau et al 2020 [166]
DNA Damage	Regorafenib	Reduction in VEGF, PDGFR, EGFR and ERK expression and suppression of DNA repair	TNBC	Mehta et al 2020[167]
Hypoxia / DNA Damage	Carbon nanotubes	Increased oxygen delivery and downregulation of Bcl-2, survivin, HIF-1α, RAD51 and Ku80	ER+ and TNBC	Jia et al 2017[160]
Hypoxia	Genetic knockdown of HIF1α	Increased DNA damage and decreased autophagy	ER+	Zhong et al 2016[161]
Hypoxia	HS-1793	Decreased HIF1α and VEGF mediated signaling	ER+	Choi et al 2016[180].
Metabolism	GLUT1 inhibition (WZB117)	Decreased levels of glucose uptake, lactate production, and intracellular ATP	Multiple	Zhao et al 2016[158]
Metabolism	Activation of PK-M2	Increased antioxidant production and glucose uptake, depletion of stem cells	TNBC	Zhang et al 2019[157]
Metabolism	Metformin	Activation of AMPK and inactivation of mTOR	ER+	Sanli et al 2010 Song et al. 2012[155,156]

Oxidative Stress	Simvastatin	Increased radiation-induced cell death in IBC and TNBC cell lines	Multiple Subtypes	Lacerda et al 2014[181]
Oxidative Stress	Overexpression of BTG1	Increased reactive oxygen species, apoptosis, chromosomal aberrations, and G_2/M arrest	ER+ and TNBC	Zhu et al. 2015 [127]
Oxidative Stress	Genetic knockdown of HuR	Increased oxidative stress and increased dsDNA damage	TNBC	Mehta et al. 2016 [162]
Oxidative Stress	Glutathione depletion or inhibition of thioredoxin reductase	Increased DNA damage and increase in reactive oxygen species	TNBC	Rodman et al 2016 [164]
Oxidative Stress	Histamine	Increased oxidative DNA damage, dsDNA breaks, and increased reactive oxygen species	Multiple	Martinel Lamas et al 2015 [163]

Table 1.2: Novel preclinical approaches to modulate the radiation response in breast cancer.

Strategies to radiosensitize breast cancer cells include a variety of compounds that target multiple different pathways, including the cell cycle, DNA damage, apoptosis, hypoxia, and autophagy.

References

1 BD, Y. *et al.* A Genetic Basis for the Variation in the Vulnerability of Cancer to DNA Damage. *Nature communications* 7, doi:10.1038/ncomms11428 (2016).

2 Early Breast Cancer Trialists' Collaborative, G. in *Lancet* Vol. 379 432-444 (2012).

3 Darby, S. *et al.* Effect of radiotherapy after breast-conserving surgery on 10-year recurrence and 15-year breast cancer death: meta-analysis of individual patient data for 10,801 women in 17 randomised trials. *Lancet* 378, 1707-1716, doi:10.1016/s0140-6736(11)61629-2 (2011).

4 Effect of radiotherapy after mastectomy and axillary surgery on 10-year recurrence and 20-year breast cancer mortality: meta-analysis of individual patient data for 8135 women in 22 randomised trials - The Lancet. doi:doi:10.1016/S0140-6736(14)60488-8 (2020).

5 Dong, J. *et al.* Cordycepin sensitizes breast cancer cells toward irradiation through elevating ROS production involving Nrf2. *Toxicol Appl Pharmacol* 364, 12-21, doi:10.1016/j.taap.2018.12.006 (2019).

6 Robinson, B. W. & Shewach, D. S. Radiosensitization by gemcitabine in p53 wild-type and mutant MCF-7 breast carcinoma cell lines. *Clin Cancer Res* 7, 2581-2589 (2001).

7 SD, S. *et al.* Involvement of p53 in Gemcitabine Mediated Cytotoxicity and Radiosensitivity in Breast Cancer Cell Lines. *Gene* 498, doi:10.1016/j.gene.2012.01.099 (2012).

8 Suh, W. W. *et al.* A phase I dose escalation trial of gemcitabine with radiotherapy for breast cancer in the treatment of unresectable chest wall recurrences. *Breast J* 10, 204-210, doi:10.1111/j.1075-122X.2004.21305.x (2004).

9 Liu, Y. L. *et al.* Concurrent use of capecitabine with radiation therapy and survival in breast cancer (BC) after neoadjuvant chemotherapy. *Clin Transl Oncol* 20, 1280-1288, doi:10.1007/s12094-018-1859-7 (2018).

10 Gaui, M. F. *et al.* A phase II study of second-line neoadjuvant chemotherapy with capecitabine and radiation therapy for anthracycline-resistant locally advanced breast cancer. *Am J Clin Oncol* 30, 78-81, doi:10.1097/01.coc.0000245475.41324.6d (2007).

11 Bourgier C, G. I., Heymann S, Barhi M, Mazouni C, Al Ghuzlan AA, Balleyguier C, Marsiglia H, Delaloge S. Effect of preoperative rescue concomitant FUN/XUN-based chemo-radiotherapy for neoadjuvant chemotherapy-refractory breast cancer. - PubMed - NCBI. *Radiother Oncol.* (2012).

12 Wang, L. *et al.* 5-aza-2'-Deoxycytidine enhances the radiosensitivity of breast cancer cells. *Cancer Biother Radiopharm* 28, 34-44, doi:10.1089/cbr.2012.1170 (2013).

13 Genet, D. *et al.* Concomitant intensive chemoradiotherapy induction in non-metastatic inflammatory breast cancer: long-term follow-up. *British Journal of Cancer* 97, 883-887, doi:doi:10.1038/sj.bjc.6603987 (2007).

14 Zellars, R. C. *et al.* Phase I/II Trial of Partial Breast Irradiation With Concurrent Dose-Dense Doxorubicin and Cyclophosphamide (ddAC) Chemotherapy in Early Stage Breast Cancer: Report of Skin Toxicity and Cosmetic Outcome. *International Journal of Radiation Oncology, Biology, Physics* 69, doi:10.1016/j.ijrobp.2007.07.046 (2007).

15 Brackstone, M. *et al.* Concurrent Neoadjuvant Chemotherapy and Radiation Therapy in Locally Advanced Breast Cancer. *Int J Radiat Oncol Biol Phys* 99, 769-776, doi:10.1016/j.ijrobp.2017.06.005 (2017).

16 Adams, S. *et al.* Preoperative concurrent paclitaxel-radiation in locally advanced breast cancer: pathologic response correlates with five-year overall survival. *Breast Cancer Res Treat* 124, 723-732, doi:10.1007/s10549-010-1181-8 (2010).
17 C, C., RA, T., D, M., P, C. & N, M. Concurrent Hormone and Radiation Therapy in Patients With Breast Cancer: What Is the Rationale? *The Lancet. Oncology* 10, doi:10.1016/S1470-2045(08)70333-4 (2009).
18 Polkinghorn, W. R. *et al.* Androgen receptor signaling regulates DNA repair in prostate cancers. *Cancer Discov* 3, 1245-1253, doi:10.1158/2159-8290.cd-13-0172 (2013).
19 Goodwin, J. F. *et al.* A hormone-DNA repair circuit governs the response to genotoxic insult. *Cancer Discov* 3, 1254-1271, doi:10.1158/2159-8290.cd-13-0108 (2013).
20 Speers, C. *et al.* Androgen receptor as a mediator and biomarker of radioresistance in triple-negative breast cancer. *NPJ Breast Cancer* 3, 29, doi:10.1038/s41523-017-0038-2 (2017).
21 Michmerhuizen, A. R. *et al.* Seviteronel, a Novel CYP17 Lyase Inhibitor and Androgen Receptor Antagonist, Radiosensitizes AR-Positive Triple Negative Breast Cancer Cells. *Front Endocrinol (Lausanne)* 11, 35, doi:10.3389/fendo.2020.00035 (2020).
22 Kale, S., Korcum, A. F., Dundar, E. & Erin, N. HSP90 inhibitor PU-H71 increases radiosensitivity of breast cancer cells metastasized to visceral organs and alters the levels of inflammatory mediators. *Naunyn Schmiedebergs Arch Pharmacol* 393, 253-262, doi:10.1007/s00210-019-01725-z (2020).
23 Ha, K. *et al.* Hsp90 inhibitor-mediated disruption of chaperone association of ATR with hsp90 sensitizes cancer cells to DNA damage. *Mol Cancer Ther* 10, 1194-1206, doi:10.1158/1535-7163.mct-11-0094 (2011).
24 Chen, X. *et al.* Estrogen Receptor Mediates the Radiosensitivity of Triple-Negative Breast Cancer Cells. *Med Sci Monit* 23, 2674-2683, doi:10.12659/msm.904810 (2017).
25 Kyndi, M. *et al.* Estrogen receptor, progesterone receptor, HER-2, and response to postmastectomy radiotherapy in high-risk breast cancer: the Danish Breast Cancer Cooperative Group. *J Clin Oncol* 26, 1419-1426, doi:10.1200/jco.2007.14.5565 (2008).
26 Gray, M. *et al.* Development and characterisation of acquired radioresistant breast cancer cell lines. *Radiat Oncol* 14, 64, doi:10.1186/s13014-019-1268-2 (2019).
27 Villalobos, M. *et al.* Interaction between ionizing radiation, estrogens and antiestrogens in the modification of tumor microenvironment in estrogen dependent multicellular spheroids. *Acta Oncol* 34, 413-417, doi:10.3109/02841869509094000 (1995).
28 Wazer, D. E., Tercilla, O. F., Lin, P. S. & Schmidt-Ullrich, R. Modulation in the radiosensitivity of MCF-7 human breast carcinoma cells by 17B-estradiol and tamoxifen. *Br J Radiol* 62, 1079-1083, doi:10.1259/0007-1285-62-744-1079 (1989).
29 Wang, J., Yang, Q., Haffty, B. G., Li, X. & Moran, M. S. Fulvestrant radiosensitizes human estrogen receptor-positive breast cancer cells. *Biochem Biophys Res Commun* 431, 146-151, doi:10.1016/j.bbrc.2013.01.006 (2013).
30 Kantorowitz, D. A., Thompson, H. J. & Furmanski, P. Effect of conjoint administration of tamoxifen and high-dose radiation on the development of mammary carcinoma. *Int J Radiat Oncol Biol Phys* 26, 89-94, doi:10.1016/0360-3016(93)90177-w (1993).
31 Pierce, L. J. *et al.* Sequencing of tamoxifen and radiotherapy after breast-conserving surgery in early-stage breast cancer. *J Clin Oncol* 23, 24-29, doi:10.1200/jco.2005.01.198 (2005).

32 Ahn, P. H. *et al.* Sequence of radiotherapy with tamoxifen in conservatively managed breast cancer does not affect local relapse rates. *J Clin Oncol* 23, 17-23, doi:10.1200/jco.2005.09.048 (2005).
33 Dalberg, K., Johansson, H., Johansson, U. & Rutqvist, L. E. A randomized trial of long term adjuvant tamoxifen plus postoperative radiation therapy versus radiation therapy alone for patients with early stage breast carcinoma treated with breast-conserving surgery. Stockholm Breast Cancer Study Group. *Cancer* 82, 2204-2211 (1998).
34 Fisher, B. *et al.* Tamoxifen, radiation therapy, or both for prevention of ipsilateral breast tumor recurrence after lumpectomy in women with invasive breast cancers of one centimeter or less. *J Clin Oncol* 20, 4141-4149, doi:10.1200/jco.2002.11.101 (2002).
35 Fyles, A. W. *et al.* Tamoxifen with or without breast irradiation in women 50 years of age or older with early breast cancer. *N Engl J Med* 351, 963-970, doi:10.1056/NEJMoa040595 (2004).
36 Guo, G. *et al.* Expression of ErbB2 enhances radiation-induced NF-kappaB activation. *Oncogene* 23, 535-545, doi:10.1038/sj.onc.1207149 (2004).
37 Hou, J. *et al.* HER2 reduces breast cancer radiosensitivity by activating focal adhesion kinase in vitro and in vivo. *Oncotarget* 7, 45186-45198, doi:10.18632/oncotarget.9870 (2016).
38 Duru, N. *et al.* HER2-associated radioresistance of breast cancer stem cells isolated from HER2-negative breast cancer cells. *Clin Cancer Res* 18, 6634-6647, doi:10.1158/1078-0432.ccr-12-1436 (2012).
39 Yamaguchi, H. *et al.* HER2-Targeted Multifunctional Silica Nanoparticles Specifically Enhance the Radiosensitivity of HER2-Overexpressing Breast Cancer Cells. *Int J Mol Sci* 19, doi:10.3390/ijms19030908 (2018).
40 Liang, K. *et al.* Sensitization of breast cancer cells to radiation by trastuzumab. *Mol Cancer Ther* 2, 1113-1120 (2003).
41 Samani, R. K. *et al.* Trastuzumab and folic acid functionalized gold nanoclusters as a dual-targeted radiosensitizer for megavoltage radiation therapy of human breast cancer. *Eur J Pharm Sci* 153, 105487, doi:10.1016/j.ejps.2020.105487 (2020).
42 Pietras, R. J. *et al.* Monoclonal antibody to HER-2/neureceptor modulates repair of radiation-induced DNA damage and enhances radiosensitivity of human breast cancer cells overexpressing this oncogene. *Cancer Res* 59, 1347-1355 (1999).
43 Horton, J. K. *et al.* Radiosensitization of chemotherapy-refractory, locally advanced or locally recurrent breast cancer with trastuzumab: a phase II trial. *Int J Radiat Oncol Biol Phys* 76, 998-1004, doi:10.1016/j.ijrobp.2009.03.027 (2010).
44 Yu, T. *et al.* Radiosensitizing effect of lapatinib in human epidermal growth factor receptor 2-positive breast cancer cells. *Oncotarget* 7, 79089-79100, doi:10.18632/oncotarget.12597 (2016).
45 Sambade, M. J. *et al.* Lapatinib in combination with radiation diminishes tumor regrowth in HER2+ and basal-like/EGFR+ breast tumor xenografts. *Int J Radiat Oncol Biol Phys* 77, 575-581, doi:10.1016/j.ijrobp.2009.12.063 (2010).
46 Sambade, M. J., Camp, J. T., Kimple, R. J., Sartor, C. I. & Shields, J. M. Mechanism of lapatinib-mediated radiosensitization of breast cancer cells is primarily by inhibition of the Raf>MEK>ERK mitogen-activated protein kinase cascade and radiosensitization of lapatinib-resistant cells restored by direct inhibition of MEK. *Radiother Oncol* 93, 639-644, doi:10.1016/j.radonc.2009.09.006 (2009).

47 Schmidt-Ullrich, R. K., Valerie, K., Fogleman, P. B. & Walters, J. Radiation-induced autophosphorylation of epidermal growth factor receptor in human malignant mammary and squamous epithelial cells. *Radiat Res* 145, 81-85 (1996).
48 Schmidt-Ullrich, R. K., Valerie, K. C., Chan, W. & McWilliams, D. Altered expression of epidermal growth factor receptor and estrogen receptor in MCF-7 cells after single and repeated radiation exposures. *Int J Radiat Oncol Biol Phys* 29, 813-819, doi:10.1016/0360-3016(94)90570-3 (1994).
49 C, S. *et al.* A Signature That May Be Predictive of Early vs. Late Recurrence After Radiation Treatment (RT) for Breast Cancer That May Inform the Biology of Early, Aggressive Recurrences. *International journal of radiation oncology, biology, physics*, doi:10.1016/j.ijrobp.2020.05.015 (2020).
50 Liang, K. *et al.* Targeting the phosphatidylinositol 3-kinase/Akt pathway for enhancing breast cancer cells to radiotherapy. *Mol Cancer Ther* 2, 353-360 (2003).
51 Holler, M. *et al.* Dual Targeting of Akt and mTORC1 Impairs Repair of DNA Double-Strand Breaks and Increases Radiation Sensitivity of Human Tumor Cells. *PLoS One* 11, e0154745, doi:10.1371/journal.pone.0154745 (2016).
52 Li, P. *et al.* Simultaneous inhibition of EGFR and PI3K enhances radiosensitivity in human breast cancer. *Int J Radiat Oncol Biol Phys* 83, e391-397, doi:10.1016/j.ijrobp.2011.12.090 (2012).
53 No, M., Choi, E. J. & Kim, I. A. Targeting HER2 signaling pathway for radiosensitization: alternative strategy for therapeutic resistance. *Cancer Biol Ther* 8, 2351-2361, doi:10.4161/cbt.8.24.10131 (2009).
54 Andrade, D. *et al.* YAP1 inhibition radiosensitizes triple negative breast cancer cells by targeting the DNA damage response and cell survival pathways. *Oncotarget* 8, 98495-98508, doi:10.18632/oncotarget.21913 (2017).
55 Hu, T., Zhou, R., Zhao, Y. & Wu, G. Integrin alpha6/Akt/Erk signaling is essential for human breast cancer resistance to radiotherapy. *Sci Rep* 6, 33376, doi:10.1038/srep33376 (2016).
56 Wang, T. *et al.* Co-activation of ERK, NF-kappaB, and GADD45beta in response to ionizing radiation. *J Biol Chem* 280, 12593-12601, doi:10.1074/jbc.M410982200 (2005).
57 Michmerhuizen, A. R. *et al.* PARP1 Inhibition Radiosensitizes Models of Inflammatory Breast Cancer to Ionizing Radiation. *Mol Cancer Ther*, doi:10.1158/1535-7163.mct-19-0520 (2019).
58 Jagsi, R. *et al.* TBCRC 024 initial results: A multicenter phase 1 study of veliparib administered concurrently with chest wall and nodal radiation therapy in patients with inflammatory or locoregionally recurrent breast cancer. *International Journal of Radiation Oncology* 93, S137 (2015).
59 Feng, F. Y. *et al.* Targeted radiosensitization with PARP1 inhibition: optimization of therapy and identification of biomarkers of response in breast cancer. *Breast Cancer Res Treat* 147, 81-94, doi:10.1007/s10549-014-3085-5 (2014).
60 Bridges, K. A. *et al.* Niraparib (MK-4827), a novel poly(ADP-Ribose) polymerase inhibitor, radiosensitizes human lung and breast cancer cells. *5*, doi:*https://www.oncotarget.com/article/2083/* (2014).
61 Wang, L. *et al.* MK-4827, a PARP-1/-2 inhibitor, strongly enhances response of human lung and breast cancer xenografts to radiation. *Invest New Drugs* 30, 2113-2120, doi:10.1007/s10637-011-9770-x (2012).

62 Sizemore, S. T. *et al.* Synthetic Lethality of PARP Inhibition and Ionizing Radiation is p53-dependent. *Mol Cancer Res* 16, 1092-1102, doi:10.1158/1541-7786.mcr-18-0106 (2018).
63 Dominguez-Gomez, G. *et al.* Nicotinamide sensitizes human breast cancer cells to the cytotoxic effects of radiation and cisplatin. *Oncol Rep* 33, 721-728, doi:10.3892/or.2014.3661 (2015).
64 M, M. *et al.* Association Between Genetic Polymorphisms in the XRCC1, XRCC3, XPD, GSTM1, GSTT1, MSH2, MLH1, MSH3, and MGMT Genes and Radiosensitivity in Breast Cancer Patients. *International journal of radiation oncology, biology, physics* 81, doi:10.1016/j.ijrobp.2010.04.023 (2011).
65 Mamon, H. J. *et al.* Differing effects of breast cancer 1, early onset (BRCA1) and ataxia-telangiectasia mutated (ATM) mutations on cellular responses to ionizing radiation. *Int J Radiat Biol* 79, 817-829, doi:10.1080/09553000310001610952 (2003).
66 Ma, Z. *et al.* The Chk1 inhibitor AZD7762 sensitises p53 mutant breast cancer cells to radiation in vitro and in vivo. *Mol Med Rep* 6, 897-903, doi:10.3892/mmr.2012.999 (2012).
67 Zhang, Y. *et al.* in *Oncotarget* Vol. 7 34688-34702 (2016).
68 Zhou, Z. *et al.* in *Acta Pharmacol Sin* Vol. 38 513-523 (2017).
69 IG, C., BW, D. & MJ, T. Sensitization of Breast Carcinoma Cells to Ionizing Radiation by Small Molecule Inhibitors of DNA-dependent Protein Kinase and Ataxia Telangiectsia Mutated. *Biochemical pharmacology* 71, doi:10.1016/j.bcp.2005.09.029 (2005).
70 Gasparini, P. *et al.* Protective role of miR-155 in breast cancer through RAD51 targeting impairs homologous recombination after irradiation. *Proc Natl Acad Sci U S A* 111, 4536-4541, doi:10.1073/pnas.1402604111 (2014).
71 Ciszewski, W. M., Tavecchio, M., Dastych, J. & Curtin, N. J. DNA-PK inhibition by NU7441 sensitizes breast cancer cells to ionizing radiation and doxorubicin. *Breast Cancer Res Treat* 143, 47-55, doi:10.1007/s10549-013-2785-6 (2014).
72 Fok, J. *et al.* AZD7648 is a potent and selective DNA-PK inhibitor that enhances radiation, chemotherapy and olaparib activity. *Nature Communications* (Nov 2019).
73 Jang, N. Y. *et al.* Radiosensitization with combined use of olaparib and PI-103 in triple-negative breast cancer. *BMC Cancer* 15, 89, doi:10.1186/s12885-015-1090-7 (2015).
74 Tu, X. *et al.* ATR Inhibition Is a Promising Radiosensitizing Strategy for Triple-Negative Breast Cancer. *Mol Cancer Ther* 17, 2462-2472, doi:10.1158/1535-7163.mct-18-0470 (2018).
75 Zenke, F. T. *et al.* Pharmacological inhibitor of DNA-PK, M3814, potentiates radiotherapy and regresses human tumors in mouse models. doi:10.1158/1535-7163.MCT-19-0734 (2020).
76 Schmid, P. *et al.* Pembrolizumab for Early Triple-Negative Breast Cancer. *https://doi.org/10.1056/NEJMoa1910549*, doi:NJ202002273820907 (2020).
77 Vanpouille-Box, C. *et al.* DNA exonuclease Trex1 regulates radiotherapy-induced tumour immunogenicity. *Nat Commun* 8, 15618, doi:10.1038/ncomms15618 (2017).
78 Deng, L. *et al.* Irradiation and anti-PD-L1 treatment synergistically promote antitumor immunity in mice. *J Clin Invest* 124, 687-695, doi:10.1172/jci67313 (2014).
79 Verbrugge, I. *et al.* Radiotherapy increases the permissiveness of established mammary tumors to rejection by immunomodulatory antibodies. *Cancer Res* 72, 3163-3174, doi:10.1158/0008-5472.can-12-0210 (2012).

80 Dovedi, S. J. *et al.* Acquired Resistance to Fractionated Radiotherapy Can Be Overcome by Concurrent PD-L1 Blockade. doi:10.1158/0008-5472.CAN-14-1258 (2014).
81 Vanpouille-Box, C. *et al.* TGFbeta Is a Master Regulator of Radiation Therapy-Induced Antitumor Immunity. *Cancer Res* 75, 2232-2242, doi:10.1158/0008-5472.can-14-3511 (2015).
82 F, B. *et al.* TGFβ1 Inhibition Increases the Radiosensitivity of Breast Cancer Cells in Vitro and Promotes Tumor Control by Radiation in Vivo. *Clinical cancer research : an official journal of the American Association for Cancer Research* 17, doi:10.1158/1078-0432.CCR-11-0544 (2011).
83 Demaria, S. *et al.* Ionizing radiation inhibition of distant untreated tumors (abscopal effect) is immune mediated. *Int J Radiat Oncol Biol Phys* 58, 862-870, doi:10.1016/j.ijrobp.2003.09.012 (2004).
84 Dewan, M. Z. *et al.* Fractionated but not single-dose radiotherapy induces an immune-mediated abscopal effect when combined with anti-CTLA-4 antibody. *Clin Cancer Res* 15, 5379-5388, doi:10.1158/1078-0432.ccr-09-0265 (2009).
85 Aguilera, T. A. *et al.* in *Nat Commun* Vol. 7 (2016).
86 Marvaso, G. *et al.* Sphingosine analog fingolimod (FTY720) increases radiation sensitivity of human breast cancer cells in vitro. *Cancer Biol Ther* 15, 797-805, doi:10.4161/cbt.28556 (2014).
87 PG, T. *et al.* Emerging Opportunities of Radiotherapy Combined With Immunotherapy in the Era of Breast Cancer Heterogeneity. *Frontiers in oncology* 8, doi:10.3389/fonc.2018.00609 (2018).
88 JC, Y. & SC, F. Integration of Radiation and Immunotherapy in Breast Cancer - Treatment Implications. *Breast (Edinburgh, Scotland)* 38, doi:10.1016/j.breast.2017.12.005 (2018).
89 Yao, Z. *et al.* EGFR inhibitor C225 Increases the Radio-Sensitivity of Human Breast Cancer Cells. *Asian Pac J Cancer Prev* 20, 311-319, doi:10.31557/apjcp.2019.20.1.311 (2019).
90 El Guerrab, A., Bamdad, M., Bignon, Y. J., Penault-Llorca, F. & Aubel, C. Anti-EGFR monoclonal antibodies enhance sensitivity to DNA-damaging agents in BRCA1-mutated and PTEN-wild-type triple-negative breast cancer cells. *Mol Carcinog* 56, 1383-1394, doi:10.1002/mc.22596 (2017).
91 Qu, Y. Y. *et al.* Nimotuzumab enhances the radiosensitivity of cancer cells in vitro by inhibiting radiation-induced DNA damage repair. *PLoS One* 8, e70727, doi:10.1371/journal.pone.0070727 (2013).
92 Rao, G. S., Murray, S. & Ethier, S. P. Radiosensitization of human breast cancer cells by a novel ErbB family receptor tyrosine kinase inhibitor. *Int J Radiat Oncol Biol Phys* 48, 1519-1528, doi:10.1016/s0360-3016(00)01358-4 (2000).
93 He, G. *et al.* Silencing human epidermal growth factor receptor-3 radiosensitizes human luminal A breast cancer cells. *Cancer Sci* 109, 3774-3782, doi:10.1111/cas.13810 (2018).
94 Contessa, J. N., Abell, A., Mikkelsen, R. B., Valerie, K. & Schmidt-Ullrich, R. K. Compensatory ErbB3/c-Src signaling enhances carcinoma cell survival to ionizing radiation. *Breast Cancer Res Treat* 95, 17-27, doi:10.1007/s10549-005-9023-9 (2006).
95 Lammering, G. *et al.* Adenovirus-mediated overexpression of dominant negative epidermal growth factor receptor-CD533 as a gene therapeutic approach radiosensitizes human carcinoma and malignant glioma cells. *Int J Radiat Oncol Biol Phys* 51, 775-784, doi:10.1016/s0360-3016(01)01714-x (2001).

96 Contessa, J. N. *et al.* The inducible expression of dominant-negative epidermal growth factor receptor-CD533 results in radiosensitization of human mammary carcinoma cells. *Clin Cancer Res* 5, 405-411 (1999).
97 Ghorab, M. M., Alsaid, M. S. & Soliman, A. M. Dual EGFR/HER2 inhibitors and apoptosis inducers: New benzo[g]quinazoline derivatives bearing benzenesulfonamide as anticancer and radiosensitizers. *Bioorg Chem* 80, 611-620, doi:10.1016/j.bioorg.2018.07.015 (2018).
98 Fukutome, M., Maebayashi, K., Nasu, S., Seki, K. & Mitsuhashi, N. Enhancement of radiosensitivity by dual inhibition of the HER family with ZD1839 ("Iressa") and trastuzumab ("Herceptin"). *Int J Radiat Oncol Biol Phys* 66, 528-536, doi:10.1016/j.ijrobp.2006.05.036 (2006).
99 Heravi, M. *et al.* ZRBA1, a Mixed EGFR/DNA Targeting Molecule, Potentiates Radiation Response Through Delayed DNA Damage Repair Process in a Triple Negative Breast Cancer Model. *Int J Radiat Oncol Biol Phys* 92, 399-406, doi:10.1016/j.ijrobp.2015.01.026 (2015).
100 Li, P. *et al.* Co-inhibition of epidermal growth factor receptor and insulin-like growth factor receptor 1 enhances radiosensitivity in human breast cancer cells. *BMC Cancer* 13, 297, doi:10.1186/1471-2407-13-297 (2013).
101 Wen, B. *et al.* Tyrphostin AG 1024 modulates radiosensitivity in human breast cancer cells. *Br J Cancer* 85, 2017-2021, doi:10.1054/bjoc.2001.2171 (2001).
102 BC, T. *et al.* Insulin-like Growth factor-I Receptor Overexpression Mediates Cellular Radioresistance and Local Breast Cancer Recurrence After Lumpectomy and Radiation. *Cancer research* 57 (1997).
103 Koo, T. *et al.* MicroRNA-200c increases radiosensitivity of human cancer cells with activated EGFR-associated signaling. *Oncotarget* 8, 65457-65468, doi:10.18632/oncotarget.18924 (2017).
104 Lee, K. M., Choi, E. J. & Kim, I. A. microRNA-7 increases radiosensitivity of human cancer cells with activated EGFR-associated signaling. *Radiother Oncol* 101, 171-176, doi:10.1016/j.radonc.2011.05.050 (2011).
105 Cao, N. *et al.* NF-kappaB-mediated HER2 overexpression in radiation-adaptive resistance. *Radiat Res* 171, 9-21, doi:10.1667/rr1472.1 (2009).
106 Lai, Y., Yu, X., Lin, X. & He, S. Inhibition of mTOR sensitizes breast cancer stem cells to radiation-induced repression of self-renewal through the regulation of MnSOD and Akt. *Int J Mol Med* 37, 369-377, doi:10.3892/ijmm.2015.2441 (2016).
107 Kuger, S. *et al.* Novel PI3K and mTOR Inhibitor NVP-BEZ235 Radiosensitizes Breast Cancer Cell Lines under Normoxic and Hypoxic Conditions. *Breast Cancer (Auckl)* 8, 39-49, doi:10.4137/bcbcr.s13693 (2014).
108 Sizemore, G. M. *et al.* Stromal PTEN determines mammary epithelial response to radiotherapy. *Nat Commun* 9, 2783, doi:10.1038/s41467-018-05266-6 (2018).
109 Weng, L. P. *et al.* PTEN suppresses breast cancer cell growth by phosphatase activity-dependent G1 arrest followed by cell death. *Cancer Res* 59, 5808-5814 (1999).
110 Toulany, M. *et al.* Impact of oncogenic K-RAS on YB-1 phosphorylation induced by ionizing radiation. *Breast Cancer Res* 13, R28, doi:10.1186/bcr2845 (2011).
111 Yan, Y., Greer, P. M., Cao, P. T., Kolb, R. H. & Cowan, K. H. RAC1 GTPase plays an important role in gamma-irradiation induced G2/M checkpoint activation. *Breast Cancer Res* 14, R60, doi:10.1186/bcr3164 (2012).

112 Albert, J. M., Kim, K. W., Cao, C. & Lu, B. Targeting the Akt/mammalian target of rapamycin pathway for radiosensitization of breast cancer. *Mol Cancer Ther* 5, 1183-1189, doi:10.1158/1535-7163.mct-05-0400 (2006).
113 S, P. *et al.* Rapamycin-sensitive Pathway Regulates Mitochondrial Membrane Potential, Autophagy, and Survival in Irradiated MCF-7 Cells. *Cancer research* 65, doi:10.1158/0008-5472.CAN-05-1083 (2005).
114 Fatehi, D., Soltani, A. & Ghatrehsamani, M. SRT1720, a potential sensitizer for radiotherapy and cytotoxicity effects of NVB-BEZ235 in metastatic breast cancer cells. *Pathol Res Pract* 214, 889-895, doi:10.1016/j.prp.2018.04.001 (2018).
115 Masoumi, H., Soltani, A. & Ghatrehsamani, M. The beneficial role of SIRT1 activator on chemo- and radiosensitization of breast cancer cells in response to IL-6. *Mol Biol Rep* 47, 129-139, doi:10.1007/s11033-019-05114-w (2020).
116 Zhang, X., Li, Y., Wang, D. & Wei, X. miR-22 suppresses tumorigenesis and improves radiosensitivity of breast cancer cells by targeting Sirt1. *Biol Res* 50, 27, doi:10.1186/s40659-017-0133-8 (2017).
117 Maggiorella, L. *et al.* Enhancement of radiation response by roscovitine in human breast carcinoma in vitro and in vivo. *Cancer Res* 63, 2513-2517 (2003).
118 Liu, X. *et al.* Genistein enhances the radiosensitivity of breast cancer cells via G(2)/M cell cycle arrest and apoptosis. *Molecules* 18, 13200-13217, doi:10.3390/molecules181113200 (2013).
119 Quereda, V. *et al.* Therapeutic Targeting of CDK12/CDK13 in Triple-Negative Breast Cancer. *Cancer Cell* 36, 545-558.e547, doi:10.1016/j.ccell.2019.09.004 (2019).
120 Pesch, A. *et al.* Short Term CDK4/6 Inhibition Radiosensitizes Estrogen Receptor Positive Breast Cancers. *Clinical Cancer Research* (2020).
121 Robinson, T. J. *et al.* RB1 status in triple negative breast cancer cells dictates response to radiation treatment and selective therapeutic drugs. *PLoS One* 8, e78641, doi:10.1371/journal.pone.0078641 (2013).
122 Fernandez-Aroca, D. M. *et al.* P53 pathway is a major determinant in the radiosensitizing effect of Palbociclib: Implication in cancer therapy. *Cancer Lett* 451, 23-33, doi:10.1016/j.canlet.2019.02.049 (2019).
123 Bao-Lei, T. *et al.* Knocking down PML impairs p53 signaling transduction pathway and suppresses irradiation induced apoptosis in breast carcinoma cell MCF-7. *J Cell Biochem* 97, 561-571, doi:10.1002/jcb.20584 (2006).
124 Wang, H., Oliver, P., Zhang, Z., Agrawal, S. & Zhang, R. Chemosensitization and radiosensitization of human cancer by antisense anti-MDM2 oligonucleotides: in vitro and in vivo activities and mechanisms. *Ann N Y Acad Sci* 1002, 217-235, doi:10.1196/annals.1281.025 (2003).
125 Zhang, Z. *et al.* Radiosensitization by antisense anti-MDM2 mixed-backbone oligonucleotide in in vitro and in vivo human cancer models. *Clin Cancer Res* 10, 1263-1273, doi:10.1158/1078-0432.ccr-0245-03 (2004).
126 X, H. *et al.* BTG2 Overexpression Increases the Radiosensitivity of Breast Cancer Cells in Vitro and in Vivo. *Oncology research* 20, doi:10.3727/096504013x13685487925211 (2013).
127 Zhu, R., Li, W., Xu, Y., Wan, J. & Zhang, Z. Upregulation of BTG1 enhances the radiation sensitivity of human breast cancer in vitro and in vivo. *Oncol Rep* 34, 3017-3024, doi:10.3892/or.2015.4311 (2015).

128 Speers, C. *et al.* Maternal Embryonic Leucine Zipper Kinase (MELK) as a Novel Mediator and Biomarker of Radioresistance in Human Breast Cancer. *Clin Cancer Res* 22, 5864-5875, doi:10.1158/1078-0432.ccr-15-2711 (2016).
129 KA, B. *et al.* MK-1775, a Novel Wee1 Kinase Inhibitor, Radiosensitizes p53-defective Human Tumor Cells. *Clinical cancer research : an official journal of the American Association for Cancer Research* 17, doi:10.1158/1078-0432.CCR-11-0650 (2011).
130 Li, C. *et al.* SKP2 promotes breast cancer tumorigenesis and radiation tolerance through PDCD4 ubiquitination. *J Exp Clin Cancer Res* 38, 76, doi:10.1186/s13046-019-1069-3 (2019).
131 Ren, Y.-q., Fu, F. & Han, J. MiR-27a Modulates Radiosensitivity of Triple-Negative Breast Cancer (TNBC) Cells by Targeting CDC27. doi:10.12659/MSM.893974 (2015).
132 Chandler, B. *et al.* (Journal of Clinical Investigation, 2019).
133 Yan, Y. *et al.* Protein phosphatase 2A has an essential role in the activation of gamma-irradiation-induced G2/M checkpoint response. *Oncogene* 29, 4317-4329, doi:10.1038/onc.2010.187 (2010).
134 Benada, J., Burdova, K., Lidak, T., von Morgen, P. & Macurek, L. Polo-like kinase 1 inhibits DNA damage response during mitosis. *Cell Cycle* 14, 219-231, doi:10.4161/15384101.2014.977067 (2015).
135 Brassesco, M. S. *et al.* PLK1 Inhibition Radiosensitizes Breast Cancer Cells, but Shows Low Efficacy as Monotherapy or in Combination with other Cytotoxic Drugs. *Anticancer Agents Med Chem* 18, 1252-1257, doi:10.2174/1871520618666180228155435 (2018).
136 Yin, L. *et al.* Niclosamide sensitizes triple-negative breast cancer cells to ionizing radiation in association with the inhibition of Wnt/beta-catenin signaling. *Oncotarget* 7, 42126-42138, doi:10.18632/oncotarget.9704 (2016).
137 Li, J. Y. *et al.* ABT-737 reverses the acquired radioresistance of breast cancer cells by targeting Bcl-2 and Bcl-xL. *J Exp Clin Cancer Res* 31, 102, doi:10.1186/1756-9966-31-102 (2012).
138 Zhou, K. X. *et al.* CXCR4 antagonist AMD3100 enhances the response of MDA-MB-231 triple-negative breast cancer cells to ionizing radiation. *Cancer Lett* 418, 196-203, doi:10.1016/j.canlet.2018.01.009 (2018).
139 Lin, F. *et al.* COX-2 promotes breast cancer cell radioresistance via p38/MAPK-mediated cellular anti-apoptosis and invasiveness. *Tumour Biol* 34, 2817-2826, doi:10.1007/s13277-013-0840-x (2013).
140 Oladghaffari, M. *et al.* MLN4924 and 2DG combined treatment enhances the efficiency of radiotherapy in breast cancer cells. *Int J Radiat Biol* 93, 590-599, doi:10.1080/09553002.2017.1294272 (2017).
141 D, Y., M, T., G, W. & Y, S. The p21-dependent Radiosensitization of Human Breast Cancer Cells by MLN4924, an Investigational Inhibitor of NEDD8 Activating Enzyme. *PloS one* 7, doi:10.1371/journal.pone.0034079 (2012).
142 Yang, D. *et al.* Smac-mimetic compound SM-164 induces radiosensitization in breast cancer cells through activation of caspases and induction of apoptosis. *Breast Cancer Research and Treatment* 133, 189-199, doi:doi:10.1007/s10549-011-1752-3 (2011).
143 Hu, X., Ding, D., Zhang, J. & Cui, J. Knockdown of lncRNA HOTAIR sensitizes breast cancer cells to ionizing radiation through activating miR-218. *Biosci Rep* 39, doi:10.1042/bsr20181038 (2019).

144 C, S. *et al.* Overexpression of Bax Sensitizes Human Breast Cancer MCF-7 Cells to Radiation-Induced Apoptosis. *International journal of cancer* 67, doi:10.1002/(SICI)1097-0215(19960703)67:1<101::AID-IJC17>3.0.CO;2-H (1996).
145 Lu, L. *et al.* Activation of STAT3 and Bcl-2 and reduction of reactive oxygen species (ROS) promote radioresistance in breast cancer and overcome of radioresistance with niclosamide. *Oncogene* 37, 5292-5304, doi:10.1038/s41388-018-0340-y (2018).
146 Zou, M. *et al.* Knockdown of CAVEOLIN-1 Sensitizes Human Basal-Like Triple-Negative Breast Cancer Cells to Radiation. *Cell Physiol Biochem* 44, 778-791, doi:10.1159/000485291 (2017).
147 Zhang, L. *et al.* Mebendazole Potentiates Radiation Therapy in Triple-Negative Breast Cancer. *Int J Radiat Oncol Biol Phys* 103, 195-207, doi:10.1016/j.ijrobp.2018.08.046 (2019).
148 Johnson, J. *et al.* Targeting PI3K and AMPKα Signaling Alone or in Combination to Enhance Radiosensitivity of Triple Negative Breast Cancer. *Cells* 9, doi:10.3390/cells9051253 (2020).
149 H, C. *et al.* Autophagy Contributes to Resistance of Tumor Cells to Ionizing Radiation. *Radiotherapy and oncology : journal of the European Society for Therapeutic Radiology and Oncology* 99, doi:10.1016/j.radonc.2011.06.002 (2011).
150 C, C. *et al.* Radiosensitization by Targeting Radioresistance-Related Genes With Protein Kinase A Inhibitor in Radioresistant Cancer Cells. *Experimental & molecular medicine* 37, doi:10.1038/emm.2005.74 (2005).
151 Apel, A., Herr, I., Schwarz, H., Rodemann, H. P. & Mayer, A. Blocked Autophagy Sensitizes Resistant Carcinoma Cells to Radiation Therapy. doi:10.1158/0008-5472.CAN-07-0562 (2008).
152 KW, K., L, M., LR, M., DK, J. & B, L. Endoplasmic Reticulum Stress Mediates Radiation-Induced Autophagy by perk-eIF2alpha in caspase-3/7-deficient Cells. *Oncogene* 29, doi:10.1038/onc.2010.74 (2010).
153 F, L. *et al.* Different Roles of CHOP and JNK in Mediating Radiation-Induced Autophagy and Apoptosis in Breast Cancer Cells. *Radiation research* 185, doi:10.1667/RR14344.1 (2016).
154 MW, H. *et al.* Autophagy Inhibition Can Overcome Radioresistance in Breast Cancer Cells Through Suppression of TAK1 Activation. *Anticancer research* 34 (2014).
155 Sanli, T. *et al.* Ionizing radiation activates AMP-activated kinase (AMPK): a target for radiosensitization of human cancer cells. *Int J Radiat Oncol Biol Phys* 78, 221-229, doi:10.1016/j.ijrobp.2010.03.005 (2010).
156 Song, C. W. *et al.* Metformin kills and radiosensitizes cancer cells and preferentially kills cancer stem cells. *Sci Rep* 2, 362, doi:10.1038/srep00362 (2012).
157 Zhang, L. *et al.* PK-M2-mediated metabolic changes in breast cancer cells induced by ionizing radiation. *Breast Cancer Res Treat* (2019).
158 Zhao, F., Ming, J., Zhou, Y. & Fan, L. Inhibition of Glut1 by WZB117 sensitizes radioresistant breast cancer cells to irradiation. *Cancer Chemother Pharmacol* 77, 963-972, doi:10.1007/s00280-016-3007-9 (2016).
159 WS, H., XF, D., M, J., CW, L. & JH, R. Hypoxia-induced Autophagy Confers Resistance of Breast Cancer Cells to Ionizing Radiation. *Oncology research* 20, doi:10.3727/096504013x13589503483012 (2012).

160 Y, J. *et al.* Increased Chemosensitivity and Radiosensitivity of Human Breast Cancer Cell Lines Treated With Novel Functionalized Single-Walled Carbon Nanotubes. *Oncology letters* 13, doi:10.3892/ol.2016.5402 (2017).
161 Zhong, R. *et al.* The role of hypoxia-inducible factor-1alpha in radiation-induced autophagic cell death in breast cancer cells. *Tumour Biol* 36, 7077-7083, doi:10.1007/s13277-015-3425-z (2015).
162 Mehta, M. *et al.* in *Oncotarget* Vol. 7 64820-64835 (2016).
163 Martinel Lamas, D. J. *et al.* Enhancement of ionizing radiation response by histamine in vitro and in vivo in human breast cancer. *Cancer Biol Ther* 16, 137-148, doi:10.4161/15384047.2014.987091 (2015).
164 Rodman, S. N. *et al.* Enhancement of Radiation Response in Breast Cancer Stem Cells by Inhibition of Thioredoxin- and Glutathione-Dependent Metabolism. *Radiat Res* 186, 385-395, doi:10.1667/rr14463.1 (2016).
165 Atkinson, R. L. *et al.* Thermal enhancement with optically activated gold nanoshells sensitizes breast cancer stem cells to radiation therapy. *Sci Transl Med* 2, 55ra79, doi:10.1126/scitranslmed.3001447 (2010).
166 Lettau, K., Zips, D. & Toulany, M. Simultaneous targeting of RSK and AKT efficiently inhibits YB-1-mediated repair of ionizing radiation-induced DNA double strand breaks in breast cancer cells. *Int J Radiat Oncol Biol Phys*, doi:10.1016/j.ijrobp.2020.09.005 (2020).
167 Mehta, M. *et al.* Regorafenib sensitizes human breast cancer cells to radiation by inhibiting multiple kinases and inducing DNA damage. *Int J Radiat Biol*, 1-12, doi:10.1080/09553002.2020.1730012 (2020).
168 Lee, Y. C. *et al.* Tribbles Homolog 3 Involved in Radiation Response of Triple Negative Breast Cancer Cells by Regulating Notch1 Activation. *Cancers (Basel)* 11, doi:10.3390/cancers11020127 (2019).
169 Peng, J. H. *et al.* Inhibition of Notch signaling pathway enhanced the radiosensitivity of breast cancer cells. *J Cell Biochem* 119, 8398-8409, doi:10.1002/jcb.27036 (2018).
170 Farhood, B. *et al.* Melatonin as an adjuvant in radiotherapy for radioprotection and radiosensitization. *Clin Transl Oncol* 21, 268-279, doi:10.1007/s12094-018-1934-0 (2019).
171 Taghizadeh, B., Ghavami, L., Nikoofar, A. & Goliaei, B. Equol as a potent radiosensitizer in estrogen receptor-positive and -negative human breast cancer cell lines. *Breast Cancer* 22, 382-390, doi:10.1007/s12282-013-0492-0 (2015).
172 Bigdeli, B. *et al.* Enterolactone: A novel radiosensitizer for human breast cancer cell lines through impaired DNA repair and increased apoptosis. *Toxicol Appl Pharmacol* 313, 180-194, doi:10.1016/j.taap.2016.10.021 (2016).
173 Ding, X. *et al.* Radiosensitization effect of Huaier on breast cancer cells. *Oncology Reports* 35, 2843-2850, doi:10.3892/or.2016.4630 (2016).
174 Su, Y. J., Huang, S. Y., Ni, Y. H., Liao, K. F. & Chiu, S. C. Anti-Tumor and Radiosensitization Effects of N-Butylidenephthalide on Human Breast Cancer Cells. *Molecules* 23, doi:10.3390/molecules23020240 (2018).
175 Wang, J. *et al.* Radiosensitization effects of berberine on human breast cancer cells. *International Journal of Molecular Medicine* 30, 1166-1172, doi:10.3892/ijmm.2012.1095 (2012).

176 Kim, M. Y. *et al.* Naphthazarin enhances ionizing radiation-induced cell cycle arrest and apoptosis in human breast cancer cells. *Int J Oncol* 46, 1659-1666, doi:10.3892/ijo.2015.2857 (2015).
177 Famoso, J. M., Laughlin, B., McBride, A. & Gonzalez, V. J. in *Adv Radiat Oncol* Vol. 3 19-24 (2018).
178 O, K.-P., LB, M. & EL, J. Pentoxifylline and Vitamin E for Treatment or Prevention of Radiation-Induced Fibrosis in Patients With Breast Cancer. *The breast journal* 24, doi:10.1111/tbj.13044 (2018).
179 M, M. *et al.* Pentoxifylline and Vitamin E Treatment for Prevention of Radiation-Induced Side-Effects in Women With Breast Cancer: A Phase Two, Double-Blind, Placebo-Controlled Randomised Clinical Trial (Ptx-5). *European journal of cancer (Oxford, England : 1990)* 45, doi:10.1016/j.ejca.2009.05.015 (2009).
180 Choi, Y. J., Heo, K., Park, H. S., Yang, K. M. & Jeong, M. H. The resveratrol analog HS-1793 enhances radiosensitivity of mouse-derived breast cancer cells under hypoxic conditions. *Int J Oncol* 49, 1479-1488, doi:10.3892/ijo.2016.3647 (2016).
181 Lacerda, L. *et al.* Simvastatin radiosensitizes differentiated and stem-like breast cancer cell lines and is associated with improved local control in inflammatory breast cancer patients treated with postmastectomy radiation. *Stem Cells Transl Med* 3, 849-856, doi:10.5966/sctm.2013-0204 (2014).

Chapter 2 : PARP1 Inhibition Radiosensitizes Models of Inflammatory Breast Cancer to Ionizing Radiation[2]

Abstract

Sustained locoregional control of disease is a significant issue in patients with inflammatory breast cancer (IBC), with local control rates of 80% or less at 5 years. Given the unsatisfactory outcomes for these patients, there is a clear need for intensification of local therapy, including radiation. Inhibition of the DNA repair protein poly adenosine diphosphate-ribose polymerase 1 (PARP1) has had little efficacy as a single agent in breast cancer outside of studies restricted to patients with BRCA mutations; however, PARP1 inhibition (PARPi) may lead to the radiosensitization of aggressive tumor types. Thus, this study investigates inhibition of PARP1 as a novel and promising radiosensitization strategy in IBC. In all existing IBC models (SUM-149, SUM-190, MDA-IBC-3), PARPi (AZD2281-olaparib and ABT-888-veliparib) had limited single agent efficacy (IC50 > 10 μM) in proliferation assays. Despite limited single agent efficacy, sub-micromolar concentrations of AZD2281 in combination with RT led to significant radiosensitization (rER 1.12-1.76). This effect was partially dependent on *BRCA1* mutational status. Radiosensitization was due, at least in part, to delayed resolution of double strand DNA breaks as measured by

[2] This chapter was published in *Molecular Cancer Therapeutics* in 2019. Experimental design, data collection, and manuscript preparation was performed in collaboration with co-first author Anna Michmerhuizen.

multiple assays. Using a SUM-190 xenograft model *in vivo*, the combination of PARPi and RT significantly delays tumor doubling and tripling times compared to PARPi or RT alone with limited toxicity. This study demonstrates that PARPi improves the effectiveness of radiotherapy in IBC models and provides the preclinical rationale for the opening phase II randomized trial of RT +/- PARPi in women with IBC (SWOG 1706, NCT03598257).

Introduction

Inflammatory breast cancer (IBC) diagnoses represent well under 5% of new breast cancer cases but account for a disproportionate share of breast cancer mortality(1). Despite aggressive, multimodal therapy, patients have high rates of locoregional recurrence and distant metastases(1). Treatment strategies for many breast cancer subtypes are largely directed against the protein drivers of each molecular subtype, including targeted therapies against the estrogen receptor (ER) or the human epidermal growth factor receptor 2 (HER2). IBC, however, represents a heterogeneous population that includes tumors across all of the molecular subtypes(2). Current treatment guidelines for IBC patients take into consideration the molecular subtype of the tumor and include anti-HER2 or anti-estrogen therapy when appropriate, but more effective and targeted therapeutic options for patients with IBC are extremely limited. Without more effective alternatives, IBC patients typically receive neoadjuvant chemotherapy followed by mastectomy and adjuvant radiation (RT) to the chest wall and regional lymphatics(1). The key molecular drivers of IBC are currently unknown, and this uncertainty manifests as ineffective clinical therapeutic strategies. In IBC, there is a critical need to identify more effective treatment strategies to decrease rates of locoregional recurrence.

In an attempt to understand the heterogeneity of IBC, a recent study of 53 IBC tumors demonstrated that over 90% of tumors studied contained actionable mutations in genes such as *PIK3CA* and *BRCA1/2* that could be targeted using therapies that are either FDA-approved or currently in clinical trial(3). In line with this finding, there are a number of phase I and phase II clinical trials seeking to repurpose other FDA-approved drugs for indication in IBC(1). Targeted therapies in these trials include agents against PD-1 (pembrolizumab), VEGF-A (bevacizumab)(4,5), JAK1/2 (ruxolitinib), and the viral agent T-VEC (talimogene

laherparepvec)(1). Many different chemotherapy and radiation therapy regimens have been explored in IBC, but rates of recurrence and overall survival have not significantly improved(6). However, the ability to sensitize IBC tumors to current treatments such as radiation represents a promising treatment strategy for patients with IBC.

Inhibition of poly adenosine diphosphate-ribose polymerase 1 (PARP1) has been explored in clinical trials for many cancer types. PARP1 inhibition (PARPi) does not demonstrate significant single agent efficacy in the treatment of most breast cancers(7),(8); however, PARPi is an effective targeted therapy in subsets of patients harboring *BRCA1/2* mutations(9). In addition to the use of PARP1 inhibitors as monotherapy, our group has shown previously that PARPi can effectively radiosensitize a large range of breast cancer cell lines, including those with functional BRCA1 and BRCA2(10). PARP1, through the addition of poly-ADP ribose (PAR) moieties to sites of single strand DNA (ssDNA) damage, plays a critical role in recognition and recruitment of DNA repair machinery for a variety of different DNA repair processes. If ssDNA lesions go unrepaired, double strand DNA (dsDNA) breaks form.

For cells with intact repair pathways, non-homologous end joining (NHEJ) or homologous recombination (HR) allows the cell to repair DNA. In the case of cancers with *BRCA1/2* mutations, where BRCA-mediated homologous recombination is already deficient, the use of PARP1 inhibitors alone can promote the lethal accumulation of dsDNA breaks, leading to selective death of tumor cells – a concept referred to as synthetic lethality. In cells with wild type BRCA, other deficiencies in DNA repair pathways – and the addition of PARPi – may predispose tumor cells to higher levels of DNA damage caused by therapeutic radiation(10). To that end, the present study aimed to determine the effect and efficacy of combining PARP1 inhibition and radiation in multiple preclinical models of IBC.

Results

Single agent PARPi does not significantly affect proliferation of IBC cell lines *in vitro*

First, we sought to characterize the effect of two PARP1 inhibitors, olaparib (AZD2281) and veliparib (ABT-888) (11), on the proliferation of IBC cell lines. In SUM-190 and MDA-IBC-3 cells, single agent PARPi with olaparib or veliparb does not cause a significant decrease in proliferation at concentrations up to 10μM (**Figure 2.1A-D**). While veliparib does not appear to impact proliferation of SUM-149 cells (IC50 > 10μM, **Figure 2.1E**), olaparib does have a modest effect as a single agent in SUM-149 cells (IC50 = 2.2μM, **Figure 2.1F**). All models tested were isolated from patients with IBC; however, SUM-149 cells are unique as they harbor a BRCA1 2288delT mutation as well as allelic loss of the wild type BRCA1 gene, rendering them BRCA1 deficient(12). Thus, SUM-149 cells may be especially sensitive to additional inhibition of DNA repair pathways(12).

PARPi leads to radiosensitization of IBC cell lines *in vitro*

While single agent PARPi with either olaparib or veliparib did not inhibit cell proliferation, we sought to determine the effect of PARP1 inhibition on the radiosensitivity of IBC cell lines. Clonogenic survival assays were performed with olaparib in each of the three IBC cell lines, as olaparib is a more potent PARP1 inhibitor compared to veliparib, with both PARP1 enzymatic inhibition efficacy and PARP trapping function. All IBC cell lines displayed significant radiosensitization as a result of pretreatment with olaparib. In SUM-190 cells, a dose-dependent radiosensitization was observed, with average radiation enhancement ratios (rER) of 1.45 ± 0.03 and 1.64 ± 0.21 at concentrations of 1μM and 2μM olaparib, respectively (**Figure 2.2A, Table 2.1A**). A similar trend was observed in MDA-IBC-3 cells, with enhancement ratios of 1.12 ± 0.08

and 1.28 ± 0.06 under the same treatment conditions (**Figure 2.2C, Table 2.1B**). Because SUM-149 cells express a truncated form of the BRCA1 protein, treatment with olaparib leads to marked radiosensitization at much lower doses. At 10nM and 20nM, the average enhancement ratios for SUM-149 cells were approximately 1.42 ± 0.01 and 1.76 ± 0.11 (**Figure 2.2E, Table 2.1C**). The enhancement ratios observed here are similar to or greater than that of cisplatin (rER=1.2-1.3), a compound well-characterized for its ability to act as a radiosensitizing agent(13),(14). Furthermore, the surviving fraction of cells at 6 Gy (**Figure 2.2B, D, F**) was significantly lower across all three inflammatory cell lines with the addition of olaparib. The radiation enhancement ratios demonstrated a marked dose-dependent increase, while toxicity from each treatment was minimal (**Table 2.1**).

PARP1 inhibition and radiation leads to delayed repair of DNA double strand breaks compared to radiation alone

In cancer cells, ionizing radiation induces both single strand and double strand DNA breaks. In situations where DNA repair is inhibited and single strand breaks go unrepaired, the collapse of replication forks can propagate chromosomal damage and lead to the accumulation of lethal dsDNA breaks. Because PARP1 is involved in the recruitment of DNA repair proteins to DNA strand breaks, we sought to understand the effect of PARP1 inhibition and radiation on the accumulation of DNA damage in IBC cell lines. In SUM-190 and SUM-149 cells, radiation treatment alone (2 Gy) induces γH2AX foci in greater than 75% of cells (**Figure 2.3A-B**). In both cell lines, dsDNA breaks are retained at significantly higher levels at 12 and 16 hours after treatment with olaparib and radiation compared to treatment with radiation alone (**Figure 2.3C-D**). Furthermore, a similar difference in dsDNA breaks was observed between RT alone and combination treatment in SUM-190 cells at 4 hours after radiation. In short, the presence of

olaparib leads to the accumulation and persistence of dsDNA breaks in the combination treatment compared to the radiation treatment alone in both SUM-190 and SUM-149 cells. In order to independently confirm these findings, we performed the neutral comet assay to assess for dsDNA breaks (**Figure 2.4A**). In SUM-190 cells, the combination of PARPi and RT in SUM-190 cells lead to a significantly longer tail moment, indicating increased dsDNA breaks compared to treatment with RT alone ($p = 0.029$). The tail moment was also significantly higher compared to cells treated with vehicle or olaparib as a single agent (**Figure 2.4A)**. Representative images for each treatment condition are shown (**Figure 2.4A**).

Olaparib effectively inhibits PAR formation in IBC cell lines

In order to determine if inhibition of PARP1 enzymatic activity occurs at concentrations of olaparib that are sufficient to induce radiosensitization, we treated cells with olaparib ± 4 Gy radiation and measured the total PAR and PARP1 levels in IBC cell lines. In SUM-190 and MDA-IBC-3 cells, PAR formation is significantly inhibited with 1μM of olaparib (**Figure 2.4B-C**). Inhibition of PAR formation, however, can also be achieved at the same level in SUM-149 cells with 20nM of olaparib (**Figure 2.4D**). Therefore, inhibition of PAR formation with olaparib occurs at low concentrations (20nM) that are sufficient to confer radiosensitization in SUM-149 cells. Though olaparib effectively inhibits PARylation at these concentrations, the amount of PARP1 in the cell lines remains relatively constant in all models (**Figure 2.4B-D**).

PARP1 inhibition significantly inhibits growth of SUM-190 xenografts *in vivo*

Having demonstrated that PARP1 inhibition can effectively radiosensitize IBC cell lines *in vitro*, we next sought to validate these findings in an *in vivo* xenograft model. For *in vivo* studies, subcutaneous tumors were allowed to reach ~80 mm^3 in CB-17 SCID mice whereupon treatment

was initiated with one of the following: vehicle, 50 mg/kg olaparib alone daily, radiation alone (8 fractions of 2 Gy), or the combination (olaparib 50 mg/kg + 2 Gy RT daily for 8 fractions) (**Figure 2.5A**). To truly assess the radiosensitizing effects of PARP1 inhibition, olaparib treatment was started one day before initiation of radiation and discontinued after the last fraction of radiation.

Consistent with the *in vitro* proliferation assays, treatment with olaparib alone did not significantly delay tumor growth or doubling time of xenograft tumors. As expected, radiation alone did lead to a decrease in tumor size initially, but tumors continued to grow after the completion of fractionated radiation (**Figure 2.5B**). Mice receiving both radiation and olaparib treatment had significantly smaller tumors after completion of the study compared to those receiving radiation alone ($p < 0.0001$). There was a significant delay in the time to tumor doubling ($p < 0.0001$, **Figure 2.5C**) and tripling ($p < 0.0001$, **Figure 2.5D**) in the animals treated with combination olaparib and RT. In addition, time to tumor doubling and tripling was not reached in the combination treated group after 35 days. Weights of the mice (**Figure 2.5E**) remained relatively constant throughout the experiment, indicating there was limited toxicity observed with combination treatment. Interestingly, the effects of the combination treatment with olaparib and radiation were found to be synergistic using the fractional tumor volume (FTV) method as previously described (**Figure 2.5F**)(15).

Immunohistochemistry studies in tumors harvested from the mice at the end of the experiment demonstrated that levels of Ki67, a marker of cell proliferation, were significantly decreased in all treatment groups compared to control mice, with the most significant decrease in the combination treated animals ($p = 0.0004$, **Figure 2.5A-B**). There was also a decrease in p16 staining levels in the mice treated with radiation alone ($p = 0.0072$) and the combination treated group ($p = 0.0385$) in the long-term experiments (**Figure 2.5C-D**), suggesting a decrease in cellular

senescence in these tumors(16). The on-target effects of olaparib were confirmed in the short-term studies (48 hours of PARPi treatment alone or 24 hours of PARPi pretreatment before radiation). As expected, total levels of PARP1 were unaffected by treatment with olaparib, radiation, or the combination treatment (**Figure 2.7A-B**), while PAR levels were significantly lower in the PARPi treated animals (**Figure 2.7C-D**).

Discussion

In this study, we demonstrate that PARP1 inhibition alone is insufficient in delaying IBC cell line growth and proliferation (**Figure 2.1**). Combination treatment with PARP1 inhibition and ionizing radiation, however, results in significant radiosensitization of IBC models *in vitro* (**Figure 2.2**), and the combination treatment results in delayed tumor growth *in vivo* (**Figure 2.5**). Additionally, we demonstrate that PARP1 inhibition in combination with radiation significantly delays resolution of dsDNA breaks using *in vitro* models of IBC (**Figure 2.3, Figure 2.4**). Taken together, these results suggest that PARP1 inhibition with radiation therapy may be a promising strategy for the treatment of inflammatory breast cancer.

Although these studies suggest that PARP1 inhibition may be an effective radiosensitization strategy for the treatment of IBC, other potential targets for treatment have also been identified. Several groups have identified molecular alterations in IBC tumors and *in vitro* models that may help to describe the aggressive phenotype associated with IBC(1). Owing to the inflammatory nature of these cancers, the use of lipid lowering agents such as statins has been met with some success(17,18). Preclinical data using statins in IBC show statin treatment can lead to increased apoptosis and radiosensitivity, inhibition of proliferation and invasion, and decreased metastatic dissemination of tumors(19). In a population-based cohort study in patients with IBC, statin use was associated with improved progression-free survival in IBC patients(19). Recent studies have sought to better define this inflammatory microenvironment, and many have noted that macrophages may be important in mediating the radiosensitivity and metastatic potential of IBC tumors(20-23). Immune regulating agents have also been implicated in the aggressiveness of IBC. In addition to the role that cytokines such as INFα and TNFα may play in pathogenesis(24), many studies have reported that PD-L1 is consistently overexpressed in IBC

tumors(25,26). Upregulation of downstream signaling proteins including mTOR and JAK2/STAT3 have also been observed(26,27). The role of RhoC in IBC has also been reported, but recent evidence suggests that downstream signaling may lead to unique metabolic regulation(28) and changes in lipid raft formation(29). Transcriptional reprogramming of IBC cells is also common, including C/EBPδ-mediated upregulation of VEGF-A(30) and upregulation of the redox-sensitive transcription factor NFκB and the E3 ubiquitin ligase XIAP(31-34). These promising studies suggest that more effective treatment strategies are on the horizon.

Although we have demonstrated the radiosensitizing effects of olaparib in our models, these studies highlight the challenges of studying IBC. This study uses most of the available preclinical models of IBC but also highlights that there are a limited number of available models in which to study IBC. Thus, the need for additional model systems is critical to gaining a better understanding of the heterogeneity and pathogenesis of inflammatory breast cancers. While our studies were conducted in IBC cell lines, an important future direction of this work will involve the use of patient-derived xenograft (PDX) models of IBC. In addition, this study primarily utilized the more potent PARPi olaparib, though our previous studies also evaluated the efficacy of radiosensitization using veliparib(10). Olaparib may be more potent given its dual functionality as a PARP enzymatic inhibitor and PARP trapper, whereas veliparib only has functions as an enzymatic inhibitor of PARP1 at the doses used for these studies(35). Although more potent, toxicity in clinical trials to date does not appear worse with olaparib and clinical data suggests that olaparib is well tolerated *in vivo*(8).

The dual functionality of some PARP inhibitors (such as olaparib) to both inhibit enzymatic activity of the PARP1 protein as well as induce PARP trapping has been well

documented(35-38). Recent literature also suggests that PARPi may cause an increase in replication fork acceleration, resulting in replicative stress that ultimately leads to cell death(39). Though the study reported here does not directly address the relative contributions of enzymatic PARP1 inhibition verses PARP trapping on radiosensitization, studies are underway to determine how these functions may differentially contribute to the compounds' radiosensitizing effects. In addition to olaparib, PARP inhibitors such as talazoparib and rucaparib are used to treat other types of breast cancer(40,41). These inhibitors may also be valuable in the treatment of IBC in combination with radiation and are currently being investigated.

While we have shown that PARP1 inhibition can be used for the radiosensitization of inflammatory breast cancer, olaparib and other PARP1 inhibitors are currently being investigated as radiosensitization agents for the treatment of triple negative breast cancer (RadioPARP/ NCT03109080), head and neck cancer(42), pancreatic cancer(43), prostate cancer(44), and ovarian cancer(45). More recent trials are testing whether PARP1 inhibition is effective in combination with radiation in squamous cell carcinoma(46) (NCT02229656), locally advanced rectal cancer (NCT02921256 and NCT01589419), high grade gliomas (NCT03212742), non-small cell lung cancer (NCT01386385 and NCT02412371), and soft tissue sarcoma(47) (NCT02787642). Thus, while this study is the first to report that PARP inhibition may be an effective strategy in patients with IBC, the concept of PARP inhibitor-mediated radiosensitization is being explored in many other cancer contexts.

IBC is a subset of breast cancer with limited treatment options and the lowest 5-year survival rates of any breast cancer type(1). Despite the limitations of the model systems, these data have provided the preclinical rationale for further clinical investigation. In a phase I trial, our group previously demonstrated that PARP1 inhibition in combination with radiation may be

a safe and effective strategy for women with IBC (and in women with locoregionally recurrent breast cancer)(48). To that end, a randomized phase II trial (SWOG 1706, NCT03598257) comparing the effects of olaparib and radiation therapy to radiation therapy alone in patients with IBC is now underway. Patients in the combination arm begin treatment with olaparib one day prior to the initiation of radiation therapy, and olaparib is administered until the final day of radiation treatment. Invasive disease-free survival of women receiving treatment with olaparib and radiation will be compared to that of the group receiving radiation alone. Secondary endpoints, such as local disease control, distant relapse-free survival and overall survival will also be assessed. In addition, correlative studies from this trial will be used to see if biomarkers of treatment response and efficacy can be identified. These correlative studies will also define the genomic and transcriptomic landscape of IBC in a large patient population and will assess how circulating tumor DNA (ctDNA) levels are affected by combination and single agent treatment.

Though it is evident from our study that PARP1 inhibition with olaparib leads to radiosensitization of IBC cell lines, further studies are needed to determine the exact mechanism of olaparib-induced radiosensitization in IBC. Future transcriptomic and proteomic analysis of current model systems across multiple platforms may provide some insight as to the mechanism of this radiosensitization, and such studies are currently underway. Finally, correlative studies from SWOG 1706 will help inform future mechanistic studies and will provide a platform in which to evaluate potential predictive or prognostic biomarkers that may be able to help more effectively guide selection of IBC patients for this approach to treatment intensification.

Methods

Cell Culture

All IBC cell lines were grown in HAMS F12 media (Gibco 11765-054) in a 5% CO_2 incubator. Media for SUM-149 cells was supplemented with 5% FBS (Atlanta Biologicals), 10mM HEPES (Thermo Fisher 15630080), 1x antibiotic-antimycotic (anti-anti, Thermo Fisher 15240062), 1µg/mL hydrocortisone (Sigma H4001), and 5µg/mL insulin (Sigma I9278). SUM-190 media was supplemented with 1% FBS, 1µg/mL hydrocortisone, 5µg/mL insulin (Sigma I0516), 50nM sodium selenite (Sigma S9133), 5µg/mL apo-Transferrin (Sigma T-8158), 10nM triiodo thyronine (T3, Sigma T5516), 10mM HEPES, and 0.03% ethanolamine (Sigma 411000). MDA-IBC-3 cells were grown with 10% FBS, 1µg/mL hydrocortisone, 1x anti-anti, and 5µg/mL insulin (Sigma I0516). SUM cell lines were obtained from Stephen Ethier at the Medical University of South Carolina, and MDA-IBC-3 cells were obtained directly from Wendy Woodward at the University of Texas MD Anderson Cancer Center. All cell lines were routinely tested for mycoplasma contamination (Lonza LT07-418) and were authenticated using fragment analysis at the University of Michigan DNA sequencing core. Olaparib (MedChem Express HY-10162) and veliparib (MedChem Express HY-10129) were reconstituted in 100% DMSO for cellular assays.

Proliferation Assays

SUM-190 and SUM-149 cells were plated in 96 well plates overnight and treated the next morning with either olaparib or veliparib using a dose range of 1pM to 10µM. After 72 hours, AlamarBlue (Thermo Fisher DAL1025) was added up to 10% of the final volume and read on a microplate reader after incubation at 37ºC for 3 hours. MDA-IBC-3 cells were plated in 6-well plates and

treated with a dose range of 1nM to 10μM of either olaparib or veliparib. After 72 hours, cells were trypsinized and counted with a hemocytometer.

Clonogenic Survival Assays

SUM-149 and SUM-190 cells were plated at various densities from single cell suspension in 6-well plates and radiated the following day after a one-hour pretreatment with olaparib. Cells were grown for up to three weeks, then fixed with methanol/acetic acid and stained with 1% crystal violet. Colonies with a minimum of 50 cells were counted for each treatment condition. Plating efficiency was determined and used to calculate toxicity. Cell survival curves were calculated as described previously(10). MDA-IBC-3 cells were grown in soft agar (Thermo Fisher 214050) with a base layer of 0.5% agar solution and a top layer of 0.4% agar containing the cell suspension. Drug treatments in supernatant media were added fresh each week. Colonies were grown for up to four weeks before staining with 0.005% crystal violet.

Immunofluorescence

Cells were plated on 18 mm coverslips in 12-well plates and allowed to adhere to coverslips overnight. The following day, cells were treated with media containing either olaparib or vehicle one hour before radiation (2 Gy), and coverslips were fixed at predetermined time points after radiation. γH2AX foci were detected using anti-phospho-histone H2AX (ser139) monoclonal antibody (Millipore 05-636), with a goat anti-mouse fluorescent secondary antibody (Invitrogen A11005). At least 100 cells were scored visually for γH2AX foci in three independent experiments. Cells containing ≥ 15 γH2AX foci were scored positive and were pooled for statistical analysis.

Immunoblotting

Cells were plated overnight and pre-treated the next morning with olaparib. Plates were irradiated one hour after pretreatment, and cells were harvested at 6 and 24 hours after radiation. Lysates were extracted using RIPA buffer (Thermo Fisher 89901) containing protease and phosphatase inhibitors (Sigma-Aldrich PHOSS-RO, CO-RO). Proteins were detected using the anti-PAR antibody (LS-B12794, 1:5000), the anti-PARP1 antibody (ab6079, 1:1000), and anti-β-Actin (8H10D10, Cell Signaling 12262S, 1:50,000).

Xenograft Models

Bilateral subcutaneous flank injections were performed on 4-6 week old CB17-SCID female mice with 1 x 10^6 SUM-190 cells resuspended in 100μL PBS with 50% Matrigel (Thermo Fisher CB-40234). Tumors were allowed to grow until reaching approximately 80mm^3. Olaparib treatment was given by intraperitoneal injection 24 hours prior to the first radiation treatment. For long term studies, mice were treated with vehicle (10% 2-hydroxylpropyl-beta-cyclodextrin in phosphate buffered saline, Thermo Fisher 10010-023), olaparib (50mg/kg) alone, radiation alone (2 Gy x 8 fractions) or the combination of olaparib + RT, with 16-20 tumors per treatment group. Tumor growth was measured three times a week using digital calipers, and mice were weighed on the same days. Tumor volume was calculated using the equation $V=(L*W^2)*\pi/6$. For short term studies, mice were treated with vehicle control, olaparib, or radiation for 48 hours before the tumors were harvested. Mice treated with both olaparib and radiation received olaparib treatment 24 hours before radiation treatment. The tumors were then harvested 48 hours after radiation. Immunohistochemical staining was performed on tumors for all four conditions. All procedures involving mice were approved by the Institutional Animal Care & Use Committee (IACUC) at the University of Michigan and conform to their relevant regulatory standards.

Irradiation

Irradiation was carried out using a Philips RT250 (Kimtron Medical) at a dose rate of approximately 2 Gy/min in the University of Michigan Experimental Irradiation Core as previously described(10). Irradiation of mouse tumors was carried out as described previously(49).

Immunohistochemistry

Immunohistochemical staining was performed on the DAKO Autostainer (Agilent, Carpinteria, CA) using Envision+ or liquid streptavidin-biotin and diaminobenzadine (DAB) as the chromogen. De-paraffinized sections were labeled with the antibodies listed in Supplemental Table 1 for 30 minutes at ambient temperature. Microwave epitope retrieval, as specified in Supplemental Table 1, was used prior to staining for all antibodies. Appropriate negative (no primary antibody) and positive controls (as listed in Supplemental Table 1) were stained in parallel with each set of slides studied. Whole-slide digital images were generated using an Aperio AT2 scanner (Leica Biosystems Imaging, Vista, CA, USA) at 20X magnification, with a resolution of 0.5 μm per pixel. The scanner uses a 20x / 0.75 NA objective and an LED light source. The same instrument and settings were used throughout the study for all whole-slide images generated. The images were checked for quality before use, and scans were repeated as necessary. Digital slides were analyzed using the Visopharm image analysis software suite (DK-2970 Hoersholm, Denmark, v2019.2) to count stained and unstained nuclei.

Comet Assay

Cells were plated in 6 well plates and allowed to adhere overnight. Cells were pretreated with olaparib for one hour before radiation and collected at designated time points after radiation. Cells were mixed with low melting point agarose (Thermo Fisher 15-455-200) and spread on

CometSlides (Trevigen 4250-050-03). The cells were lysed with lysis solution (Trevigen 4250-050-01), and DNA was separated by electrophoresis. Propidium iodide (Thermo Fisher P3566) was used to stain DNA. A fluorescent microscope was used to take images of at least 50 cells/treatment. Images were analyzed using Comet Assay IV Software Version 4.3 to calculate the Olive tail moment. Results were pooled for statistical analyses.

Statistical Analyses

GraphPad Prism 7.0 was used to perform statistical tests. *In vitro* statistical analyses were performed using the two-tailed student's t-test or a one-way ANOVA in the case of multiple comparisons. For *in vivo* studies, a two way ANOVA was used to compare tumor growth, and the fractional tumor volume (FTV) method for assessing synergy *in vivo* was used as previously described(15,50).

Acknowledgements

The authors would like to thank the Breast Cancer Research Foundation (through a grant to L. Pierce), The Komen for the Cure Foundation (through a grant to R. Jagsi), and the University of Michigan Rogel Cancer Center (through a grant to C. Speers). A. Michmerhuizen, A. Pesch, and B. Chandler are supported by the following training grants: T32-GM007315, T32-GM007767, T32-CA140044. The authors would also like to thank Wendy Woodward at MD Anderson Cancer Center for providing MDA-IBC-3 cells, and Stephen Ethier at the Medical University of South Carolina for providing SUM-149 and SUM-190 cells. This work was completed and published with the following co-authors: Anna Michmerhuizen, Leah Moubadder, Benjamin Chandler, Kari Wilder-Romans, Meleah Cameron, Eric Olsen, Dafydd Thomas, Amanda Zhang, Nicole Hirsh, Cassandra Ritter, Meilan Liu, Shyam Nyati, Lori J. Pierce, Reshma Jagsi, and Corey Speers.

Figures

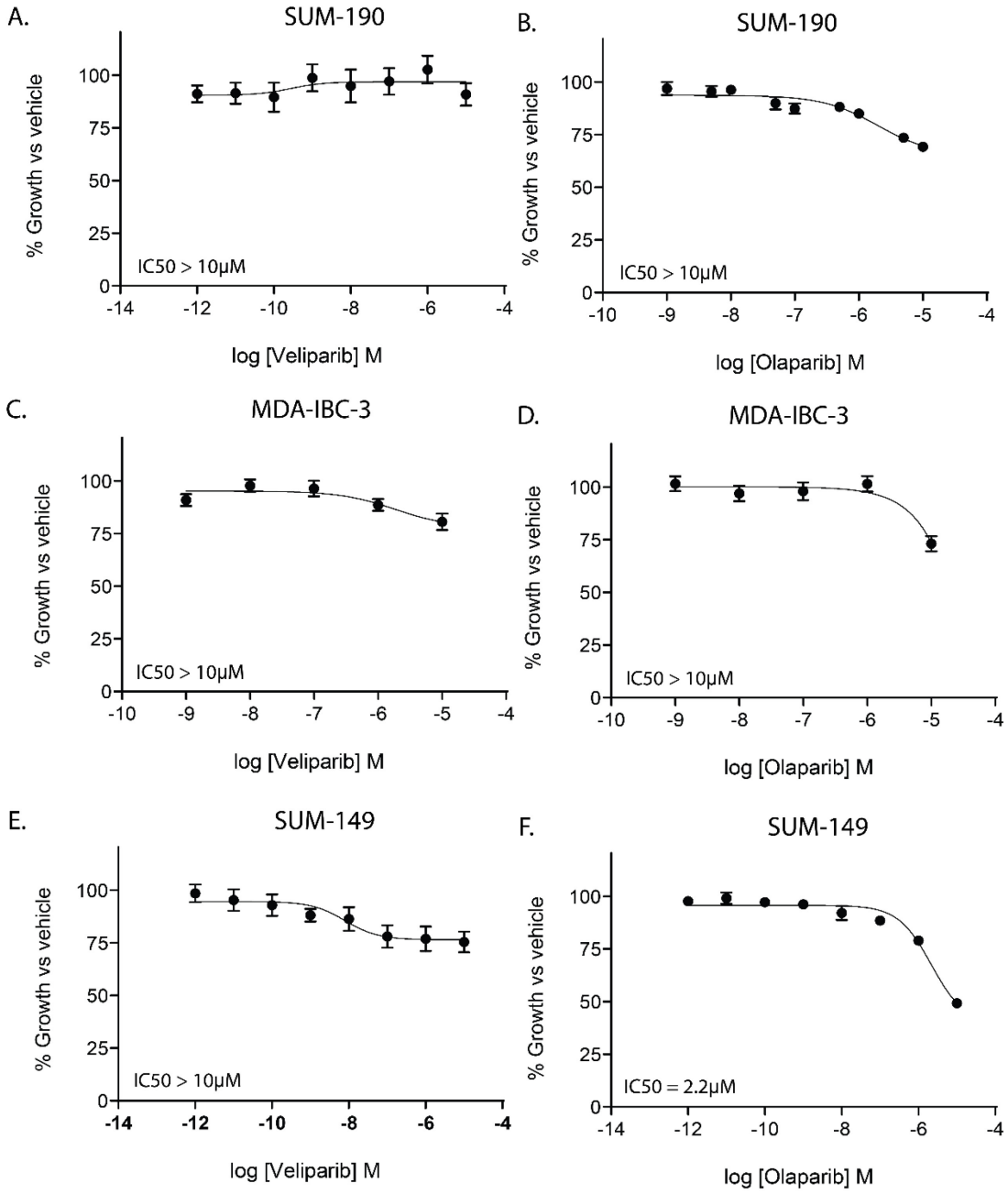

IBC cell lines were treated with either olaparib or veliparib and cell viability was measured 72 hours after treatment. In SUM-190 (**A,B**) and MDA-IBC-3 (**C,D**) cells, neither veliparib or olaparib showed significant effects on proliferation at doses up to 10μM. In SUM-149 cells (**E,F**), olaparib, but not veliparib, can inhibit proliferation at high doses (2.2μM). Graphs are shown as the average of three independent experiments ± SEM.

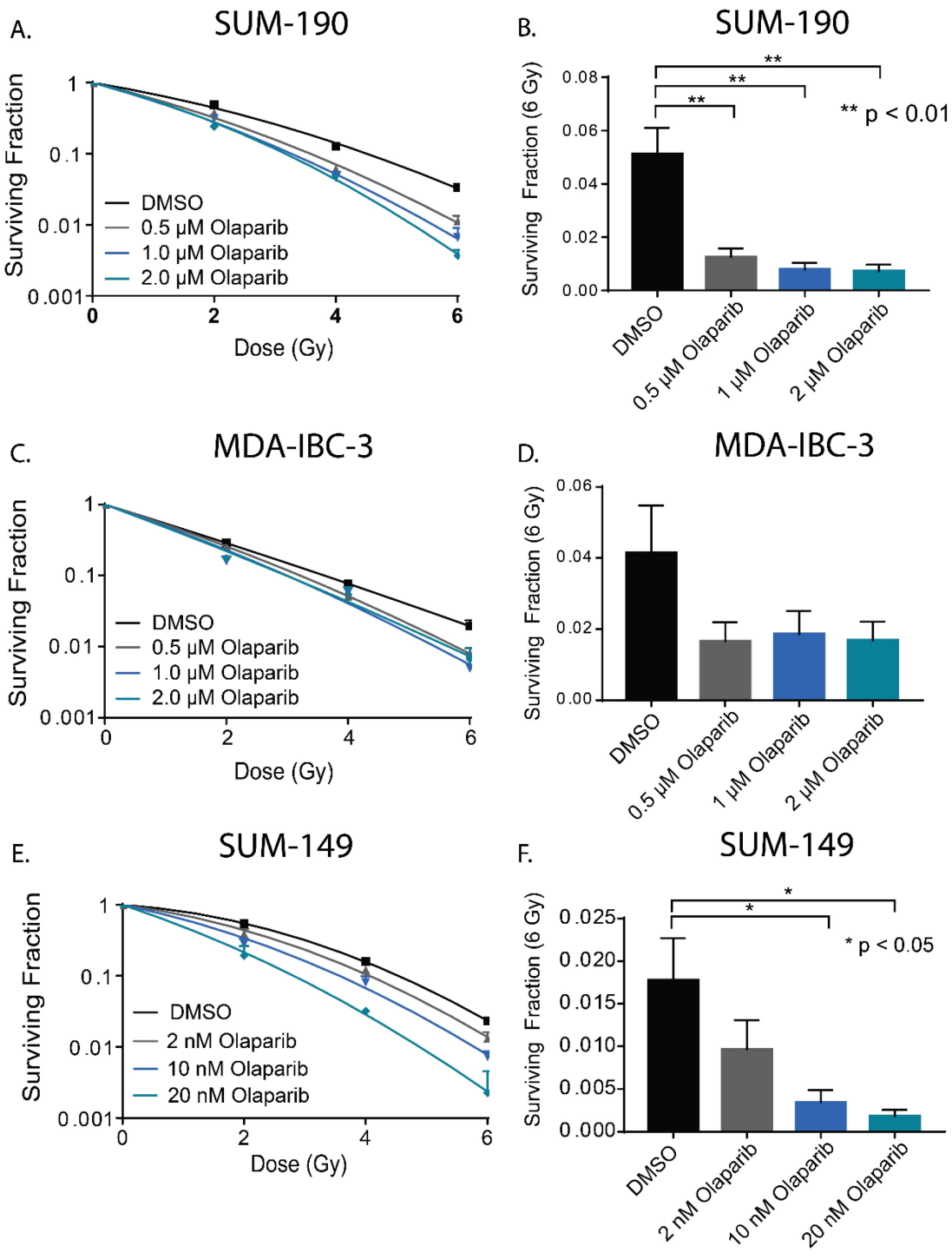

Olaparib treatment results in a dose-dependent reduction in survival fraction of SUM-190 (**A**), MDA-IBC-3 (**C**), and SUM-149 (**E**) cell lines. Representative data from single experiments are shown for each cell line. The surviving fraction of cells after 6 Gy (**B, D, F**) was calculated as the mean of three independent experiments and depicted ± SEM for each cell line. ($p < 0.05$ = *, $p < 0.01$ = **)

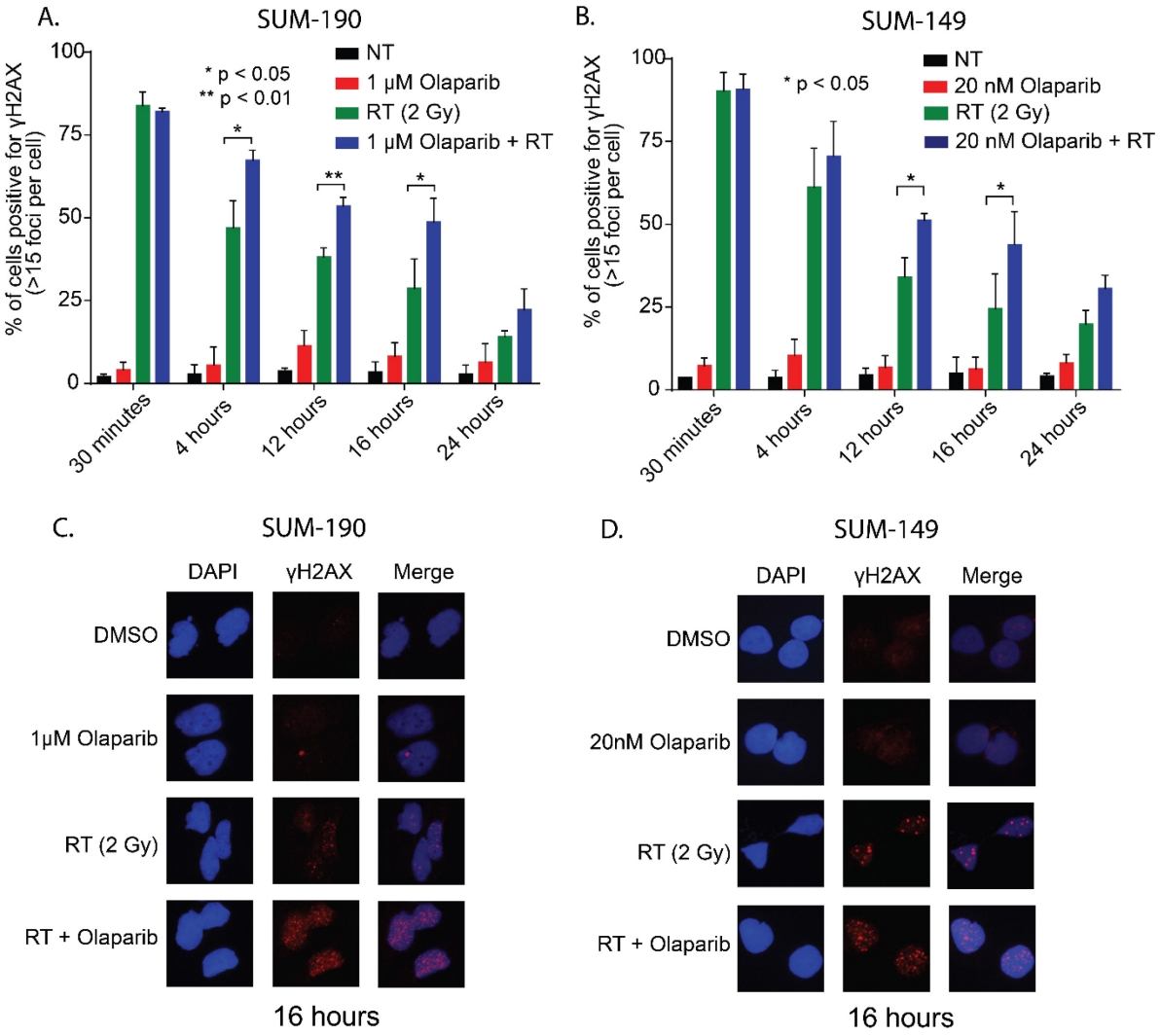

Immunofluorescence microscopy was used to measure γH2AX foci in SUM-190 (**A**) and SUM-149 (**B**) cells. Cells were pretreated for one hour with olaparib and fixed at 0.5, 4, 12, 16, and 24 hours after radiation, then stained for DAPI and γH2AX. Cells containing ≥ 15 foci were scored as positive. In SUM-190 cells at 4, 12, and 16 hours, there were significantly higher levels of cells positive for γH2AX for those treated with the combination of 2 Gy radiation and 1μM olaparib compared to cells treated with 2 Gy radiation alone. In SUM-149 cells, 20nM olaparib and 2 Gy radiation results in a higher percentage of γH2AX positive cells compared to cells treated with radiation alone at both 12 and 16 hours. Representative images of γH2AX foci in SUM-190 (**C**) and SUM-149 (**D**) cells at 16 hours are shown for all treatment groups. Graphs represent the average of three independent experiments ± SD. ($p < 0.05$ = *).

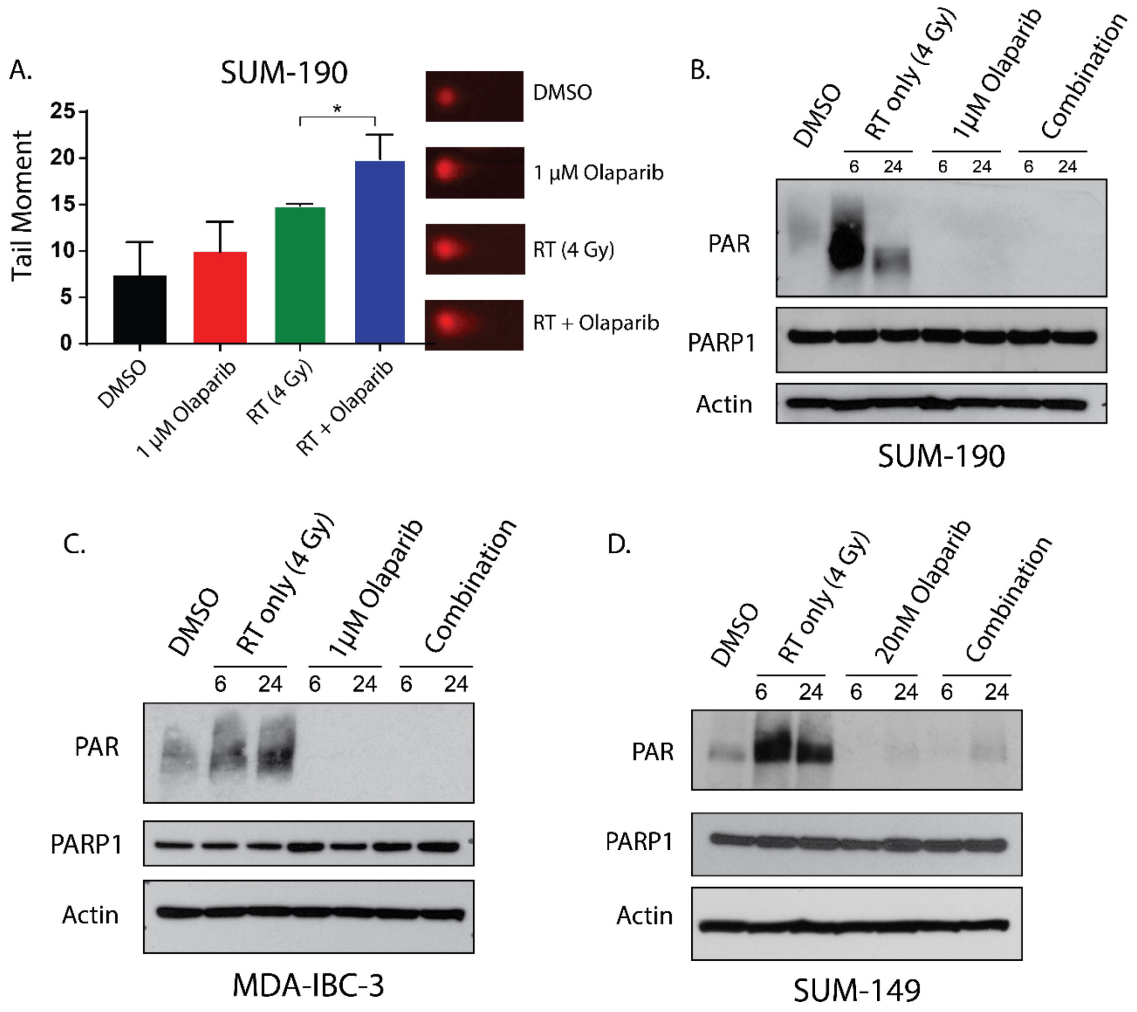

Neutral comet assay in SUM-190 cells (**A**) shows higher levels of dsDNA damage at 4 hours in cells treated with radiation and olaparib compared to untreated cells, or cells treated with RT or olaparib alone ($p < 0.05$ = *). Graphs represent the average of three independent experiments ± SD and representative images for each treatment are shown. In SUM-190 (**B**) and MDA-IBC-3 (**C**) cells, radiation induced DNA damage causes an increase in PAR formation at both 6 and 24 hours after 4 Gy radiation. In the combination group that receives a one-hour pretreatment of 1µM olaparib before radiation, PAR formation is significantly lower at 6 and 24 hours after RT. In SUM-149 (**D**) cells, this same trend can be observed at a much lower dose of olaparib (20nM). Though the enzymatic activity of PARP1 is efficiently inhibited at these doses, total levels of PARP are not significantly different across the treatment conditions.

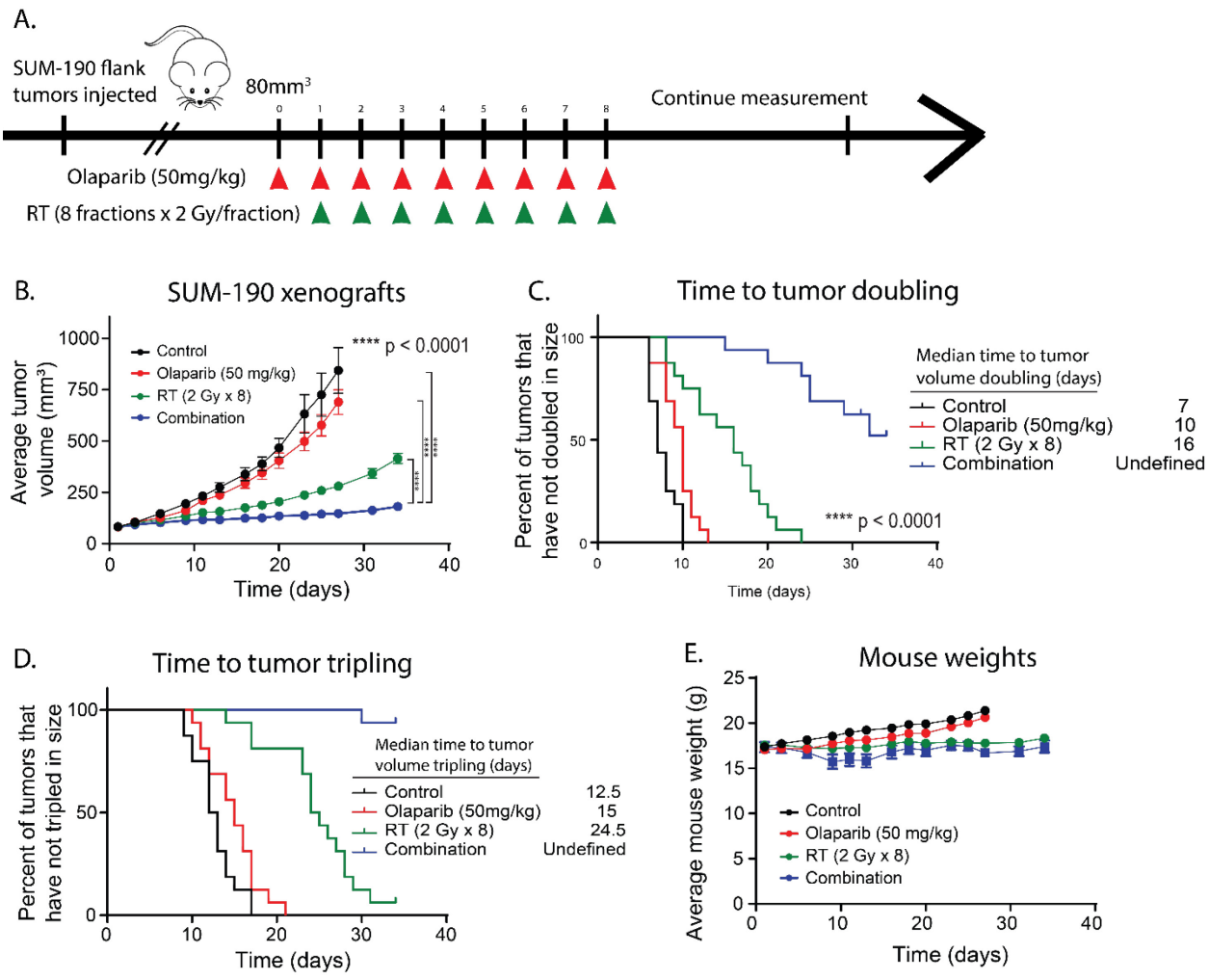

F.

SUM-190 Xenografts: Fractional Tumor Volume (FTV)					
			Combination		
Day	RT	Olaparib	Expected	Observed	Ratio
9	0.798	0.862	0.688	0.701	**0.981**
16	0.690	0.818	0.564	0.573	**0.985**
23	0.367	0.765	0.281	0.209	**1.344**
25	0.344	0.759	0.261	0.186	**1.403**
27	0.325	0.790	0.257	0.166	**1.549**

SUM-190 cells were subcutaneously injected into CB17-SCID mice, and treatment was started when tumors reached approximately 80 mm^3 (**A**). Olaparib treatment began one day before the initiation of radiation treatment and ended on the same day as the last fraction of radiation. With this paradigm, the combination treatment leads to delayed growth of tumors (**B**) and an increased time to tumor doubling (**C**) and tumor tripling (**D**) ($p < 0.0001$ = ****). The treatment did not display significant toxicities, and animal weights were not significantly different between the treatment groups (**E**). Using the FTV method, there was a synergistic effect with olaparib and RT treatment to antagonize tumor growth (ratios >1 indicate synergism) (**F**). A two-way ANOVA was performed to compare tumor volume between experimental groups.

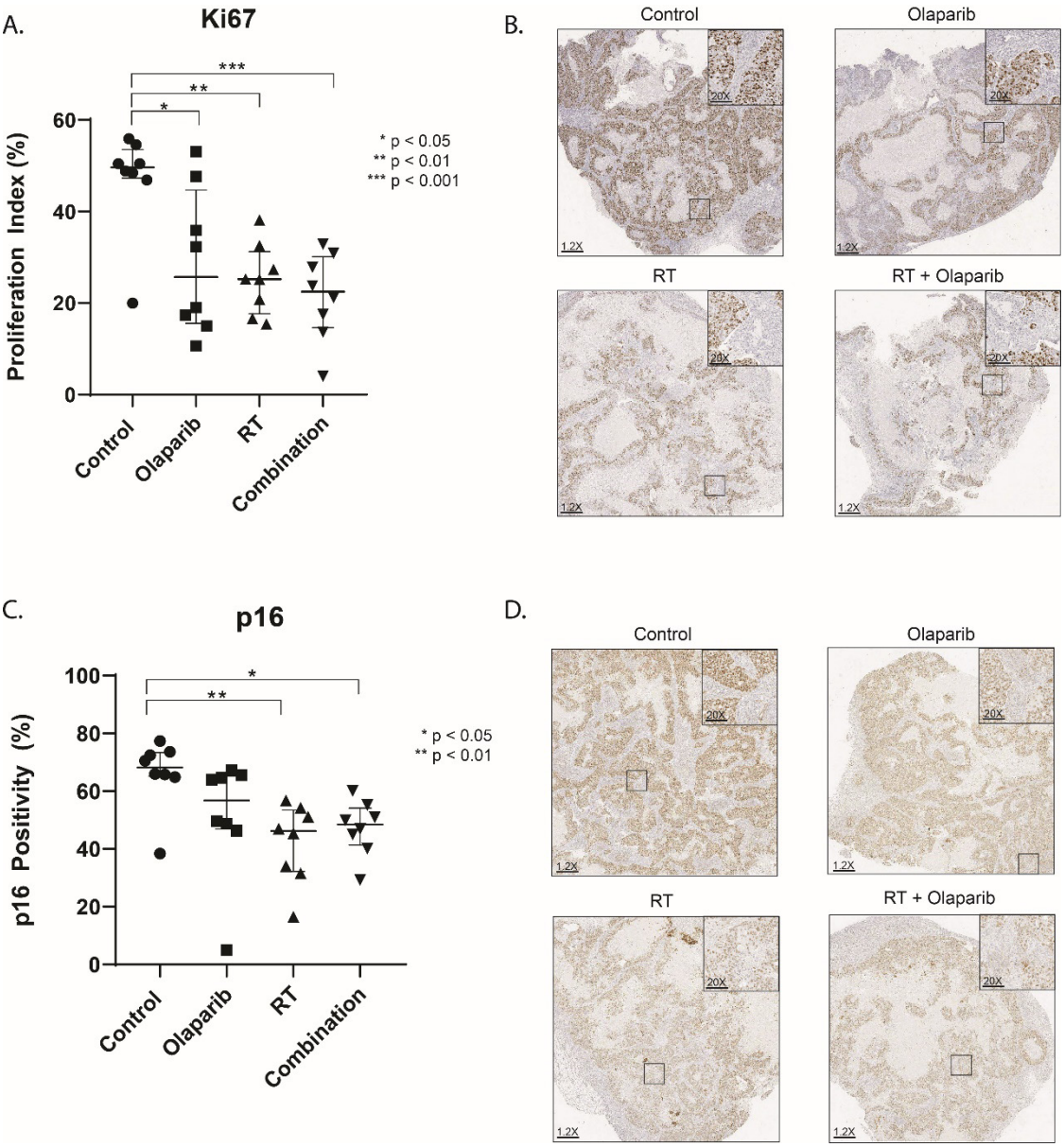

Figure 2.6: Ki67 and p16 levels are decreased in tumors from animals treated with radiation and combination PARP-inhibitor and radiation.

SUM-190 xenograft tumors that were harvested from mice at the completion of the long-term *in vivo* study. Protein expression levels were assessed by immunohistochemical staining. Levels of Ki67, a marker of proliferation, are significantly decreased in all treatment groups (**A**), and p16 levels are significantly decreased in the RT-alone and combination treated groups (**B**). Representative images from each group are shown (**C,D**). (* $p < 0.05$, ** $p < 0.01$, *** $p < 0.001$).

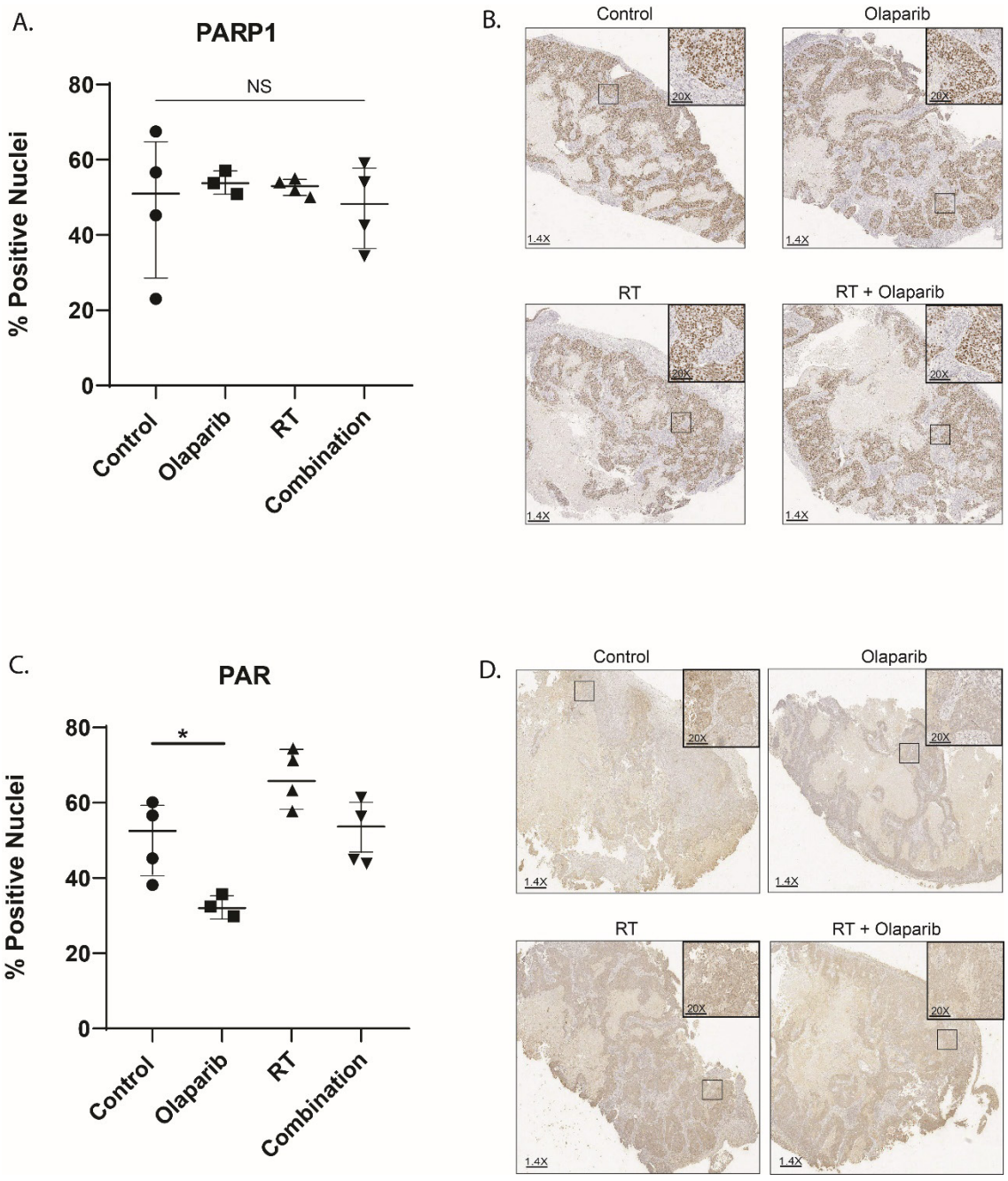

Figure 2.7: Total PARP1 levels do not change with treatment but PAR levels are decreased by PARPi.

Total levels of PARP1 were assessed in tumors from mice treated with olaparib. Olaparib treatment did not affect PARP1 protein expression by IHC in olaparib-alone, RT alone, or combination treated animals (**A**). Representative images of PARP1 staining are shown for all treatment conditions (**B**). PAR levels were, however, significantly decreased in the animals treated with olaparib alone (**C**). Representative images of PAR staining are shown for all treatment conditions (**D**). (NS: not significant, * $p < 0.05$)

A.

SUM-190 Clonogenic Survival Assay		
Treatment	Enhancement Ratio	Cytotoxicity
DMSO	1.0	1.0
0.5 μM	1.25 ± 0.06	0.77 ± 0.02
1 μM	1.45 ± 0.03	0.62 ± 0.13
2 μM	1.64 ± 0.21	0.63 ± 0.10

B.

MDA-IBC-3 Clonogenic Survival Assay		
Treatment	Enhancement Ratio	Cytotoxicity
DMSO	1.0	1.0
0.5 μM	1.20 ± 0.39	0.61 ± 0.39
1 μM	1.12 ± 0.08	0.46 ± 0.27
2 μM	1.28 ± 0.06	0.43 ± 0.31

C.

SUM-149 Clonogenic Survival Assay		
Treatment	Enhancement Ratio	Cytotoxicity
DMSO	1.0	1.0
2 nM	1.22 ± 0.05	0.82 ± 0.23
10 nM	1.42 ± 0.01	0.49 ± 0.24
20 nM	1.76 ± 0.11	0.39 ± 0.23

Average radiation enhancement ratio (rER) and toxicity values are shown for each treatment in SUM-190 (**A**), MDA-IBC-3 (**B**), and SUM-149 (**C**) cells.

Ab	Company	Cat #	Source	Clone	Dilution	Epitope retrieval	Detection	Control Tissue
Ki67	AbCam	Ab16667	Rabbit MonoAb	SP-6	1:250	pH6 HIER	Env+	Tonsil
p16 (INK4a)	AbCam	Ab108349	Rabbit MonoAb	EPR1473	1:2000	pH6 HIER	Env+	Kidney
PARP1	AbCam	Ab191217	Rabbit MonoAb	EPR18461	1:1000	pH6 HIER	Env+	HeLa cell pellet
PAR	AbCam	Ab14460	Chicken		1:500	pH6 HIER	LSAB+	Pancreas

HIER: Heat induced epitope retrieval
LSAB+: Liquid streptavidin Biotin
Env+: Envision+ Polymer HRP Second antibody

Antibodies used in all of the immunohistochemistry experiments are listed with each of the corresponding dilutions, retrieval techniques, and positive controls.

References

1. Menta A, Fouad TM, Lucci A, Le-Petross H, Stauder MC, Woodward WA*, et al.* Inflammatory Breast Cancer: What to Know About This Unique, Aggressive Breast Cancer. Surg Clin North Am 2018;98(4):787-800 doi 10.1016/j.suc.2018.03.009.
2. Li J, Xia Y, Wu Q, Zhu S, Chen C, Yang W*, et al.* Outcomes of patients with inflammatory breast cancer by hormone receptor-and HER2-defined molecular subtypes: A population-based study from the SEER program. Oncotarget 2017;8(30):49370.
3. Ross JS, Ali SM, Wang K, Khaira D, Palma NA, Chmielecki J*, et al.* Comprehensive genomic profiling of inflammatory breast cancer cases reveals a high frequency of clinically relevant genomic alterations. Breast Cancer Res Treat 2015;154(1):155-62 doi 10.1007/s10549-015-3592-z.
4. Wedam SB, Low JA, Yang SX, Chow CK, Choyke P, Danforth D*, et al.* Antiangiogenic and antitumor effects of bevacizumab in patients with inflammatory and locally advanced breast cancer. J Clin Oncol 2006;24(5):769-77 doi 10.1200/jco.2005.03.4645.
5. Yang SX, Steinberg SM, Nguyen D, Wu TD, Modrusan Z, Swain SM. Gene expression profile and angiogenic marker correlates with response to neoadjuvant bevacizumab followed by bevacizumab plus chemotherapy in breast cancer. Clin Cancer Res 2008;14(18):5893-9 doi 10.1158/1078-0432.ccr-07-4762.
6. Bourgier C, Pessoa EL, Dunant A, Heymann S, Spielmann M, Uzan C*, et al.* Exclusive alternating chemotherapy and radiotherapy in nonmetastatic inflammatory breast cancer: 20 years of follow-up. Int J Radiat Oncol Biol Phys 2012;82(2):690-5 doi 10.1016/j.ijrobp.2010.11.040.
7. Gelmon KA, Tischkowitz M, Mackay H, Swenerton K, Robidoux A, Tonkin K*, et al.* Olaparib in patients with recurrent high-grade serous or poorly differentiated ovarian carcinoma or triple-negative breast cancer: a phase 2, multicentre, open-label, non-randomised study. Lancet Oncol 2011;12(9):852-61 doi 10.1016/s1470-2045(11)70214-5.
8. Dent RA, Lindeman GJ, Clemons M, Wildiers H, Chan A, McCarthy NJ*, et al.* Phase I trial of the oral PARP inhibitor olaparib in combination with paclitaxel for first- or second-line treatment of patients with metastatic triple-negative breast cancer. Breast Cancer Res. Volume 152013. p R88.
9. Comen EA, Robson M. Poly(ADP-Ribose) Polymerase Inhibitors in Triple-Negative Breast Cancer. Cancer J 2010;16(1):48-52 doi 10.1097/PPO.0b013e3181cf01eb.
10. Feng FY, Speers C, Liu M, Jackson WC, Moon D, Rinkinen J*, et al.* Targeted radiosensitization with PARP1 inhibition: optimization of therapy and identification of biomarkers of response in breast cancer. Breast Cancer Res Treat 2014;147(1):81-94 doi 10.1007/s10549-014-3085-5.
11. Donawho CK, Luo Y, Penning TD, Bauch JL, Bouska JJ, Bontcheva-Diaz VD*, et al.* ABT-888, an orally active poly(ADP-ribose) polymerase inhibitor that potentiates DNA-damaging agents in preclinical tumor models. Clin Cancer Res 2007;13(9):2728-37 doi 10.1158/1078-0432.ccr-06-3039.
12. Elstrodt F, Hollestelle A, Nagel JH, Gorin M, Wasielewski M, van den Ouweland A*, et al.* BRCA1 mutation analysis of 41 human breast cancer cell lines reveals three new deleterious mutants. Cancer Res 2006;66(1):41-5 doi 10.1158/0008-5472.can-05-2853.

13. Skov K, Macphail S. Interaction of platinum drugs with clinically relevant x-ray doses in mammalian cells: a comparison of cisplatin, carboplatin, iproplatin, and tetraplatin. International Journal of Radiation Oncology* Biology* Physics 1991;20(2):221-5.
14. Zhang X, Yang H, Gu K, Chen J, Rui M, Jiang G-L. In vitro and in vivo study of a nanoliposomal cisplatin as a radiosensitizer. International journal of nanomedicine 2011;6:437.
15. Matar P, Rojo F, Cassia R, Moreno-Bueno G, Di Cosimo S, Tabernero J*, et al.* Combined epidermal growth factor receptor targeting with the tyrosine kinase inhibitor gefitinib (ZD1839) and the monoclonal antibody cetuximab (IMC-C225): superiority over single-agent receptor targeting. Clinical cancer research : an official journal of the American Association for Cancer Research 2004;10(19):6487-501 doi 10.1158/1078-0432.ccr-04-0870.
16. Althubiti M, Lezina L, Carrera S, Jukes-Jones R, Giblett SM, Antonov A*, et al.* Characterization of novel markers of senescence and their prognostic potential in cancer. Cell Death Dis 2014;5:e1528 doi 10.1038/cddis.2014.489.
17. Wolfe AR, Debeb BG, Lacerda L, Larson R, Bambhroliya A, Huang X*, et al.* Simvastatin prevents triple-negative breast cancer metastasis in pre-clinical models through regulation of FOXO3a. Breast Cancer Res Treat 2015;154(3):495-508 doi 10.1007/s10549-015-3645-3.
18. Van Wyhe RD, Rahal OM, Woodward WA. Effect of statins on breast cancer recurrence and mortality: a review. Breast Cancer (Dove Med Press) 2017;9:559-65 doi 10.2147/bctt.s148080.
19. Brewer TM, Masuda H, Liu DD, Shen Y, Liu P, Iwamoto T*, et al.* Statin use in primary inflammatory breast cancer: a cohort study. British journal of cancer 2013;109(2):318-24 doi 10.1038/bjc.2013.342.
20. Reddy JP, Atkinson RL, Larson R, Burks JK, Smith D, Debeb BG*, et al.* Mammary stem cell and macrophage markers are enriched in normal tissue adjacent to inflammatory breast cancer. Breast Cancer Res Treat 2018;171(2):283-93 doi 10.1007/s10549-018-4835-6.
21. Allen SG, Chen Y-C, Madden JM, Fournier CL, Altemus MA, Hiziroglu AB*, et al.* Macrophages enhance migration in inflammatory breast cancer cells via RhoC GTPase signaling. Scientific reports 2016;6:39190.
22. Rahal OM, Wolfe AR, Mandal PK, Larson R, Tin S, Jimenez C*, et al.* Blocking Interleukin (IL)4- and IL13-Mediated Phosphorylation of STAT6 (Tyr641) Decreases M2 Polarization of Macrophages and Protects Against Macrophage-Mediated Radioresistance of Inflammatory Breast Cancer. Int J Radiat Oncol Biol Phys 2018;100(4):1034-43 doi 10.1016/j.ijrobp.2017.11.043.
23. Wolfe AR, Trenton NJ, Debeb BG, Larson R, Ruffell B, Chu K*, et al.* Mesenchymal stem cells and macrophages interact through IL-6 to promote inflammatory breast cancer in pre-clinical models. Oncotarget 2016;7(50):82482-92 doi 10.18632/oncotarget.12694.
24. Bertucci F, Finetti P, Vermeulen P, Van Dam P, Dirix L, Birnbaum D*, et al.* Genomic profiling of inflammatory breast cancer: a review. Breast 2014;23(5):538-45 doi 10.1016/j.breast.2014.06.008.
25. Bertucci F, Finetti P, Colpaert C, Mamessier E, Parizel M, Dirix L*, et al.* PDL1 expression in inflammatory breast cancer is frequent and predicts for the pathological response to chemotherapy. Oncotarget 2015;6(15):13506-19 doi 10.18632/oncotarget.3642.

26. Hamm CA, Moran D, Rao K, Trusk PB, Pry K, Sausen M*, et al.* Genomic and Immunological Tumor Profiling Identifies Targetable Pathways and Extensive CD8+/PDL1+ Immune Infiltration in Inflammatory Breast Cancer Tumors. Mol Cancer Ther 2016;15(7):1746-56 doi 10.1158/1535-7163.mct-15-0353.
27. Jhaveri K, Teplinsky E, Silvera D, Valeta-Magara A, Arju R, Giashuddin S*, et al.* Hyperactivated mTOR and JAK2/STAT3 pathways: molecular drivers and potential therapeutic targets of inflammatory and invasive ductal breast cancers after neoadjuvant chemotherapy. Clinical breast cancer 2016;16(2):113-22. e1.
28. Wynn ML, Yates JA, Evans CR, Van Wassenhove LD, Wu ZF, Bridges S*, et al.* RhoC GTPase is a potent regulator of glutamine metabolism and N-acetylaspartate production in inflammatory breast cancer cells. Journal of Biological Chemistry 2016;291(26):13715-29.
29. Joglekar M, Elbezanti WO, Weitzman MD, Lehman HL, van Golen KL. Caveolin-1 mediates inflammatory breast cancer cell invasion via the Akt1 pathway and RhoC GTPase. J Cell Biochem 2015;116(6):923-33 doi 10.1002/jcb.25025.
30. Balamurugan K, Sterneck E. The Many Faces of C/EBPδ and their Relevance for Inflammation and Cancer. Int J Biol Sci. Volume 92013. p 917-33.
31. Allensworth JL, Evans MK, Bertucci F, Aldrich AJ, Festa RA, Finetti P*, et al.* Disulfiram (DSF) acts as a copper ionophore to induce copper-dependent oxidative stress and mediate anti-tumor efficacy in inflammatory breast cancer. Mol Oncol. Volume 92015. p 1155-68.
32. Arora J, Sauer SJ, Tarpley M, Vermeulen P, Rypens C, Van Laere S*, et al.* Inflammatory breast cancer tumor emboli express high levels of anti-apoptotic proteins: use of a quantitative high content and high-throughput 3D IBC spheroid assay to identify targeting strategies. Oncotarget. Volume 82017. p 25848-63.
33. Lerebours F, Vacher S, Andrieu C, Espie M, Marty M, Lidereau R*, et al.* NF-kappa B genes have a major role in Inflammatory Breast Cancer. BMC Cancer. Volume 82008. p 41.
34. Van Laere SJ, Van der Auwera I, Van den Eynden GG, van Dam P, Van Marck EA, Vermeulen PB*, et al.* NF-κB activation in inflammatory breast cancer is associated with oestrogen receptor downregulation, secondary to EGFR and/or ErbB2 overexpression and MAPK hyperactivation. Br J Cancer. Volume 972007. p 659-69.
35. Murai J, Huang Sy N, Das BB, Renaud A, Zhang Y, Doroshow JH*, et al.* Differential trapping of PARP1 and PARP2 by clinical PARP inhibitors. Cancer Res 2012;72(21):5588-99 doi 10.1158/0008-5472.can-12-2753.
36. Menear KA, Adcock C, Boulter R, Cockcroft XL, Copsey L, Cranston A*, et al.* 4-[3-(4-cyclopropanecarbonylpiperazine-1-carbonyl)-4-fluorobenzyl]-2H-phthalazin- 1-one: a novel bioavailable inhibitor of poly(ADP-ribose) polymerase-1. J Med Chem 2008;51(20):6581-91 doi 10.1021/jm8001263.
37. Parsels LA, Karnak D, Parsels JD, Zhang Q, Velez-Padilla J, Reichert ZR*, et al.* PARP1 Trapping and DNA Replication Stress Enhance Radiosensitization with Combined WEE1 and PARP Inhibitors. Mol Cancer Res 2018;16(2):222-32.
38. Murai J, Zhang Y, Morris J, Ji J, Takeda S, Doroshow JH*, et al.* Rationale for Poly(ADP-ribose) Polymerase (PARP) Inhibitors in Combination Therapy with Camptothecins or Temozolomide Based on PARP Trapping versus Catalytic Inhibition. J Pharmacol Exp Ther. Volume 3492014. p 408-16.

39. Maya-Mendoza A, Moudry P, Merchut-Maya JM, Lee M, Strauss R, Bartek J. High speed of fork progression induces DNA replication stress and genomic instability. Nature 2018;559(7713):279-84 doi 10.1038/s41586-018-0261-5.
40. Drew Y, Ledermann J, Hall G, Rea D, Glasspool R, Highley M*, et al.* Phase 2 multicentre trial investigating intermittent and continuous dosing schedules of the poly(ADP-ribose) polymerase inhibitor rucaparib in germline BRCA mutation carriers with advanced ovarian and breast cancer. Br J Cancer 2016;114(7):723-30 doi 10.1038/bjc.2016.41.
41. Litton JK, Rugo HS, Ettl J, Hurvitz SA, Goncalves A, Lee KH*, et al.* Talazoparib in Patients with Advanced Breast Cancer and a Germline BRCA Mutation. N Engl J Med 2018;379(8):753-63 doi 10.1056/NEJMoa1802905.
42. Karam SD, Reddy K, Blatchford PJ, Waxweiler T, DeLouize AM, Oweida A*, et al.* Final Report of a Phase I Trial of Olaparib with Cetuximab and Radiation for Heavy Smoker Patients with Locally Advanced Head and Neck Cancer. Clin Cancer Res 2018;24(20):4949-59 doi 10.1158/1078-0432.ccr-18-0467.
43. Vance S, Liu E, Zhao L, Parsels JD, Parsels LA, Brown JL*, et al.* Selective radiosensitization of p53 mutant pancreatic cancer cells by combined inhibition of Chk1 and PARP1. Cell Cycle 2011;10(24):4321-9 doi 10.4161/cc.10.24.18661.
44. Han S, Brenner JC, Sabolch A, Jackson W, Speers C, Wilder-Romans K*, et al.* Targeted radiosensitization of ETS fusion-positive prostate cancer through PARP1 inhibition. Neoplasia 2013;15(10):1207-17 doi 10.1593/neo.131604.
45. Bi Y, Verginadis, II, Dey S, Lin L, Guo L, Zheng Y*, et al.* Radiosensitization by the PARP inhibitor olaparib in BRCA1-proficient and deficient high-grade serous ovarian carcinomas. Gynecol Oncol 2018;150(3):534-44 doi 10.1016/j.ygyno.2018.07.002.
46. Wurster S, Hennes F, Parplys AC, Seelbach JI, Mansour WY, Zielinski A*, et al.* PARP1 inhibition radiosensitizes HNSCC cells deficient in homologous recombination by disabling the DNA replication fork elongation response. Oncotarget 2016;7(9):9732-41.
47. Mangoni M, Sottili M, Salvatore G, Meattini I, Desideri I, Greto D*, et al.* Enhancement of Soft Tissue Sarcoma Cell Radiosensitivity by Poly(ADP-ribose) Polymerase-1 Inhibitors. Radiat Res 2018;190(5):464-72 doi 10.1667/rr15035.1.
48. Jagsi R, Griffith K, Bellon J, Woodward W, Horton J, Ho A*, et al.* TBCRC 024 initial results: A multicenter phase 1 study of veliparib administered concurrently with chest wall and nodal radiation therapy in patients with inflammatory or locoregionally recurrent breast cancer. International Journal of Radiation Oncology 2015;93(3):S137.
49. Speers C, Zhao SG, Kothari V, Santola A, Liu M, Wilder-Romans K*, et al.* Maternal Embryonic Leucine Zipper Kinase (MELK) as a Novel Mediator and Biomarker of Radioresistance in Human Breast Cancer. Clinical cancer research : an official journal of the American Association for Cancer Research 2016;22(23):5864-75.
50. Yokoyama Y, Dhanabal M, Griffioen AW, Sukhatme VP, Ramakrishnan S. Synergy between angiostatin and endostatin: inhibition of ovarian cancer growth. Cancer Res 2000;60(8):2190-6.

Chapter 3 : Short Term CDK4/6 Inhibition Radiosensitizes Estrogen Receptor Positive Breast Cancers[3]

Abstract

Cyclin-dependent kinase 4/6 (CDK4/6) inhibitors have improved progression free survival for metastatic, estrogen receptor positive (ER+) breast cancers, but their role in the non-metastatic setting remains unclear. We sought to understand the effects of CDK4/6 inhibition (CDK4/6i) and radiation (RT) in multiple preclinical breast cancer models. Transcriptomic and proteomic analyses were used to identify significantly altered pathways after CDK4/6i. Clonogenic assays were used to quantify the RT enhancement ratio (rER). DNA damage was quantified using γH2AX staining and the neutral comet assay. DNA repair was assessed using RAD51 foci formation and non-homologous end joining (NHEJ) reporter assays. Orthotopic xenografts were used to assess the efficacy of combination therapy. Palbociclib significantly radiosensitized multiple ER+ cell lines at low nanomolar, sub IC_{50} concentrations (rER: 1.21 – 1.52) and led to a decrease in the surviving fraction of cells at 2 Gy ($p < 0.001$). Similar results were observed in ribociclib- (rER: 1.08 - 1.68) and abemaciclib-treated (rER: 1.19 - 2.05) cells. Combination treatment decreased RAD51 foci formation ($p < 0.001$), leading to a suppression of HR activity,

[3] This chapter was published in *Clinical Cancer Research* in September 2020.

but did not affect NHEJ efficiency ($p > 0.05$). Immortalized breast epithelial cells and cells with acquired resistance to CDK4/6i did not demonstrate radiosensitization (rER: 0.94 – 1.11) or changes in RAD51 foci. In xenograft models, concurrent palbociclib and RT led to a significant decrease in tumor growth. These studies provide preclinical rationale to test CDK4/6i + RT in women with locally-advanced ER+ breast cancer at high risk for locoregional recurrence.

Statement of Translational Relevance

Although CDK4/6 inhibitors are currently indicated for patients with metastatic, ER+ breast cancer, their utility in the non-metastatic setting is still being established. Our understanding of the interaction between CDK4/6 inhibitors and the ionizing radiation given as part of the standard of care is lacking, and the utility of this approach in women at high risk for locoregional failure is unknown. In this manuscript, we demonstrate using multiple non-overlapping *in vitro* and *in vivo* models that combination therapy with RT and each of the three clinically approved CDK4/6 inhibitors is more effective at decreasing cell proliferation and tumor growth when compared to either RT or CDK4/6 inhibition alone. Further, this sensitization is due, at least in part, through the suppression of homologous recombination (HR)-mediated DNA repair. In contrast, preclinical models with acquired resistance to CDK4/6 inhibition do not demonstrate radiosensitization or suppression of HR. These data suggest that combination CDK4/6 inhibition and RT represent a novel indication for CDK4/6 inhibitors and a clinically feasible strategy for the radiosensitization of ER+ breast cancers that warrants clinical exploration.

Introduction

The treatment of breast cancer is guided, in part, by the presence or absence of hormone receptors including the estrogen receptor (ER). Nearly 75% of new breast cancer diagnoses will be classified as estrogen receptor positive (ER+) disease(1). For these patients, precision medicine strategies that target the ER using selective estrogen receptor modulators (SERMs), selective estrogen receptor degraders (SERDs), and aromatase inhibitors (AIs) that block ER signaling have resulted in significant improvements in recurrence-free and overall survival rates(1). While many women with ER+ metastatic breast cancer initially respond to endocrine therapy, nearly all will become refractory to endocrine therapy(1). Treatment options in the metastatic setting are expanding, and the recent introduction of cyclin-dependent kinase 4 and 6 (CDK4/6) inhibitors into the clinic has significantly improved outcomes for these patients(2,3).

In contrast to anti-estrogen therapies, CDK4/6 inhibitors work by targeting the cell cycle(4). When cells are actively proliferating, the levels of cyclin proteins rise and fall in a series of predetermined, cyclic patterns. The activation of specific cyclins at fixed points in the cell cycle is crucial for proper regulation of cyclin-dependent kinases (CDKs). CDKs are serine/threonine kinases that act as master regulators of the cell cycle; they phosphorylate downstream target proteins necessary to proceed through cell cycle "checkpoints" designed to control abnormal proliferation(4). For example, cyclin D1 forms a complex with CDK4/6 and leads to the phosphorylation of many downstream targets – including the inactivation of the retinoblastoma (RB1) tumor suppressor(4). The ability of cancer cells to evade growth suppressors, one of the hallmarks of cancer, has long been appreciated in many cancer types based on the dysregulation of cyclins and cyclin-dependent kinases (CDKs)(4).

With the development of selective CDK4/6 inhibitors including palbociclib, the ability to selectively target this cell cycle dysregulation in metastatic, ER+ breast cancer became possible. There are currently 3 FDA-approved CDK4/6 inhibitors: palbociclib (PD0332991)(5), ribociclib (LEE011)(6) and abemaciclib (LY2835219)(7). All three are orally bioavailable ATP-competitive inhibitors of CDK4 and CDK6. Early preclinical studies suggested that ER+ breast cancer cell lines are more sensitive to the antiproliferative effects of specific CDK4/6 inhibitors compared to other breast cancer subtypes, including triple negative breast cancer, where alterations in *RB1* are more frequent(5). This differential response, later validated by others, provided the rationale to restrict early clinical trials to ER+ breast cancers(3). Based on several practice changing clinical trials(2,3,8,9), CDK4/6 inhibitors are now standard-of-care for women diagnosed with metastatic ER+ breast cancer in combination with hormone therapies such as letrozole or tamoxifen.

For patients with metastatic, ER+ breast cancer, CDK4/6 inhibitors have improved progression free survival, but acquired resistance to these drugs remains a critical clinical issue(4). While the exact mechanism(s) of therapy resistance remain unclear, recent data suggest changes in phosphorylation of RB1(5,10,11), and changes in cyclin/CDK expression(12-16), may contribute to drug resistance; however, currently there is no known consensus pathway of resistance. CDK4/6 inhibitors have also demonstrated the ability to slow progression in many types of cancers as well as the potential to synergize with other agents for more durable responses.

Although use of CDK4/6 inhibitors is currently limited to the metastatic setting, there are ongoing efforts to evaluate the efficacy of CDK4/6 inhibitors in the upfront setting for women with locally advanced or high-risk ER+ disease(17). This resistance may become a more critical issue as these inhibitors make their way into the clinical management of patients with locally advanced, non-metastatic disease where cure remains the therapeutic goal. Thus, there is a critical

unmet need to identify strategies to improve the local efficacy of CDK4/6 inhibitor therapy in patients with ER+ breast cancer.

Radiation (RT) therapy remains a mainstay in the treatment of women with locally advanced ER+ breast cancer(18). Despite its ubiquitous use, combination studies testing the use of RT in combination with CDK4/6 inhibition are lacking. It is well established that pharmacological CDK4/6 inhibition interferes with cell cycle regulation(4), but recent studies have also shown that single agent palbociclib can also affect regulation of the DNA damage response pathways(19,20). However, our understanding of this interaction and the resulting effects of CDK4/6 inhibitor therapy and RT is incomplete. Therefore, we sought to determine whether combining CDK4/6 inhibitors with RT would prove to be more effective than either treatment alone in multiple models of ER+ breast cancer, and to evaluate the physiological significance of this phenomenon *in vivo*.

Results

Single-agent CDK4/6 inhibition leads to a suppression of cell cycle and DNA damage response pathways

To determine the effects of CDK4/6 inhibition in breast cancer, we performed proliferation assays and calculated the IC_{50} values of palbociclib, ribociclib, and abemaciclib in the estrogen-dependent, ER+ breast cancer cell lines MCF-7, T47D, (**Figure 3.1**), CAMA-1, and ZR-75-1 (**Figure 3.2**). In order to understand the biological changes that are induced by short term CDK4/6 inhibition, we analyzed transcriptomic changes of T47D cells treated with 40nM palbociclib for 16 hours (**Figure 3.3A**). Overrepresentation (pORA) and total pathway accumulation (pAcc) were computed using iPathway (Advaita) to find pathways that were significantly differentially expressed.

As expected, the cell cycle pathway was differentially expressed between vehicle-treated and palbociclib-treated T47D cells ($p = 9.283 \times 10^{-5}$) and expression of RB1, a canonical target of CDK4/6, was significantly decreased compared to control cells ($p = 2.014 \times 10^{-4}$). Surprisingly, pathway analysis identified DNA damage response as the pathway most significantly overrepresented after palbociclib treatment. These significantly altered pathways (with FDR-corrected p values) include DNA replication ($p = 6.198 \times 10^{-23}$), Mismatch repair ($p = 3.209 \times 10^{-7}$), Base excision repair ($p = 1.249 \times 10^{-5}$), Fanconi anemia ($p = 1.585 \times 10^{-5}$), nucleotide excision repair ($p = 4.935 \times 10^{-5}$), and homologous recombination ($p = 8.874 \times 10^{-5}$). Cell cycle downregulation also led to the global suppression of cell cycle genes (**Figure 3.3D**) including Cyclin E2 (*CCNE2*), the transcription factor E2F (*E2F1*), and RB1 (*RB1*). T47D cells treated with either 100nM ribociclib (**Figure 3.3B**) or 20nM abemaciclib (**Figure 3.3C**) demonstrated similar pathway changes in cell cycle and DNA damage response pathways. MCF-7 cells treated with low

concentrations of CDK4/6 inhibition for 16 hours (**Figure 3.4**) showed less robust changes in gene expression overall and no significant changes in DNA damage response pathways, but showed some change in cell cycle response along with significant changes in interleukin and chemokine signaling.

To understand how these pathway changes might be altered after the development of CDK4/6 inhibitor resistance, we developed models of acquired resistance (**Figure 3.3E**) to palbociclib (Pal_{AR}) ribociclib, (Rib_{AR}) and abemaciclib (Abe_{AR}) in MCF-7 and T47D cells. After selection, CDK4/6 inhibitor resistant MCF-7 and T47D cells demonstrated a 10-100 fold greater resistance to CDK4/6 inhibition as evident by a significant shift in the dose-response curves (**Figure 3.1**). CDK4/6 inhibitor resistant cell lines also developed cross resistance to all three CDK4/6 inhibitors, suggesting commonality in resistance mechanisms (**Figure 3.5**). In contrast to the changes observed after CDK4/6 inhibition in CDK4/6 inhibitor-sensitive parental cell lines, short term treatment of palbociclib-resistant T47D Pal_{AR} cells with 40nM palbociclib (**Figure 3.3F**) predominately led to changes in pathways involved in adhesion, cytokine signaling, and immune regulation, which has been demonstrated by others(19). T47D Rib_{AR} (**Figure 3.3G**) and T47D Abe_{AR} (**Figure 3.3H**) cells and CDK4/6 inhibitor-resistant MCF-7 cells (**Figure 3.4D-F**) also showed minimal changes in cell cycle and DNA damage response pathways, suggesting that CDK4/6 inhibitor-resistant cell lines are not as susceptible to manipulations of DNA repair and DNA damage as their wild-type counterparts.

In order to confirm these observed transcriptomic changes, we used reverse phase protein array to quantify changes in protein and phosphoprotein expression in MCF-7 and MCF-7 Pal_{AR} cells 16 hours after treatment with 75nM palbociclib. Along with expected changes in cell cycle proteins – including decreased pRB1 in MCF-7 parental cells – we saw a decrease in the expression

of a significant number of proteins and phospho-proteins involved in the DNA damage response (**Figure 3.3I**). CDK4/6 inhibition with palbociclib did not cause significant suppression of these proteins in MCF-7 Pal_{AR} cells treated with 75nM palbociclib, suggesting that CDK4/6 inhibitor-resistant cells are no longer susceptible to CDK4/6 inhibitor-mediated suppression of DNA repair.

CDK4/6 inhibition radiosensitizes CDK4/6 inhibitor-naïve ER+ breast cancer cell lines

Because CDK4 and CDK6 act at the G_1/S checkpoint, it has been hypothesized that the use of CDK4/6 inhibitors would be radioprotective by arresting cells in the G_1 phase; cells are typically most sensitive to RT in G_2/M. Our data demonstrating significant changes in DNA damage response proteins and phosphoproteins suggested that CDK4/6 inhibitors may be directly impacting these pathways independent of the cell cycle effects and may potentiate the effects of DNA damaging agents (including ionizing RT). In order to assess the ability of CDK4/6 inhibition to influence the radiosensitivity of ER+ breast cancer cell lines, we performed clonogenic cell survival assays. In these assays, ER+ breast cancer cells were pretreated with low-concentration CDK4/6 inhibition one hour prior to RT to minimize potential confounding effects of cell cycle reassortment.

We demonstrate that escalating doses of palbociclib produced a dose-dependent increase in radiosensitization in MCF-7 cells (rER 1.15 – 1.67) at concentrations at or below the IC_{50} value (**Figure 3.6A**). The radiation enhancement ratio (rER) of clinically approved radiosensitizing agents such as cisplatin(27) is ~1.2, suggesting that this radiosensitization is clinically meaningful(27,28). Similar results were observed in T47D (rER: 1.12 – 1.65, **Figure 3.6B**), CAMA-1 (rER: 1.14 – 1.42, **Figure 3.2D**), and ZR-75-1 cells (rER: 1.12 – 1.43, **Figure 3.2F**) when treated with sub-IC_{50} concentrations of palbociclib. Radiosensitization occurred in MCF-7 and T47D cells to a similar degree with ribociclib (**Figure 3.6C-D**) and abemaciclib (**Figure**

3.6E&F), suggesting that all three CDK4/6 inhibitors led to comparable levels of radiosensitization *in vitro*. Furthermore, all three drugs showed modest single agent toxicity (**Table 3.1**), predominately at concentrations closer to the IC_{50} value. However, at these concentrations, CDK4/6 inhibition did not significantly radiosensitize the transformed, mammary epithelial cell line MCF-10A (**Figure 3.7**), suggesting that the combination treatment would be unlikely to cause significant toxicity to normal breast tissue when treated with RT (**Table 3.3**).

Because CDK4/6 inhibitors change the cell cycle distribution of exponentially growing ER+ breast cancer cells, we sought to understand how cell cycle changes may play a role in the radiosensitization. To that end, we performed propidium iodide-based cell cycle analysis in T47D and MCF-7 cells (**Figure 3.8A,C**) to determine the time course of G_1 arrest in our cell lines. In T47D cells, G_1 arrest did not occur at 1 or 6 hours after CDK4/6 inhibitor treatment, but cells were significantly arrested by 16 hours and remained arrested at 24 and 48 hours. MCF-7 cells did not arrest after 1 hour of drug treatment - equivalent to our one hour pretreatment in other assays – but did demonstrate cell cycle arrest at 48 hours even at these low concentrations. In addition, we performed clonogenic assays in MCF-7 cells with varied CDK4/6 inhibitor pretreatment times before radiation. In spite of these differences in cell cycle accumulation, pretreatment with 50-100nM palbociclib for either 6 or 24 hours led to nearly equivalent levels of radiosensitization in MCF-7 cells (rER 1.29-1.58 at 6 hours, 1.13-1.71 at 24 hours; **Figure 3.8E-F, Table 3.4**), suggesting that radiosensitization is cell cycle independent and that radiosensitization occurs even in cells arresting at the G_1 checkpoint.

Given that CDK4/6 inhibitor-resistant cell lines respond differently to short-term CDK4/6 inhibition compared to their parental cell lines, we were interested in understanding whether CDK4/6 inhibitor resistance would play a role in the response of ER+ breast cancer cells to

ionizing radiation. As expected, cell cycle analysis demonstrated that CDK4/6 inhibitor-resistant MCF-7 and T47D cells did not arrest at G_1 after treatment with palbociclib, ribociclib, or abemaciclib (**Figure 3.8B,D**) even after 48 hours. Much higher concentrations of all 3 drugs (100-500nM) also failed to radiosensitize CDK4/6 inhibitor-resistant MCF-7 **(Figure 3.9A,C,E)** and T47D cells **(Figure 3.9B,D,F)** in clonogenic cell survival assays. Because these cells were selected for acquired resistance to CDK4/6 inhibitor monotherapy, single agent toxicity (**Table 3.2**) was minimal, as expected.

Short term CDK4/6 inhibition leads to a decrease in homologous recombination efficiency

Radiosensitization can occur through a variety of mechanisms, including changes in the efficiency of the DNA damage response, cell cycle reassortment, changes in oxygenation, and upregulation of other cellular response pathways such as apoptosis or senescence. Given that we observed cellular changes in multiple DNA damage response pathways at the transcriptomic and proteomic/phospho-proteomic level after short term CDK4/6 inhibition, we wanted to understand whether CDK4/6 inhibition affects specific DNA damage response pathways, including the two major double-strand break repair pathways of homologous recombination (HR) and non-homologous end joining (NHEJ).

To assess HR-mediated effects, we performed RAD51 foci formation assays. RAD51 is a recombinase responsible for protecting single stranded DNA at the site of DNA strand breaks and initiating the catalysis of HR-mediated DNA repair. RAD51 foci are indicative of active HR and can be quantified using immunofluorescence microscopy to assess HR competency. In MCF-7 (**Figure 3.10A**) and T47D (**Figure 3.10B**) cells, RT (4 Gy) led to an increase in RAD51 foci at 6 and 16 hours following RT. In contrast, a 1-hour pretreatment with either palbociclib, ribociclib, or abemaciclib led to a significant decrease in RAD51 foci at 6 and 16 hours post-RT compared to

RT alone. The inability of ER+ breast cancer cells to respond to and repair double stranded breaks using HR cannot solely be attributed to an absence of RAD51 protein (**Figure 3.10C**), though there was a slight decrease in total RAD51 protein levels in the palbociclib- and combination-treated groups in T47D cells at these time points. In contrast to CDK4/6 inhibitor-sensitive cell lines, CDK4/6 inhibitor-resistant $MCF7_{AR}$ (**Figure 3.10D-F**) and $T47D_{AR}$ cells (**Figure 3.10G-I**) did not demonstrate changes in RAD51 foci formation at either 6 or 16 hours. CDK4/6 inhibitor resistant cell lines still formed RAD51 foci and retained the ability to perform HR, but the addition of a CDK4/6 inhibitor did not further suppress the repair capacity of these cells. Representative foci are shown in both CDK4/6 inhibitor-sensitive (**Figure 3.11A&B**) and CDK4/6 inhibitor-resistant (**Figure 3.11C&D**) cells.

CDK4/6 inhibition does not suppress NHEJ repair

To understand how CDK4/6 inhibition may affect NHEJ efficiency, we used a transient GFP reporter system(22) to assess NHEJ proficiency in MCF-7 (**Figure 3.12A**) and CAMA-1 (**Figure 3.12B**) cells. In this system, CDK4/6 inhibitor monotherapy did not affect NHEJ efficiency in either cell line compared to vehicle controls. As a control, treatment with 1μM NU7441 (a DNAPK inhibitor) significantly decreases NHEJ activity in both MCF-7 and CAMA-1 cells, but the CHK1/2 inhibitor AZD7762 does not affect NHEJ repair efficiency. Furthermore, when combined with RT, we observed stable or increased expression of the NHEJ protein mediator pKu80 in MCF-7 (**Figure 3.12C**), CAMA-1 (**Figure 3.12D**), and T47D cells (**Figure 3.12E**) suggesting that NHEJ repair was not inhibited and may be activated in response to decreases in HR. In addition, at concentrations that are double the IC_{50} values of each CDK4/6 inhibitor in MCF-7 cells, pKu80 expression was significantly higher in cells treated with the combination of drug and RT (**Figure 3.12F**).

If CDK4/6 inhibition suppresses the ability of ER+ breast cancer cells to undergo HR, NHEJ becomes the predominant form of dsDNA break repair. Thus, we hypothesized that combining CDK4/6 inhibition with pharmacological or genetic inhibition of proteins in the NHEJ pathway would be synergistic. In both MCF-7 and T47D cells (**Figure 3.12G, 3.12J**), palbociclib in combination with 500nM NU7441 leads to extremely significant levels of radiosensitization (rER: 1.80 – 3.46) compared to either compound alone. However, in MCF-7 cells, pharmacologic CHK1/2 inhibition is not synergistic with CDK4/6 inhibition – consistent with the hypothesis that CDK4/6 inhibitors act redundantly to suppress HR repair. Similar results were obtained using genetic knockdown of Ku70 (XRCC6) and RAD51 (RAD51) in MCF-7 cells (**Figure 3.12H,I**). Although the ability of single agent DNAPK inhibition to radiosensitize MCF-7 cells is retained in MCF-7 Pal_{AR} cells (**Figure 3.12K**), the addition of palbociclib does not lead to additional or synergistic levels of radiosensitization.

These studies demonstrate that CDK4/6 inhibition impairs the ability of cells to undergo HR and may shunt dsDNA break repair through the NHEJ pathway. In our models, neither immunofluorescent γH2AX foci (**Figure 3.13A,B,E,F**) or γH2AX total protein (**Figure 3.13C&D)** were significantly different between cells treated with RT alone (2 Gy) or the combination of RT and palbociclib, suggesting that combination treatment did not significantly affect the persistence of dsDNA damage in the cell. In our proteomic analysis using RPPA we did not see any changes in γH2AX (pS139) expression in our MCF-7 cells treated with 75nM palbociclib (**Figure 3.3I**). To further confirm this, we performed the neutral COMET assay in MCF-7 cells to detect changes in dsDNA breaks (**Figure 3.13G-H**). Although RT (4 Gy) caused an increase in dsDNA breaks at both 6 and 16 hours after RT, CDK4/6 inhibition did not potentiate a delay in dsDNA break repair. Thus, the ability of cells to repair dsDNA breaks in

breast cancer cells treated with CDK4/6 inhibition and RT may be limited to low-fidelity NHEJ repair.

CDK4/6 inhibition radiosensitizes ER+ breast cancer cells *in vivo*

To understand if CDK4/6 inhibition leads to clinically relevant levels of radiosensitization *in vivo*, we generated orthotopic xenograft models with the MCF-7 cells (**Figure 3.14A**). In the combination group, palbociclib treatment was started one day before fractionated RT and was discontinued after the last fraction in order to measure the radiosensitizing effects of CDK4/6 inhibition with palbociclib independent from its single agent efficacy. Treatment with the combination of palbociclib and RT significantly suppressed tumor growth ($p < 0.01$, **Figure 3.14B**) and prolonged time to tumor doubling ($p < 0.0001$, **Figure 3.14C**) compared to mice treated with RT or palbociclib alone. These treatments did not lead to any visible toxicities or significant changes in body weights of mice (**Figure 3.14D**) throughout the duration of the study, suggesting that the therapy was generally well-tolerated. In addition, we calculated the expected and observed fractional tumor volume (FTV)(26) for each treatment condition (**Table 3.6**) and our results suggest that combination treatment with palbociclib and RT has synergistic (expected/observed ratio > 1) rather than additive effects.

Discussion

In this study, we demonstrate that short term treatment of ER+ breast cancer cell lines with the CDK4/6 inhibitors palbociclib, ribociclib, and abemaciclib led to alterations in many cellular pathways, including suppression of cell cycle signaling and changes in the DNA damage response (**Figure 3.3**). In ER+ breast cancer cells that are sensitive to CDK4/6 inhibitor monotherapy, the combination of CDK4/6 inhibition and ionizing RT led to significant radiosensitization with each of the three clinically approved CDK4/6 inhibitors (**Figure 3.6**). This radiosensitizing ability, however, was lost in ER+ breast cancer cells with acquired resistance to CDK4/6 inhibition and was not observed in normal breast epithelial cells (**Figure 3.7, Figure 3.9**). Mechanistically, the radiosensitization observed in CDK4/6 inhibitor sensitive models was mediated by impaired homologous recombination that shunted dsDNA break repair towards error-prone NHEJ (**Figure 3.10**). In contrast, both HR and NHEJ repair remained intact in CDK4/6 inhibitor-resistant cell lines. In xenograft models of ER+ breast cancer, CDK4/6 inhibition led to tumor radiosensitization (**Figure 3.14**). Taken together, these results demonstrate that the combination of CDK4/6 inhibition and RT is a potentially effective strategy for the radiosensitization of ER+ breast cancer that is lost in cells that have become resistant to CDK4/6 inhibitor monotherapy. Our data also suggest that concurrent administration of CDK4/6 inhibition with RT (instead of adjuvant therapy) may be a more effective strategy to decrease the rates of disease recurrence in patients with ER+ breast cancer at high risk of locoregional recurrence and that this strategy warrants clinical investigation.

In contrast to the conventional use of CDK4/6 inhibitors in the metastatic setting, our work challenges the standard treatment paradigm and highlights the therapeutic potential of using CDK4/6 inhibitors in combination with ionizing RT to radiosensitize CDK4/6 inhibitor-naïve ER+

breast cancers. In contrast to studies that seek to overcome CDK4/6 inhibitor resistance or propose therapeutic alternatives for CDK4/6 inhibitor-resistant tumors, our approach in combining CDK4/6 inhibitors and RT is a novel therapeutic strategy that can be utilized prior to the development of drug resistance; thus, this approach has the potential to cure women prior to the development of metastatic disease. Finally, in our study, all three clinically approved CDK4/6 inhibitors demonstrated the ability to radiosensitize ER+ breast cancer cell lines at similar concentrations, suggesting that this effect could be achieved in patients regardless of the specific CDK4/6 inhibitor chosen for therapy.

In current practice, RT is only given in combination with CDK4/6 inhibitors for palliative management in patients with metastatic disease. While there have been a few studies that report additional skin and GI toxicities for these patients(29,30), recent analyses report that combination therapy in the palliative setting has been generally well-tolerated(31-34). Our data in normal breast epithelial cells suggested that CDK4/6 inhibition did not potentiate radiation effects and therefore should be well tolerated by the normal breast tissue when translated clinically.

It is important to note that our *in vivo* murine studies were designed to test the effect of low dose CDK4/6 inhibition (25mg/kg) as a radiosensitizing strategy, rather than the efficacy of continued combination therapy at standard, optimal doses (50-100mg/kg). Because drug was not continued after completion of fractionated RT, we would expect that long term CDK4/6 inhibition after completion of RT would lead to even further reduction in overall tumor burden. Importantly, our data suggest that much lower doses of CDK4/6 inhibition can confer radiosensitivity, and one potential translational strategy would be to use these low doses in combination with RT which would potentially limit the frequency of systemic toxicities that lead to the discontinuation of therapy. Alternatively, future studies will assess if monotherapy doses of CDK4/6 inhibition led

to an even greater degree of radiosensitization with an acceptably low toxicity profile. These two competing strategies are currently being considered in the planned phase I/II clinical trials testing this combination treatment.

While this work may be beneficial for ER+ breast cancer patients, our study may also provide valuable mechanistic insights that could be applied to other cancers where CDK4/6 inhibitors are being studied preclinically. Indeed, whether CDK4/6 inhibitor-mediated radiosensitization is clinically effective in other subtypes of breast cancer (basal-like, HER2 enriched, etc.) remains an unanswered question, as well as if this is effective in other histologies, including invasive lobular or inflammatory breast cancer. Previous studies have, however, demonstrated that CDK4/6 inhibition may radiosensitize head and neck squamous cell carcinomas(35,36), glioblastomas(37,38), and colorectal and lung cancer cell lines(39). In line with findings in head and neck squamous cell carcinoma cell lines(35,36), impaired HR efficiency might be important for CDK4/6 inhibitor-mediated radiosensitization in multiple cancer types.

Along the same lines, other preclinical studies performed in pancreatic cancer(40) and triple negative breast cancer(20,41) cell lines have suggested that CDK4/6 inhibition impairs homologous recombination efficiency after administration of cytotoxic chemotherapies or RT(42). This will be an important clinical consideration for future studies with CDK4/6 inhibitors as radiosensitizing agents, as cytotoxic chemotherapies are routinely used to treat patients with ER+ breast cancer in the neoadjuvant setting. However, in contrast to studies in lung and colorectal cancer cell lines that suggest that radiosensitization is p53-dependent(39), our data showed that CDK4/6 inhibitor-mediated radiosensitization occurs in both p53 wild type (MCF-7, ZR-75-1) and p53 mutant (T47D, CAMA-1) models. However, all of our models express the tumor suppressor RB1 which has recently been shown to directly promote HR in breast cancer cell lines(43).

There are some limitations to this study that need to be considered. Although we focused on CDK4/6 inhibition and the DNA damage response, other mechanisms of radiosensitization may play a minor role in this phenotype. CDK4/6 inhibitor monotherapy has been shown to increase apoptosis in triple negative breast cancer cell lines(44-46), but in our models we did not see an increase in apoptosis with CDK4/6 inhibition or combination treatment (**Figure 3.15**). There are conflicting reports about the effect of CDK4/6 inhibition on senescence in breast and other cancer types(47-52), and further studies could address any potential contributions of senescence to the radiosensitization phenotype that we see in ER+ breast cancer models. We also did not explore mechanisms of single strand break repair, such as mismatch repair, base excision repair, or nucleotide excision repair, but our transcriptomic data (**Figure 3.3**) suggested that these pathways could play a minor role in radiosensitization. Finally, confirmatory animal studies demonstrating radiosensitization in CDK4/6 inhibitor-treatment naïve PDX models and lack of radiosensitization in CDK4/6 inhibitor-resistant PDXs (from women whose disease progressed on CDK4/6 inhibitor therapy) are needed. These studies were underway when the COVID-19 pandemic arose and are still planned when circumstances allow.

It is possible that other CDK inhibitors may be able to radiosensitize ER+ breast cancer cells. Flavopiridol, a nonspecific CDK inhibitor, has been shown to radiosensitize cancer cell lines(53,54) and to potentiate cell death after cytotoxic therapy(55), though it is has an unacceptable safety profile that has prevented its clinical development(56). Furthermore, studies of CDK12/13 in triple negative breast cancer have demonstrated changes in radiation sensitivity based on direct interaction with transcriptional machinery and changes in polyadenylation(57), and support the idea that radiosensitization in ER+ breast cancers may be achieved with inhibition of other cyclin-dependent kinases as well. Finally, there is recent evidence to suggest that hormone

therapy and CDK4/6 inhibitor resistance may lead to alterations in genes such as *AKT1* and *AURKA* that are involved in DNA repair(58), which may have important clinical implications for patients receiving both types of therapy.

In conclusion, our results suggest that CDK4/6 inhibitor therapy would be effective in decreasing tumor growth in ER+ breast cancer patients by radiosensitizing tumor cells during fractionated RT. Our data also suggests that the development of CDK4/6 inhibitor resistance with one drug leads to cross-resistance with the others in its class, consistent with what others have shown, which is an important clinical consideration as clinicians start to use CDK4/6 inhibitors in the adjuvant setting with RT. We also found that CDK4/6 inhibitor-mediated radiosensitization can be used as a therapeutic strategy in the absence (or prior to) the initiation of hormone therapies, but future studies will seek to understand the interaction between CDK4/6 inhibition and RT with concurrent endocrine therapy. A complete understanding of the mechanism of CDK4/6 inhibitor-mediated radiosensitization will provide further insight into future treatment protocols and strategies to more effectively treat patients with ER+ breast cancers.

Methods

Cell Culture

All cell lines were obtained from ATCC and cultured at 37ºC and 5% CO_2 at subconfluent densities. MCF-7 and T47D cells were maintained in DMEM (#11965-092), 10% fetal bovine serum (FBS) (Atlanta Biologicals), and 1% Pen/Strep (Thermo #15070063). CAMA-1 cells were maintained in EMEM (#12-611F), 10% FBS, and 1% Pen/Strep. MCF-10A cells were maintained in DMEM/F-12 (#11330-032) containing 5% horse serum (Invitrogen #16050-122), 1% Pen/Strep, 20ng/mL EGF (Thermo #PHG0311), 0.5mg/mL hydrocortisone (Sigma #H-0888), 100ng/mL cholera toxin (Sigma #C-8052), and 10µg/mL insulin (Sigma #1-5500). Parental cell lines (MCF-7, T47D, CAMA-1, ZR-75-1) are ER+ breast cancer cells that are sensitive to both estrogen supplementation and hormone therapies. CDK4/6 inhibitor-resistant cell lines were developed through serial passaging with dose-escalation of either palbociclib, ribociclib, or abemaciclib every 2-3 weeks. Cells were selected for approximately three months (**Figure 3.1D**) and resistant pools were continuously cultured in 1µM CDK4/6 inhibitor. Before use in assays, drug was removed for at least 24 hours and cells were plated in drug-free media. The identity of the cell lines was confirmed by STR profiling and mycoplasma testing was done monthly (Lonza #LT07-318).

Drugs

All drugs were solubilized in 100% DMSO for a stock concentration of 10mM for use in all cell culture assays. Palbociclib (Sigma #PZ0199), ribociclib (Med Chem Express #HY-15777A), abemaciclib (Med Chem Express #HY-16297A), staurosporine (Sigma #S6942), NU7441 (Selleck #S2638), and AZD7762 (Sigma #SML0350) were all purchased commercially.

Clonogenic Survival assay

Cells were seeded at single cell density in 6 well plates and allowed to adhere overnight. The following morning, cells were pretreated with drug for one hour (except where indicated otherwise) and radiated. Colony counts were used to determine toxicity, the surviving fraction of cells at 2 Gy (SF 2 Gy), and the radiation enhancement ratio (rER) for each treatment condition. Clonogenic data were fit to a linear-quadratic model and enhancement ratios were calculated as the ratio of the area under the curve (AUC) from control cells / experimental conditions.

Immunoblotting

Cell lysates were prepared with RIPA buffer (Thermo Fisher #89901) containing commercially available phosphatase and protease inhibitor tablets (Sigma #PHOSS-RO, #CO-RO). Protein lysates were sonicated and reduced with 2% β-Mercaptoethanol and 4x Nu-Page buffer (Life Technologies #NP0007). Immunoreactivity was detected using the following antibodies: anti-RAD51 (Millipore ABE257 1:1000, pKu80 (Invitrogen #38118, 1:1000), Ku80 (CST #2180S, 1:1000), γH2AX (Milipore #05-636, 1:1000), cleaved PARP (CST #5625S, 1:1000), PARP1 (CST # 9542S, 1:1000), anti-β-Actin-HRP (CST #12262S, 1:50,000).

Proliferation Assays

Cells were plated in 96-well plates (~2000 cells/well) and treated the next morning with drugs ranging from 1nM - 10μM or vehicle. Cells were cultured for 72 hours and then Alamar blue (Invitrogen #DAL1100) was added at a concentration of 10% of the final volume. Plates were read 3-4 hours after the addition of Alamar blue with a microplate reader (BioTek Cytation 3) and

fluorescence was measured for each well. Readings were blank-corrected and normalized in comparison to the vehicle (DMSO-treated) controls. Cell growth curves were generated using the GraphPad Prism v7 software and fit with nonlinear regression to calculate the half maximal inhibitory concentration (IC_{50}). IC_{50} concentrations (unique to each of the three drugs in each cell line) were used in subsequent assays for most experiments where single treatment with drug was indicated.

Comet Assay

MCF-7 cells cultured in 6-well plates were treated with either vehicle or 75nM palbociclib one hour prior to RT (4 Gy). At 6 and 16 hours post-radiation, cells were trypsinized and plated on CometSlides (Trevigen #4250-050-03) after dilution in low melting point agarose (Thermo Fisher #15-455-200). Lysis solution (Trevigen #4250-050-01) overnight allowed for electrophoretic separation of DNA fragments and propidium iodide (Thermo Fisher #P3566) was used to stain the DNA fragments. At least 50 cells per treatment group were imaged and images were analyzed with Comet Assay IV Software Version 4.3 to calculate the tail moment.

Flow Cytometry

For cell cycle determinations, exponentially growing cells were trypsinized and fixed with 70% ethanol. Fixed cells were then stained with 1x PBS containing 50µg/mL propidium iodide and 100µg/mL RNAse (Qiagen #19101) approximately 30 minutes before analysis on the Bio-Rad ZE5 Cell Analyzer at the University of Michigan Flow Cytometry core. Cell cycle analysis and curve fitting was performed using FCS Express 7. For apoptosis experiments, live cells were

trypsinized and stained with Annexin V and propidium iodide according to the manufacturer's protocol (Roche #11858777001) before analysis.

Immunofluorescence

Cells were plated in 12 well plates containing glass coverslips and treated with either vehicle or CDK4/6 inhibitor the following day. Coverslips were fixed at predetermined timepoints using 2% sucrose (S0389) and 0.2% Triton X-100 (Sigma #T8787) in 4% paraformaldehyde (Thermo Fisher #J19943K2). Cells were permeabilized with 0.5% Triton X-100 and blocked with 5% goat serum (Thermo Fisher #16210064) containing 0.5% BSA and 0.05% Triton X-100 before staining with RAD51 (GeneTex GTX70230 1:300) or γH2AX (Millipore #05-636, 1:2000) primary antibodies. Goat anti-mouse secondary (Life Technologies #A11005, 1:2000) was used and slides were mounted with ProLong Gold containing DAPI (Invitrogen #P36931) before imaging.

siRNA Clonogenics

SiRAD51 (#J-003530-10), siXRCC6 (#L-005084-00-0020), and siNT (#D-001810-10) were all obtained from Dharmacon. Lipofectamine RNAiMAX (Thermo #13378030) was used to transfect cells in Opti-MEM (Invitrogen #31985-062) and antibiotic-free media. Cells were plated at sub-confluent densities in 6-well plates overnight and siRNA were used at a final concentration at 25nM. 24 hours post-transfection, cells were re-plated at single cell density for clonogenic cell survival assays. The next morning, cells were pretreated for one hour before radiation (0, 2, 4, 6 Gy) and clonogenic assays grew for 1-3 weeks before fixing with methanol/acetic acid and staining with crystal violet.

Irradiation

Irradiation was carried out as described previously in the University of Michigan Experimental Irradiation Core(21,22). Briefly, a Philips RT250 (Kimtron Medical), which is calibrated to meet the standards of the National Institute of Standards and Technology (NIST), was used at a dose rate of approximately 2 Gy/min for both *in vitro* and *in vivo* irradiation experiments.

NHEJ Reporter and qPCR

NHEJ reporter assays were performed as described previously(21,22). Briefly, a linearized GFP reporter plasmid was transfected into cells using lipofectamine 2000 (Invitrogen #11668) in Opti-MEM media (Invitrogen 31985-062) after a 1-hour pretreatment and plasmid DNA was isolated to perform comparative qPCR ($\Delta\Delta C_t$) using GFP and internal control primers. The Qiaprep Spin Miniprep Kit (Qiagen #27204) was used to isolate plasmid DNA. Fast Sybr Green was used to perform comparative qPCR ($\Delta\Delta C_t$) on a QuantStudio6 Flex Real Time qPCR system using GFP (GCTGGTTTAGTGAACCGTCAG, GCTGAACTTGTGGCCGTTTA) and internal control (TACATCAATGGGCGTGGATA, AAGTCCCGTTGATTTTGGTG) primers. All C_t values were normalized to untreated control cells.

Xenograft Studies

MCF-7 cells ($n = 4 \times 10^6$) were injected bilaterally into the mammary fat pads of 8-10 week old CB17-SCID female mice in 50% Matrigel (Thermo #CB-40234). Estrogen pellets (Innovative Research of America, #SE-121) were implanted subcutaneously in the nape of the neck on the day of tumor injection and removed after visible tumor formation. When tumors reached

approximately 80mm^3, mice were randomized into four groups (14-16 tumors per group): vehicle (Sodium L-Lactate, 50mmol/L pH 4.0, Sigma #L-7022), palbociclib only, RT only, or combination treatment. Mice in the palbociclib only or combination groups were treated with 25mg/kg palbociclib by oral gavage for 6 days. Mice receiving RT only received fractions of 2 Gy for five days. Mice in the combination group started palbociclib treatment one day before RT, but drug in all groups was discontinued after the last RT fraction. Tumor growth was measured 1-3 times a week and tumor volume was calculated using the equation $V=(L*W2)*\pi/6$. All xenograft experiments and procedures were done with the approval of the Institutional Animal Care & Use Committee (IACUC) at the University of Michigan.

Transcriptomic Analysis

RNA was isolated using QIAzol and the RNeasy mini kit (Qiagen #74104) and sent to the University of Michigan Advanced Genomics Core. For transcriptomic analyses, expression values were calculated using a robust multi-array average (RMA)(23) to convert probe values into log2 expression values for each gene which were then fit using linear models(24). The standard error (SE) for each gene was standardized across all arrays used for a median SE of 1. All p-values were corrected for a false discovery rate. Analyses were done using the oligo and limma packages of Bioconductor in R at the University of Michigan Bioinformatics Core. Data from this study is publicly available through GEO (GSE155570).

Statistical Analysis

The SF-2 Gy values and the NHEJ reporter data were compared to control cells using a one-way ANOVA with Dunnett's Test. A *t*-test was used to compare RT and combination groups in the immunofluorescence experiments, and p-values were corrected for multiple comparisons. All *in vitro* experiments were completed as the average of at least three independent experiments and pooled for statistical analysis. Xenograft tumor size and mouse weights were compared using a two-way ANOVA, and survival curves were compared using the log-rank (Mantel-Cox) test. Fractional tumor volume (FTV) was calculated in a manner consistent with previous studies(22,26).

Pathway Analysis

The data (significantly impacted pathways, biological processes, molecular interactions, miRNAs, SNPs, etc.) were analyzed using Advaita Bio's iPathwayGuide. This software analysis tool implements the 'Impact Analysis' approach that takes into consideration the direction and type of all signals on a pathway, the position, role and type of every gene, etc., as described previously(27-30). The pathway plot displays the unique character of iPathwayGuide's Impact Analysis, which accounts for both over-representation (enrichment) of differentially expressed genes on a pathway AND the topology of the pathway. The x-axis measures the p-value obtained using the classical over-representation analysis (pORA). The y-axis represents the p-value obtained from total perturbation accumulation (pAcc) in the pathway. The first probability, pORA, expresses the probability of observing the number of DE genes in a given pathway that is greater than or equal to the number observed, by random chance(27,30). The second probability, pAcc, is calculated based on the amount of total accumulation measured in each pathway.

Proteomic Analysis

Protein for reverse phase protein array (RPPA) was extracted from cells and standardized to 1.5 μg/μL in RIPA buffer. Cell lysate was reduced with β-mercaptoethanol and 4x SDS and sent to the Functional Proteomics RPPA Core Facility at M.D. Anderson Cancer Center for analysis(25). Briefly, serial dilutions of each sample were prepared and used to capture the linear antibody/antigen reaction for accurate data analysis using validated antibodies. In addition, 48 unique cell lysates were printed on each slide and served as controls to develop Replicate-Based-Normalization used for quality control for data generation and analysis and RPPA data merging across different slides. Subsequent algorithms of spatial correction, quality control of antibody probing, protein loading correction, replicate-based-normalization, and quality of antibody batches were performed with each run and an automated program for RPPA Pipeline processing was used. Each sample was quantitated and run in triplicate for each condition.

Acknowledgements

AP is supported by T32-GM007767, F31-CA254138, and the University of Michigan Center for the Education of Women (CEW+) Irma M. Wyman Fund, AM is supported by T32-GM007315 and T32-GM113900, and BC is supported by T32-CA140044. AP, AM, and BC are all supported by Rackham Graduate School Research Grants. The authors would also like to thank the Breast Cancer Research Foundation (N02600 to LP, N003173 to JR) and the University of Michigan Rogel Cancer Center (P30CA046592 and G023324). Finally, the authors greatly appreciate the contributions of the University of Michigan core facilities (Flow Cytometry, Advanced Genomics, Bioinformatics), and the M.D. Anderson Functional Proteomics RPPA Core Facility (NCI #CA16672) for support and technical assistance with the experiments in this manuscript. This

work was completed and published with the following co-authors: Nicole Hirsh, Benjamin Chandler, Anna Michmerhuizen, Cassandra Ritter, Marlie Androsiglio, Kari Wilder-Romans, Meilan Liu, Christina Gersch, José Larios, Lori Pierce, James Rae, and Corey Speers.

Figures

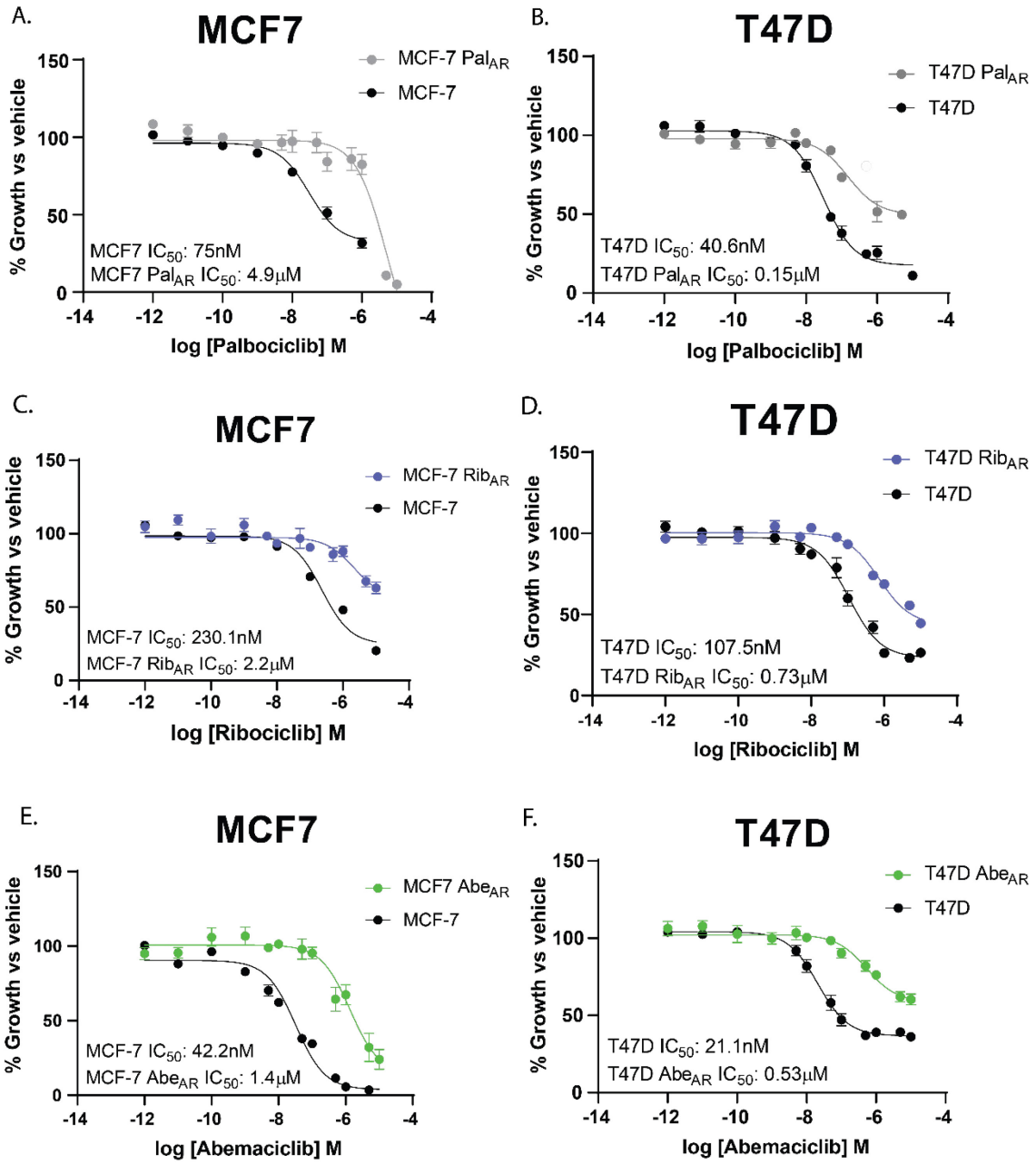

Figure 3.1: Proliferation of ER+ breast cancer cells following CDK4/6 inhibition.

MCF-7 and T47D cells (black lines) were treated with various concentrations of palbociclib (**A, B**), ribociclib (**C,D**), or abemaciclib (**E,F**) and allowed to grow for 72 hours before the addition of Alamar Blue. CDK4/6 inhibitor resistant MCF-7 and T47D cells (colored lines) were treated with the same range of drug and demonstrated decreased sensitivity to CDK4/6 inhibitor monotherapy. IC_{50} values were calculated for each treatment condition using the dose-response curve and all values were normalized to vehicle (DMSO) control wells. Data points represent the average ± SEM.

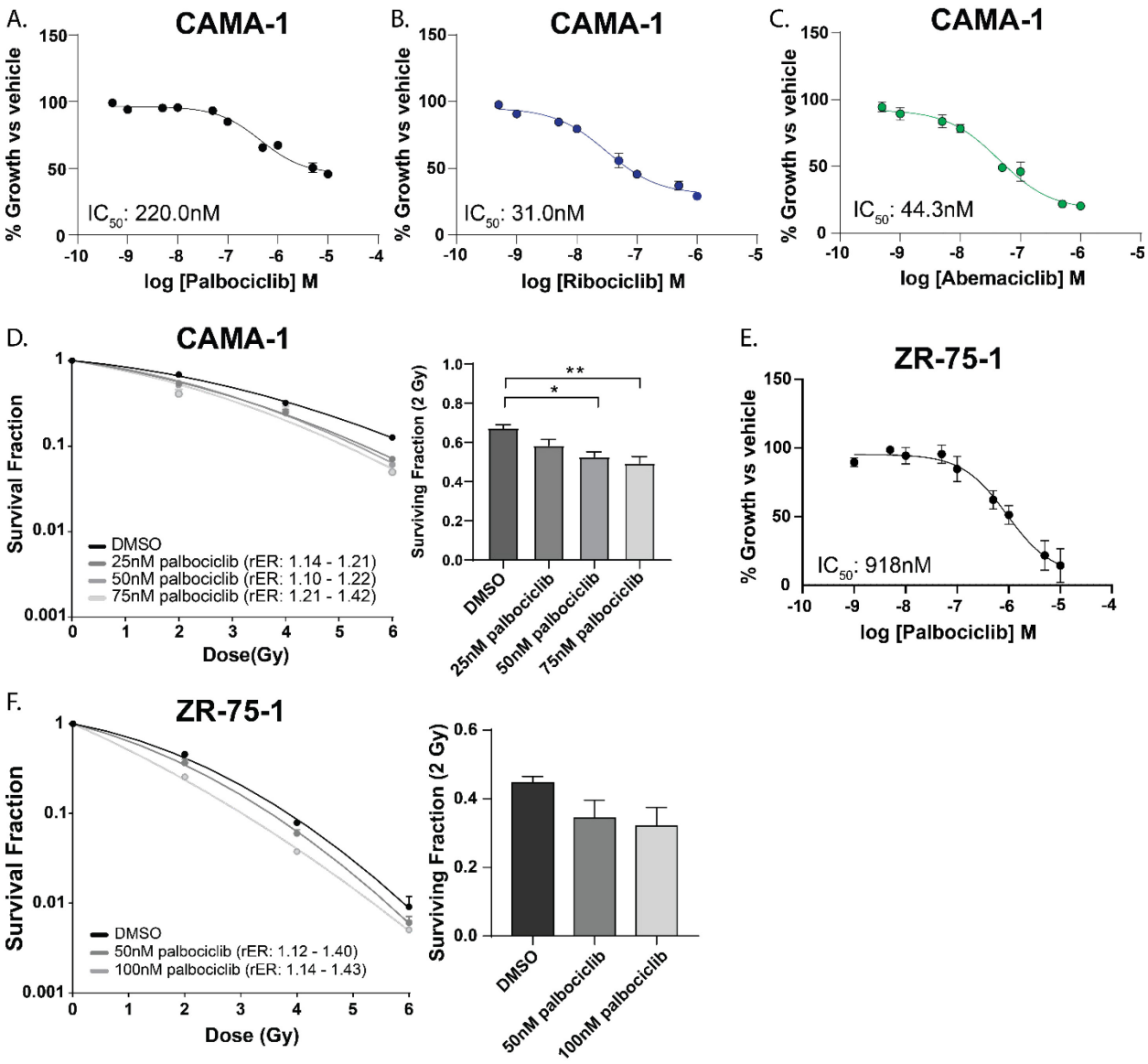

Figure 3.2: CDK4/6 inhibition radiosensitizes CAMA-1 and ZR-75-1 cells.

Proliferation assays were used to assess single agent efficacy of CDK4/6 inhibition in CAMA-1 (**A-C**) and ZR-75-1 (**E**) cells. In clonogenic cell survival assays, CAMA-1 (**D**) and ZR-75-1 (**F**) cells were treated with vehicle or palbociclib and the surviving fraction of cells was calculated for each condition.

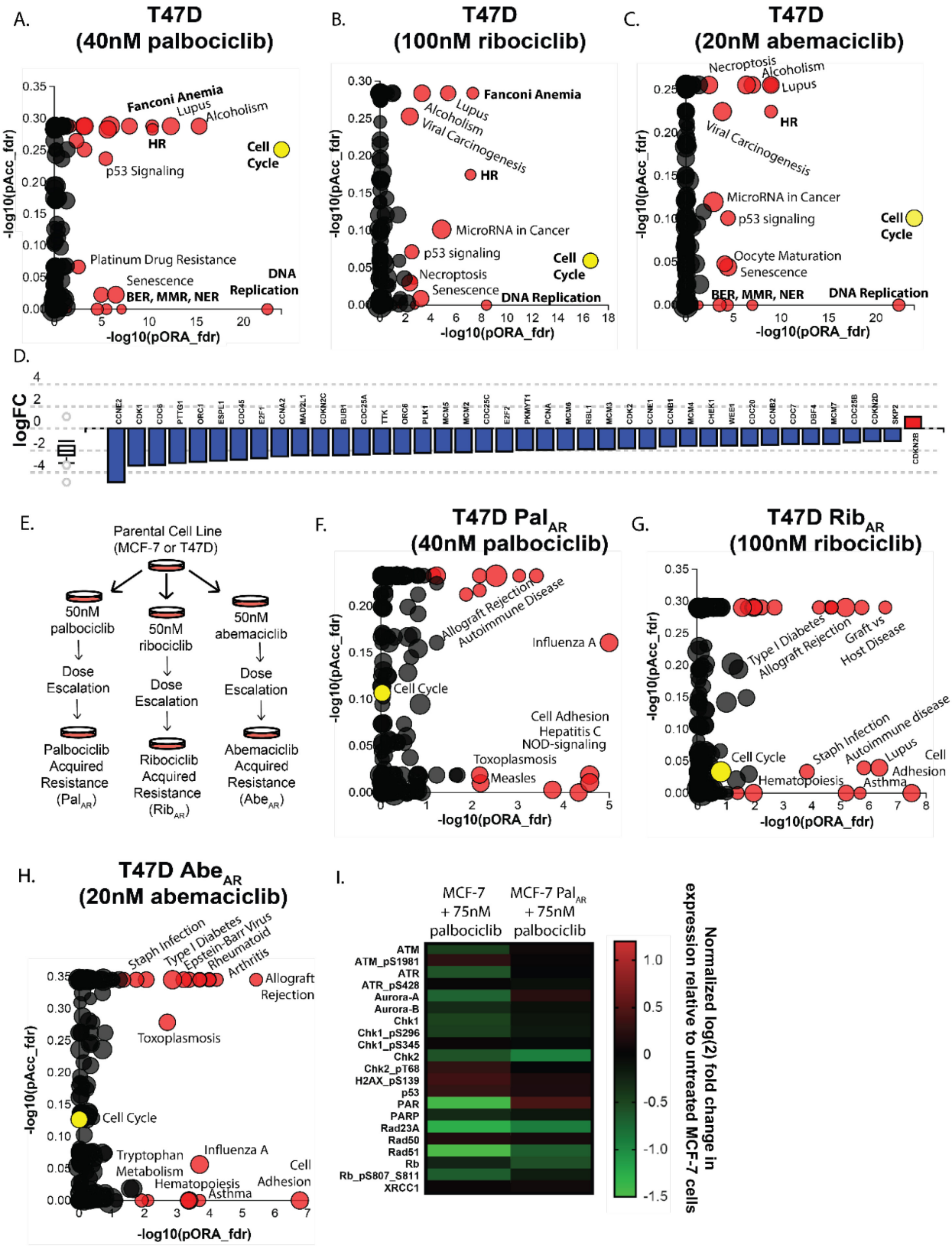
A.
T47D
(40nM palbociclib)
Fanconi Anemia
Lupus
Alcoholism
HR
Cell Cycle
p53 Signaling
Platinum Drug Resistance
Senescence
BER, MMR, NER
DNA Replication
-log10(pAcc_fdr)
-log10(pORA_fdr)
B.
T47D
(100nM ribociclib)
Fanconi Anemia
Lupus
Alcoholism
Viral Carcinogenesis
HR
MicroRNA in Cancer
p53 signaling
Cell Cycle
Necroptosis
Senescence
DNA Replication
C.
T47D
(20nM abemaciclib)
Necroptosis
Alcoholism
Lupus
HR
Viral Carcinogenesis
MicroRNA in Cancer
p53 signaling
Cell Cycle
Oocyte Maturation
Senescence
BER, MMR, NER
DNA Replication
D.
logFC
CCNE2 CDK1 CDC6 PTTG1 ORC1 ESPL1 CDC45 E2F1 CCNA2 MAD2L1 CDKN2C BUB1 CDC25A TTK ORC6 PLK1 MCM5 MCM2 CDC25C E2F2 PKMYT1 PCNA MCM6 RBL1 MCM3 CDK2 CCNE1 CCNB1 MCM4 CHEK1 WEE1 CDC20 CCNB2 CDC7 DBF4 MCM7 CDC25B CDKN2D SKP2 CDKN2B
E.
Parental Cell Line
(MCF-7 or T47D)
50nM palbociclib
50nM ribociclib
50nM abemaciclib
Dose Escalation
Palbociclib Acquired Resistance (Pal$_{AR}$)
Ribociclib Acquired Resistance (Rib$_{AR}$)
Abemaciclib Acquired Resistance (Abe$_{AR}$)
F.
T47D Pal$_{AR}$
(40nM palbociclib)
Allograft Rejection
Autoimmune Disease
Influenza A
Cell Cycle
Cell Adhesion
Hepatitis C
NOD-signaling
Toxoplasmosis
Measles
G.
T47D Rib$_{AR}$
(100nM ribociclib)
Type I Diabetes
Allograft Rejection
Graft vs Host Disease
Staph Infection
Autoimmune disease
Lupus
Cell Adhesion
Cell Cycle
Hematopoiesis
Asthma
H.
T47D Abe$_{AR}$
(20nM abemaciclib)
Staph Infection
Type I Diabetes
Epstein-Barr Virus
Rheumatoid Arthritis
Allograft Rejection
Toxoplasmosis
Cell Cycle
Tryptophan Metabolism
Influenza A
Hematopoiesis
Asthma
Cell Adhesion
I.
MCF-7 + 75nM palbociclib
MCF-7 Pal$_{AR}$ + 75nM palbociclib
ATM
ATM_pS1981
ATR
ATR_pS428
Aurora-A
Aurora-B
Chk1
Chk1_pS296
Chk1_pS345
Chk2
Chk2_pT68
H2AX_pS139
p53
PAR
PARP
Rad23A
Rad50
Rad51
Rb
Rb_pS807_S811
XRCC1
Normalized log(2) fold change in expression relative to untreated MCF-7 cells

Figure 3.3: Multi-omic analysis of ER+ breast cancer cells after CDK4/6 inhibition.

T47D cells were treated with 40nM palbociclib (**A**), 100nM ribociclib (**B**), or 20nM abemaciclib (**C**) for 16 hours to assess transcriptomic changes at the pathway level. Genes related to the cell cycle are globally suppressed in T47D cells treated with palbociclib (**D**). CDK4/6 inhibitor-resistant MCF-7 and T47D cell lines were generated using long term selection (**E**). Differentially expressed pathways in CDK4/6 inhibitor-resistant T47D Pal_{AR} (**F**), Rib_{AR} (**G**), or Abe_{AR} (**H**) cells treated with a CDK4/6 inhibitor for 16 hours compared to parental T47D cells treated with the corresponding CDK4/6 inhibitor. (**I**) Reverse phase protein lysate array (RPPA) data from MCF-7 and MCF-7 Pal_{AR} cells treated with 75nM palbociclib for 16 hours. Protein and phosphoprotein log2 expression values were normalized for total protein loading and shown as the fold change in expression over untreated MCF-7 cells. All p-values and pathway plots were FDR corrected, where red dots indicate significantly differentially expressed pathways and (unlabeled) grey pathways are not significantly changed. The yellow dot in panels A-F is used to denote the cell cycle.

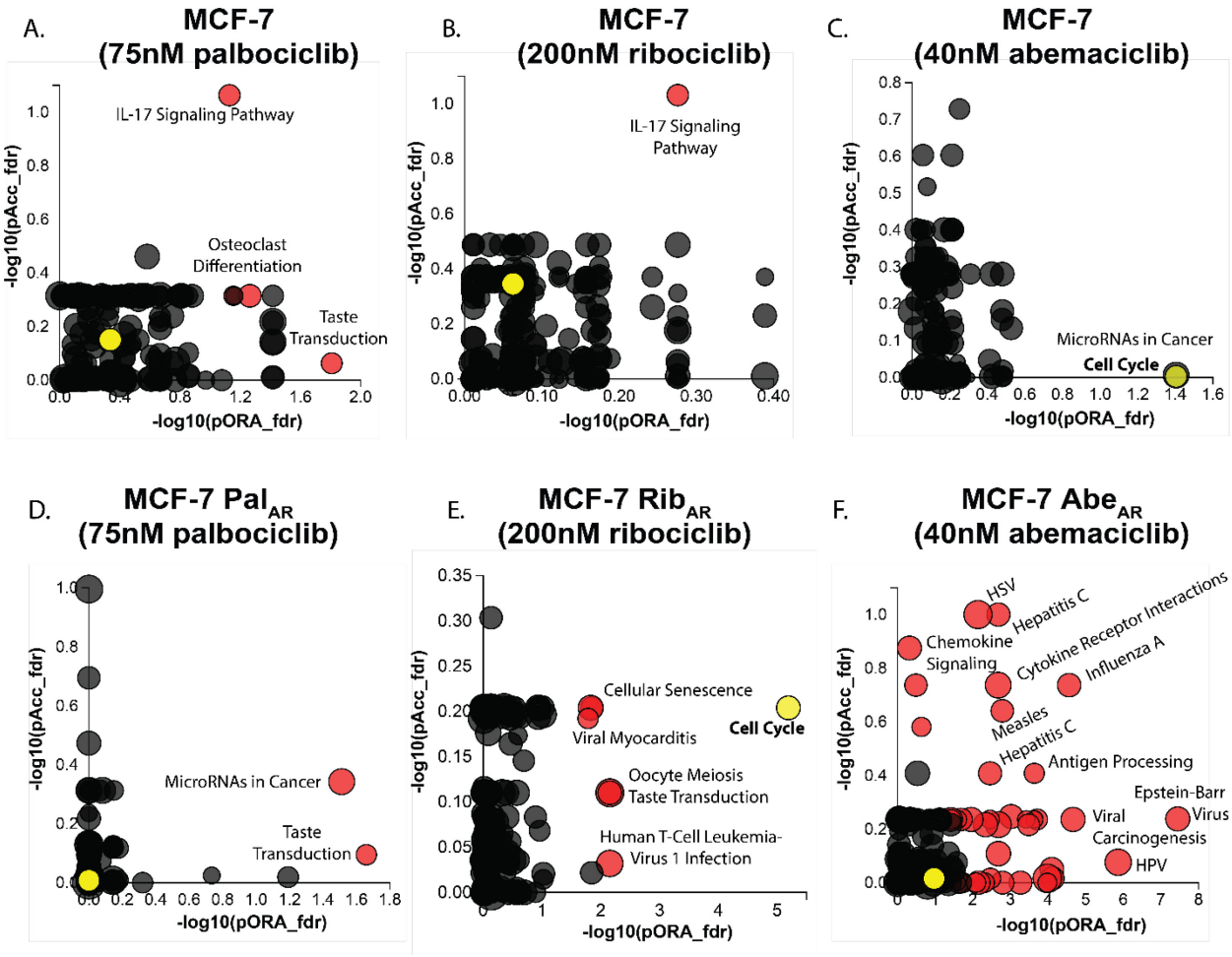

Figure 3.4: **Transcriptomic analysis of MCF-7 cells following CDK4/6 inhibition.**

MCF-7 cells were treated with 75nM palbociclib (**A**), 200nM ribociclib (**B**), or 40nM abemaciclib (**C**) for 16 hours and analyzed for pathways that were differentially expressed between parental cells and CDK4/6 inhibitor-treated cells. MCF7 Pal$_{AR}$ (**D**), Rib$_{AR}$ (**E**), and Abe$_{AR}$ (**F**) cells were also treated with CDK4/6 inhibition and compared to the wild-type MCF-7 parental cells treated with the corresponding CDK4/6 inhibitor. Red dots represent differentially expressed pathways, grey dots represent non-significant pathway changes, and the yellow dot is used to highlight the cell cycle pathway.

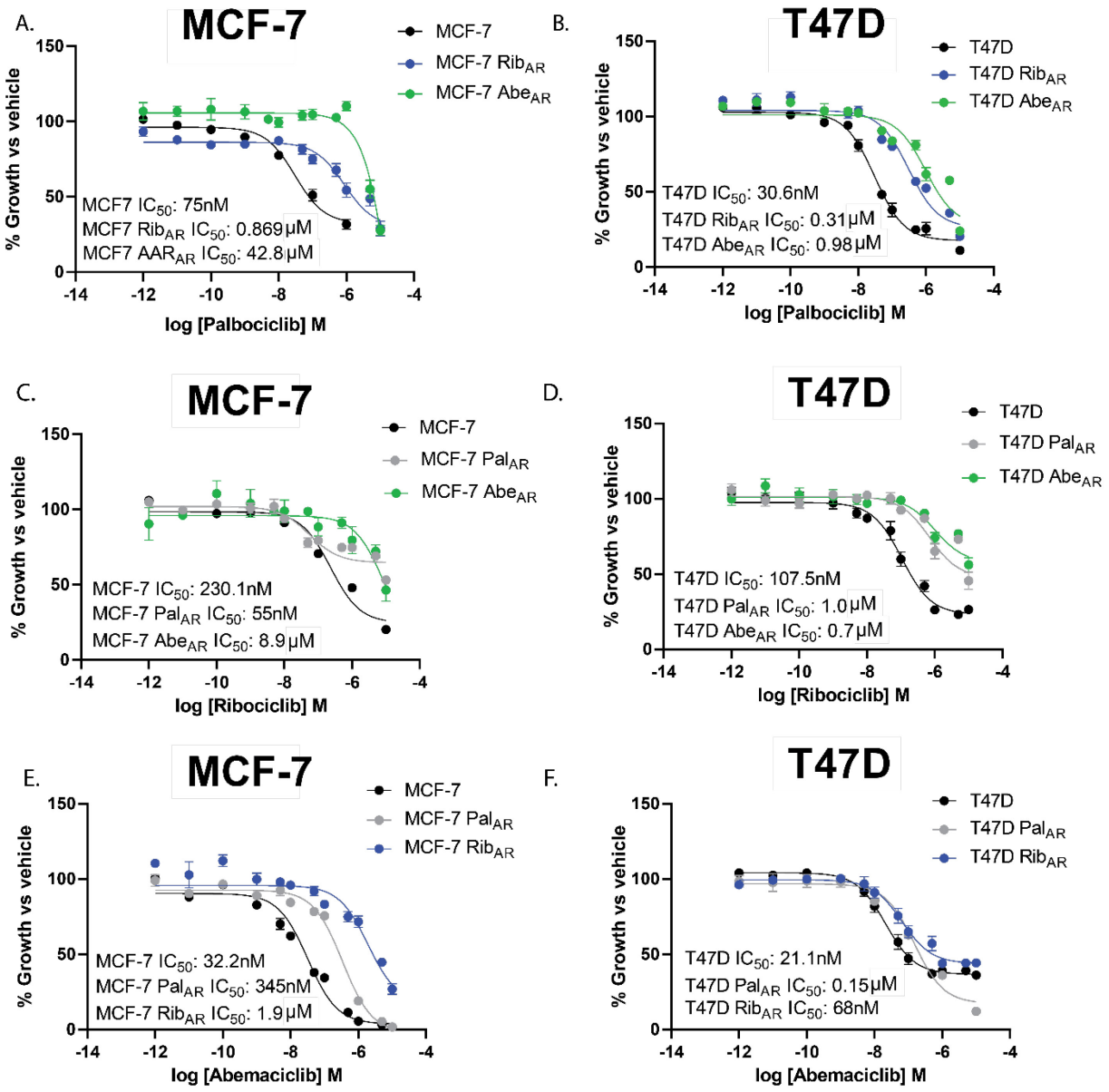

Figure 3.5: CDK4/6 inhibitor-resistant cells demonstrate cross-resistance.

CDK4/6 inhibitor resistant MCF-7 (**A, C, E**) and T47D (**B, D, F**) cells were treated with either palbociclib (**A,B**), ribociclib (**C,D**), or abemaciclib (**E,F**). Cell lines selected for resistance against one drug (such as Pal$_{AR}$ cells and palbociclib) were treated with each of the other two CDK4/6 inhibitors for 72 hours and viability was measured compared to vehicle (DMSO-treated) controls.

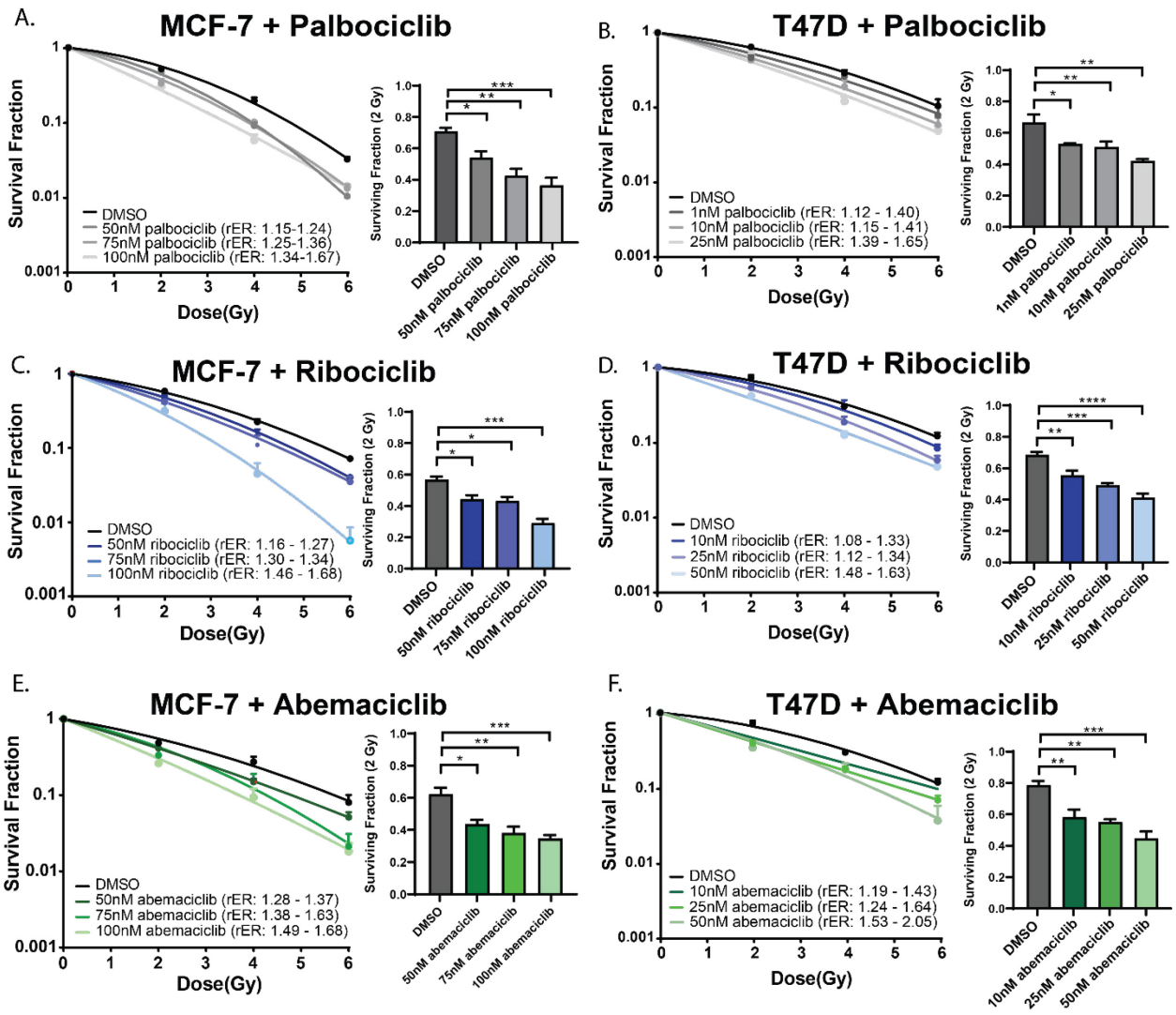

Figure 3.6: Concurrent pharmacological inhibition of CDK4/6 in ER+ breast cancer cell lines confers radiosensitivity.

Clonogenic survival assays were performed in MCF-7 (**A**) and T47D (**B**) cells with 1-hour pretreatment of the CDK4/6 inhibitor palbociclib at 1-100nM palbociclib. Clonogenics were also performed with ribociclib (**C,D**) and abemaciclib (**E,F**) and the surviving fraction of cells was calculated for each treatment condition at 2 Gy. Radiation enhancement ratios (rER) are shown. ($p < 0.05$ = *, $p < 0.01$ = **, $p < 0.001$ = ***).

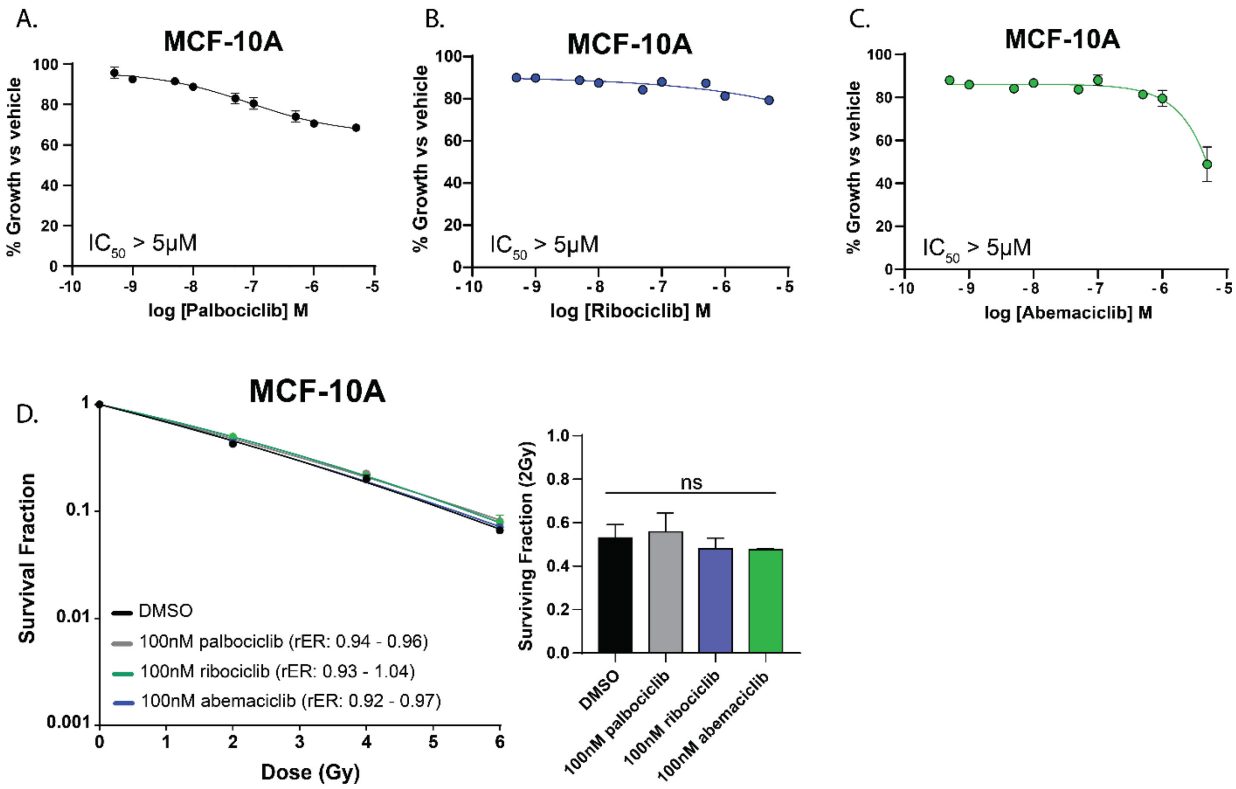

Figure 3.7: CDK4/6 inhibition and RT does not radiosensitize normal breast tissue cells.

CDK4/6 inhibition with palbociclib (**A**), ribociclib (**B**), and abemaciclib (**C**) in MCF-10A cells was assessed using Alamar blue-based proliferation assays. The surviving fraction of cells was calculated in clonogenic survival assays using 100nM of each of the three CDK4/6 inhibitors (**D**).

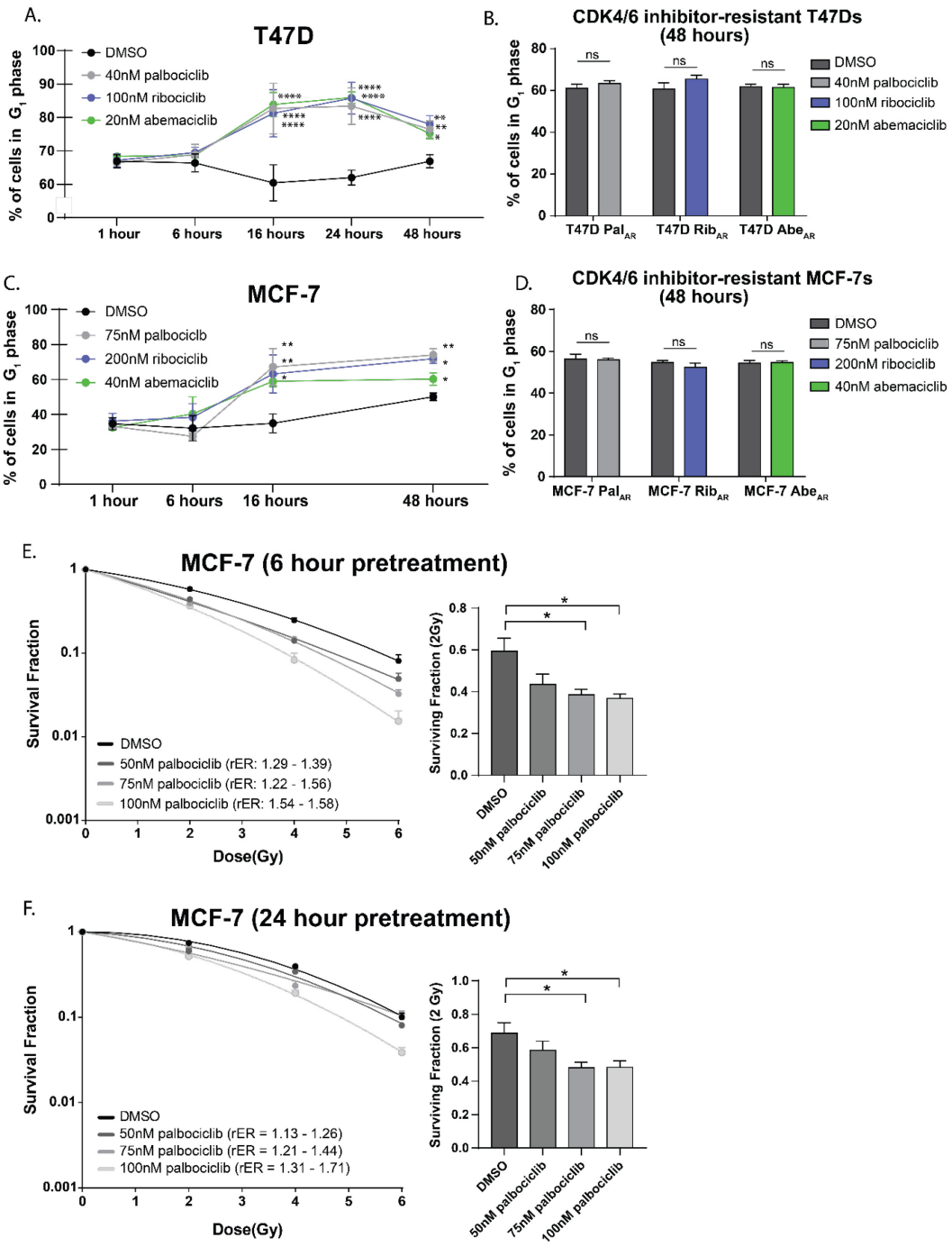

Figure 3.8: CDK4/6 inhibitor effects on radiosensitization are not explained exclusively by cell cycle changes.

Cell cycle changes were assessed in T47D (**A**) and MCF-7 (**C**) cells at predetermined timepoints after treatment with each of the CDK4/6 inhibitors (colored lines) using propidium iodide-based flow cytometry. CDK4/6 inhibitor resistant T47D (**B**) and MCF-7 (**D**) cells were treated ± CDK4/6 inhibition and cell cycle changes were assessed at 48 hours. Clonogenic survival assays were repeated in MCF-7 cells with a 6 hour pretreatment (**E**) or a 24 hour pretreatment (**F**) in contrast to the conventional one hour pretreatment used in all other assays.

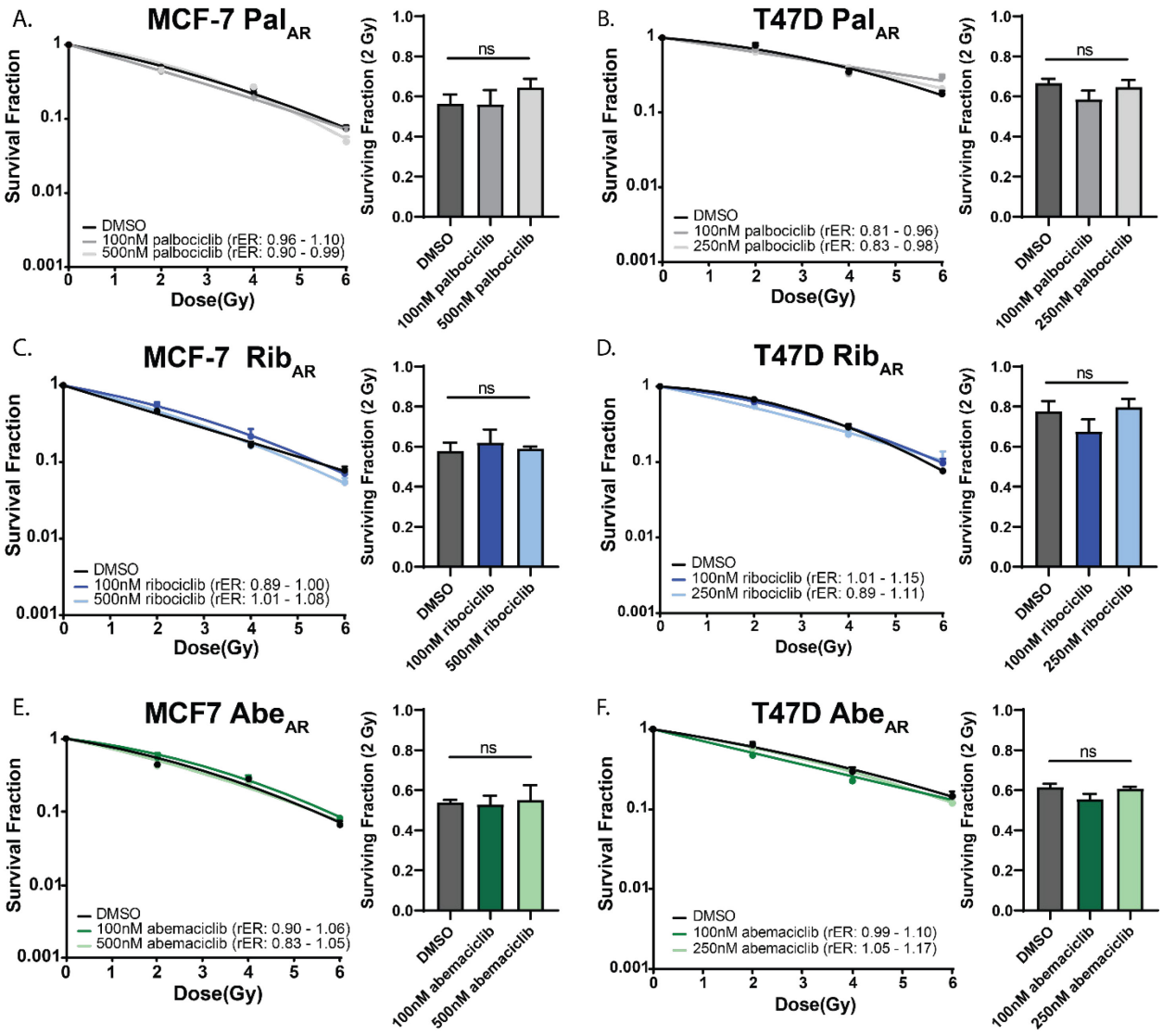

Figure 3.9: CDK4/6 inhibition does not radiosensitize CDK4/6 inhibitor-resistant cell lines.

After three months of selection in CDK4/6 inhibitor-containing media, clonogenic survival assays were repeated in MCF-7 Pal_{AR} (**A**) and T47D Pal_{AR} cells (**B**). Ribociclib- (**C,D**) and abemaciclib-resistant (**E,F**) cell lines were also unaffected by combination therapy. Radiation enhancement ratios (rER) are shown. Data are graphed as the mean ± SEM.

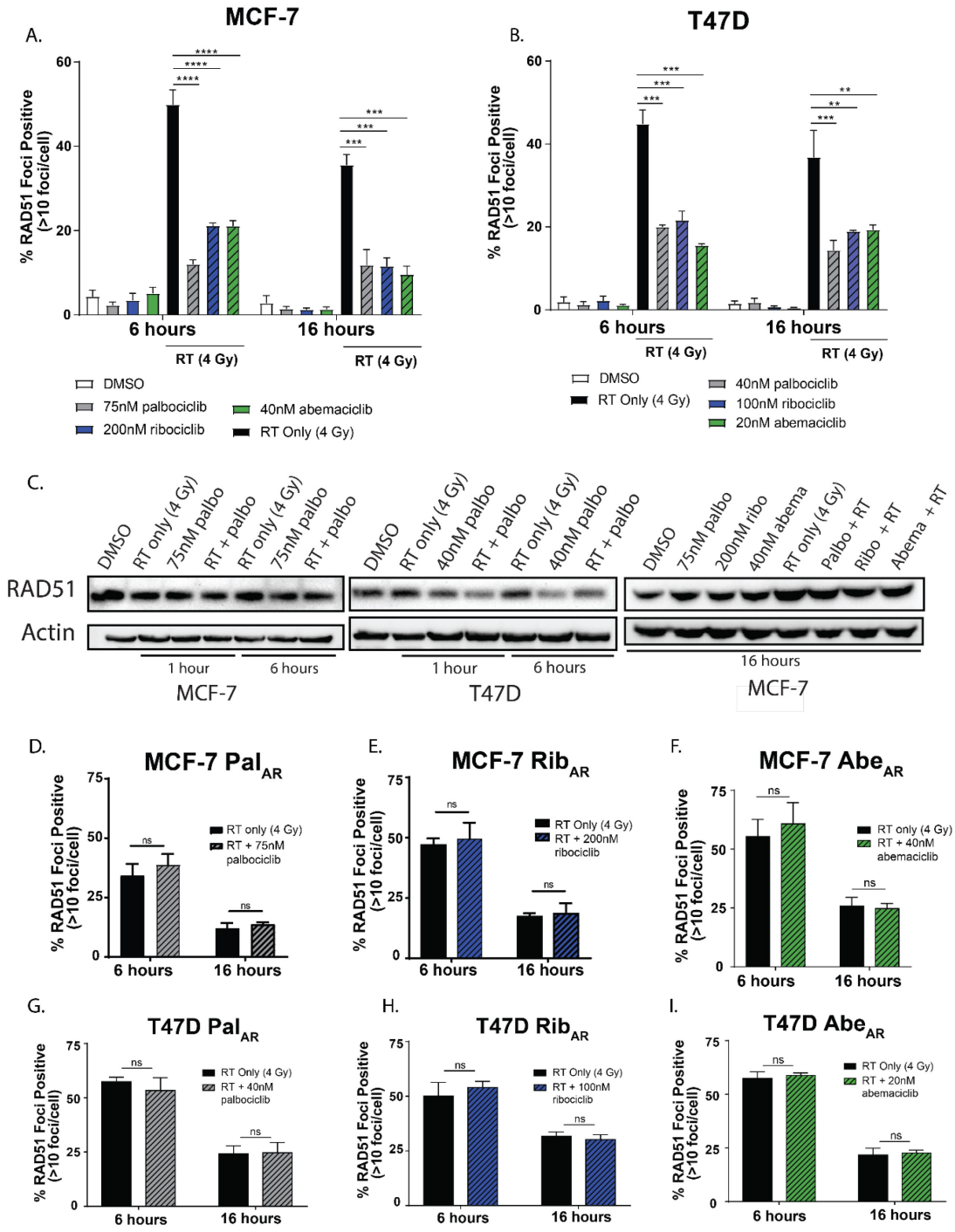

Figure 3.10: CDK4/6 inhibition suppresses HR in CDK4/6 inhibitor-sensitive cells.

After a 1-hour pretreatment ± CDK4/6 inhibition (colored bars), MCF-7 (**A**) and T47D (**B**) cells were treated ± 4 Gy RT (black / patterned bars) and slides were stained for immunofluorescent RAD51 foci 6- and 16-hours after radiation. Total RAD51 protein levels were assessed by western blot (**C**) at 1, 6, or 16 hours following radiation, with a one hour drug treatment prior to RT (4 Gy). CDK4/6 inhibitor-resistant cell lines were also used to assess RAD51 foci formation by immunofluorescence (**D-I**). Data points represent the average ± SEM.

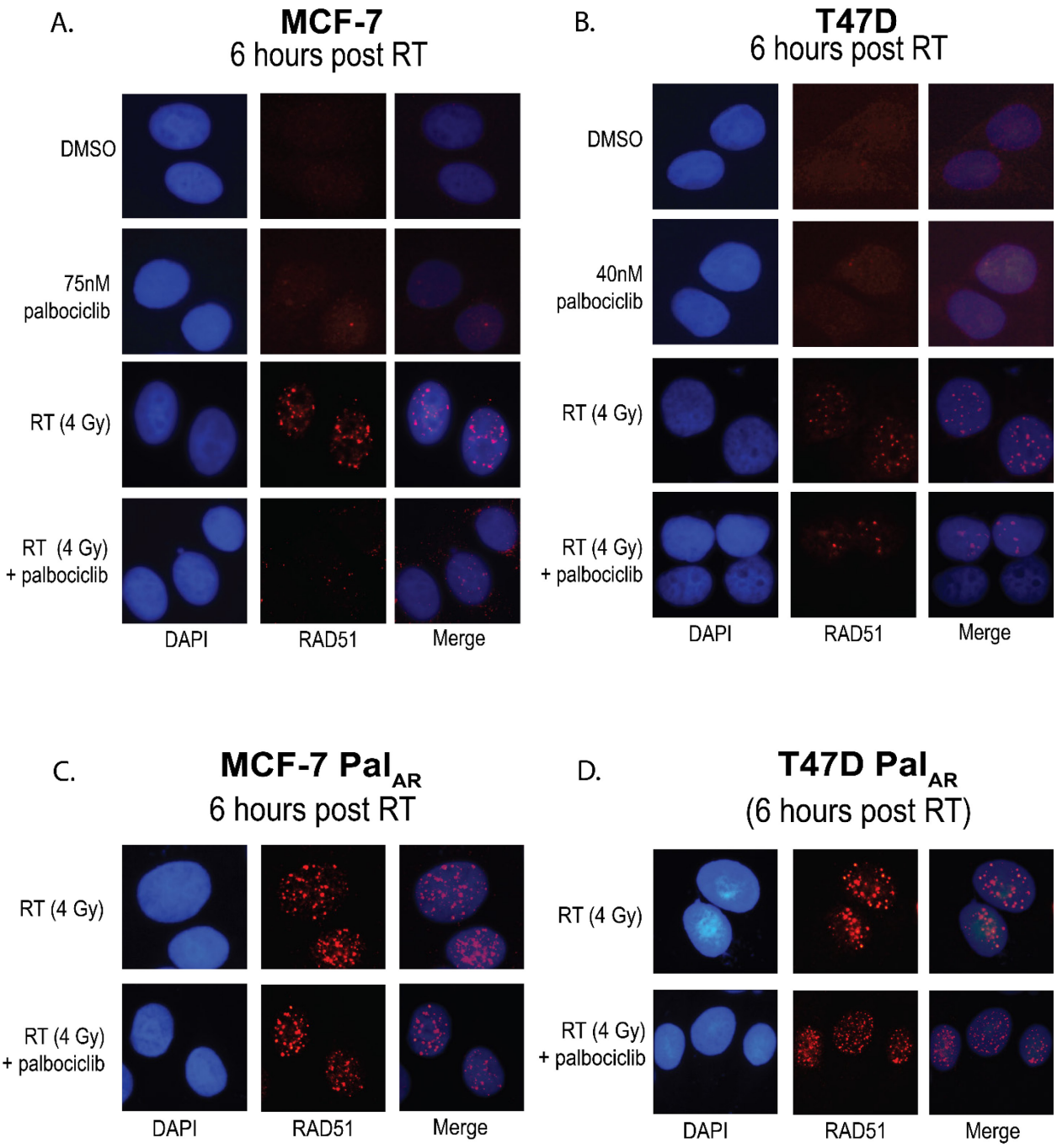

Figure 3.11: Representative Images for RAD51 immunofluorescence.

Sample images from MCF-7 (**A**) and T47D (**B**) cells treated ± palbociclib and ± 4 Gy RT are shown for all treatment conditions. Foci from the MCF-7 Pal$_{AR}$ (**C**) and T47D Pal$_{AR}$ cells (**D**) are shown for the RT (4 Gy) and combination treated groups. All images are from the 6 hour timepoint.

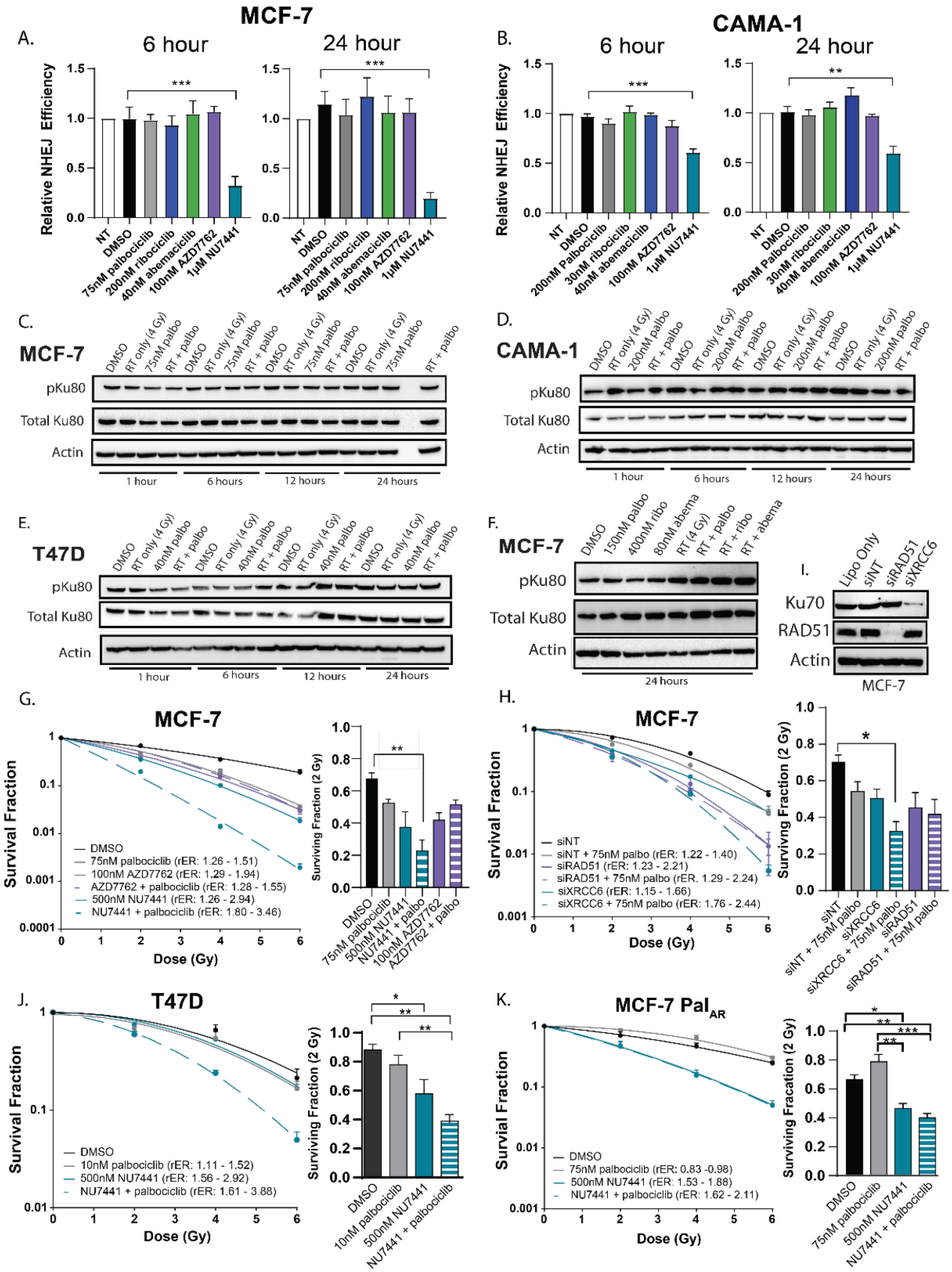
MCF-7
A.
6 hour
24 hour
Relative NHEJ Efficiency
NT
DMSO
75nM palbociclib
200nM ribociclib
40nM abemaciclib
100nM AZD7762
1μM NU7441
B.
CAMA-1
200nM Palbociclib
30nM ribociclib
C.
pKu80
Total Ku80
Actin
1 hour
6 hours
12 hours
24 hours
D.
E.
T47D
40nM palbo
F.
150nM palbo
400nM ribo
80nM abema
RT (4 Gy)
RT + palbo
RT + ribo
RT + abema
I.
Lipo Only
siNT
siRAD51
siXRCC6
Ku70
RAD51
G.
Survival Fraction
Dose (Gy)
DMSO
75nM palbociclib (rER: 1.26 - 1.51)
100nM AZD7762 (rER: 1.29 - 1.94)
AZD7762 + palbociclib (rER: 1.28 - 1.55)
500nM NU7441 (rER: 1.26 - 2.94)
NU7441 + palbociclib (rER: 1.80 - 3.46)
Surviving Fraction (2 Gy)
H.
siNT
siNT + 75nM palbo (rER: 1.22 - 1.40)
siRAD51 (rER: 1.23 - 2.21)
siRAD51 + 75nM palbo (rER. 1.29 - 2.24)
siXRCC6 (rER: 1.15 - 1.66)
siXRCC6 + 75nM palbo (rER: 1.76 - 2.44)
J.
T47D
10nM palbociclib (rER: 1.11 - 1.52)
500nM NU7441 (rER: 1.56 - 2.92)
NU7441 + palbociclib (rER: 1.61 - 3.88)
K.
MCF-7 Pal$_{AR}$
75nM palbociclib (rER: 0.83 -0.98)
500nM NU7441 (rER: 1.53 - 1.88)
NU7441 + palbociclib (rER: 1.62 - 2.11)

Figure 3.12: CDK4/6 inhibition does not suppress NHEJ efficiency in breast cancer cells.

A GFP reporter system was used to assess relative NHEJ efficiency in MCF-7 (**A**) and CAMA1 (**B**) cells at 6- and 24-hours following CDK4/6 inhibitor treatment. DNAPK inhibition (1μM NU7441) was used as a positive control and CHK1/2 inhibition (100nM AZD7762) was used as a negative control in this assay. Western blots (**C-E**) were used to assess pKu80 and Ku80 expression at 1, 6, 12, and 24 hours after RT (4 Gy) and a 1-hour drug pretreatment. Western blots were also used to assess pKu80/Ku80 expression at 24 hours after treatment of MCF-7 cells with higher concentrations of CDK4/6 inhibition (**F**). Clonogenics were performed in MCF-7 (**G**), T47D (**J**), and MCF-7 Pal_{AR} cells (**K**) with palbociclib in combination with RT and either NU7441 (teal) and/or AZD7762 (purple). MCF-7 cells were also used for clonogenics with siXRCC6 and siRAD51 (**H**) ± 75nM palbociclib. Protein was harvested 48 hours after transfection (the timepoint at which clonogenics are radiated) to demonstrate successful RAD51 and Ku70 protein knockdown (**I**). Data points represent the average ± SEM ($p < 0.05$ = *, $p < 0.01$ = **, $p < 0.001$ = ***).

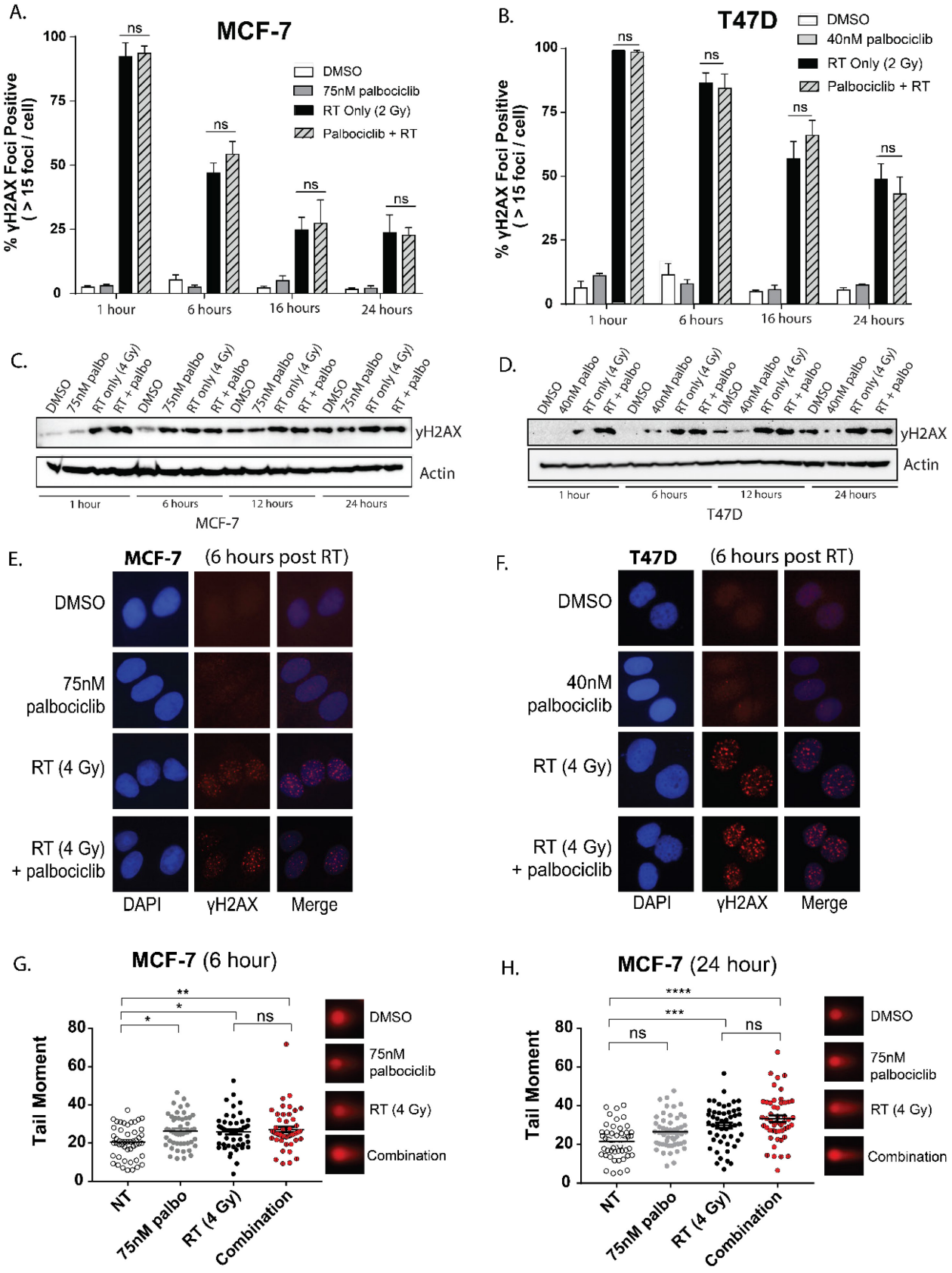
A.
MCF-7
% γH2AX Foci Positive (> 15 foci / cell)
DMSO
75nM palbociclib
RT Only (2 Gy)
Palbociclib + RT
ns
1 hour
6 hours
16 hours
24 hours
B.
T47D
DMSO
40nM palbociclib
RT Only (2 Gy)
Palbociclib + RT
C.
DMSO
75nM palbo
RT only (4 Gy)
RT + palbo
γH2AX
Actin
1 hour
6 hours
12 hours
24 hours
MCF-7
D.
DMSO
40nM palbo
RT only (4 Gy)
RT + palbo
T47D
E.
MCF-7 (6 hours post RT)
DMSO
75nM palbociclib
RT (4 Gy)
RT (4 Gy) + palbociclib
DAPI
γH2AX
Merge
F.
T47D (6 hours post RT)
40nM palbociclib
G.
MCF-7 (6 hour)
Tail Moment
NT
75nM palbo
RT (4 Gy)
Combination
H.
MCF-7 (24 hour)

Figure 3.13: dsDNA breaks are not potentiated with CDK4/6 inhibition.

In MCF-7 (**A**) and T47D (**B**) cells, γH2AX foci formation was measured at 1, 6, 16, and 24 hours after RT (2 Gy) and a one hour palbociclib pretreatment. Representative foci are shown at the 6 hour timepoint (**E,F**). Total γH2AX was assessed by western blot (**C,D**) with the same pretreatment and post-radiation time points. The neutral COMET assay **(G, H)** was used to quantify the tail moment (a surrogate measure for dsDNA breaks) in MCF-7 cells at 6 and 24 hours ± RT (4 Gy) and ± a one hour, 75nM pretreatment with palbociclib. ($p < 0.05$ = *, $p < 0.01$ = **, $p < 0.001$ = ***, $p < 0.0001$ = ****).

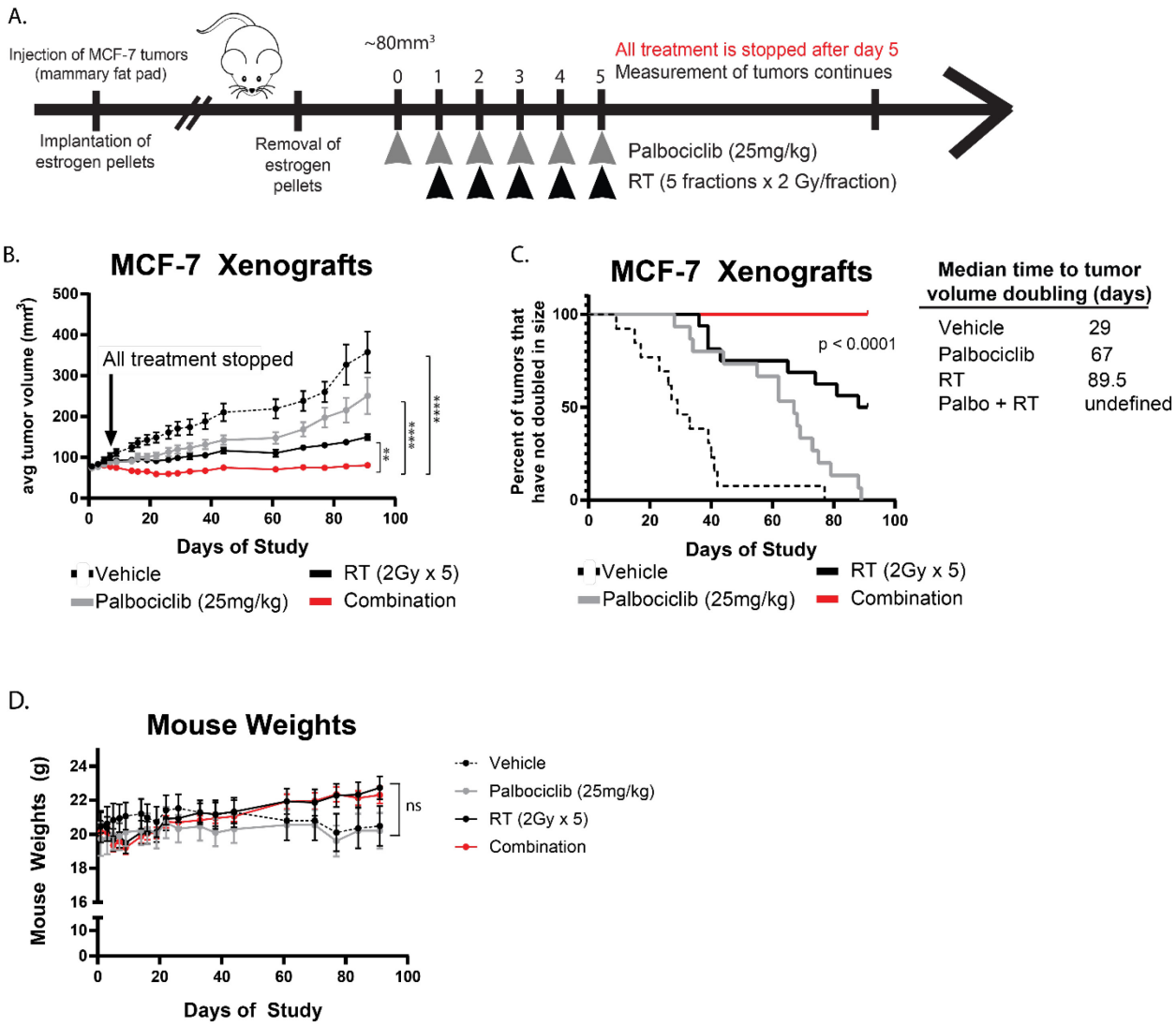

Figure 3.14: CDK4/6 inhibition radiosensitizes ER+ breast cancer cells *in vivo*.

MCF-7 cells were used to generate orthotopic xenograft tumors in the mammary fat pads of CB17-SCID mice. Once tumors reached 80mm^3, mice were treated with either vehicle, palbociclib alone (25mg/kg), RT alone (5 x 2 Gy), or the combination and all treatment was stopped on the 5th day as indicated (**A**). Tumor size (**B**) was measured throughout the duration of the study and used to calculate the time to tumor doubling (**C**). Mouse weights (**D**) were recorded on the same days that tumor measurements were taken. ($p < 0.05$ = *, $p < 0.01$ = **, $p < 0.001$ = ***).

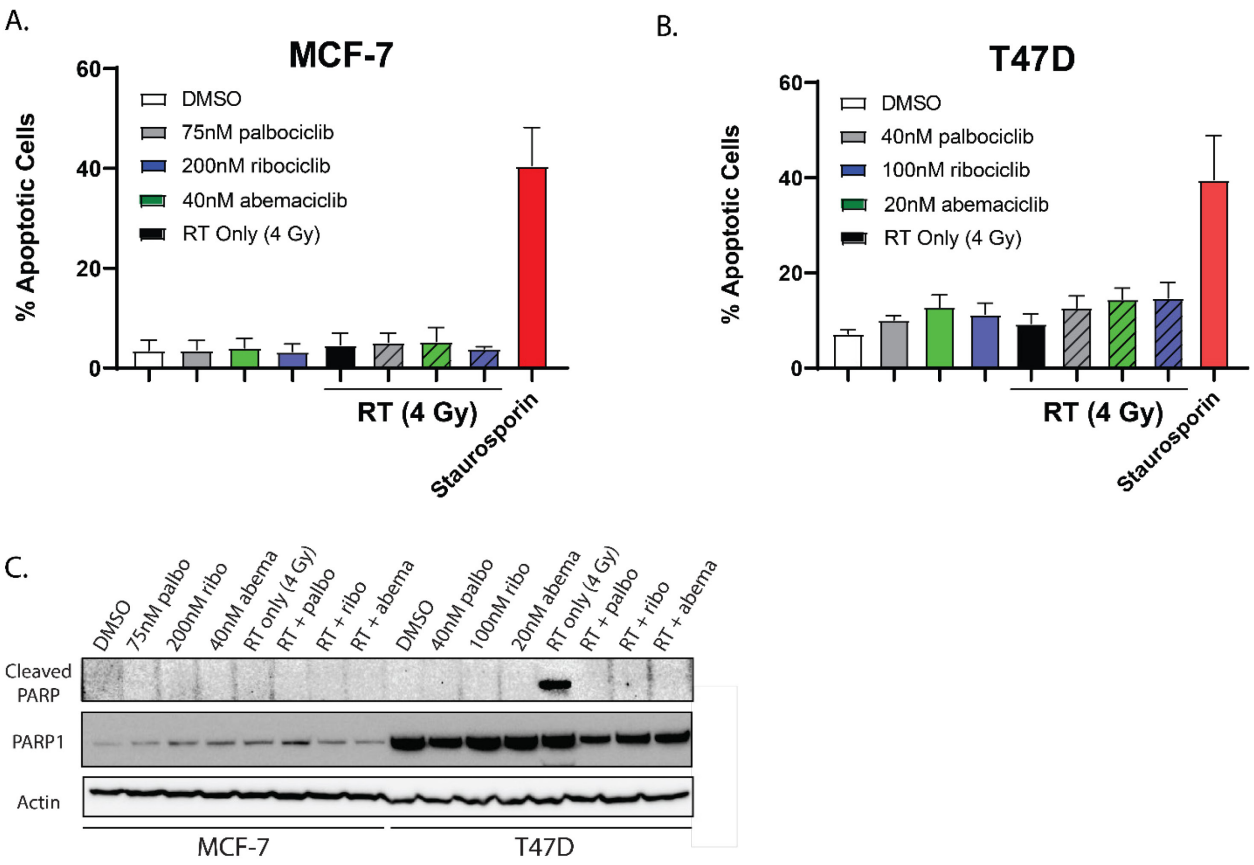

Figure 3.15: CDK4/6 inhibition + RT does not increase apoptosis.

Flow cytometry was used to assess apoptosis in live MCF-7 (**A**) and T47D (**B**) cells based on annexin V (FITC) and propidium iodide staining. The percentages of early and late apoptotic cells were added together and the total number of apoptotic cells was graphed as a percent of the total cells assayed. 500nM staurosporin (red) was used as a positive control. Cells were treated with drug alone (colored bars), 4 Gy RT alone (black bar) or the combination (patterned bars) and harvested at 48 hours for analysis. In combination treated cells, drug was added 1 hour before RT. Using the same experimental conditions, cells were also harvested for western blot analysis (**C**) of cleaved PARP and total PARP1 protein.

A.

MCF-7 Clonogenic Survival Assay (Palbociclib)		
Treatment	Enhancement Ratio	Cytotoxicity
DMSO	1.0	1.0
50 nM palbociclib	1.22 ± 0.06	0.70 ± 0.12
75 nM palbociclib	1.31 ± 0.06	0.67 ± 0.14
100 nM palbociclib	1.52 ± 0.14	0.53 ± 0.08

MCF-7 Clonogenic Survival Assay (Ribociclib)		
Treatment	Enhancement Ratio	Cytotoxicity
DMSO	1.0	1.0
50 nM ribociclib	1.20 ± 0.05	0.88 ± 0.04
75 nM ribociclib	1.33 ± 0.02	0.69 ± 0.10
100 nM ribociclib	1.58 ± 0.11	0.64 ± 0.02

MCF-7 Clonogenic Survival Assay (Abemaciclib)		
Treatment	Enhancement Ratio	Cytotoxicity
DMSO	1.0	1.0
50 nM abemaciclib	1.34 ± 0.05	0.78 ± 0.05
75 nM abemaciclib	1.51 ± 0.15	0.80 ± 0.09
100 nM abemaciclib	1.59 ± 0.13	0.44 ± 0.06

B.

T47D Clonogenic Survival Assay (Palbociclib)		
Treatment	Enhancement Ratio	Cytotoxicity
DMSO	1.0	1.0
1 nM palbociclib	1.23 ± 0.15	0.99 ± 0.14
10 nM palbociclib	1.29 ± 0.13	0.54 ± 0.11
25 nM palbociclib	1.50 ± 0.13	0.29 ± 0.05

T47D Clonogenic Survival Assay (Ribociclib)		
Treatment	Enhancement Ratio	Cytotoxicity
DMSO	1.0	1.0
10 nM ribociclib	1.20 ± 0.12	0.85 ± 0.13
25 nM ribociclib	1.28 ± 0.11	0.78 ± 0.15
50 nM ribociclib	1.58 ± 0.07	0.57 ± 0.15

T47D Clonogenic Survival Assay (Abemaciclib)		
Treatment	Enhancement Ratio	Cytotoxicity
DMSO	1.0	1.0
10 nM abemaciclib	1.31 ± 0.11	0.88 ± 0.22
25 nM abemaciclib	1.38 ± 0.23	0.74 ± 0.20
50nM abemaciclib	1.81 ± 0.26	0.69 ± 0.11

C

CAMA-1 Clonogenic Survival Assay (Palbociclib)		
Treatment	Enhancement Ratio	Cytotoxicity
DMSO	1.0	1.0
25nM palbociclib	1.17 ± 0.04	0.92 ± 0.13
50nM palbociclib	1.16 ± 0.06	0.72 ± 0.05
75nM palbociclib	1.30 ± 0.09	0.51 ± 0.10

D.

ZR-75-1 Clonogenic Assay (Palbociclib)		
Treatment	Enhancement Ratio	Cytotoxicity
DMSO	1.0	1.0
50 nM palbociclib	1.21 ± 0.15	0.81 ± 0.14
100 nM palbociclib	1.27 ± 0.14	0.47 ± 0.16

Table 3.1: Toxicity and radiation enhancement ratios for MCF-7, T47D, CAMA-1, and ZR-75-1 cells treated with CDK4/6 inhibition and RT.

A.

MCF-7 Pal_{AR} Clonogenic Assay (Palbociclib)		
Treatment	Enhancement Ratio	Cytotoxicity
DMSO	1.0	1.0
100nM palbociclib	1.03 ± 0.07	0.95 ± 0.04
500nM palbociclib	0.95 ± 0.05	0.82 ± 0.13

B.

T47D Pal_{AR} Clonogenic Assay (Palbociclib)		
Treatment	Enhancement Ratio	Cytotoxicity
DMSO	1.0	1.0
100nM palbociclib	0.90 ± 0.07	0.75 ± 0.17
250nM palbociclib	0.92 ± 0.08	0.70 ± 0.32

C.

MCF-7 Rib_{AR} Clonogenic Assay (Ribociclib)		
Treatment	Enhancement Ratio	Cytotoxicity
DMSO	1.0	1.0
100nM ribociclib	0.97 ± 0.11	0.75 ± 0.19
500nM ribociclib	1.03 ± 0.04	0.85 ± 0.06

D.

T47D Rib_{AR} Clonogenic Assay (Ribociclib)		
Treatment	Enhancement Ratio	Cytotoxicity
DMSO	1.0	1.0
100nM ribociclib	1.08 ± 0.07	0.47 ± 0.11
250nM ribociclib	1.01 ± 0.11	0.33 ± 0.13

E.

MCF-7 Abe_{AR} Clonogenic Assay (Abemaciclib)		
Treatment	Enhancement Ratio	Cytotoxicity
DMSO	1.0	1.0
100nM abemaciclib	0.96 ± 0.08	0.85 ± 0.08
500nM abemaciclib	0.92 ± 0.11	0.81 ± 0.26

F.

T47D Abe_{AR} Clonogenic Assay (Abemaciclib)		
Treatment	Enhancement Ratio	Cytotoxicity
DMSO	1.0	1.0
100nM abemaciclib	1.06 ± 0.06	0.95 ± 0.16
250nM abemaciclib	1.10 ± 0.06	0.58 ± 0.15

Table 3.2: Toxicity and radiation enhancement ratios for CDK4/6 inhibitor-resistant MCF-7 and T47D cells treated with CDK4/6 inhibition and RT.

A.

MCF-10A Clonogenic Assay		
Treatment	Enhancement Ratio	Cytotoxicity
DMSO	1.0	1.0
100nM palbociclib	0.95 ± 0.01	0.47 ± 0.13
100nM ribociclib	0.99 ± 0.08	0.87 ± 0.09
100nM abemaciclib	0.95 ± 0.02	0.54 ± 0.03

Table 3.3: Toxicity and radiation enhancement ratios for MCF10A cells treated with CDK4/6 inhibition and RT.

MCF-7 Clonogenic Assay (6 hour pretreatment)		
Treatment	Enhancement Ratio	Cytotoxicity
DMSO	1.0	1.0
50 nM palbociclib	1.33 ± 0.05	0.81 ± 0.10
75 nM palbociclib	1.37 ± 0.17	0.66 ± 0.06
100 nM palbociclib	1.57 ± 0.02	0.64 ± 0.11

B.

MCF-7 Clonogenic Assay (24 hour pretreatment)		
Treatment	Enhancement Ratio	Cytotoxicity
DMSO	1.0	1.0
50 nM palbociclib	1.29 ± 0.07	0.74 ± 0.16
75 nM palbociclib	1.33 ± 0.11	0.67 ± 0.16
100 nM palbociclib	1.48 ± 0.20	0.59 ± 0.10

Table 3.4: Toxicity and radiation enhancement ratios for MCF-7 cells treated with CDK4/6 inhibition and RT with either a 6 hour or 24 hour pretreatment.

A.

MCF-7 Clonogenic Assay (NU7441, AZD7762)		
Treatment	Enhancement Ratio	Cytotoxicity
DMSO	1.0	1.0
75nM palbociclib	1.35 ± 0.11	0.83 ± 0.07
500nM NU7441	1.97 ± 0.71	0.99 ± 0.19
NU7441 + palbo	2.70 ± 0.87	0.85 ± 0.04
100nM AZD7762	1.60 ± 0.29	0.24 ± 0.05
AZD7762 + palbo	1.36 ± 0.13	0.28 ± 0.04

B.

MCF-7 Clonogenic Assay (siNT, siRAD51, siXRCC6)		
Treatment	Enhancement Ratio	Cytotoxicity
siNT	1.0	1.0
siNT + 75nM palbo	1.33 ± 0.11	0.79 ± 0.18
siXRCC6	1.44 ± 0.26	0.36 ± 0.20
siXRCC6 + palbo	2.08 ± 0.34	0.15 ± 0.15
siRAD51	1.69 ± 0.51	0.09 ± 0.05
siRAD51 + palbo	1.87 ± 0.58	0.04 ± 0.03

C.

T47D Clonogenic Assay (NU7441)		
Treatment	Enhancement Ratio	Cytotoxicity
DMSO	1.0	1.0
10nM palbociclib	1.29 ± 0.17	1.26 ± 0.15
500nM NU7441	2.22 ± 0.70	1.03 ± 0.60
NU7441 + palbo	2.51 ± 0.09	1.28 ± 0.36

D.

MCF7 Pal_{AR} Clonogenic Assay (NU7441)		
Treatment	Enhancement Ratio	Cytotoxicity
DMSO	1.0	1.0
75nM palbociclib	0.89 ± 0.08	0.82 ± 0.06
500nM NU7441	1.67 ± 0.19	0.91 ± 0.09
NU7441 + palbo	1.88 ± 0.24	0.89 ± 0.09

Table 3.5: Toxicity and radiation enhancement ratios for MCF-7 and T47D cells.

Cells were treated with either NU7441, AZD7762, and palbociclib (**A,C**), MCF-7 cells transfected with siNT, siXRCC6, or siRAD51 and palbociclib (**B**), or MCF-7 Pal_{AR} cells treated with NU7441 and palbociclib (**D**).

MCF-7 Xenografts (FTV)			Combination		
Day	RT	Palbo	Expected	Observed	Ratio
9	0.822	0.795	0.654	0.671	0.974
26	0.584	0.704	0.411	0.373	1.103
38	0.558	0.699	0.390	0.358	1.090
61	0.505	0.674	0.340	0.323	1.055
77	0.499	0.759	0.379	0.286	1.326

Table 3.6: Synergy calculations for the expected and observed tumor sizes in MCF-7 xenografts. Synergy is indicated by a ratio of expected/observed > 1.

References

1. Menta A, Fouad TM, Lucci A, Le-Petross H, Stauder MC, Woodward WA*, et al.* Inflammatory Breast Cancer: What to Know About This Unique, Aggressive Breast Cancer. Surg Clin North Am 2018;98(4):787-800 doi 10.1016/j.suc.2018.03.009.
2. Li J, Xia Y, Wu Q, Zhu S, Chen C, Yang W*, et al.* Outcomes of patients with inflammatory breast cancer by hormone receptor-and HER2-defined molecular subtypes: A population-based study from the SEER program. Oncotarget 2017;8(30):49370.
3. Ross JS, Ali SM, Wang K, Khaira D, Palma NA, Chmielecki J*, et al.* Comprehensive genomic profiling of inflammatory breast cancer cases reveals a high frequency of clinically relevant genomic alterations. Breast Cancer Res Treat 2015;154(1):155-62 doi 10.1007/s10549-015-3592-z.
4. Wedam SB, Low JA, Yang SX, Chow CK, Choyke P, Danforth D*, et al.* Antiangiogenic and antitumor effects of bevacizumab in patients with inflammatory and locally advanced breast cancer. J Clin Oncol 2006;24(5):769-77 doi 10.1200/jco.2005.03.4645.
5. Yang SX, Steinberg SM, Nguyen D, Wu TD, Modrusan Z, Swain SM. Gene expression profile and angiogenic marker correlates with response to neoadjuvant bevacizumab followed by bevacizumab plus chemotherapy in breast cancer. Clin Cancer Res 2008;14(18):5893-9 doi 10.1158/1078-0432.ccr-07-4762.
6. Bourgier C, Pessoa EL, Dunant A, Heymann S, Spielmann M, Uzan C*, et al.* Exclusive alternating chemotherapy and radiotherapy in nonmetastatic inflammatory breast cancer: 20 years of follow-up. Int J Radiat Oncol Biol Phys 2012;82(2):690-5 doi 10.1016/j.ijrobp.2010.11.040.
7. Gelmon KA, Tischkowitz M, Mackay H, Swenerton K, Robidoux A, Tonkin K*, et al.* Olaparib in patients with recurrent high-grade serous or poorly differentiated ovarian carcinoma or triple-negative breast cancer: a phase 2, multicentre, open-label, non-randomised study. Lancet Oncol 2011;12(9):852-61 doi 10.1016/s1470-2045(11)70214-5.
8. Dent RA, Lindeman GJ, Clemons M, Wildiers H, Chan A, McCarthy NJ*, et al.* Phase I trial of the oral PARP inhibitor olaparib in combination with paclitaxel for first- or second-line treatment of patients with metastatic triple-negative breast cancer. Breast Cancer Res. Volume 152013. p R88.
9. Comen EA, Robson M. Poly(ADP-Ribose) Polymerase Inhibitors in Triple-Negative Breast Cancer. Cancer J 2010;16(1):48-52 doi 10.1097/PPO.0b013e3181cf01eb.
10. Feng FY, Speers C, Liu M, Jackson WC, Moon D, Rinkinen J*, et al.* Targeted radiosensitization with PARP1 inhibition: optimization of therapy and identification of biomarkers of response in breast cancer. Breast Cancer Res Treat 2014;147(1):81-94 doi 10.1007/s10549-014-3085-5.
11. Donawho CK, Luo Y, Penning TD, Bauch JL, Bouska JJ, Bontcheva-Diaz VD*, et al.* ABT-888, an orally active poly(ADP-ribose) polymerase inhibitor that potentiates DNA-damaging agents in preclinical tumor models. Clin Cancer Res 2007;13(9):2728-37 doi 10.1158/1078-0432.ccr-06-3039.
12. Elstrodt F, Hollestelle A, Nagel JH, Gorin M, Wasielewski M, van den Ouweland A*, et al.* BRCA1 mutation analysis of 41 human breast cancer cell lines reveals three new deleterious mutants. Cancer Res 2006;66(1):41-5 doi 10.1158/0008-5472.can-05-2853.

13. Skov K, Macphail S. Interaction of platinum drugs with clinically relevant x-ray doses in mammalian cells: a comparison of cisplatin, carboplatin, iproplatin, and tetraplatin. International Journal of Radiation Oncology* Biology* Physics 1991;20(2):221-5.
14. Zhang X, Yang H, Gu K, Chen J, Rui M, Jiang G-L. In vitro and in vivo study of a nanoliposomal cisplatin as a radiosensitizer. International journal of nanomedicine 2011;6:437.
15. Matar P, Rojo F, Cassia R, Moreno-Bueno G, Di Cosimo S, Tabernero J*, et al.* Combined epidermal growth factor receptor targeting with the tyrosine kinase inhibitor gefitinib (ZD1839) and the monoclonal antibody cetuximab (IMC-C225): superiority over single-agent receptor targeting. Clinical cancer research : an official journal of the American Association for Cancer Research 2004;10(19):6487-501 doi 10.1158/1078-0432.ccr-04-0870.
16. Althubiti M, Lezina L, Carrera S, Jukes-Jones R, Giblett SM, Antonov A*, et al.* Characterization of novel markers of senescence and their prognostic potential in cancer. Cell Death Dis 2014;5:e1528 doi 10.1038/cddis.2014.489.
17. Wolfe AR, Debeb BG, Lacerda L, Larson R, Bambhroliya A, Huang X*, et al.* Simvastatin prevents triple-negative breast cancer metastasis in pre-clinical models through regulation of FOXO3a. Breast Cancer Res Treat 2015;154(3):495-508 doi 10.1007/s10549-015-3645-3.
18. Van Wyhe RD, Rahal OM, Woodward WA. Effect of statins on breast cancer recurrence and mortality: a review. Breast Cancer (Dove Med Press) 2017;9:559-65 doi 10.2147/bctt.s148080.
19. Brewer TM, Masuda H, Liu DD, Shen Y, Liu P, Iwamoto T*, et al.* Statin use in primary inflammatory breast cancer: a cohort study. British journal of cancer 2013;109(2):318-24 doi 10.1038/bjc.2013.342.
20. Reddy JP, Atkinson RL, Larson R, Burks JK, Smith D, Debeb BG*, et al.* Mammary stem cell and macrophage markers are enriched in normal tissue adjacent to inflammatory breast cancer. Breast Cancer Res Treat 2018;171(2):283-93 doi 10.1007/s10549-018-4835-6.
21. Allen SG, Chen Y-C, Madden JM, Fournier CL, Altemus MA, Hiziroglu AB*, et al.* Macrophages enhance migration in inflammatory breast cancer cells via RhoC GTPase signaling. Scientific reports 2016;6:39190.
22. Rahal OM, Wolfe AR, Mandal PK, Larson R, Tin S, Jimenez C*, et al.* Blocking Interleukin (IL)4- and IL13-Mediated Phosphorylation of STAT6 (Tyr641) Decreases M2 Polarization of Macrophages and Protects Against Macrophage-Mediated Radioresistance of Inflammatory Breast Cancer. Int J Radiat Oncol Biol Phys 2018;100(4):1034-43 doi 10.1016/j.ijrobp.2017.11.043.
23. Wolfe AR, Trenton NJ, Debeb BG, Larson R, Ruffell B, Chu K*, et al.* Mesenchymal stem cells and macrophages interact through IL-6 to promote inflammatory breast cancer in pre-clinical models. Oncotarget 2016;7(50):82482-92 doi 10.18632/oncotarget.12694.
24. Bertucci F, Finetti P, Vermeulen P, Van Dam P, Dirix L, Birnbaum D*, et al.* Genomic profiling of inflammatory breast cancer: a review. Breast 2014;23(5):538-45 doi 10.1016/j.breast.2014.06.008.
25. Bertucci F, Finetti P, Colpaert C, Mamessier E, Parizel M, Dirix L*, et al.* PDL1 expression in inflammatory breast cancer is frequent and predicts for the pathological response to chemotherapy. Oncotarget 2015;6(15):13506-19 doi 10.18632/oncotarget.3642.

26. Hamm CA, Moran D, Rao K, Trusk PB, Pry K, Sausen M*, et al.* Genomic and Immunological Tumor Profiling Identifies Targetable Pathways and Extensive CD8+/PDL1+ Immune Infiltration in Inflammatory Breast Cancer Tumors. Mol Cancer Ther 2016;15(7):1746-56 doi 10.1158/1535-7163.mct-15-0353.
27. Jhaveri K, Teplinsky E, Silvera D, Valeta-Magara A, Arju R, Giashuddin S*, et al.* Hyperactivated mTOR and JAK2/STAT3 pathways: molecular drivers and potential therapeutic targets of inflammatory and invasive ductal breast cancers after neoadjuvant chemotherapy. Clinical breast cancer 2016;16(2):113-22. e1.
28. Wynn ML, Yates JA, Evans CR, Van Wassenhove LD, Wu ZF, Bridges S*, et al.* RhoC GTPase is a potent regulator of glutamine metabolism and N-acetylaspartate production in inflammatory breast cancer cells. Journal of Biological Chemistry 2016;291(26):13715-29.
29. Joglekar M, Elbezanti WO, Weitzman MD, Lehman HL, van Golen KL. Caveolin-1 mediates inflammatory breast cancer cell invasion via the Akt1 pathway and RhoC GTPase. J Cell Biochem 2015;116(6):923-33 doi 10.1002/jcb.25025.
30. Balamurugan K, Sterneck E. The Many Faces of C/EBPδ and their Relevance for Inflammation and Cancer. Int J Biol Sci. Volume 92013. p 917-33.
31. Allensworth JL, Evans MK, Bertucci F, Aldrich AJ, Festa RA, Finetti P*, et al.* Disulfiram (DSF) acts as a copper ionophore to induce copper-dependent oxidative stress and mediate anti-tumor efficacy in inflammatory breast cancer. Mol Oncol. Volume 92015. p 1155-68.
32. Arora J, Sauer SJ, Tarpley M, Vermeulen P, Rypens C, Van Laere S*, et al.* Inflammatory breast cancer tumor emboli express high levels of anti-apoptotic proteins: use of a quantitative high content and high-throughput 3D IBC spheroid assay to identify targeting strategies. Oncotarget. Volume 82017. p 25848-63.
33. Lerebours F, Vacher S, Andrieu C, Espie M, Marty M, Lidereau R*, et al.* NF-kappa B genes have a major role in Inflammatory Breast Cancer. BMC Cancer. Volume 82008. p 41.
34. Van Laere SJ, Van der Auwera I, Van den Eynden GG, van Dam P, Van Marck EA, Vermeulen PB*, et al.* NF-κB activation in inflammatory breast cancer is associated with oestrogen receptor downregulation, secondary to EGFR and/or ErbB2 overexpression and MAPK hyperactivation. Br J Cancer. Volume 972007. p 659-69.
35. Murai J, Huang Sy N, Das BB, Renaud A, Zhang Y, Doroshow JH*, et al.* Differential trapping of PARP1 and PARP2 by clinical PARP inhibitors. Cancer Res 2012;72(21):5588-99 doi 10.1158/0008-5472.can-12-2753.
36. Menear KA, Adcock C, Boulter R, Cockcroft XL, Copsey L, Cranston A*, et al.* 4-[3-(4-cyclopropanecarbonylpiperazine-1-carbonyl)-4-fluorobenzyl]-2H-phthalazin- 1-one: a novel bioavailable inhibitor of poly(ADP-ribose) polymerase-1. J Med Chem 2008;51(20):6581-91 doi 10.1021/jm8001263.
37. Parsels LA, Karnak D, Parsels JD, Zhang Q, Velez-Padilla J, Reichert ZR*, et al.* PARP1 Trapping and DNA Replication Stress Enhance Radiosensitization with Combined WEE1 and PARP Inhibitors. Mol Cancer Res 2018;16(2):222-32 doi 10.1158/1541-7786.mcr-17-0455.
38. Murai J, Zhang Y, Morris J, Ji J, Takeda S, Doroshow JH*, et al.* Rationale for Poly(ADP-ribose) Polymerase (PARP) Inhibitors in Combination Therapy with Camptothecins or Temozolomide Based on PARP Trapping versus Catalytic Inhibition. J Pharmacol Exp Ther. Volume 3492014. p 408-16.

39. Maya-Mendoza A, Moudry P, Merchut-Maya JM, Lee M, Strauss R, Bartek J. High speed of fork progression induces DNA replication stress and genomic instability. Nature 2018;559(7713):279-84 doi 10.1038/s41586-018-0261-5.
40. Drew Y, Ledermann J, Hall G, Rea D, Glasspool R, Highley M*, et al.* Phase 2 multicentre trial investigating intermittent and continuous dosing schedules of the poly(ADP-ribose) polymerase inhibitor rucaparib in germline BRCA mutation carriers with advanced ovarian and breast cancer. Br J Cancer 2016;114(7):723-30 doi 10.1038/bjc.2016.41.
41. Litton JK, Rugo HS, Ettl J, Hurvitz SA, Goncalves A, Lee KH*, et al.* Talazoparib in Patients with Advanced Breast Cancer and a Germline BRCA Mutation. N Engl J Med 2018;379(8):753-63 doi 10.1056/NEJMoa1802905.
42. Karam SD, Reddy K, Blatchford PJ, Waxweiler T, DeLouize AM, Oweida A*, et al.* Final Report of a Phase I Trial of Olaparib with Cetuximab and Radiation for Heavy Smoker Patients with Locally Advanced Head and Neck Cancer. Clin Cancer Res 2018;24(20):4949-59 doi 10.1158/1078-0432.ccr-18-0467.
43. Vance S, Liu E, Zhao L, Parsels JD, Parsels LA, Brown JL*, et al.* Selective radiosensitization of p53 mutant pancreatic cancer cells by combined inhibition of Chk1 and PARP1. Cell Cycle 2011;10(24):4321-9 doi 10.4161/cc.10.24.18661.
44. Han S, Brenner JC, Sabolch A, Jackson W, Speers C, Wilder-Romans K*, et al.* Targeted radiosensitization of ETS fusion-positive prostate cancer through PARP1 inhibition. Neoplasia 2013;15(10):1207-17 doi 10.1593/neo.131604.
45. Bi Y, Verginadis, II, Dey S, Lin L, Guo L, Zheng Y*, et al.* Radiosensitization by the PARP inhibitor olaparib in BRCA1-proficient and deficient high-grade serous ovarian carcinomas. Gynecol Oncol 2018;150(3):534-44 doi 10.1016/j.ygyno.2018.07.002.
46. Wurster S, Hennes F, Parplys AC, Seelbach JI, Mansour WY, Zielinski A*, et al.* PARP1 inhibition radiosensitizes HNSCC cells deficient in homologous recombination by disabling the DNA replication fork elongation response. Oncotarget 2016;7(9):9732-41 doi 10.18632/oncotarget.6947.
47. Mangoni M, Sottili M, Salvatore G, Meattini I, Desideri I, Greto D*, et al.* Enhancement of Soft Tissue Sarcoma Cell Radiosensitivity by Poly(ADP-ribose) Polymerase-1 Inhibitors. Radiat Res 2018;190(5):464-72 doi 10.1667/rr15035.1.
48. Jagsi R, Griffith K, Bellon J, Woodward W, Horton J, Ho A*, et al.* TBCRC 024 initial results: A multicenter phase 1 study of veliparib administered concurrently with chest wall and nodal radiation therapy in patients with inflammatory or locoregionally recurrent breast cancer. International Journal of Radiation Oncology 2015;93(3):S137.
49. Speers C, Zhao SG, Kothari V, Santola A, Liu M, Wilder-Romans K*, et al.* Maternal Embryonic Leucine Zipper Kinase (MELK) as a Novel Mediator and Biomarker of Radioresistance in Human Breast Cancer. Clinical cancer research : an official journal of the American Association for Cancer Research 2016;22(23):5864-75 doi 10.1158/1078-0432.ccr-15-2711.
50. Yokoyama Y, Dhanabal M, Griffioen AW, Sukhatme VP, Ramakrishnan S. Synergy between angiostatin and endostatin: inhibition of ovarian cancer growth. Cancer Res 2000;60(8):2190-6.

Chapter 4 : RB Expression Confers Sensitivity to CDK4/6 Inhibitor-Mediated Radiosensitization Across Breast Cancer Subtypes[4]

Abstract

Standard radiation (RT) therapy does not reliably provide locoregional control for women with multi-node positive and triple-negative (TNBC) breast cancers. We hypothesized that CDK4/6 inhibition (CDK4/6i) would increase the radiosensitivity not only of estrogen receptor positive (ER+) cells, but also TNBC that express retinoblastoma (RB) protein. We found that CDK4/6i radiosensitized RB wild-type TNBC (n=4, rER 1.49 – 2.22), but failed to radiosensitize RB-null TNBC (n=3, rER: 0.84 – 1.00). RB expression predicted response to CDK4/6i + RT (R2=0.84), and radiosensitization was lost in ER+/TNBC cells (rER: 0.88 – 1.13) after RB1 knockdown in isogenic and non-isogenic models. CDK4/6i suppressed homologous recombination (HR) in RB wild-type cells, but not in RB-null cells or isogenic models of RB1 loss; HR competency was rescued with RB re-expression. Radiosensitization was independent of non-homologous end joining and the known effects of CDK4/6i on cell cycle arrest. Mechanistically, RB and RAD51 interact *in vitro* to promote HR repair. CDK4/6i produced RB-dependent radiosensitization in TNBC xenografts, but not in isogenic RB-null xenografts. Our data provide the preclinical rationale for a clinical trial expanding the use of CDK4/6i + RT to

[4] This chapter was published in *JCI Insight* in January 2022.

difficult to control RB-intact breast cancers (including TNBC) and nominate RB status as a predictive biomarker of therapeutic efficacy.

Introduction

Breast cancer is a heterogeneous group of diseases where treatment options – and often treatment outcomes – are tied to the presence or absence of molecular markers including the estrogen receptor (ER), progesterone receptor (PR), and the human epidermal growth factor receptor 2 (HER2). These receptors serve as drivers of tumorigenesis and disease progression, and ER+ or HER2-expressing tumors respond to inhibitors targeting either hormone-mediated or HER2-mediated signaling pathways, respectively. In triple negative breast cancers (TNBC) that lack ER, PR, and HER2, this results in a limited number of targeted treatment options. Consequently, locoregional control remains a challenge in women with TNBC and multi-node positive estrogen receptor-positive (ER+) breast cancers (1, 2).

Traditionally, endocrine therapies including tamoxifen, fulvestrant, and aromatase inhibitors are used for the treatment of ER+ breast cancer following surgery, RT, and/or chemotherapy (3). For patients whose cancers develop resistance to these therapies and who develop locoregional recurrences or metastatic disease, treatment with CDK4/6 inhibitors including palbociclib (4), ribociclib (5), and abemaciclib (6) has demonstrated an increase in progression free survival time and decreased tumor metastasis (7). Mechanistically, pharmacological CDK4/6 inhibition prevents phosphorylation of downstream cell cycle proteins such as RB that control cell cycle progression through the G_1/S checkpoint (4). Although first approved in the metastatic setting for ER+ breast cancers, current clinical trials in hormone receptor-positive (HR+) breast cancer including PALLAS, monarchE, PENELOPE-B, and NATALEE seek to study the potential utility of CDK4/6 inhibitors in non-metastatic HR+ breast cancer. Varying results have been reported, but based on improved invasive disease-free survival in the MonarchE trial, abemaciclib was the first CDK4/6 inhibitor to be approved as an adjuvant

therapy in women with high-risk, non-metastatic, ER+ breast cancer with a high Ki67 score (8-10). Thus far, clinical trials using CDK4/6 inhibitors have been mostly restricted to women with ER+, HER2- breast cancer, and their potential role in treating TNBC remains unclear.

Multiple preclinical studies support the hypothesis that CDK4/6 inhibition can improve the efficacy of standard chemotherapy treatments (such as paclitaxel and cisplatin) in TNBC and other cancer types by inducing apoptosis or potentiating DNA damage and causing increased cell death (11-16). Previous studies combining low doses of CDK4/6 inhibition with RT demonstrate clinically-meaningful radiosensitization in ER+ breast cancer models (17), though others have since suggested that combination treatment may be most effective when RT is administered prior to CDK4/6 inhibitor therapy (18). There is evidence to suggest that CDK4/6 inhibition can increase tumor cell sensitivity to proton therapy through impaired RAD51 foci formation (19), but at present our understanding of the relationship between simultaneous radiation treatment and CDK4/6 inhibitor therapy in the treatment of TNBC is insufficient.

When compared to ER+ breast cancers, loss-of-function mutations in the retinoblastoma tumor suppressor *RB1* (RB) are more common in TNBC (7% vs. < 4%), and RB pathway alterations have been reported in up to 30% of TNBC (20, 21). *RB1* loss in breast cancer is associated with resistance to many therapies, including chemotherapy and radiation, and the presence of wild-type RB protein is an important determinant for the efficacy of CDK4/6 inhibitor monotherapy (4). However, in addition to CDK4/6-mediated phosphorylation of RB that is required to drive forward the G_1/S cell cycle transition, there is growing evidence that RB is essential for multiple processes involved in the DNA damage response (22-24). For example, RB null TNBC are more sensitive to gamma irradiation and less susceptible to CDK4/6 inhibitor

monotherapy (4, 25, 26). Further studies also suggest that RB localizes to double strand DNA (dsDNA) breaks and helps recruit factors such as BRG1 necessary for proper dsDNA repair (27).

Taken together, the lack of targeted treatment options and the failure to achieve locoregional control of aggressive breast cancers – including TNBC – represents a clear unmet clinical need, but our understanding of the potential of combined CDK4/6 inhibitor therapy and radiotherapy in TNBC remains insufficient. In this study, we first sought to evaluate the efficacy of combining CDK4/6 inhibitors with radiotherapy in multiple preclinical models of TNBC. Next, we utilized isogenic models of breast cancer to explore how the presence or absence of RB led to changes in intrinsic cellular radiosensitivity as well as the mitigation of CDK4/6 inhibitor-mediated radiosensitization in ER+ and TNBC. Finally, we investigated the effects of RB expression on homologous recombination (HR) efficiency and the role of RB in CDK4/6 inhibitor-mediated radiosensitization both *in vitro* and *in vivo*.

Results

CDK4/6 inhibition radiosensitizes TNBC with wild-type *RB1*

To understand the single agent effects of CDK4/6 inhibition on the proliferation of TNBC cell lines, we calculated the half-maximal inhibitory concentration (IC_{50}) of proliferation after a 72-hour treatment with palbociclib, ribociclib, or abemaciclib (**Figure 4.1A, Figure 4.2A-B**). All three drugs had minimal to moderate effects as monotherapies, especially in TNBC cell lines that lack expression of RB (MDA-MB-468 and CAL-851, $IC_{50} > 1\mu M$; dotted lines), consistent with prior literature (4). RB expression varied across both ER+ and TNBC cell lines, and normalized breast epithelial tissue (MCF10A) expressed very low levels of RB (**Figure 4.1B**).

To determine if short term CDK4/6 inhibition altered sensitivity of TNBC cell lines to ionizing radiation, we performed clonogenic cell survival assays using a one-hour CDK4/6 inhibitor pretreatment with concentrations at or near the IC_{50} value for each TNBC cell line (**Table 4.1 & Table 4.2**). After a one-hour pretreatment, the concentrations of all three CDK4/6 inhibitors used in both ER+ and TNBC cell lines led to a decrease in RB phosphorylation at both serine 780 (S780) and serine 807 (S807), suggesting that these concentrations and this time scale were sufficient to produce relevant physiological effects (**Figure 4.3**).

A concentration-dependent increase in radiosensitization and a concentration-dependent decrease in cell survival was observed in TNBC cell lines with wild type RB protein including MDA-MB-231 (rER: 1.49 ± 0.10), CAL-120 (rER: 1.50 ± 0.07), CAL-51 (rER 2.22 ± 0.26), and SUM-159 (rER 1.69 ± 0.12) with a one-hour pretreatment of palbociclib before radiation (**Figure 4.1D-G**). Pretreatment with ribociclib or abemaciclib led to similar levels of radiosensitization in MDA-MB-231 and CAL-120 cells (rER: 1.33 – 1.34 for ribociclib and 2.14

– 2.20 for abemaciclib; **Figure 4.2D-G**), demonstrating that all three drugs affected radiosensitization to a similar degree *in vitro*. To assess the time dependence of the combination therapy, we repeated clonogenic survival assays in MDA-MB-231 cells with sequential treatment (radiation treatment first followed by drug treatment 6 hours post-RT, **Figure 4.2I**). In this model, palbociclib-mediated radiosensitization was maintained at similar or slightly diminished levels compared to clonogenics performed with drug pretreatment prior to RT.

The observed rER values after CDK4/6 inhibition + RT suggest that this radiosensitization is similar in magnitude to that of other clinically used radiosensitizers such as cisplatin (28), with an rER threshold of > 1.2. In contrast, in the TNBC cell lines MDA-MB-468 (rER 0.96 – 1.0), CAL-851 (rER 0.84 – 0.95), and BT-549 (rER: 0.91 – 0.93) that harbor inactivating *RB1* mutations, combination treatment with RT and palbociclib did not lead to radiosensitization (**Figure 4.1H-I, Figure 4.2H**). In addition, combined palbociclib and RT in normal mammary epithelial (MCF10A) cells is not significantly more toxic than palbociclib treatment alone (**Figure 4.2C**), suggesting that the combination treatment does not potentiate toxicities in normal breast tissue. Using rER values calculated from clonogenic survival assays (**Figure 4.1D-I**) and the relative RB expression from each cell line (**Figure 4.1B**), we calculated the correlation coefficient between RB expression and the degree of palbociclib-mediated radiosensitization observed *in vitro*. RB mutant cell lines were not sensitized (average radiation enhancement ratio rER: 0.92 ± 0.05, white open circles) to radiation after palbociclib treatment, whereas RB wild type TNBC cells (black circles) were radiosensitized (average rER at highest palbociclib concentrations: 1.66 ± 0.14; **Figure 4.1C**) by palbociclib. Enhancement ratios (**Table 4.3**) for RB wild type ER+ cell lines (17) were also predictive of efficacy of the combination

therapy. Thus, RB expression status was predictive of CDK4/6 inhibitor-mediated radiosensitization in our models ($R^2 = 0.73$ for all cell lines and $R^2 = 0.84$ for TNBC only).

CDK4/6 inhibition suppresses HR in TNBC

CDK4/6 inhibition is known to affect HR activity in ER+ breast cancer cells (17), which we confirmed in our experimental model system. We used a stable MCF-7 cell line expressing a GFP-based homologous recombination reporter system (29) and demonstrated a 22.1- 46.0% decrease in HR efficiency at 6 hours after CDK4/6 inhibition (**Figure 4.4A**). Using this reporter system, we examined HR repair in TNBC stable cell lines to determine if radiosensitization was due to changes in double stranded DNA (dsDNA) break repair efficiency. In two separate MDA-MB-231 HR reporter clones, palbociclib, ribociclib, and abemaciclib pretreatment led to a significant decrease in HR efficiency (19.1 - 58.7%) compared to vehicle treated cells. The magnitude of HR suppression was similar to that of the CHK1/2 inhibitor AZD7762 (average decrease of 47.1% compared to vehicle), which is known to suppress HR activity and was used as a positive experimental control (30) (**Figure 4.4B-C**). As an additional control, pretreatment with NU7441, a known inhibitor of DNA-dependent protein kinase (DNAPK) involved in NHEJ, led to an increase (average of 104.7% increase compared to vehicle) in HR efficiency by blocking NHEJ-mediated dsDNA repair. HR suppression did not occur in the RB null cell line BT-549 with 500 nM CDK4/6 inhibitor pretreatment (**Figure 4.5A,B**).

To further understand the implications of CDK4/6 inhibitor-mediated radiosensitization and its effects on HR in a non-overlapping model system, we quantified RAD51 foci formation after radiation using immunofluorescence microscopy. RAD51 is a recombinase that initiates the catalysis of HR-mediated DNA repair through involvement in the strand pairing process, and RAD51 foci formation is a surrogate measure for active HR activity (31). In MDA-MB-231

(**Figure 4.4D**), CAL-120 cells (**Figure 4.4E, Table 4.6**), and SUM-159 cells (**Figure 4.5C**) that express wild type RB, irradiation with 4 Gy led to a sharp increase in the presence of RAD51 foci at both 6 and 16 hours post radiotherapy (average increase of 50.4-67.54% compared to DMSO). However, in cells with a 1-hour palbociclib pretreatment, RAD51 foci at both 6 and 16 hours post radiotherapy significantly decreased compared to radiation alone (average decrease of 26.6-31.56% at 6 hours and 18.1-31.2% at 16 hours), indicating suppression of HR (**Figure 4.4D-E, Figure 4.5C**). The decrease in RAD51 foci formation in MDA-MB-231, CAL-120, and SUM-159 cells was not explained by the absence of RAD51 protein, which remained constant at 6 hours post-RT (**Figure 4.4F, Figure 4.5D**) with only a modest decrease of RAD51 expression after palbociclib or combination treatment in the latest time point (16 hours).

In contrast to RB wild-type TNBC cell lines, MDA-MB-468 (**Figure 4.4G**) and CAL-851 TNBC cells (**Figure 4.4H**) that lack RB formed equivalent levels of RAD51 foci after RT despite pretreatment with 1μM palbociclib (average of 46.3% percent positive in RT only cells and 53.0% in combination-treated cells at 6 hours). Thus, CDK4/6 inhibitor pretreatment did not lead to HR suppression at 6 or 16 hours (**Table 4.6**). In these RB null cell lines, RAD51 expression levels also remained relatively constant at both 6 hours and 16 hours post RT (**Figure 4.4I**). Representative immunofluorescent images of RAD51 foci are shown in both MDA-MB-231 cells and CAL-851 cells (**Figure 4.5E-F**) 6 hours after RT.

To better understand the dynamic regulation of dsDNA break repair in our models, we used a transient pEYFP reporter system to assess the capacity of TNBC cell lines to conduct non-homologous end joining-mediated DNA repair after CDK4/6 inhibition. Although we observed HR suppression 6 hours after CDK4/6 inhibition, treatment of RB wild type MDA-MB-231 and CAL-120 TNBC cells with the IC_{50} concentration of palbociclib, ribociclib, or abemaciclib did

not affect NHEJ efficiency after 6 hours (**Figure 4.6A-B**). As expected, treatment with NU7441 (DNAPK inhibitor) significantly decreased NHEJ activity (average of 46.8% decreased compared to vehicle in MDA-MB-231 and 46.1% in CAL-120), but the CHK1/2 inhibitor AZD7762 (which inhibits HR) did not affect NHEJ repair efficiency in this system.

Next, we used immunofluorescence to measure γ-phosphorylation of histone 2AX (γH2AX foci) to assess the total number of dsDNA breaks and the kinetics of DNA repair in TNBC cell lines treated with RT and palbociclib. Consistent with previous literature (17, 26), CDK4/6 inhibition did not potentiate the number of total dsDNA or delay repair time in TNBC cell lines after radiation, remaining relatively constant at 0.5, 6, 16, and 24 hours after RT (**Figure 4.6C-D, Table 4.7**). NHEJ is much faster than HR, and with CDK4/6 inhibition the burden of dsDNA repair is increasingly shifted to error-prone NHEJ even prior to cell cycle arrest in G_1. Representative images for γH2AX foci are shown in both MDA-MB-231 and CAL-120 cells (**Figure 4.6E-F**).

RB1 loss eliminates radiosensitivity to CDK4/6 inhibitors

To investigate whether intact RB protein expression was necessary for radiosensitization in breast cancer cell lines, we first sought to determine how *RB1* loss would affect the radiation response in breast cancer cell lines. CDK4/6 inhibitor-mediated radiosensitization was preserved in control siNT cells treated with palbociclib and RT (MCF-7 rER 1.40 ± 0.10, MDA-MB-231 rER: 1.53 ± 0.21) compared to cells treated with RT alone (**Figure 4.7A-B**). Transient knockdown of *RB1*, however, abolished palbociclib-mediated radiosensitization of MCF-7 (rER 1.05 ± 0.10) and MDA-MB-231 (rER 0.95 ± 0.17) cells compared to si*RB1*-transfected cells treated with vehicle. Notably, transient loss of RB expression was associated with an overall

increase in the intrinsic radiosensitivity of breast cancer cells, particularly in MDA-MB-231 cells.

To further confirm these studies, we generated isogenic models of RB loss in ER+ and TNBC cell lines utilizing the CRISPR-Cas9 system. Loss of RB in MDA-MB-231, CAL-120, MCF-7, and T47D cells led to a decrease in potency – but not a complete absence of effect – for all three CDK4/6 inhibitors as monotherapies (**Table 4.1, Figure 4.8**). Control cell lines expressing the Cas9 protein did not show significant differences in the IC_{50} value compared to parental cell lines.

RB knockout also affected CDK4/6 inhibitor-mediated cell cycle arrest in *RB1* knockout cell lines. In parental cell lines that express RB (CAL-120, MDA-MB-231; **Figure 4.9A,D**), treatment with a CDK4/6 inhibitor led to cell cycle arrest in G_1 after 24-48 hours. Although Cas9 control cells retained the ability to undergo CDK4/6 inhibitor-mediated G_1 arrest (**Figure 4.9B,E,H),** ER+ and TNBC *RB1* knockout cell lines fail to arrest in G_1 after 24-48 hour treatment with palbociclib, ribociclib, or abemaciclib (**Figure 4.9C,F,I**). These results are consistent with the RB null cell line MDA-MB-468 which also fails to arrest in G_1 phase after CDK4/6 inhibitor treatment (**Figure 4.9G**).

To determine the effect of RB protein levels on radiosensitivity in isogenic models, we performed clonogenic survival assays. We observed a complete loss of radiosensitization in MDA-MB-231 (rER: 0.97 – 1.07**, Figure 4.7C**) and CAL-120 *RB1* CRISPR cells (rER: 0.99 – 1.06, **Figure 4.10A**), despite using higher concentrations of palbociclib, ribociclib, or abemaciclib compared those used to treat parental TNBC cell lines. Similar results were obtained in the ER+ cell lines MCF-7 and T47D (**Figure 4.7D, Figure 4.10B**; rER: 0.88 – 1.07) where we failed to observe a concentration-dependent increase in radiosensitization or a decrease in the

surviving fraction of cells at 2Gy. As expected, Cas9-expressing control cell lines retained palbociclib-mediated radiosensitization at levels comparable to the respective parental cell lines (rER: 1.26 – 1.60, **Figure 4.10C,D**). When compared to wild type MDA-MB-231 and CAL-120 cells, mean rER values for each CDK4/6 inhibitor significantly decreased in MDA-MB-231 and CAL-120 CRISPR *RB1* knockout cells (**Figure 4.7E, Figure 4.10F**), consistent with RB-dependent radiosensitization. In *RB1* knockout cells, western blots were used to confirm successful knockout of RB at the protein level (**Figure 4.7F-H, Figure 4.10E**).

In order to test if re-expression of RB was sufficient to rescue the radiosensitization phenotype, we engineered a Cas9-resistant RB expression plasmid using site directed mutagenesis of a GFP-tagged RB plasmid. By creating four synonymous mutations in the coding sequence recognized by the CRISPR gRNA, we were able to overexpress RB protein in our ER+ and TNBC models of *RB1* loss without changing the amino acid sequence of the RB protein. Re-expression of RB protein in *RB1* CRISPR cells was radioprotective, leading to an increase in the surviving fraction of cells at 2Gy and an upward deflection of the surviving fraction curve (solid purple). After re-introduction of RB, radiosensitization was restored after palbociclib pretreatment (MCF-7 rER: 1.66 ± 0.04, MDA-MB-231 rER: 1.27 ± 0.03); **Figure 4.7I,J**). In addition, transient expression of RB protein in MDA-MB-468 or BT-549 cells led to modest radiosensitization ([rER: 1.27 – 1.36], **Figure 4.10G-I**), though we only tested this effect up to a concentration of 1μM palbociclib.

We also engineered models of RB loss through serial culture of MDA-MB-231 cells in palbociclib-containing media to create CDK4/6 inhibitor-resistant MDA-MB-231 subclones (MDA-MB-231 PalboR, **Figure 4.11A**, IC_{50} > 5μM for all CDK4/6 inhibitors). These cells demonstrated decreased sensitivity to all 3 CDK4/6 inhibitors and, similar to MDA-MB-231 *RB1*

CRISPR clones, MDA-MB-231 PalboR cells demonstrated a loss of RB protein. In clonogenic survival assays MDA-MB-231 PalboR cells were not radiosensitized with palbociclib, ribociclib, or abemaciclib pretreatment (rER: 0.97 – 1.09) (**Figure 4.11B**). To reaffirm the RB-dependence of radiosensitivity to CDK4/6 inhibition, we transiently expressed the GFP-RB protein in MDA-MB-231 PalboR cells which rescued palbociclib-mediated radiosensitization (**Figure 4.11C**).

Because there is data to suggest that other mutations in other tumor suppressor proteins – such as *TP53* – may play a role in response to CDK4/6 inhibitor monotherapy or combination therapy (32), we generated additional isogenic models of *TP53* loss in *TP53* wild-type ER+ (MCF-7) and TNBC (CAL-51) cell lines (**Figure 4.12A-B**) and performed clonogenic survival assays. Radiosensitization was maintained in CAL-51 and MCF-7 *TP53* CRISPR cells (**Figure 4.12C-D**) compared to Cas9 controls (**Figure 4.12B,D**), though the magnitude of the effect was slightly diminished at the highest concentrations used. Nonetheless, these findings corroborate earlier data in p53 mutant parental TNBC cell lines (**Figure 4.1D-G**) suggesting that *TP53* status does not predict response to CDK4/6 inhibition + RT.

CDK4/6 inhibition radiosensitizes RB-expressing TNBC tumors *in vivo*

To characterize the effects of combined CDK4/6 inhibition and radiation in an *in vivo* model, we generated xenografts using MDA-MB-231 cells injected into the mammary fat pads of female mice (**Figure 4.13A**). Mice received either vehicle, 100mg/kg palbociclib alone, radiation alone, or a combination of palbociclib and radiation. Palbociclib treatment in the combination group was started one day prior to the start of radiotherapy that was delivered in 6 fractions at 2 Gy/fraction; all treatment was halted after the last fraction of radiation. Combination treatment with palbociclib and RT significantly suppressed tumor growth in mice compared to treatment with RT or palbociclib alone (**Figure 4.13B**). There was significant delay

in time to tumor doubling (**Figure 4.14A,** $p<0.001$) and tripling (**Figure 4.13C,** $p<0.001$) in the combination treated group (undefined) compared to tripling times for vehicle (11 days), palbociclib alone (19 days), or radiation treated mice (23.5 days). Short term treatment of mice with palbociclib and RT demonstrated suppression of Ki67 staining in combination treated groups, demonstrating on-target effects of palbociclib and RT (**Figure 4.14C-D**).

To elucidate the RB-dependence of CDK4/6 inhibitor-mediated radiosensitization *in vivo*, we utilized isogenic MDA-MB-231 xenograft models expressing either Cas9 alone or the Cas9 and the *RB1* CRISPR guide (**Figure 4.13D**). In Cas9-expressing xenografts, RT and abemaciclib (50mg/kg) demonstrated modest single agent efficacy, but combined abemaciclib + RT led to significant radiosensitization *in vivo* **Figure 4.13**, $p < 0.01$). Although *RB1* CRISPR xenograft tumors (**Figure 4.13**) were not radiosensitized by abemaciclib + RT ($p > 0.05$), *RB1* CRISPR xenografts demonstrated increased single agent sensitivity to RT, consistent with the proposed role of RB in responding to DNA damage. Despite *RB1* knockout, modest single agent effects of abemaciclib were observed - likely due to the effects of abemaciclib on other CDKs such as CDK5 and CDK9.

Overall, all treatments were tolerated without significant weight loss (**Figure 4.14B, E-F**). Synergy between CDK4/6 inhibition with palbociclib (**Table 4.4**) and abemaciclib (**Table 4.5**) and radiation was calculated, as described previously (33). Combination treatments were synergistic – not just additive – in RB-expressing xenografts by the end of the study (parental and Cas9 control xenografts; ratio > 1), which did not occur in *RB1* CRISPR xenografts (**Table 4.5**), as expected.

RB is involved in HR-mediated dsDNA repair

To assess whether or not changes in the intrinsic sensitivity of *RB1* CRISPR cells was mediated through aberrant mitosis and increased mitotic catastrophe, we performed immunofluorescence to quantify micronuclei formation in MCF-7 and MDA-MB-231 cells 72 hours after 4 Gy RT (**Figure 4.15**) (34). As expected, *RB1* wild type parental cells, radiation led to an increase in micronucleated cells (23.1% in MDA-MB-231, 26.0% in MCF-7 cells). However, RT-induced micronuclei formation was not potentiated in the *RB1* CRISPR cell lines and occurred at similar magnitudes (16.9% increase in MDA-MB-231 *RB1* CRISPR cells after RT and 22.9% increase in MCF-7 *RB1* CRISPR cells) to the parental cell lines.

To further elucidate the effects of *RB1* loss in ER+ and TNBC cell lines, we quantified RAD51 foci formation after transient *RB1* knockdown or CRISPR-mediated *RB1* loss. In MCF-7 and MDA-MB-231 cells, transient RB loss resulted in a decrease in the overall induction of RAD51 foci following radiation (4Gy) treatment (average of 53.9% percent positive in siNT cells after RT and 37.8% positive in si*RB1* cells after RT; **Figure 4.16A,B, Table 4.8**). While control cells demonstrate CDK4/6 inhibitor-mediated suppression of RAD51 foci formation, indicative of HR suppression, si*RB1* cells do not demonstrate suppression of RAD51 foci formation after palbociclib treatment.

Consistent with models of transient *RB1* knockdown, MCF-7 and MDA-MB-231 *RB1* CRISPR cells display global suppression of RAD51 foci formation compared to Cas-9 control cell lines (average of 68.2% percent positive in Cas9 cells after RT and 42.6% positive in *RB1* CRISPR cells after RT; **Figure 4.16C,D**). Overexpression of RB protein in *RB1* CRISPR cells increased the overall quantity of radiation-induced RAD51 foci and increased susceptibility of TNBC and ER+ cells to CDK4/6 inhibitor-mediated HR suppression (**Figure 4.16C-D**). Representative images of RAD51 foci are shown for MCF-7 and MDA-MB-231 cells transfected

with si*RB1* (**Figure 4.17A,B**) as well as MCF-7 and MDA-MB-231 Cas9 and *RB1* CRISPR cells (**Figure 4.17C-E**) 6 hours post RT (**Table 4.9**).

With a clear decrease in HR activity (RAD51 foci) driven by RB-dependent CDK4/6 inhibitor-mediated radiosensitization, we next sought to determine the molecular mechanism linking RB to HR. Thus, we co-transfected HEK-293T cells with GFP-RB or Myc-tagged RAD51 and performed immunoprecipitation 24 hours after transfection (**Figure 4.16E**). Pulldown of GFP-RB (green boxes) also resulted in pulldown of myc-RAD51 protein, and the reverse occurred with pulldown of myc-RAD51 (black boxes) resulting in pulldown of GFP-RB protein. In contrast, the NHEJ mediator Ku80 was not pulled down with either GFP-RB pulldown or myc-RAD51 pulldown, suggesting that it may not be necessary for RB-dependent repair of dsDNA breaks. This interaction between GFP-RB and myc-RAD51 was also observed in the ER+ breast cancer cell line MCF-7 (**Figure 4.16F**) and the TNBC cell line MDA-MB-231 (**Figure 4.16G**). To control for nonspecific effects of overexpression we also performed immunoprecipitation with GFP-RB and myc-MCL1, a mitochondria-associated protein involved in apoptosis, and did not observe nonspecific pulldown of GFP-RB as an artifact of overexpression (**Figure 4.17F**).

Discussion

In this study, we demonstrate that CDK4/6 inhibition and radiotherapy led to an RB-dependent increase in both radiosensitization and breast cancer cell death in multiple, non-overlapping ER + and TNBC models *in vitro* (**Figure 4.1**) and in vivo (**Figure 4.13**). Cells treated with a CDK4/6 inhibitor in the presence of RB were radiosensitized through cell cycle-independent impairment of HR activity and not NHEJ (**Figure 4.6**); neither radiation sensitivity nor HR activity was affected in RB null TNBC cell lines (**Figure 4.4**). The blockade of CDK4/6 inhibitor-mediated radiosensitization produced by transient knockdown or complete knockout of *RB1* could be rescued with transient overexpression of RB protein (**Figure 4.7**), further confirming the key role of RB in radiosensitization. Finally, our findings suggest that RB may affect HR by interacting with key protein members of HR repair (such as RAD51) in breast cancer cell lines (**Figure 4.16**). These results demonstrate that the combination of CDK4/6 inhibition and radiotherapy is a potentially effective strategy not just for ER+ breast cancers, but for the radiosensitization of other *RB1* wild type cancers including TNBC, which have disproportionately high rates of locoregional recurrence after RT (**Figure 4.18**).

Although the role of RB in cell cycle progression through the G_1/S checkpoint is well characterized, recent reports have implicated RB expression as a necessity for promoting efficient DNA damage response in cancer cells (35). RB expression can be used to predict sensitivity of cancer cells to antimitotic and cytotoxic chemotherapies (12, 16), and recent evidence suggests that CDK4/6 inhibitors can be used to suppress the DNA damage response in RB-dependent cancers (24). Finally, the ataxia telangiectasia mutated (ATM) protein, which sits at the apex of dsDNA break repair, has been shown to phosphorylate RB (36) or E2F1 (27), leading to RB-dependent repair of dsDNA breaks.

The role of RB in DNA damage repair has been implicated in both NHEJ-mediated(37) and HR-mediated repair (27, 38). CDK4/6 inhibitor-mediated G_1 arrest in TNBC cell lines shifts the DNA damage response away from HR to the more error-prone dsDNA repair pathway, NHEJ, resulting in increased DNA damage (11, 26). Additionally, loss of RB may modulate expression of γH2AX, a measure for the total number of dsDNA breaks, in cancer cell lines (39, 40). Although we were unable to reproduce the finding that RB protein forms foci after radiation that are co-localized with γH2AX at dsDNA break sites (27), we instead demonstrated that RB interacts within the same protein complex as RAD51 in the process of HR-dependent DNA repair. Although further studies are needed to determine the complex dynamics of RB and RAD51 interaction and the time course of recruitment for additional DNA damage response proteins, we have demonstrated here that manipulation of RB expression changes both the radiosensitivity of breast cancer cells and their susceptibility to CDK4/6 inhibitor-mediated suppression of homologous recombination. Specifically, we show that the absence of RB impairs the recruitment of RAD51 to sites of dsDNA damage (resulting in less RAD51 foci), but overexpression of GFP-RB can increase RAD51 recruitment (more RAD51 foci).

There is a growing body of evidence suggesting that other cyclin-dependent kinases including CDK7, CDK8, CDK9, and CDK12 may also be important for modulating the sensitivity of cancer cells to the effects of ionizing radiation (41-43). In contrast to CDK4/6 inhibitor-mediated radiosensitization in breast cancer that is primarily mediated through suppression of HR, inhibition of other CDK proteins leads to increased apoptosis, senescence, and/or inhibition of RNA Polymerase II function that leads to radiosensitization (41-43). Furthermore, specific inhibition of CDK9 may be mediated through suppression of Axl-mediated signaling pathways (44). In our study, abemaciclib – which inhibits other CDK proteins

including CDK9 – was consistently the most potent and effective radiosensitization agent compared to palbociclib and ribociclib, which are more selective for CDK4/6. Although pan-CDK inhibitors such as roscovitine, flavorpiridiol, and roniciclib have also demonstrated potential as radiosensitization agents in a variety of cancer types, targeted inhibition of individual CDK proteins provides a more targeted therapeutic approach with greatly reduced side effect profiles (45-50). Future studies are needed in this setting to explore if there are additional mechanisms – beyond HR suppression – that could be exploited with the use of CDK inhibition + RT in ER+ and TNBC.

CDK4/6 inhibitors may be administered with other types of therapies – particularly endocrine therapies in ER+ disease or novel immune checkpoint inhibitors in TNBC – which may influence cell survival when administered concurrently with radiation. CDK4/6 inhibition has been shown to promote anti-tumor immunity (51-54), leading to greater immunogenicity of TNBC cells *in vivo*. Radiation is known to stimulate the immune system in breast cancer (55, 56) and immunotherapies have recently been approved for use in TNBC (57). Many combination treatments with CDK4/6 inhibition and immune checkpoint inhibitors (targeting PD-1 and CTLA-4) have been proposed (58), but the effects of CDK4/6 inhibition on radiation-induced anti-tumor immunity – and the potential for those effects to be altered in the presence of immune checkpoint inhibitor therapy – have yet to be elucidated and are an important future direction of this work.

CDK4/6 inhibitors are currently only approved for use to treat ER+ breast cancers, but our data builds on a growing body of evidence that suggests there may be clinical relevance in expanding the use of CDK4/6 inhibition in combination with DNA damaging or cytotoxic agents to treat TNBC and other cancer types. Although the rates of RB mutation are higher in TNBC

(7%) (20), the RB-dependence of CDK4/6 inhibitor-mediated radiosensitization may be an important consideration in patient selection for future clinical trials in both ER+ breast cancer and TNBC. Furthermore, in additional cancers such as oral squamous cell carcinoma and hepatocellular carcinoma, palbociclib significantly inhibits cellular growth, accelerates senescence and apoptosis, and suppresses RAD51 foci formation (59, 60). Thus, CDK4/6 inhibition + RT may be a viable therapeutic strategy in other cancer types.

We have demonstrated the potential for radiosensitization of TNBC models utilizing all three of the clinically approved CDK4/6 inhibitors, but future studies we will evaluate whether this strategy is effective in other histopathological classifications or subtypes of breast cancer, such as inflammatory breast cancer, lobular breast cancer, and HER2-enriched breast cancer. In addition, future studies are needed to address optimal sequencing of drug and radiation in both ER+ and TNBC in order to optimize treatment efficacy (18). These studies will determine whether pretreatment, concurrent, treatment, or continued adjuvant treatment of tumors with drug in relation to RT are most effective, and these studies will be critical to phase I/II clinical trial design in women with RB intact breast cancers at high risk for locoregional recurrence. Finally, animal studies utilizing patient-derived xenograft (PDX) models will help offer additional compelling evidence that combinatory treatment with CDK4/6 inhibition and radiotherapy may be a clinically relevant strategy for TNBC.

Taken together, our results suggest that CDK4/6 inhibition + RT is a promising strategy to decrease recurrence and increase local disease control across ER+ and TNBC and that RB may be a potential biomarker for efficacy. Concerns about the safety of concurrent CDK4/6 inhibition and RT remain, and to date, small studies exploring outcomes in patients with MBC receiving palliative radiation and CDK4/6 inhibitor therapy have conflicting results regarding

toxicity, depending on the dose/fractionation of radiation and the regions targeted in the metastatic setting (visceral organs) (61-64). Reassuringly, no studies to date have demonstrated more pronounced side effects of CDK4/6 inhibitors, such as cytopenias and skin desquamation, in women receiving concurrent therapy to the breast or axillary regions. To answer this question directly, we have developed a phase I trial to assess the safety, tolerability, and preliminary efficacy of this combination in women with multi-node positive ER+ breast cancer which is opening soon. In our proposed study, all subjects would receive breast/chest wall and regional nodal therapy with highly conformal techniques designed to minimize dose to adjacent organs. We do not anticipate that concurrent radiation therapy and CDK4/6 inhibition will exacerbate the known potential toxicities of these agents, however the effect of CDK4/6 inhibition on skin toxicities during postoperative RT will be carefully assessed on study.

Provided that the combination therapy is well tolerated, these data will also inform the planned phase II randomized clinical trial evaluating the efficacy of combined CDK4/6i and RT in women with multiple lymph node (LN) positive ER+ breast cancer (>3 LN). The preclinical studies described herein provide the rationale for expanding the eligibility for these trials into women with RB intact TNBC for whom locoregional control remains a significant clinical issue. Finally, this proposed combination therapy has the potential to provide an effective “targeted therapy” for the treatment of TNBC with radiation where no such targeted therapy currently exists.

Methods

Cell Culture

Cell lines were grown at 37°C and 5% CO_2. T47D, MCF-7, MDA-MB-231, MDA-MB-468, and CAL-120 cells were grown in DMEM (ThermoFisher #11965-092) with 10% FBS (Atlanta Biologicals). BT-549 were grown in RPMI and CAL-851 cells were grown in DMEM (ThermoFisher #11995-040) with 10% FBS. SUM-159 cells were grown in HAMS F-12 (ThermoFisher #11765-054) with 5% FBS, 0.01M HEPES (ThermoFisher #15630080), 6μg/mL insulin (Sigma #I9278), and 1μg/mL hydrocortisone. All cell lines were supplemented with 5% penicillin/streptomycin (Invitrogen #15140122) and used for experiments at sub-confluent densities. Cell lines were authenticated with STR profiling and mycoplasma testing (Lonza # LT07-701) was performed monthly. Palbociclib-resistant cells (PalboR) were generated by culturing MDA-MB-231 cells in dose-escalating concentrations of palbociclib (50nM – 1μM) over a period of 3 months.

Drugs

Palbociclib (Sigma, #PZ0199), abemaciclib (Med Chem Express, #HY-16297A), and ribociclib (Med Chem Express, #HY-15777A) were used to make 10mM stocks in 100% DMSO for *in vitro* assays. NU7441 (SelleckChem #S2638) and AZD7762 (SelleckChem #S1532) were also obtained commercially in 10mM DMSO.

Clonogenic Survival assay

Cells plated at single cell density were pretreated with CDK4/6 inhibitor one hour prior to RT. Plates were radiated (0 – 6 Gy) and returned to the incubator for 1-3 weeks before methanol and acetic acid fixation (7:1) and staining with crystal violet (1%). Drug-containing media remained

on the cells during the incubation phase, but drug was not replaced or replenished at any time after the initial day of treatment. Colonies were defined as 50+ cells and counted from each treatment condition to calculate the surviving fraction for each treatment group. Survival curves were calculated as described previously (33, 65) and enhancement ratios were calculated by taking a ratio of the area under each of the surviving fraction curves, with the area for the control (RT only) condition divided by the area under the curve for each experimental condition.

Immunofluorescence

100,000 cells were plated onto coverslips in 12-well plates and treated the next morning with either palbociclib or vehicle (DMSO) one hour prior to radiation (4 Gy). Coverslips were fixed at 6 hours or 16 hours post RT (4 Gy) for RAD51, and γH2AX foci were fixed at 0.5, 6, 16, and 24 hours post RT (2 Gy). Cells were fixed in 4% paraformaldehyde (ThermoFisher #J19943K2) with 2% sucrose (Sigma #S9378) and 0.2% Triton X-100 (Sigma #T8532), permeabilized with 0.5% Triton X-100, and blocked in 1x PBS containing 5% goat serum (ThermoFisher #16210064), 0.5% BSA, and 0.05% Triton X-100. The phospho-histone H2AX (ser139) monoclonal antibody (Millipore #05-636, 1:2000) or the anti-RAD51 antibody (GeneTex #GTX70230 1:300) were used with the goat anti-mouse fluorescent secondary antibody (Invitrogen #A11005, 1:2000) to stain foci. A minimum of 100 cells were used to score and analyze formation of γH2AX and RAD51 foci. To quantify the exact number of foci per cell, ImageJ was used to count image maxima. Cells with more than 15 γH2AX foci or more than 10 RAD51 foci were scored as positive. To quantify micronuclei formation, cells were radiated at 4 Gy and fixed in 4% paraformaldehyde after 72 hours before mounting directly on coverslips with DAPI stain (34).

Immunoblotting

After treatment, cells were washed using PBS and lysed using RIPA buffer (ThermoFisher, #89901) with protease and phosphatase inhibitors (Sigma #PHOSS-RO, #CO-RO). Western blotting was done using anti-RB (CST #9313S), anti-GFP (CST #2956S), anti-phospho-RB (Ser807/811; CST #8516 or Ser780; CST #8180), anti-Cas9 (CST #14697S), anti-myc (Millipore #05419), and anti-RAD51 (Millipore ABE257) antibodies. All primary antibodies were diluted at a 1:1000 dilution in 1% milk; HRP-conjugated β-actin (CST #12262S) was diluted 1:50,000. Visualization was performed using 1:10,000 HRP-conjugated secondary antibodies (CST # 7074S, #7076S) and ECL prime (Cytiva #RPN2236). RB expression was quantified using ImageJ, normalized to β-actin expression for each lane, and calculated relative to the median RB expression of the blot.

Xenograft Studies

2 x 10^6 wild type, *RB1* CRISPR, or Cas9 control MDA-MB-231 cells were injected into the mammary fat pads of 6-8 week old CB17-SCID female mice with Matrigel (ThermoFisher #CB-40234) with 14-16 tumors per group. Once tumor volume reached 80-100mm^3, mice were randomly assigned to either vehicle treatment, drug alone, radiation alone, or the combination. CDK4/6 inhibitor was given by oral gavage with either palbociclib (100mg/kg) in 50 mmol/L pH 4.0 sodium L-lactate (Sigma, #L-7022) or abemaciclib (50mg/kg) in 25mM phosphate buffer pH 2.0 (Sigma #09568) with 1% hydroxyethylcellulose. Mice in the combination groups were treated 24 hours prior to the first RT dose, dosed concurrently with radiation for 5 days, and treatment for all groups was stopped at day 6. Tumor growth was measured using calipers and tumor volume was calculated using the equation $V = (L*W2)*\pi/6$. For short term studies, mice were treated with palbociclib one day (24 hours) prior to RT and continued concurrently with RT

(1 hour pretreatment each day) for two days. Tumors were harvested 1 hour after the last fraction of RT (2 fractions x 2 Gy) and immunohistochemistry was performed with the help of the University of Michigan Research Histology and Immunohistochemistry Core. Ki67 slides were imaged at 40x and 5 high powered fields from 4 tumors (20 total) were quantified per treatment condition using ImageJ.

Homologous Recombination Repair Efficiency Assay

The HR DR-GFP reporter plasmid transfected into cell lines and, after 48 hours, selection of stable clones was performed with geneticin (ThermoFisher #10131027). Flow cytometry was used to sort for GFP+ cells and verified single clones were expanded. Cells were plated and pretreated with CDK4/6 inhibitor, 1.5μM NU7441, or 200nM AZD7762 for 1 hour, after which SceI adenovirus was added for 48 hours to induce dsDNA breaks. Cells were then harvested, ethanol-fixed, and analyzed using flow cytometry to detect GFP+ cells.

Transfections and siRNA

Pooled siRNA guides targeting *RB1* (Dharmacon #L-003296-02) and control siRNA (Dharmacon #D-001810-10) were used at a stock concentration of 20μM and a final concentration of 25nM. Lipofectamine 2000 (Thermo #11668030) was used to transfect cells in Opti-MEM (Invitrogen #31985-062) and antibiotic-free media. Transfected cells were re-plated for *in vitro* assays 24 hours post-transfection and treated with CDK4/6 inhibitor/RT 48 hours post-transfection.

CRISPR

The lentiCRISPRv2 plasmid (Addgene #98290) was digested with BsmBI for 15 minutes at 55 degrees and gel-purified using the QIAquick Gel Extraction Kit (Qiagen #28706X4).

Oligos from IDT were annealed at 95 degrees cooled at 5 degrees/minute. The *RB1* guide sequence (5' CACCGGGTTCTTTGAGCAACATGGG 3') or the *TP53* guide sequence (5' CACCGCCATTGTTCAATATCGTCCG 3') was ligated into the CRISPR plasmid and transformed into Stbl3 bacteria. For preparation of lentivirus, 1.0 x 10^6 HEK-293T cells were transfected with 1.5µg PAX2 (Addgene #12260) + 0.3µg MD2g (Addgene #12259) + 1.5µg plasmid in OPTImem media. DMEM + 30% FBS was used to collect virus-containing media at 24 and 48 hours, which was spun down and cleared through a 0.45 micron filter before adding to cells with 0.8µg/mL polybrene. For *RB1* CRISPR cells, puromycin selection was performed at 1µg/mL (MDA-MB-231, MCF-7) or 2µg/mL (T47D, CAL-120) and single clones were isolated and used for all assays. Cas9-only control cell lines utilized an *AAVS1* control guide (5' CACCGGGGGCCACTAGGGACAGGAT 3'). For *TP53* CRISPR MCF-7 and CAL-51 cells, hygromycin selection was performed at 500 µg/mL.

Mutagenesis

The GFP-RB plasmid (AddGene 16004) was mutated using PCR by introducing 4 synonymous mutations into phosphorylated primers targeting the *RB1* sequence recognized by the gRNA. Q5 polymerase (NEB #M0491) and Taq DNA ligase (NEB #M0647S) were used according to the manufacturer's protocol (including cycling parameters) for PCR extension and ligation of the plasmid with two sequential rounds of mutagenesis (2 base pair changes each time). The PCR was DpnI-treated (NEB # R0176L) for 1 hour at 37ºC and transformed into XL10 Gold bacteria (Agilent #200314). Colonies were expanded for minipreps (Qiagen #27104) and sanger sequenced (U6 primer) to confirm successful mutagenesis.

Proliferation Assays

Cells plated in 96-well plates were treated with a CDK4/6 inhibitor at concentrations from 0-10μM. After 72 hours, AlamarBlue was added to the wells at a concentration of 10% of the well volume. After incubation, viability was calculated with the relative absorbance from each well using a plate reader.

Irradiation

Irradiation was conducted at the University of Michigan Experimental Irradiation Core using a Kimtron IC-225 at a dose rate of approximately 2 Gy/min. The irradiator was calibrated using dosimetry directly traceable to a National Institute of Standards and Technology (NIST) standard. *In vitro* experiments were performed with a 0.1 mm added Cu filter and a half-value-length of 0.51 mm Cu. *In vivo* experiments were performed with a Thoraeus filter (0.4 mm Sn + 0.25 mm Cu) and a half-value-length of 2.29 mm Cu.

Immunoprecipitation

Cells were plated in 10cm dishes and transfected the next morning with 6μg GFP-RB plasmid, 6μg myc-RAD51 plasmid or the combination. 24 hours later, cells were lysed in 1.0mL RIPA buffer with protease and phosphatase inhibitor, rocked for one hour at 4 degrees then spun down and the pellet discarded. A BCA assay was used to standardize protein concentrations: ~100mg was removed for input and ~1000mg was used for the IP. Lysates were precleared by incubation with 20μL of A/G Plus agarose beads (sc-2003) for 1 hour at 4°C, then GFP-Trap Magnetic Beads (Chromotek #GTD-20), Myc-Trap Magnetic Beads (Chromotek #YTMA-20) or Binding Control Magnetic Agarose Beads (Chromotek #BMAB-20) beads were added to the cleared lysate which was left to slowly rock overnight at 4°C. Beads were washed the next morning with

RIPA buffer and bound proteins were eluted in 50uL RIPA buffer with 1x NuPAGE and 2% βeta-mercaptoethanol.

Statistical Analysis and Randomization

In vitro experiments are graphed as the average ± the standard error of the mean (SEM). Experimental conditions in clonogenic survival assays and HR/NHEJ reporter assays were compared to vehicle (DMSO) controls using a one-way ANOVA with Dunnett's post-hoc test. Immunofluorescence experiments were blinded for analysis of RAD51 or γH2AX and analyzed with an unpaired, two-sided student's t-test between paired RT and combination values for each group, with a correction for a number of time points (6 and 16 hours post radiotherapy). Xenograft tumors were randomized on the first day of treatment and tumor volume was compared using a one-way ANOVA at the study endpoint.

Study Approval

All xenograft mice model experiments were done with consent from the Institutional Animal Care & Use Committee (IACUC) at the University of Michigan.

Acknowledgements

The authors would like to thank the ASTRO, the Breast Cancer Research Foundation, and the University of Michigan Rogel Cancer Center for generously supporting this work (N003173 to JM Rae, ASTRO-BCRF Career Development Award to End Cancer N029402 to CW Speers, F049977 to CW Speers). In addition, the authors would like to thank Stephen Ethier at the Medical University of South Carolina for the SUM-159 cells and the Lawrence/Morgan labs at the University of Michigan for the myc-RAD51 plasmid. This work was also supported by multiple T32 training grants including the Pharmacological Sciences Training Program (T32GM007767; A. Pesch & K. Jungles), the Training Program in Translational Research (T32-GM113900, A. Michmerhuizen), and the Program in Cellular and Molecular Biology (T32GM007315), the Medical Scientist Training Program (T32GM007863), and a Ruth L. Kirschstein NRSA F31 award (F31CA254138, A. Pesch). A. Pesch and A. Michmerhuizen are supported by Rackham Graduate School Research Grants. A. Michmerhuizen is supported by the Rackham Predoctoral Fellowship and K. Jungles is supported by the Rackham Merit Fellowship. In addition, the authors would like to thank the University of Michigan Research Histology and Immunohistochemistry Core (P30-CA04659229) and the Flow Cytometry Core for assistance in data collection and analysis and BioRender for assistance with figure generation. This manuscript was completed and published with the following co-authors: Nicole Hirsh, Anna Michmerhuizen, Kassidy Jungles, Kari Wilder-Romans, Benjamin Chandler, Meilan Liu, Lynn Lerner, Charles Nino, Connor Ward, Erin Cobain, Theodore Lawrence, Lori Pierce, James Rae, and Corey Speers.

Figures

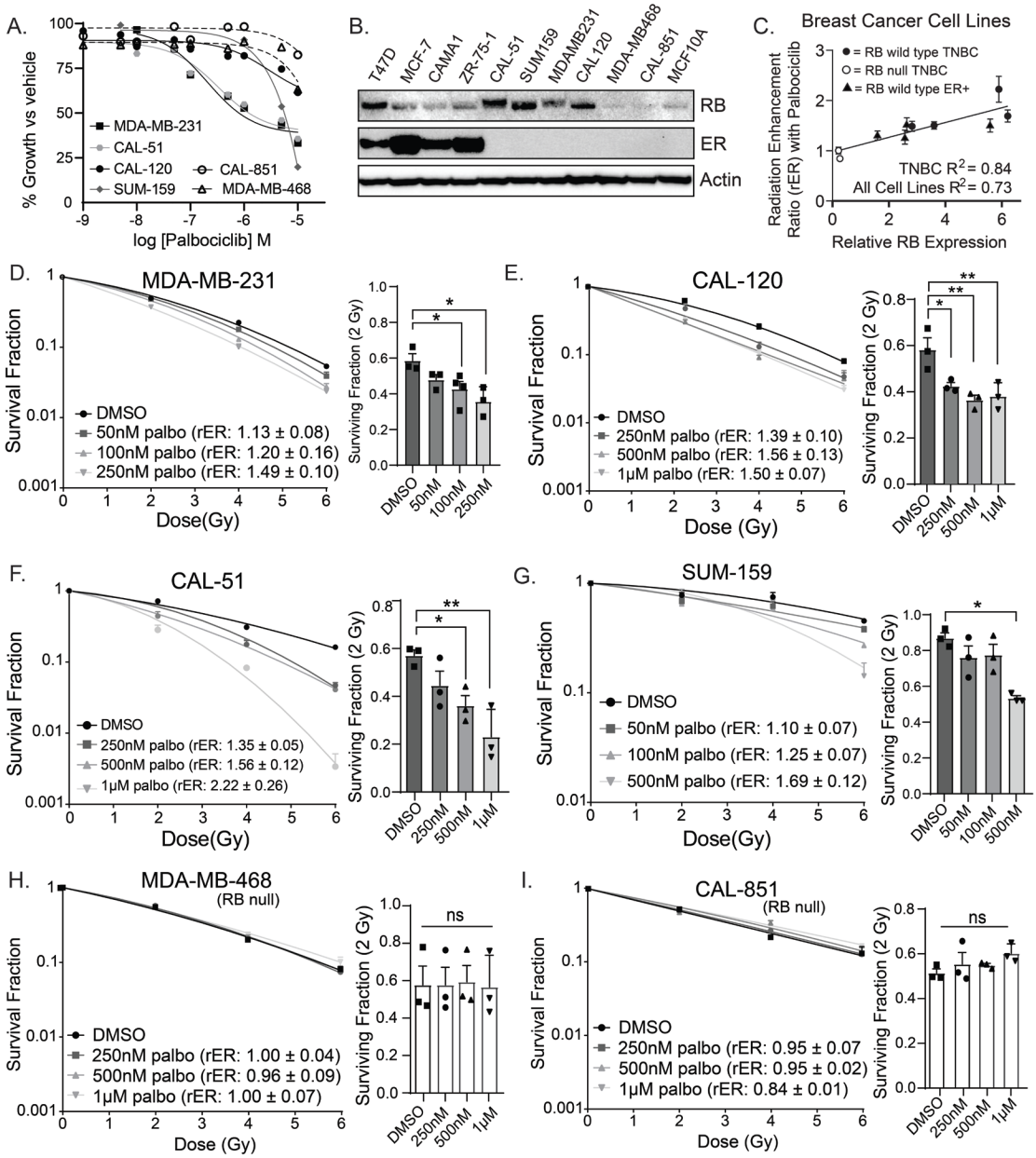

Figure 4.1: CDK4/6 inhibition with palbociclib radiosensitizes TNBC with wild-type *RB1*

Cell viability was measured in RB wild type (solid lines) and RB null (dashed lines) TNBC cell lines 72 hours after treatment with palbociclib (**A**). Western blots were used to assess protein expression in various breast cancer cell lines (**B**). RB expression was quantified using ImageJ and the correlation coefficient between RB expression and mean rER ratios (highest concentration of palbociclib for each cell line) were compared between ER+ (solid triangles), wild type *RB1* TNBC (solid circles), or RB null TNBC (open circles) (**C**). Clonogenic survival assays were performed in the RB wild type (**D-G**) and mutant (H-I) cell lines.

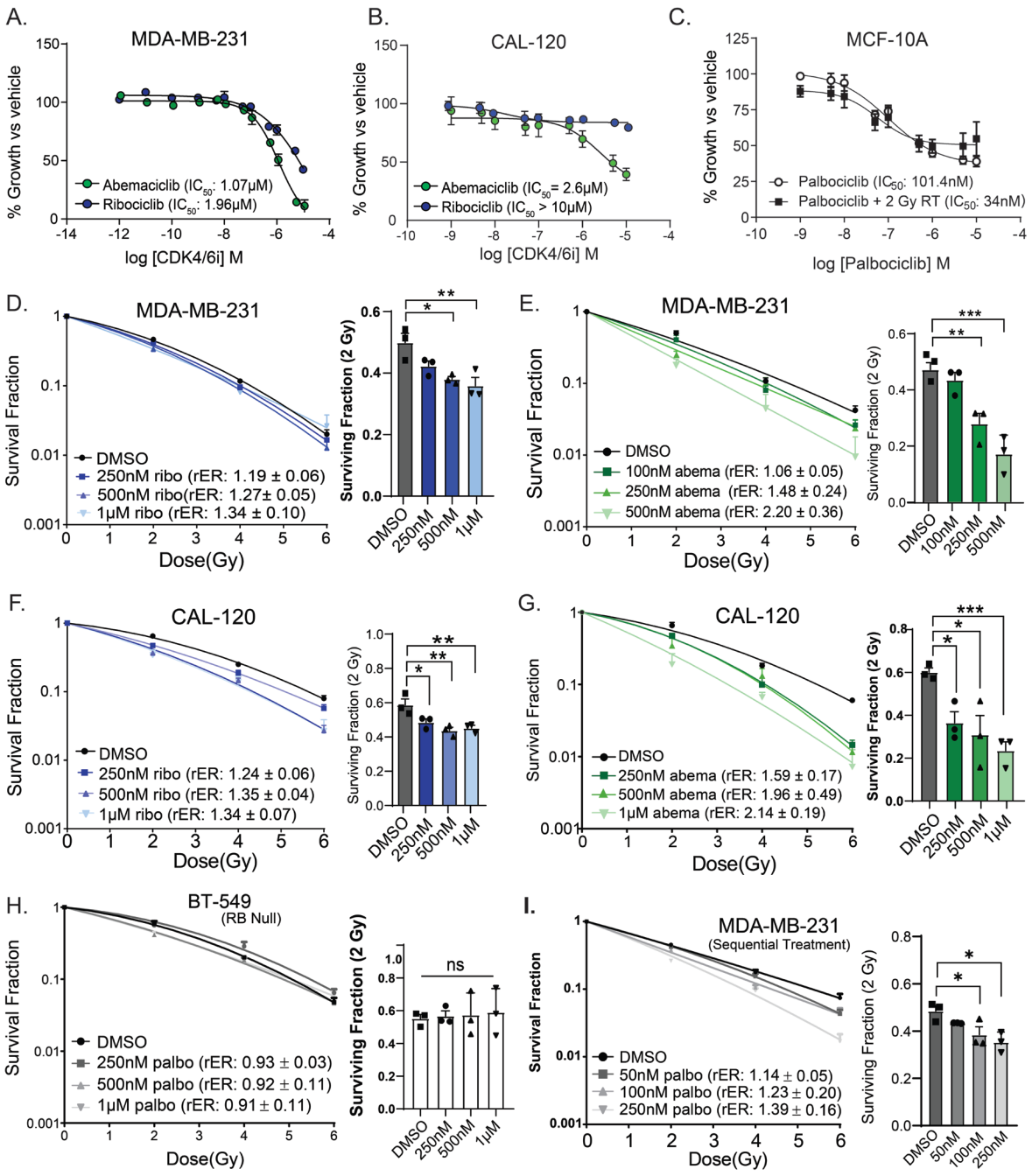

Figure 4.2: Abemaciclib and ribociclib radiosensitize TNBC with wild-type *RB1*

Cell viability was measured in each cell line 72 hours after treatment with either abemaciclib (green) or ribociclib (blue) in RB wild type MDA-MB-231 (**A**) and CAL-120 (**B**) cells to calculate IC_{50} values. MCF10A cells (**C**) were treated with palbociclib alone (open circles) or palbociclib + RT (filled squares). Clonogenic survival assays were performed in MDA-MB-231 (**D-E**) and CAL-120 (**F-G**) cells with varying doses of either ribociclib or abemaciclib and a one-hour drug pretreatment. RB null BT-549 cells were treated with palbociclib + RT (**H**). MDA-MB-231 cells were treated with palbociclib 6 hours after RT (**I**). (*, $P < 0.05$; **, $P < 0.01$; ***, $P < 0.001$).

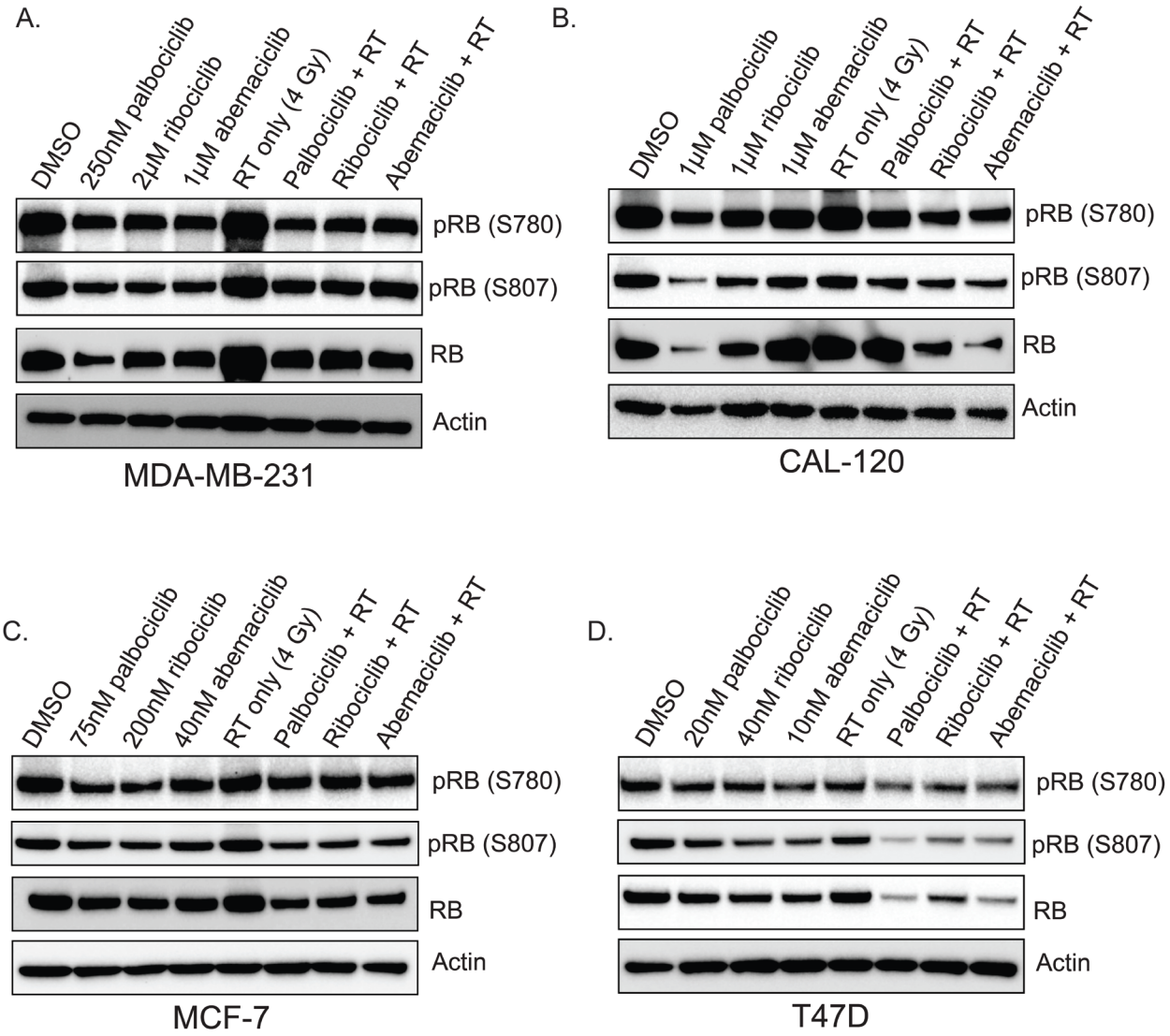

Figure 4.3: pRB levels decrease with CDK4/6 inhibition

Western blots were used to assess expression of pRB (S807), pRB (S780), and total RB in RB expressing breast cancer cell lines including MDA-MB-231 (**A**), CAL-120 (**B**), MCF-7 (**C**), and T47D (**D**) cells. Cells were pretreated with a CDK4/6 inhibitor one hour prior to radiation (4 Gy) and harvested 30 minutes after radiation treatment.

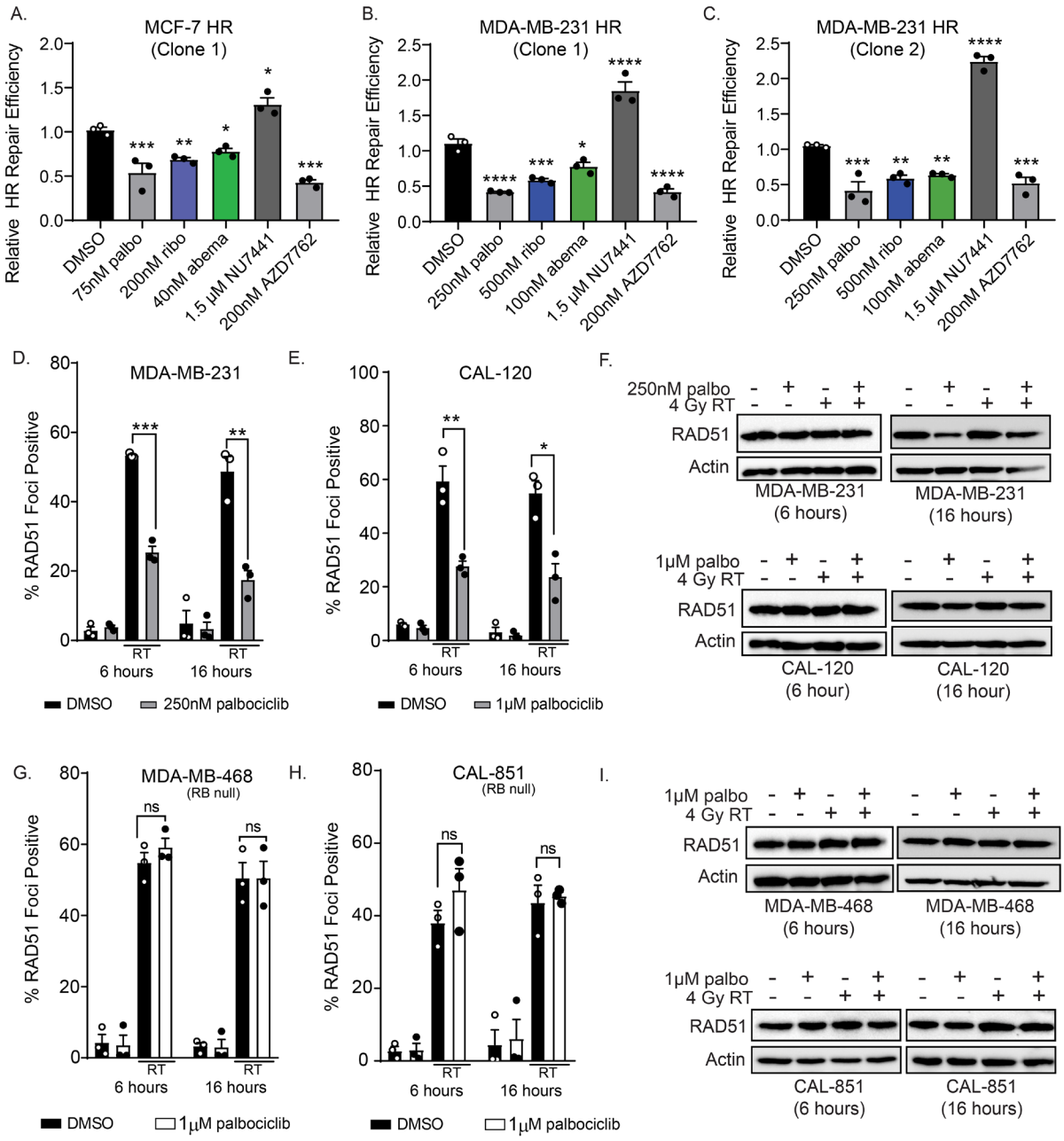

Figure 4.4: CDK4/6 inhibition suppresses HR in RB wild type TNBC

A GFP reporter was used to measure relative HR repair efficiency in RB wild type (**A**-**C**) cells after treatment with in IC_{50} concentration of palbociclib (grey), ribociclib (blue), or abemaciclib (green). A CHK1/2 inhibitor (AZD7762) was used as a positive control and a DNAPK inhibitor (NU7441) was used as the negative control. For RAD51 immunofluorescence, cells were pretreated for one hour with palbociclib and coverslips were fixed 6 hours and 16 hours after 4 Gy radiation in RB wild type MDA-MB-231 (**D**) and CAL-120 (**E**) cells as well as RB null MDA-MB-468 (**G**) and CAL-851 (**H**) TNBC cells. T-tests were performed between radiation and combination treated groups at each time point. Western blots were used to assess RAD51 protein expression at the same timepoints (**F, I**).

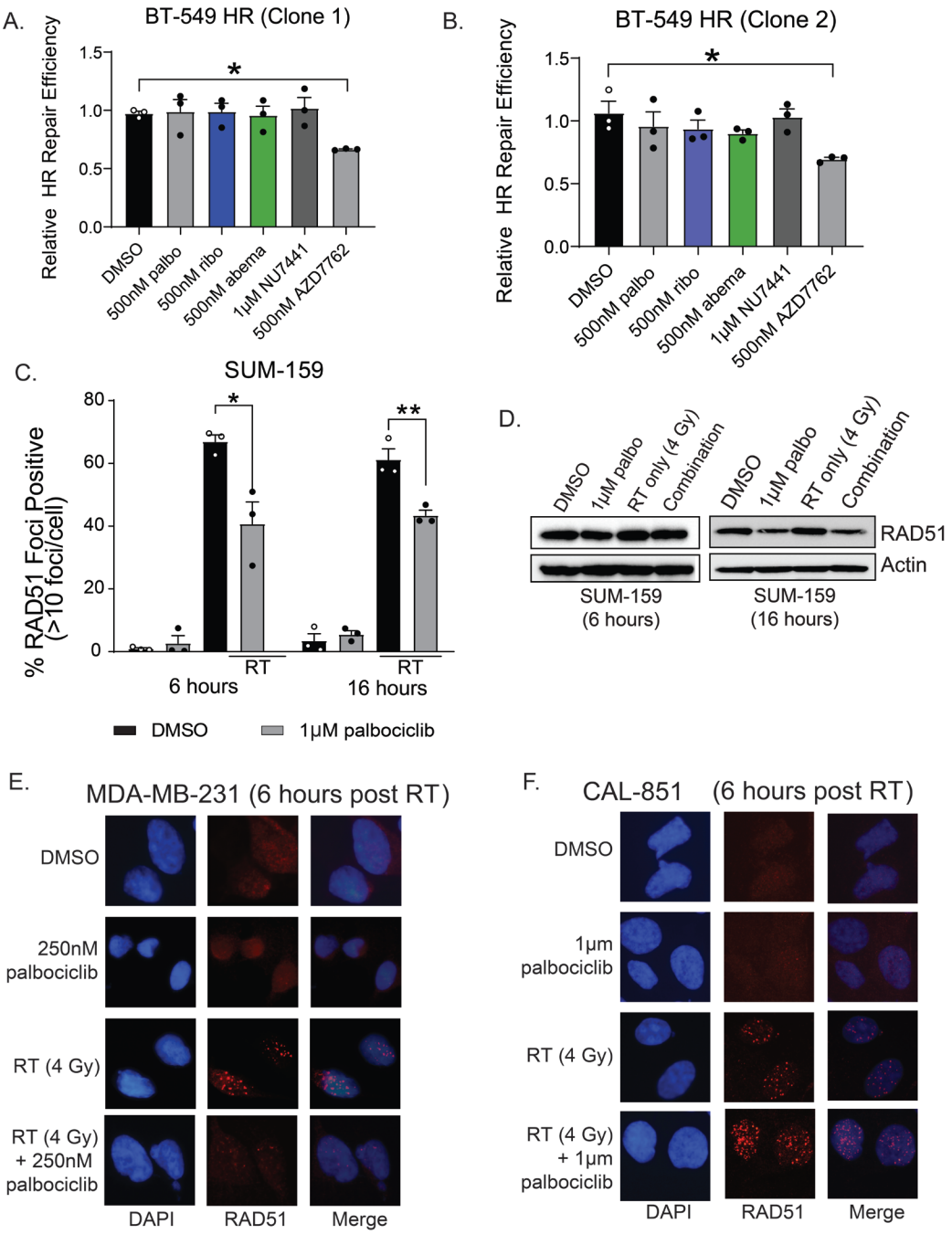

Figure 4.5: CDK4/6 inhibition impairs HR in TNBC *in vitro*

Two stable BT-549 HR reporter clones were pretreated ± 500nM CDK4/6 inhibitor one hour before SceI-induction of dsDNA breaks (**A,B**). After a 1-hour pretreatment with ± 1μM palbociclib and ± 4 Gy radiation, coverslips were stained for RAD51 foci 6 hours and 16 hours after radiation in RB wild type SUM-159 cells (**C**). T-tests were performed between paired radiation and combination treated groups at each timepoint, correcting for multiple comparisons. Western blots were used to assess RAD51 protein expression (**D**). Representative images of RAD51 foci (red) 6 hours post radiation are shown in MDA-MB-231 cells (**E**) and CAL-851 cells (**F**).

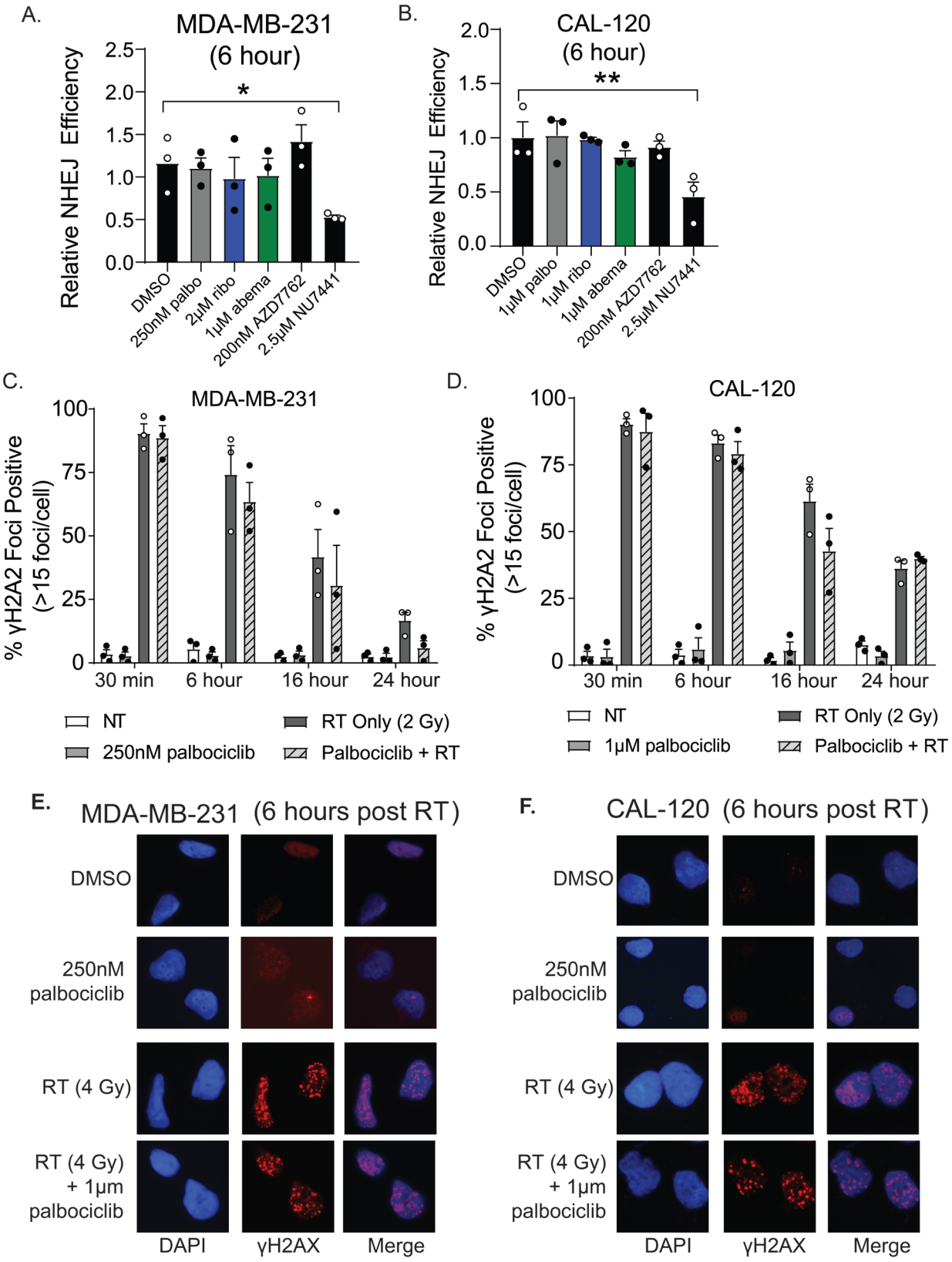
A.
MDA-MB-231
(6 hour)
Relative NHEJ Efficiency
2.5
2.0
1.5
1.0
0.5
0.0
*
DMSO
250nM palbo
2μM ribo
1μM abema
200nM AZD7762
2.5μM NU7441
B.
CAL-120
(6 hour)
Relative NHEJ Efficiency
2.0
1.5
1.0
0.5
0.0
**
DMSO
1μM palbo
1μM ribo
1μM abema
200nM AZD7762
2.5μM NU7441
C.
MDA-MB-231
% γH2A2 Foci Positive
(>15 foci/cell)
100
75
50
25
0
30 min
6 hour
16 hour
24 hour
NT
250nM palbociclib
RT Only (2 Gy)
Palbociclib + RT
D.
CAL-120
% γH2A2 Foci Positive
(>15 foci/cell)
100
75
50
25
0
30 min
6 hour
16 hour
24 hour
NT
1μM palbociclib
RT Only (2 Gy)
Palbociclib + RT
E.
MDA-MB-231 (6 hours post RT)
DMSO
250nM palbociclib
RT (4 Gy)
RT (4 Gy) + 1μm palbociclib
DAPI
γH2AX
Merge
F.
CAL-120 (6 hours post RT)
DMSO
250nM palbociclib
RT (4 Gy)
RT (4 Gy) + 1μm palbociclib
DAPI
γH2AX
Merge

Figure 4.6: CDK4/6 inhibition does not suppress NHEJ efficiency

A eYFP reporter system was used to measure relative NHEJ repair efficiency in RB wild type MDA-MB-231 (**A**) and CAL-120 (**B**) cells after treatment with palbociclib (grey), ribociclib (blue), or abemaciclib (green). The CHK1/2 inhibitor (200nM AZD7762) was used as a negative control and the DNAPK inhibitor (2.5μM NU7441) was used as a positive control. Cells were fixed 0.5, 6, 16, and 24 hours post RT (2Gy) in RB wild type MDA-MB-231 (**C**,**E**) and CAL-120 (**D**,**F**) cells and cells were stained for γH2AX foci (red) and DAPI (blue). (*, $P < 0.05$). All experiments represent the mean of n=3 independent experiments and t-tests were used to compare the RT and combination treated groups at each γH2AX timepoint.

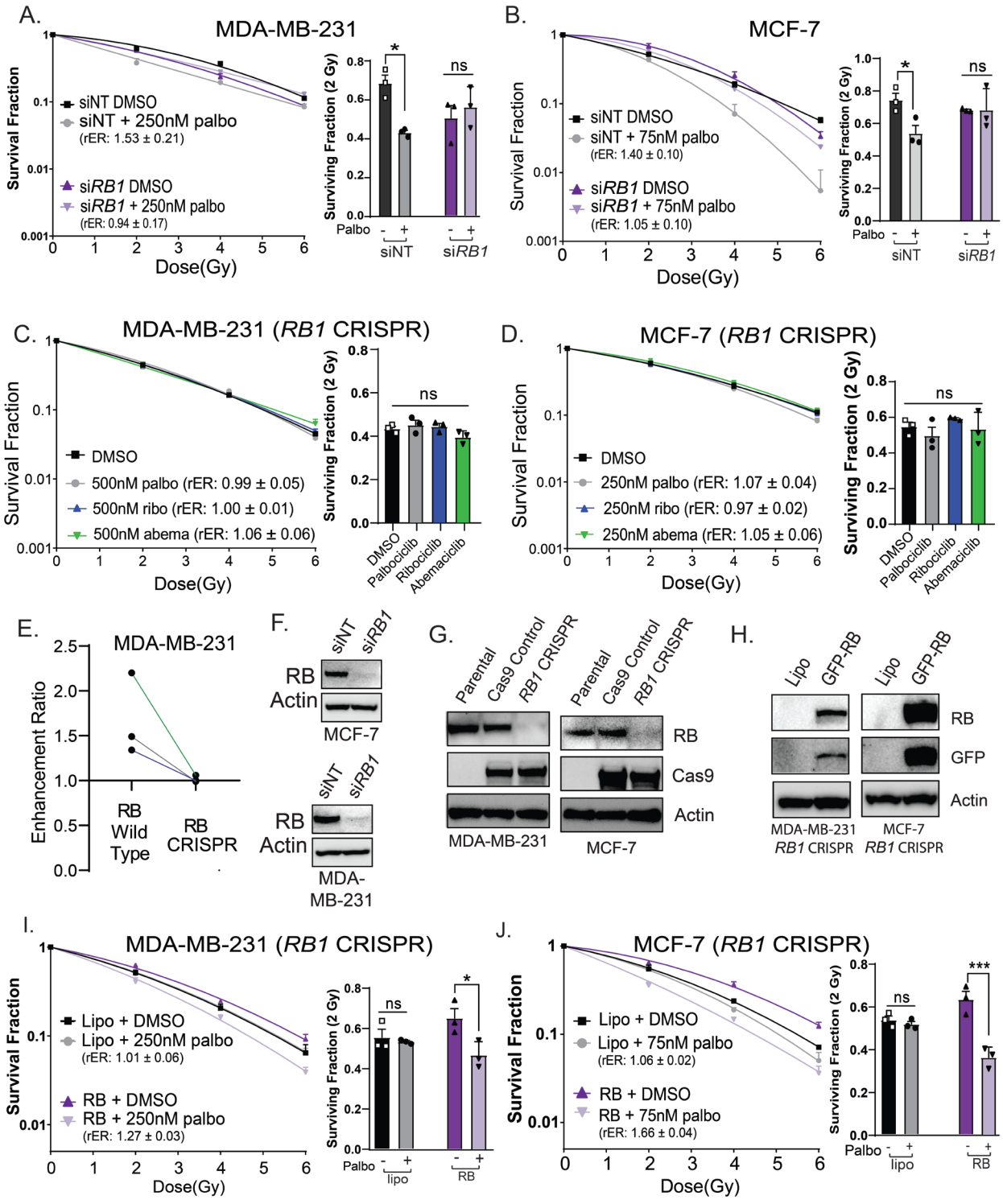
A.
MDA-MB-231
Survival Fraction
siNT DMSO
siNT + 250nM palbo
(rER: 1.53 ± 0.21)
siRB1 DMSO
siRB1 + 250nM palbo
(rER: 0.94 ± 0.17)
Dose(Gy)
Surviving Fraction (2 Gy)
Palbo
siNT
siRB1
B.
MCF-7
siNT DMSO
siNT + 75nM palbo
(rER: 1.40 ± 0.10)
siRB1 DMSO
siRB1 + 75nM palbo
(rER: 1.05 ± 0.10)
C.
MDA-MB-231 (RB1 CRISPR)
DMSO
500nM palbo (rER: 0.99 ± 0.05)
500nM ribo (rER: 1.00 ± 0.01)
500nM abema (rER: 1.06 ± 0.06)
Palbociclib
Ribociclib
Abemaciclib
D.
MCF-7 (RB1 CRISPR)
250nM palbo (rER: 1.07 ± 0.04)
250nM ribo (rER: 0.97 ± 0.02)
250nM abema (rER: 1.05 ± 0.06)
E.
Enhancement Ratio
RB Wild Type
RB CRISPR
F.
siNT
siRB1
RB
Actin
MCF-7
MDA-MB-231
G.
Parental
Cas9 Control
RB1 CRISPR
Cas9
H.
Lipo
GFP-RB
GFP
I.
MDA-MB-231 (RB1 CRISPR)
Lipo + DMSO
Lipo + 250nM palbo
(rER: 1.01 ± 0.06)
RB + DMSO
RB + 250nM palbo
(rER: 1.27 ± 0.03)
J.
MCF-7 (RB1 CRISPR)
Lipo + 75nM palbo
(rER: 1.06 ± 0.02)
RB + 75nM palbo
(rER: 1.66 ± 0.04)

Figure 4.7: RB is required for the radiosensitization of TNBC cell lines

Clonogenic survival assays were performed in breast cancer cell lines with transient knockdown of *RB1* (**A,B**) or CRISPR *RB1* knockout (**C,D**). Average radiation enhancement ratios (rER) were compared between parental MDA-MB-231 cells and MDA-MB-231 *RB1* CRISPR cells **(E**). The efficiency of siRNA mediated knockdown (**F**), CRISPR *RB1* knockout (**G**), and RB overexpression (**H**) were assessed using western blots, where transfected samples were harvested 48 hours post-transfection. RB was transiently overexpressed in MDA-MB-231 (**I**) and MCF-7 (**J**) *RB1* CRISPR cell lines and clonogenic survival assays were used to assess rescue of the radiosensitization phenotype. For CRISPR cells a one-way ANOVA with Dunnett's post hoc test was used to compare CDK4/6 inhibitor-treated cells to vehicle-treated cells. (*, $P < 0.05$; ***, $P < 0.001$).

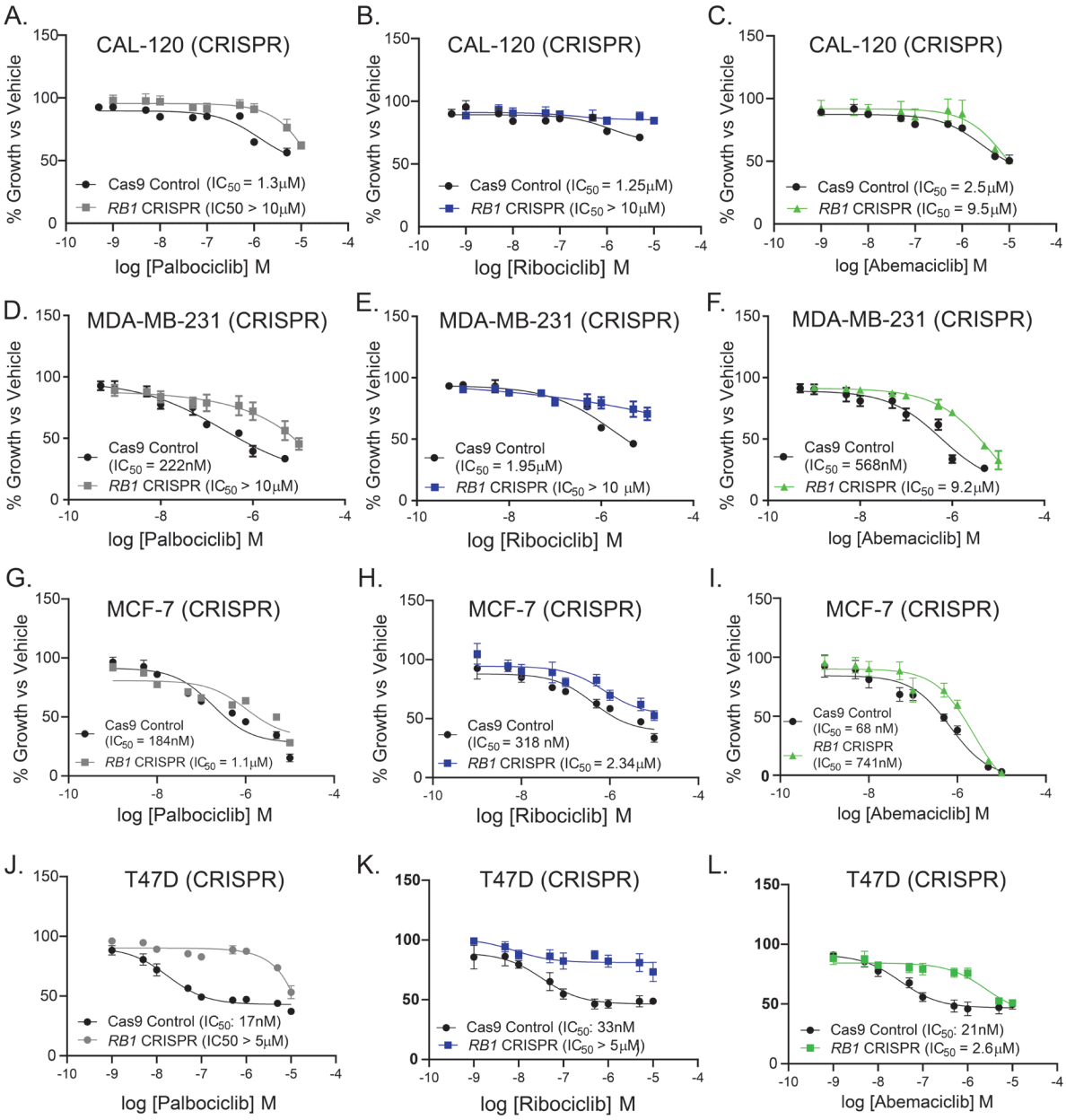

Figure 4.8: *RB1* knockout decreases CDK4/6 inhibitor potency in ER+ and TNBC cell lines

Cell viability was measured 72 hours after treatment with either palbociclib (grey), ribociclib (blue), or abemaciclib (green) in Cas9-expressing control cell lines (black circles) or *RB1* CRISPR knockout cells (colored squares). Dose-response curves were generated for each drug in CAL-120 (**A-C**), MDA-MB-231 (**D-F**), MCF-7 (**G-H**), and T47D (**J-L**) cell lines to calculate IC_{50} values after *RB1* knockout. IC_{50} experiments represent the aggregate of 3 independent replicates and data points display average with SEM.

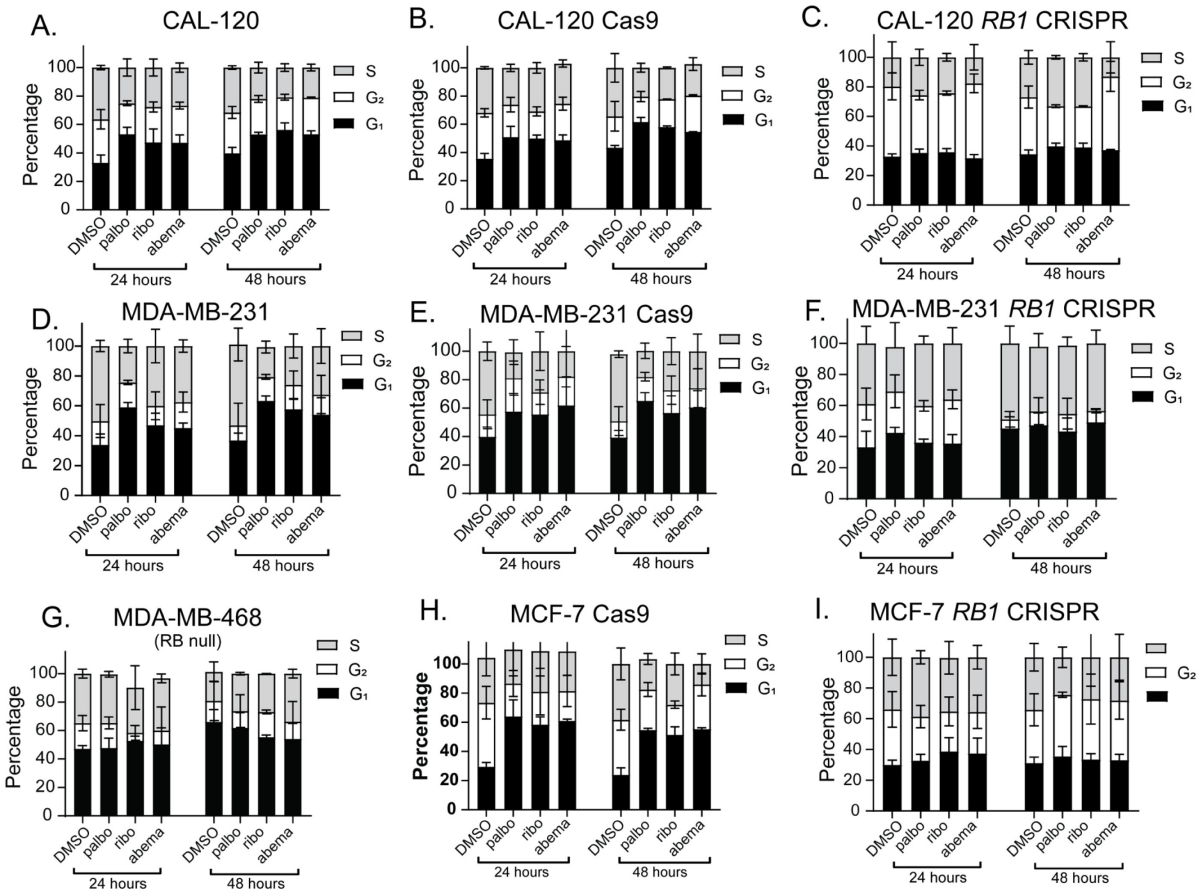

Figure 4.9: *RB1* is essential for G_1 cell-cycle arrest

Flow cytometry was used to quantify cell cycle distribution in G_1 (black), G_2 (white), and S (grey) phase after CDK4/6 inhibition using propidium iodine (PI) staining in CAL-120 cells (**A, B**), MDA-MB-231 cells (**D,E**) and MCF-7 cells **(H)** with intact *RB1*. Cell cycle progression was also quantified in RB null MDA-MB-468 cells (**G**) and in models of *RB1* knockout (**C,F,I**). Cells were fixed at 24 hours and 48 hours post drug treatment with the IC_{50} concentration of palbociclib, abemaciclib, and ribociclib in all cell lines.

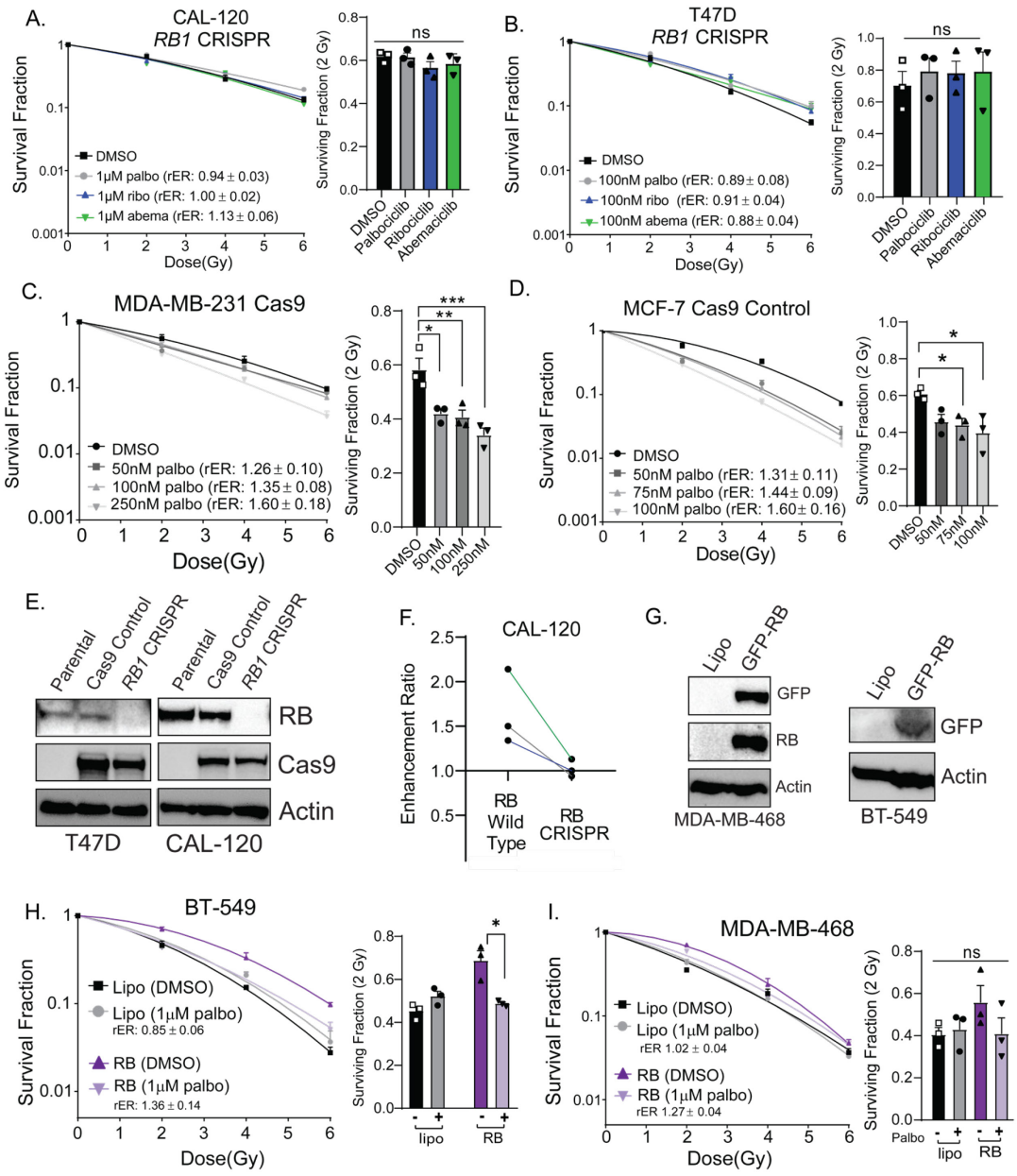

Figure 4.10: Loss of *RB1* diminishes CDK4/6 inhibitor-mediated radiosensitivity

Clonogenic survival assays were performed in CAL-120 (**A**) and T47D (**B**) *RB1* CRISPR cells along with MDA-MB-231 (**C**) and MCF-7 (**D**) Cas9 control cells to quantify radiosensitization and calculate radiation enhancement ratios (rER). Western blots were used to confirm successful knockout of RB in CAL-120 and T47D cells (**E**)**.** rER were compared between parental CAL-120 cells and CAL-120 *RB1* CRISPR knockout cells (**F**). Overexpression of RB was performed in MDA-MB-468 and BT-549 cells in order to assess radiosensitivity in clonogenic survival assays (**G-I**). All clonogenics represent the pooled results of 3 independent replicates. (*, $P < 0.05$; **, $P < 0.01$; ***, $P < 0.001$, ****, $P < 0.0001$).

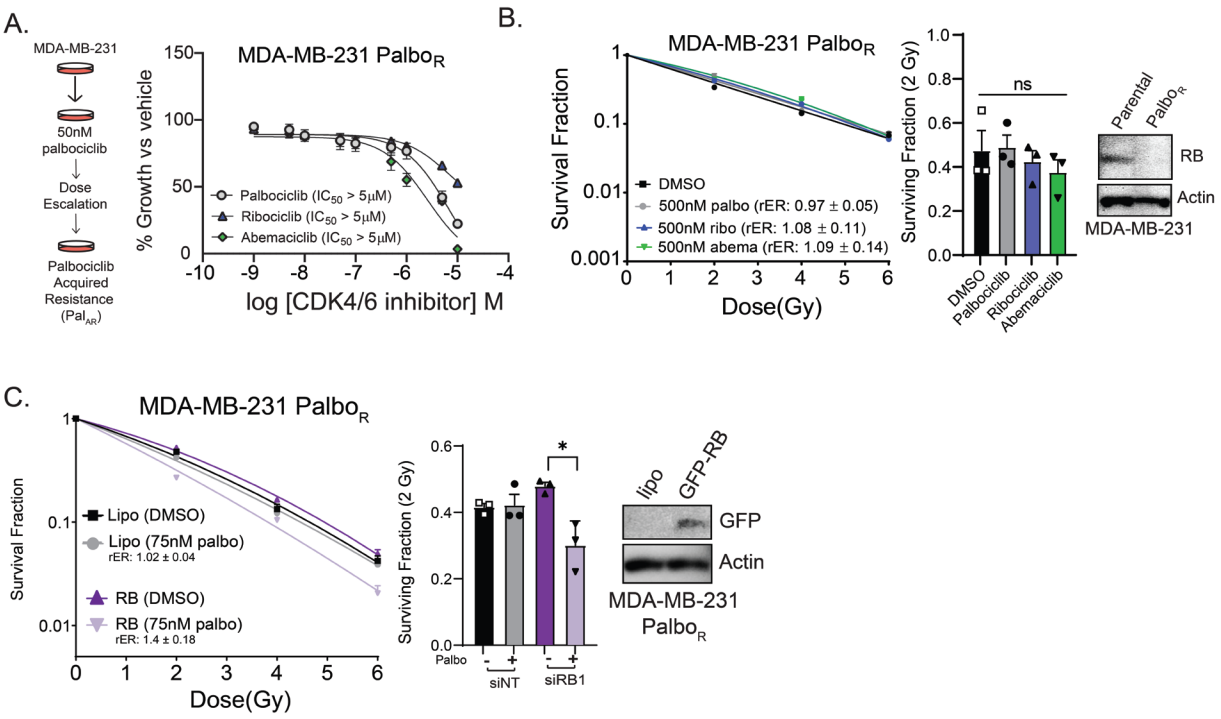

Figure 4.11: Palbociclib-resistant TNBC cells demonstrate loss of both RB protein and CDK4/6 inhbitor-mediated radiosensitization.

Palbociclib-resistant MDA-MB-231 cells were generated through continuous culture in drug-containing media (**A**) and 72 hour cell viability was used to assess acquired resistance to palbociclib, ribociclib, or abemaciclib. Clonogenic survival assays were performed to quantify the rER for PalboR cells and western blots were used to assess RB expression compared to parental MDA-MB-231 cells (**B**). Radiosensitization was assessed after transient overexpression of GFP-RB and pretreament ± palbociclib (**C**).

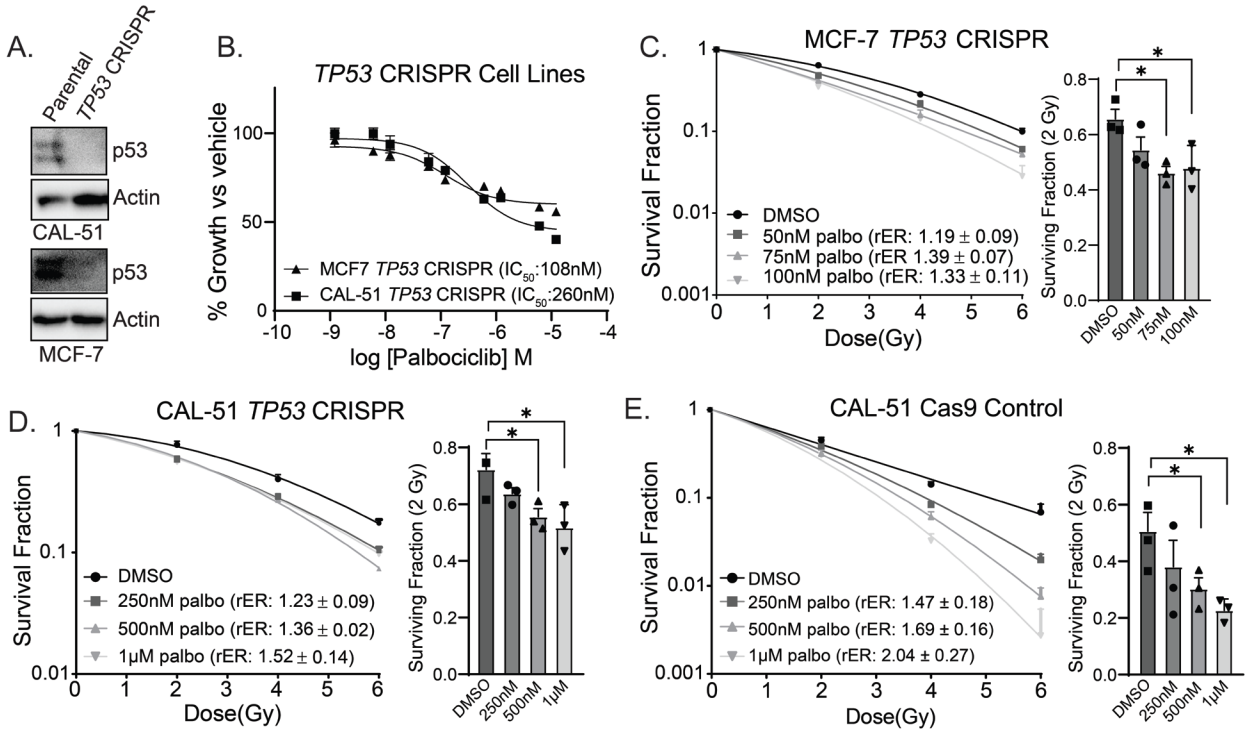

Figure 4.12 Loss of p53 expression does not significantly impact radiosensitization

Knockout of p53 protein was assessed by western blot (**A**) and the viability of *TP53* CRISPR cell lines was assessed using Alamar Blue 72 hours after treatment with varying concentrations of palbociclib (**B**). Clonogenic survival assays were used to assess palbociclib-mediated radiosensitization in *TP53* knockout cell lines (**C,D**) and Cas9 control cells (**E**) using a one hour pretreatment. A one-way ANOVA with Dunnett's post hoc test was used to compare SF 2 Gy values for each cell line (*, $P < 0.05$).

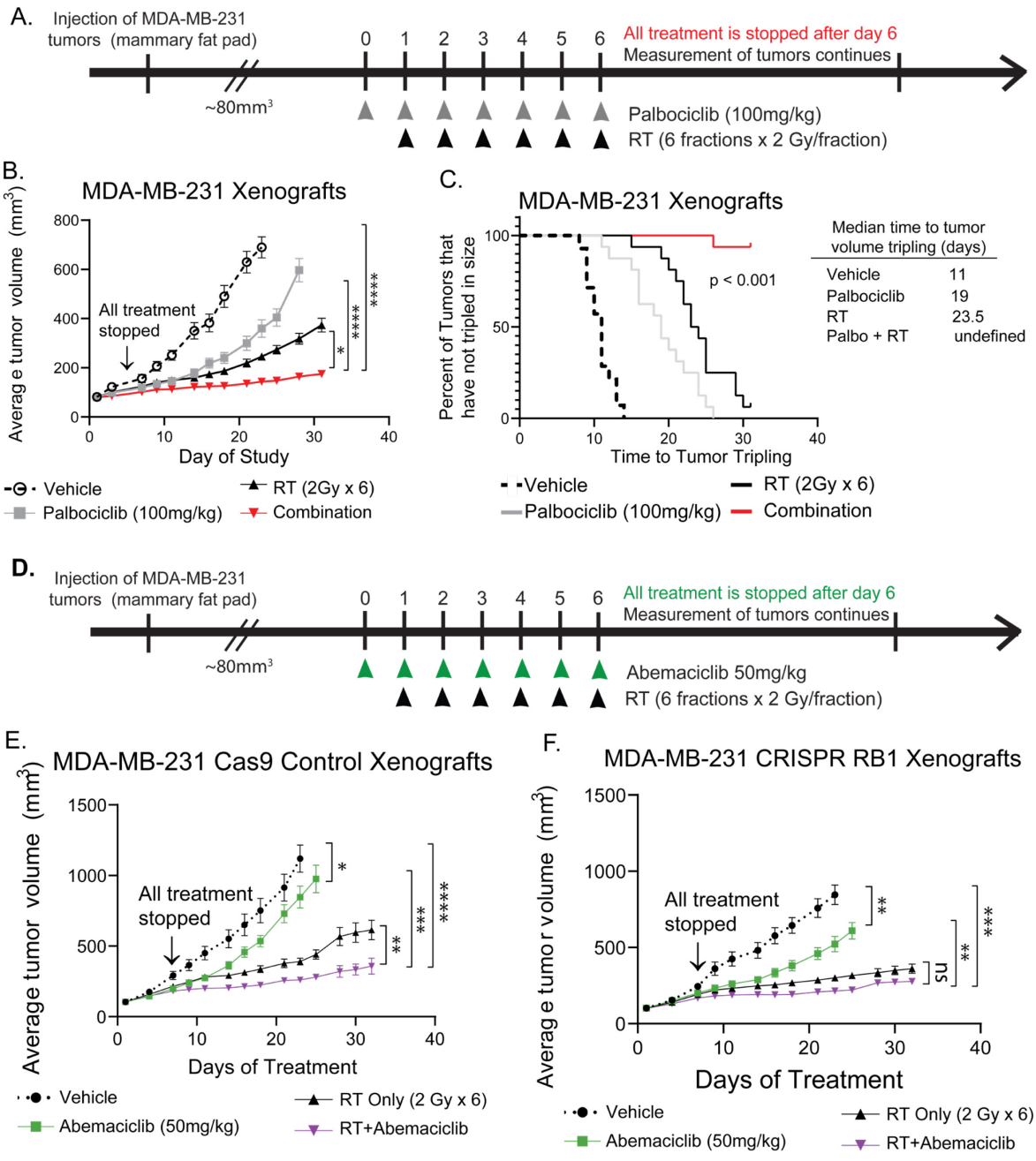

Figure 4.13: CDK4/6 inhibition radiosensitizes TNBC cells *in vivo*

Mice bearing parental (RB wild type) MDA-MB-231 xenografts were randomized to four treatment groups (8-9 tumors per group): vehicle, RT only, 100mg/kg palbociclib, and the combination (**A**). Tumor size was measured 2-3 times a week and used to calculate average tumor volume (**B**; graphed as average ± SEM) and time to tumor tripling **(C;** log-rank Mantel-Cox test). Xenografts with CRISPR MDA-MB-231 cells (**D**) expressing either Cas9 only (**E**) or Cas9 and the *RB1* guide RNA (**F**) were treated in a similar treatment schedule using 50mg/kg abemaciclib or the combination of abemaciclib + RT. Tumor volume was compared using a one-way ANOVA comparing average tumor size at the end of the study across the treatment groups.

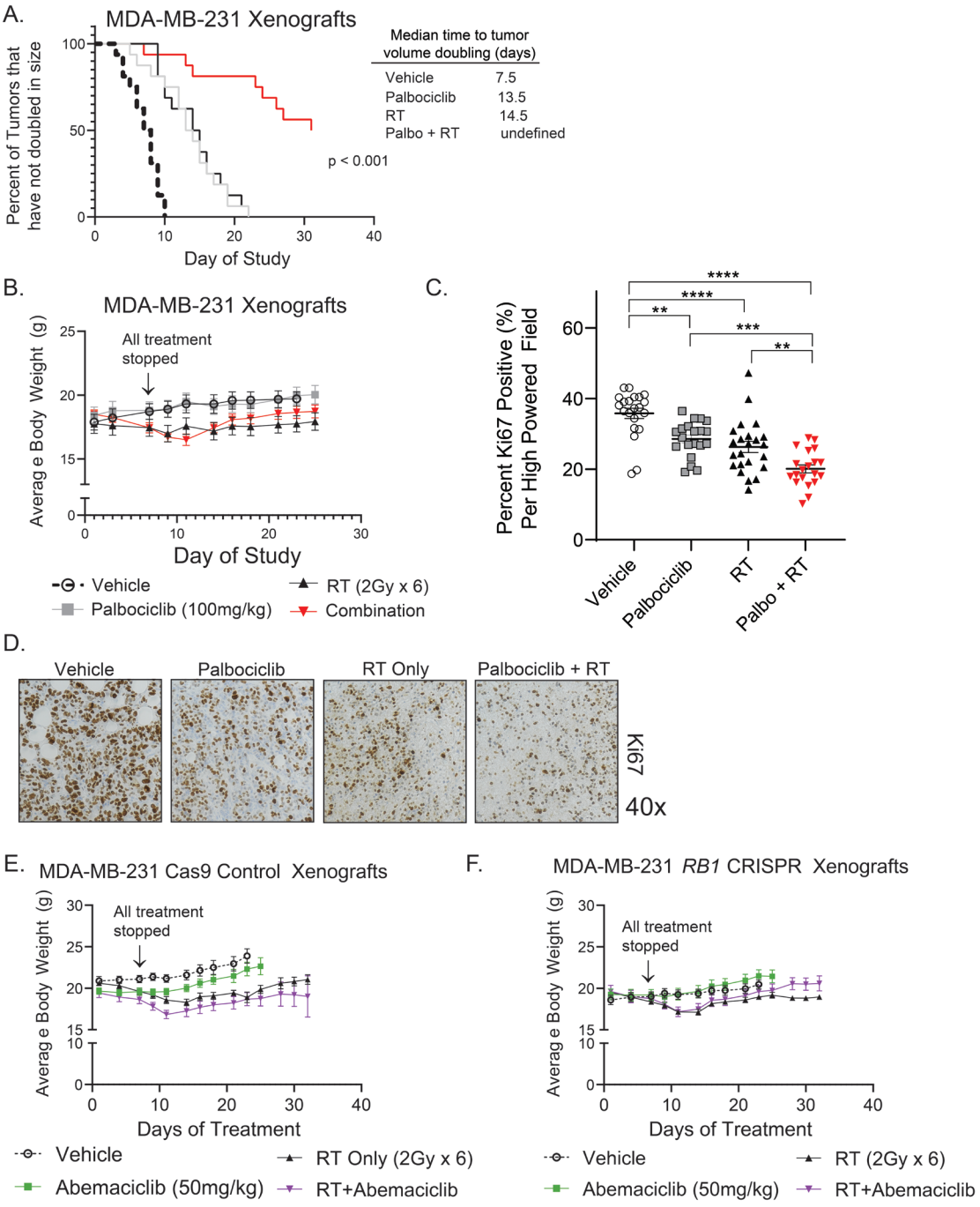

Figure 4.14: CDK4/6 inhibitor-mediated radiosensitization of TNBC *in vivo*

Time to tumor doubling is shown for MDA-MB-231 parental (RB wild type, **A**) xenografts treated with palbociclib, and a log-rank (Mantel-Cox) test was used to compare survival curves. Weights are shown for mice with parental (**B**), Cas9 control (**E**), and *RB1* CRISPR (**F**) xenografts throughout the study. Ki67 staining (imaged at 40x) was used to assess proliferation of tumor cells in mice treated with short term palbociclib and/or RT (**C,D**). A one-way ANOVA with Tukey's post hoc test was used to compare Ki67 staining across treatment groups.

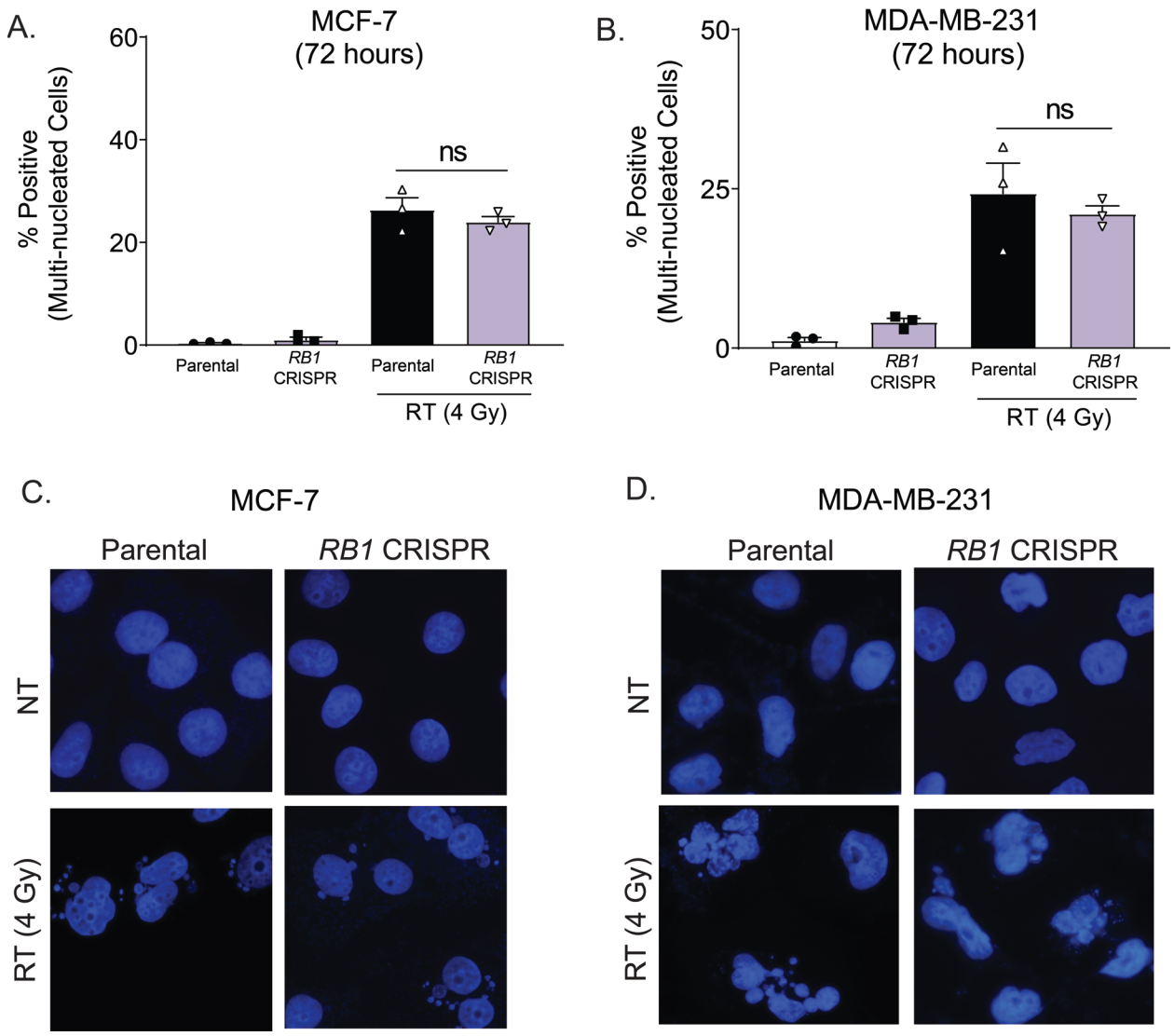

Figure 4.15: *RB1* loss does not result in increased micronuclei formation following ionizing RT

Immunofluorescence was used to quantify micronuclei formation following 4 Gy RT in parental and *RB1* CRISPR MCF-7 **(A)** and MDA-MB-231 cells (**B**) 72 hours after RT. Representative DAPI-stained slides are shown for all treatment groups (**C,D**).

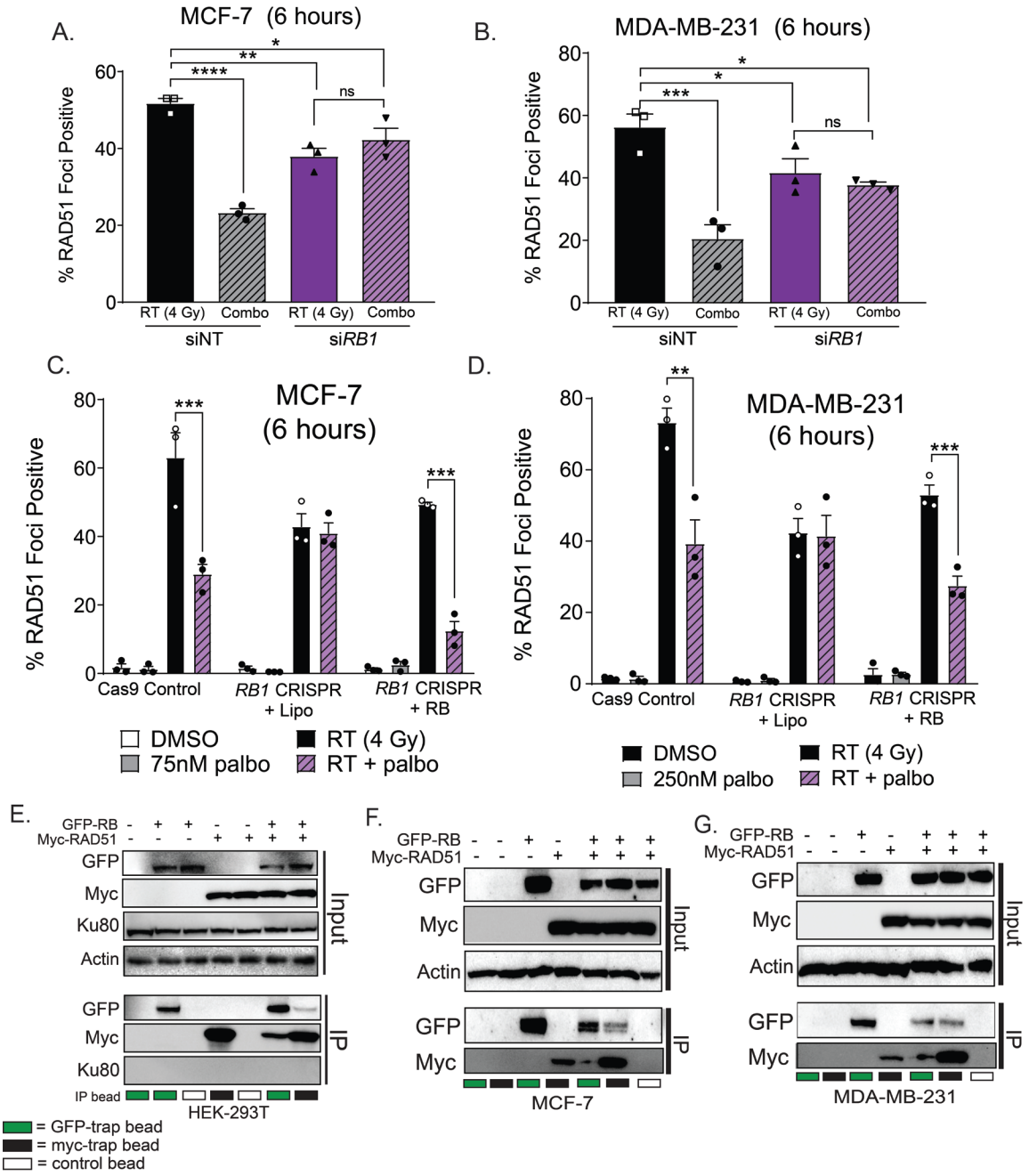

Figure 4.16: RB is required for efficient repair of dsDNA breaks through HR

RAD51 foci formation was used to assess HR competency with transient (**A,B**) knockdown or CRISPR knockout (**C,D**) of *RB1* in MCF-7 and MDA-MB-231 cells at 6 hours post radiation. Cells transfected with a control siRNA or cells expressing Cas9 with control guides (*AAVS1*) were used for comparison. Immunoprecipitation of GFP-RB and myc-RAD51 was performed 24 hours after transfection of HEK-293T cells (**E**), MCF-7 cells (**F**), or MDA-MB-231 cells (**G**) using myc-trap beads (black boxes), GFP-trap beads (green boxes), or control beads (white boxes). Expression of myc-RAD51 and GFP-RB was assessed in protein inputs and IP lysates with western blotting.

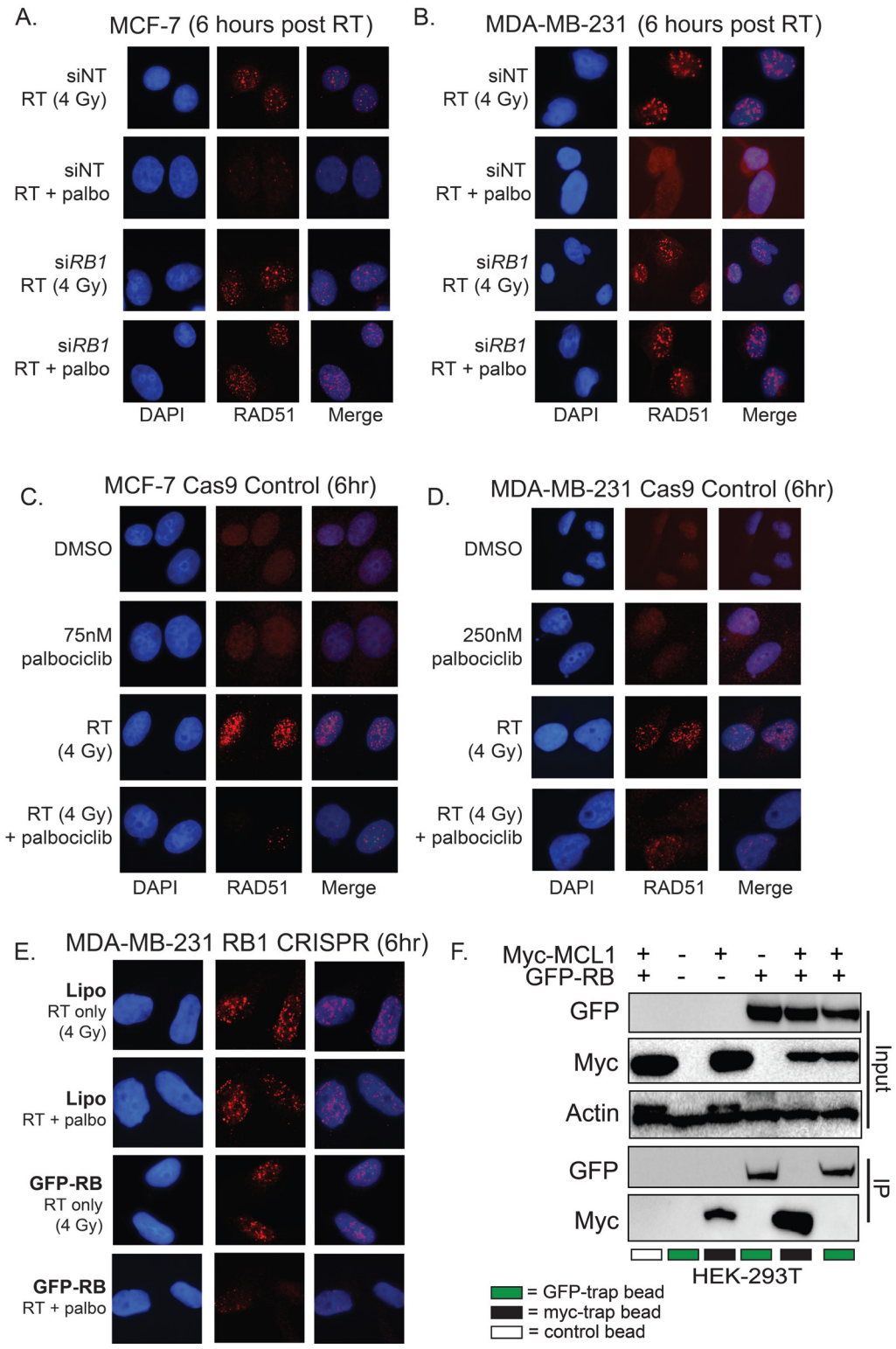

Figure 4.17: CDK4/6 inhibition suppresses RAD51 foci formation

Representative images of RAD51 foci at 6 hours post RT (4 Gy) are shown (**A-E**). As a control for immunoprecipitation, GFP-RB and myc-MCL1 were transfected into HEK-293T cells and immunoprecipitation was performed 24 hours later (**F**).

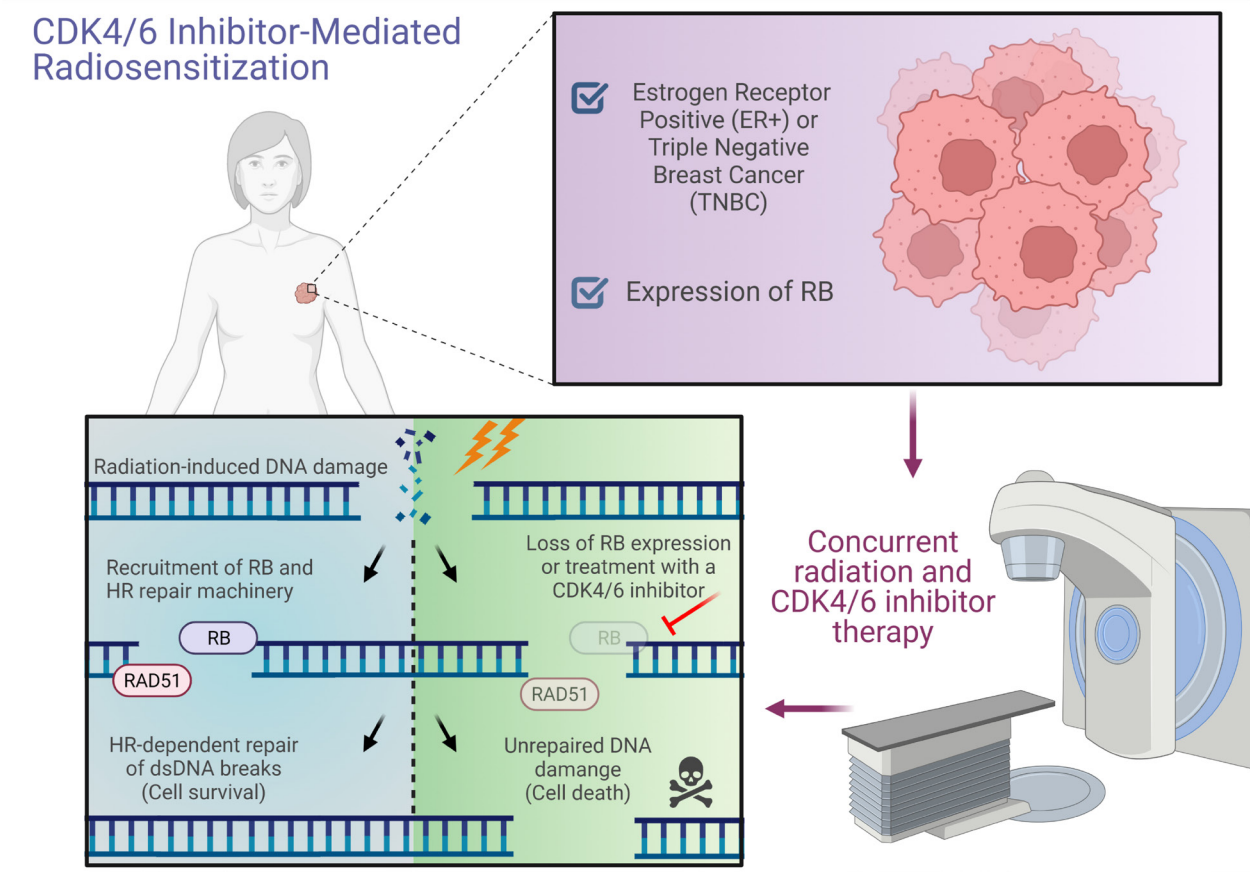

Figure 4.18: Graphical abstract describing the mechanism of CDK4/6 inhibitor-mediated radiosensization in ER+ and TNBC.

	Palbociclib			Ribociclib			Abemaciclib		
	IC_{50}	**CRISPR *RB1* IC_{50}**	**Cas9 Only IC_{50}**	**IC_{50}**	**CRISPR *RB1* IC_{50}**	**Cas9 Only IC_{50}**	**IC_{50}**	**CRISPR *RB1* IC_{50}**	**Cas9 Only IC_{50}**
MDA-MB-231	241.6nM	>10 μM	222nM	1.99μM	>10 μM	1.95μM	1.07μM	9.2 μM	568nM
CAL-120	2.9μM	>10 μM	1.3μM	1.77μM	>10 μM	1.25μM	2.61μM	9.5 μM	2.54μM
T47D	20nM	> 5μM	17nM	40nM	> 5 uM	33nM	10nM	2.6μM	21nM
MCF-7	75nM	1.047 μM	184nM	200nM	741 nM	317.7nM	40nM	2.34μM	68nM

Table 4.1: IC_{50} values for parental and CRISPR TNBC and ER+ breast cancer cell lines

Palbociclib	Cell Line	IC_{50}	RB
	SUM-159	5.5μM	Wild Type
	CAL-51	330nM	Wild Type
	MDA-MB-468	>10μM	Null
	CAL-851	>10μM	Null

Table 4.2: IC_{50} values for additional TNBC cell lines

	Cell Line	Concentration	rER	RB
Palbociclib	MCF-7	100nM	1.52 + 0.14	Wild Type
	T47D	25nM	1.50 + 0.13	Wild Type
	CAMA1	75nM	1.32 + 0.09	Wild Type
	ZR-75-1	100nM	1.27 + 0.14	Wild Type

Table 4.3: Radiation enhancement ratios for ER+ breast cancer cell lines treated with palbociclib

MDA-MB-231	Palbociclib			Combination		
	Day	**RT**	**Palbo**	**Expected**	**Observed**	**Ratio**
	7	0.790	0.762	0.602	0.651	0.925
	16	0.455	0.572	0.260	0.325	0.801
	18	0.381	0.490	0.187	0.257	0.725
	21	0.348	0.476	0.165	0.215	0.768
	Final	0.462	0.866	0.400	0.238	**1.682**

Table 4.4: Fractional tumor volume Calculations for MDA-MB-231 xenografts treated with palbociclib.

		Abemaciclib		Combination		
	Day	**RT**	**Abema**	**Expected**	**Observed**	**Ratio**
MDA-MB-231 Cas9 CRISPR	7	0.738	0.678	0.500	0.624	0.801
	11	0.625	0.608	0.380	0.446	0.852
	16	0.482	0.703	0.338	0.329	1.030
	18	0.448	0.712	0.319	0.299	1.067
	Final	0.549	0.872	0.479	0.320	1.499
MDA-MB-231 *RB1* CRISPR	7	0.782	0.818	0.640	0.684	0.935
	11	0.546	0.613	0.335	0.444	0.754
	16	0.440	0.579	0.254	0.327	0.778
	18	0.416	0.591	0.246	0.298	0.824
	Final	0.427	0.721	0.308	0.327	0.939

Table 4.5: Fractional tumor volume calculations for MDA-MB-231 Cas9 Control and *RB1* CRISPR xenografts treated with abemaciclib.

	Timepoint	Treatment	Average Foci / Cell	Average Foci / Positive Cell
CAL-120	**6 hours**	*DMSO*	3.66 ± 0.74	
		Palbociclib	2.82 ± 1.34	
		RT (4 Gy)	11.28 ± 3.39	19.56 ± 6.37
		RT + Palbo	7.38 ± 3.02	26.71 ± 10.37
	16 hours	*DMSO*	0.91± 0.64	
		Palbociclib	1.14 ± 0.67	
		RT (4 Gy)	11.86 ± 2.01	21.51 ± 2.00
		RT + Palbo	3.48 ± 0.92	17.46 ± 6.07
MDA-MB-231	**6 hours**	*DMSO*	6.67 ± 4.77	
		Palbociclib	2.84 ± 1.65	
		RT (4 Gy)	12.81 ± 4.85	25.30 ± 8.16
		RT + Palbo	4.12 ± 2.89	31.92 ± 15.83
	16 hours	*DMSO*	1.54 ± 0.49	
		Palbociclib	1.85 ± 0.34	
		RT (4 Gy)	6.43 ± 0.55	12.07 ± 1.01
		RT + Palbo	4.47 ± 3.02	18.11 ± 7.32
MDA-MB-468	**6 hours**	*DMSO*	2.72 ± 1.13	
		Palbociclib	2.18 ± 1.96	
		RT (4 Gy)	15.57 ± 4.02	29.13 ± 8.61
		RT + Palbo	11.39 ± 1.62	19.67 ± 3.47
	16 hours	*DMSO*	1.92 ± 0.52	
		Palbociclib	1.86 ± 0.84	
		RT (4 Gy)	9.04 ± 0.51	18.18 ± 1.39
		RT + Palbo	7.66 ± 0.32	15.51 ± 1.52
CAL-851	**6 hours**	*DMSO*	1.07 ± 0.47	
		Palbociclib	1.27 ± 0.80	
		RT (4 Gy)	16.17 ± 2.71	44.24 ± 10.49
		RT + Palbo	14.51 ± 3.80	34.48 ± 7.25
	16 hours	*DMSO*	1.51 ± 0.60	
		Palbociclib	2.46 ± 0.56	
		RT (4 Gy)	7.97 ± 2.33	16.06 ± 4.38
		RT + Palbo	9.32 ± 2.95	20.84 ± 6.95

Table 4.6: Quantification of RAD51 foci in RB wild type and RB null TNBC cell lines.

	Timepoint	Treatment	Average Foci / Cell	Average Foci / Positive Cell
CAL-120	**30 min**	*DMSO*	2.29 ± 0.52	
		Palbociclib	2.31 ± 0.30	
		RT (4 Gy)	20.40 ± 1.03	22.58 ± 0.64
		RT + Palbo	21.16 ± 1.68	24.21 ± 0.89
	6 hours	*DMSO*	2.73 ± 1.40	
		Palbociclib	2.51 ± 0.47	
		RT (4 Gy)	17.05 ± 0.60	21.51 ± 0.35
		RT + Palbo	14.51 ± 0.29	17.49 ± 0.54
	16 hours	*DMSO*	2.77 ± 1.04	
		Palbociclib	1.16 ± 0.65	
		RT (4 Gy)	13.40 ± 4.23	26.06 ± 0.34
		RT + Palbo	10.85 ± 2.5	24.70 ± 1.42
	24 hours	*DMSO*	1.55 ± 0.59	
		Palbociclib	1.87 ± 1.02	
		RT (4 Gy)	7.32 ± 1.11	20.83 ± 4.66
		RT + Palbo	8.27 ± 1.45	20.80 ± 3.96
MDA-MB-231	**30 min**	*DMSO*	1.24 ± 0.51	
		Palbociclib	0.91 ± 0.34	
		RT (4 Gy)	12.84 ± 5.96	19.20 ± 0.90
		RT + Palbo	18.94 ± 1.36	21.34 ± 0.80
	6 hours	*DMSO*	2.28 ± 0.76	
		Palbociclib	0.50 ± 0.02	
		RT (4 Gy)	11.63 ± 3.57	14.76 ± 3.05
		RT + Palbo	12.07 ± 2.32	18.76 ± 2.71
	16 hours	*DMSO*	1.02 ± 0.13	
		Palbociclib	1.29 ± 0.49	
		RT (4 Gy)	10.08 ± 2.02	23.11 ± 1.52
		RT + Palbo	7.00 ± 4.85	20.52 ± 1.01
	24 hours	*DMSO*	0.69 ± 0.18	
		Palbociclib	1.17 ± 0.54	
		RT (4 Gy)	3.78 ± 0.91	18.75 ± 3.49
		RT + Palbo	2.52 ± 1.30	20.17 ± 2.21

Table 4.7: Quantification of γH2AX foci after RT and CDK4/6 inhibition.

	Timepoint	Treatment	Average Foci / Cell	Average Foci / Positive Cell
MCF-7	**6 hours**	*RT (siNT)*	17.07 ± 0.17	33.04 ± 0.66
		RT + Palbo (siNT)	4.71 ± 1.07	20.71 ± 5.63
		RT (siRB1)	6.5 ± 0.82	17.40 ± 2.98
		RT + Palbo (siRB1)	10.13 ± 1.72	23.74 ± 2.73
MDA-MB-231	**6 hours**	*RT (siNT)*	11.57 ± 3.75	28.58 ± 3.25
		RT + Palbo (siNT)	5.65 ± 0.37	18.68 ± 3.01
		RT (siRB1)	5.18 ± 0.38	12.56 ± 0.88
		RT + Palbo (siRB1)	7.99 ± 1.10	21.18 ± 3.10

Table 4.8: Quantification of RAD51 foci in MCF-7 and MDA-MB-231 cells after RT and CDK4/6 inhibition ± si*RB1*.

Treatment			Average Foci / Cell	Average Foci / Positive Cell
MCF-7 Cas9	**6 hours**	*NT*	2.51 ± 0.68	
		Palbociclib	1.31 ± 05.1	
		RT (4 Gy)	22.96 ± 4.26	35.79 ± 3.30
		RT + Palbociclib	10.65 ± 1.59	37.61 ± 6.77
MCF-7 *RB1* CRISPR	**6 hours**	*NT*	2.02 ± 0.70	
		Palbociclib	0.71 ± 0.29	
		RT (4 Gy)	15.24 ± 2.83	35.38 ± 5.82
		RT + Palbociclib	14.55 ± 3.19	34.82 ± 5.40
MCF-7 *RB1* CRISPR + GFP-RB	**6 hours**	*NT*	2.11 ± 1.29	
		Palbociclib	2.42 ± 0.75	
		RT (4 Gy)	19.98 ± 3.42	40.57 ± 7.33
		RT + Palbociclib	6.68 ± 2.87	50.70 ± 12.39
MDA-MB-231 Cas9	**6 hours**	*NT*	2.60 ± 1.12	
		Palbociclib	3.61 ± 0.49	
		RT (4 Gy)	24.69 ± 5.25	33.14 ± 5.86
		RT + Palbociclib	8.36 ± 3.24	22.32 ± 9.56
MDA-MB-231 *RB1* CRISPR	**6 hours**	*NT*	4.36 ± 1.35	
		Palbociclib	3.29 ± 0.39	
		RT (4 Gy)	12.52 ± 0.76	23.60 ± 0.96
		RT + Palbociclib	9.01 ± 0.23	33.14 ± 2.29
MDA-MB-231 *RB1* CRISPR + GFP-RB	**6 hours**	*NT*	1.09 ± 0.73	
		Palbociclib	1.51 ± 0.79	
		RT (4 Gy)	20.42 ± 4.99	45.81 ± 6.48
		RT + Palbociclib	14.97 ± 2.51	38.74 ± 10.26

Table 4.9: Quantification of RAD51 foci in MCF-7 and MDA-MB-231 Cas9 control and RB1 CRISPR cells ± transient GFP-RB overexpression.

References

1. Clarke M, et al. Effects of radiotherapy and of differences in the extent of surgery for early breast cancer on local recurrence and 15-year survival: an overview of the randomised trials. Lancet. 2005;366(9503):2087-106.
2. Voduc KD, et al. Breast cancer subtypes and the risk of local and regional relapse. J Clin Oncol. 2010 Apr 1;28(10):1684-91.
3. Early Breast Cancer Trialists' Collaborative Group (EBCTCG). Effects of chemotherapy and hormonal therapy for early breast cancer on recurrence and 15-year survival: an overview of the randomised trials. Lancet. 2005 May 14-20;365(9472):1687-717.
4. Finn RS, et al. PD 0332991, a selective cyclin D kinase 4/6 inhibitor, preferentially inhibits proliferation of luminal estrogen receptor-positive human breast cancer cell lines in vitro. Breast Cancer Res. 2009;11(5):R77.
5. Tripathy D, Bardia A, Sellers WR. Ribociclib (LEE011): Mechanism of Action and Clinical Impact of This Selective Cyclin-Dependent Kinase 4/6 Inhibitor in Various Solid Tumors. Clin Cancer Res. 2017;23(13):3251-62.
6. Gelbert LM, et al. Preclinical characterization of the CDK4/6 inhibitor LY2835219: in-vivo cell cycle-dependent/independent anti-tumor activities alone/in combination with gemcitabine. Invest New Drugs. 2014 Oct;32(5):825-37. 7.
7. Finn RS, et al. The cyclin-dependent kinase 4/6 inhibitor palbociclib in combination with letrozole versus letrozole alone as first-line treatment of oestrogen receptor-positive, HER2-negative, advanced breast cancer (PALOMA-1/TRIO-18): a randomised phase 2 study. Lancet Oncol. 2015;16(1):25-35.
8. Mayer EL, et al. Palbociclib with adjuvant endocrine therapy in early breast cancer (PALLAS): interim analysis of a multicentre, open-label, randomised, phase 3 study. Lancet Oncol. 2021 Feb;22(2):212-222.
9. Johnston SRD, et al. Abemaciclib Combined With Endocrine Therapy for the Adjuvant Treatment of HR+, HER2-, Node-Positive, High-Risk, Early Breast Cancer (monarchE). J Clin Oncol. 2020 Dec 1;38(34):3987-3998.
10. Slamon DJ, et al. NATALEE: Phase III study of ribociclib (RIBO) + endocrine therapy (ET) as adjuvant treatment in hormone receptor–positive (HR+), human epidermal growth factor receptor 2–negative (HER2–) early breast cancer (EBC). Journal of Clinical Oncology 2019 37:15_suppl, TPS597-TPS597.
11. Cretella D, et al. Pre-treatment with the CDK4/6 inhibitor palbociclib improves the efficacy of paclitaxel in TNBC cells. Sci Rep. 2019 Sep 10;9(1):13014.
12. Salvador-Barbero B, et al. CDK4/6 Inhibitors Impair Recovery from Cytotoxic Chemotherapy in Pancreatic Adenocarcinoma. Cancer Cell. 2020 Mar 16;37(3):340-353.e6.
13. Roberts PJ, et al. Chemotherapy and CDK4/6 Inhibitors: Unexpected Bedfellows. Mol Cancer Ther. 2020 Aug;19(8):1575-1588.
14. Gao Y, et al. Inhibition of CDK4 sensitizes multidrug resistant ovarian cancer cells to paclitaxel by increasing apoptosiss. Cell Oncol (Dordr). 2017;40(3):209-18.
15. Huang Y, Wu H, and Li X. Novel sequential treatment with palbociclib enhances the effect of cisplatin in RB-proficient triple-negative breast cancer. Cancer Cell International. 2020;20(1):1-14.

16. O'Brien N, et al. Preclinical Activity of Abemaciclib Alone or in Combination with Antimitotic and Targeted Therapies in Breast Cancer. Mol Cancer Ther. 2018 May;17(5):897-907.
17. Pesch AM, et al. Short Term CDK4/6 Inhibition Radiosensitizes Estrogen Receptor Positive Breast Cancers. Clin Cancer Res. 2020 Dec 15;26(24):6568-6580.
18. Petroni G, et al. Radiotherapy Delivered before CDK4/6 Inhibitors Mediates Superior Therapeutic Effects in ER+ Breast Cancer. Clin Cancer Res. 2021 Apr 1;27(7):1855-1863.
19. Choi C, et al. Cyclin D1 is Associated with Radiosensitivity of Triple-Negative Breast Cancer Cells to Proton Beam Irradiation. Int J Mol Sci. 2019 Oct 7;20(19):4943.
20. Tate JG, et al. COSMIC: the Catalogue Of Somatic Mutations In Cancer. Nucleic Acids Res. 2019 Jan 8;47(D1):D941-D947.
21. Witkiewicz AK, Knudsen ES. Retinoblastoma tumor suppressor pathway in breast cancer: prognosis, precision medicine, and therapeutic interventions. Breast Cancer Res. 2014 May 7;16(3):207.
22. Hashizume R, et al. Inhibition of DNA damage repair by the CDK4/6 inhibitor palbociclib delays irradiated intracranial atypical teratoid rhabdoid tumor and glioblastoma xenograft regrowth. Neuro Oncol. 2016 Nov;18(11):1519-1528.
23. Marshall AE, et al. *RB1* Deletion in Retinoblastoma Protein Pathway-Disrupted Cells Results in DNA Damage and Cancer Progression. Mol Cell Biol. 2019 Jul 29;39(16):e00105-19.
24. Knudsen KE, et al. RB-dependent S-phase response to DNA damage. Mol Cell Biol. 2000 Oct;20(20):7751-63.
25. Robinson TJ, et al. RB1 status in triple negative breast cancer cells dictates response to radiation treatment and selective therapeutic drugs. PLoS One. 2013 Nov 12;8(11):e78641.
26. Dean JL, McClendon AK, and Knudsen ES. Modification of the DNA damage response by therapeutic CDK4/6 inhibition. J Biol Chem. 2012 Aug 17;287(34):29075-87.
27. Vélez-Cruz R, et al. RB localizes to DNA double-strand breaks and promotes DNA end resection and homologous recombination through the recruitment of BRG1. Genes Dev. 2016 Nov 15;30(22):2500-2512.
28. Zhang X, et al. *In vitro* and *in vivo* study of a nanoliposomal cisplatin as a radiosensitizer. Int J Nanomedicine. 2011;6:437-44.
29. Seluanov A, Mao Z, and Gorbunova V. Analysis of DNA double-strand break (DSB) repair in mammalian cells. J Vis Exp. 2010 Sep 8;(43):2002.
30. Morgan MA, et al. Mechanism of radiosensitization by the Chk1/2 inhibitor AZD7762 involves abrogation of the G2 checkpoint and inhibition of homologous recombinational DNA repair. Cancer Res. 2010 Jun 15;70(12):4972-81.
31. Cruz C, et al. RAD51 foci as a functional biomarker of homologous recombination repair and PARP inhibitor resistance in germline BRCA-mutated breast cancer. Ann Oncol. 2018;29(5):1203-10.
32. Fernández-Aroca DM, et al. P53 pathway is a major determinant in the radiosensitizing effect of Palbociclib: Implication in cancer therapy. Cancer Lett. 2019 Jun 1;451:23-33.
33. Chandler BC, et al. TTK inhibition radiosensitizes basal-like breast cancer through impaired homologous recombination. J Clin Invest. 2020 Feb 3;130(2):958-973.

34. Kobayashi D, Shibata A, Oike T, Nakano T. One-step Protocol for Evaluation of the Mode of Radiation-induced Clonogenic Cell Death by Fluorescence Microscopy. J Vis Exp. 2017 Oct 23;(128):56338.
35. Liao CC, et al. RB·E2F1 complex mediates DNA damage responses through transcriptional regulation of ZBRK1. J Biol Chem. 2010 Oct 22;285(43):33134-33143.
36. Pizarro JG, et al. ATM is involved in cell-cycle control through the regulation of retinoblastoma protein phosphorylation. J Cell Biochem. 2010 May;110(1):210-8.
37. Cook R, et al. Direct involvement of retinoblastoma family proteins in DNA repair by non-homologous end-joining. Cell Rep. 2015 Mar 31;10(12):2006-18.
38. Jiang Y, et al. RB Regulates DNA Double Strand Break Repair Pathway Choice by Mediating CtIP Dependent End Resection. Int J Mol Sci. 2020 Dec 1;21(23):9176.
39. Seoane M, et al. Retinoblastoma loss modulates DNA damage response favoring tumor progression. PLoS One. 2008;3(11):e3632.
40. Shamma A, et al. Rb Regulates DNA damage response and cellular senescence through E2F-dependent suppression of N-ras isoprenylation. Cancer Cell. 2009 Apr 7;15(4):255-69.
41. Veo B, et al. Transcriptional control of DNA repair networks by CDK7 regulates sensitivity to radiation in MYC-driven medulloblastoma. Cell Rep. 2021 Apr 27;35(4):109013.
42. Chen B, et al. Antagonizing CDK8 Sensitizes Colorectal Cancer to Radiation Through Potentiating the Transcription of e2f1 Target Gene apaf1. Front Cell Dev Biol. 2020 Jun 12;8:408.
43. Quereda V, et al. Therapeutic Targeting of CDK12/CDK13 in Triple-Negative Breast Cancer. Cancer Cell. 2019 Nov 11;36(5):545-558.e7.
44. Veeranki OL, et al. Targeting cyclin-dependent kinase 9 by a novel inhibitor enhances radiosensitization and identifies Axl as a novel downstream target in esophageal adenocarcinoma. Oncotarget. 2019 Jul 23;10(45):4703-4718.
45. Maggiorella L, et al. Cooperative effect of roscovitine and irradiation targets angiogenesis and induces vascular destabilization in human breast carcinoma. Cell Prolif. 2009;42(1):38-48.
46. Maggiorella L, et al. Enhancement of radiation response by roscovitine in human breast carcinoma *in vitro* and *in vivo*. Cancer Res. 2003;63(10):2513-7.
47. Syn NL, et al. Pan-CDK inhibition augments cisplatin lethality in nasopharyngeal carcinoma cell lines and xenograft models. Signal Transduction and Targeted Therapy. 2018;3(1):1-9.
48. Camphausen K, et al. Flavopiridol enhances human tumor cell radiosensitivity and prolongs expression of gammaH2AX foci. Mol Cancer Ther. 2004;3(4):409-16.
49. Motwani M, et al. d Schwartz GK. Flavopiridol Enhances the Effect of Docetaxel in Vitro and in Vivo in Human Gastric Cancer Cells1. 2003.
50. Raju U, et al. Flavopiridol, a cyclin-dependent kinase inhibitor, enhances radiosensitivity of ovarian carcinoma cells. Cancer Res. 2003;63(12):3263-7.
51. Goel S, et al. Overcoming Therapeutic Resistance in HER2-Positive Breast Cancers with CDK4/6 Inhibitors. Cancer Cell. 2016 Mar 14;29(3):255-269.
52. Kettner NM, et al. Combined Inhibition of STAT3 and DNA Repair in Palbociclib-Resistant ER-Positive Breast Cancer. Clin Cancer Res. 2019;25(13):3996-4013.

53. Zhang J, et al. Cyclin D–CDK4 kinase destabilizes PD-L1 via cullin 3–SPOP to control cancer immune surveillance. Nature. 2017;553(7686):91-5.
54. Wang Q, et al. Single-cell profiling guided combinatorial immunotherapy for fast-evolving CDK4/6 inhibitor-resistant HER2-positive breast cancer. Nat Commun. 2019;10(1):3817.
55. Vanpouille-Box C, et al. DNA exonuclease Trex1 regulates radiotherapy-induced tumour immunogenicity. Nat Commun. 2017 Jun 9;8:15618.
56. Ho AY, et al. Optimizing Radiation Therapy to Boost Systemic Immune Responses in Breast Cancer: A Critical Review for Breast Radiation Oncologists. Int J Radiat Oncol Biol Phys. 2020 Sep 1;108(1):227-241.
57. Cortes J, et al. Pembrolizumab plus chemotherapy versus placebo plus chemotherapy for previously untreated locally recurrent inoperable or metastatic triple-negative breast cancer (KEYNOTE-355): a randomised, placebo-controlled, double-blind, phase 3 clinical trial. Lancet. 2020 Dec 5;396(10265):1817-1828.
58. Teo ZL, et al. Combined CDK4/6 and PI3Kα Inhibition Is Synergistic and Immunogenic in Triple-Negative Breast Cancer. Cancer Res. 2017 Nov 15;77(22):6340-6352.
59. Wang TH, et al. Palbociclib induces DNA damage and inhibits DNA repair to induce cellular senescence and apoptosis in oral squamous cell carcinoma. J Formos Med Assoc. 2020 Dec 18:S0929-6646(20)30609-4.
60. Huang CY, et al. Palbociclib enhances radiosensitivity of hepatocellular carcinoma and cholangiocarcinoma via inhibiting ataxia telangiectasia-mutated kinase-mediated DNA damage response. Eur J Cancer. 2018 Oct;102:10-22.
61. Beddok A, et al. Concurrent use of palbociclib and radiation therapy: single-centre experience and review of the literature. Br J Cancer. 2020 Sep;123(6):905-908.
62. Bosacki C et al. CDK 4/6 inhibitors combined with radiotherapy: A review of literature. Clin Transl Radiat Oncol. 2020 Dec 1;26:79-85.
63. David S, et al. Enhanced toxicity with CDK 4/6 inhibitors and palliative radiotherapy: Non-consecutive case series and review of the literature. Transl Oncol. 2021 Jan;14(1):100939.
64. Guerini AE et al. A single-center retrospective safety analysis of cyclin-dependent kinase 4/6 inhibitors concurrent with radiation therapy in metastatic breast cancer patients. Sci Rep. 2020 Aug 12;10(1):13589.
65. Michmerhuizen AR, et al. PARP1 Inhibition Radiosensitizes Models of Inflammatory Breast Cancer to Ionizing Radiation. Mol Cancer Ther. 2019 Nov;18(11):2063-2073.

Chapter 5 : Bcl-xL Inhibition Radiosensitizes *PIK3CA/PTEN* Wild Type Triple Negative Breast Cancers in an Mcl-1-Dependent Manner[5]

Abstract

Patients with radioresistant breast cancers, including a large percentage of women with triple negative breast cancer (TNBC), demonstrate limited response to radiation (RT), increased locoregional recurrence, and lower rates of overall survival; thus, strategies to increase the efficacy of RT in TNBC are critically needed. We demonstrate that pan Bcl-2 family inhibition (ABT-263, rER: 1.06-1.74) or Bcl-xL specific inhibition (WEHI-539, A-1331852; rER: 1.13 – 2.14) radiosensitized wild-type *PIK3CA/PTEN* wild-type TNBC (MDA-MB-231, CAL-120) but failed to radiosensitize mutant *PIK3CA/PTEN* TNBC (rER: 0.87-1.18; MDA-MB-468, CAL-51, SUM-159). Specific inhibition of Bcl-2 or Mcl-1 did not induce radiosensitization, regardless of *PIK3CA/PTEN* status (rER: 0.91 – 1.21). In wild-type *PIK3CA/PTEN* TNBC, pan Bcl-2 family inhibition or Bcl-xL specific inhibition and RT led to increased levels of apoptosis ($p < 0.001$) and an increase in cleaved PARP. CRISPR-mediated *PTEN* knockout in wild-type *PIK3CA/PTEN* MDA-MB-231 and CAL-120 cells induced expression of pAKT/Akt and Mcl-1 and abolished Bcl-xL inhibitor-mediated radiosensitization (rER: 0.95 – 1.13). Similarly, Mcl-1 overexpression

[5] This chapter was a collaboration between co-first authors Andrea Pesch and Benjamin Chandler and submitted for publication in January 2022.

abolished radiosensitization in MDA-MB-231 and CAL-120 cells (rER: 0.99 – 1.09) but transient *MCL1* knockdown in CAL-51 cells promoted Bcl-xL-inhibitor mediated radiosensitization (rER 2.35 ± 0.05). *In vivo*, ABT-263 or A-1331852 in combination with RT decreased tumor growth and increased tumor tripling time ($p < 0.0001$) in *PIK3CA/PTEN* wild-type TNBC cell line and patient-derived xenografts. Collectively, this study provides the preclinical rationale for early phase clinical trials testing the safety, tolerability, and efficacy of Bcl-xL inhibition and RT in women with wild-type *PIK3CA/PTEN* wild-type TNBC at high risk for recurrence.

Introduction

Triple negative breast cancer (TNBC) is an aggressive subtype of breast cancer with poor rates of locoregional control even after treatment with radiation (RT) therapy (1). TNBC do not express molecular drivers of tumorigenesis and proliferation such as the estrogen receptor (ER), progesterone receptor, or the human epidermal growth factor receptor 2 (HER2), and, consequently, cannot be treated with small molecule and/or targeted therapeutic options. Although radiation is a mainstay in the treatment of breast cancer, patients with TNBC tend to have tumors enriched for intrinsic radioresistance (2) and additional strategies are needed to increase local disease control and reduce the occurrence of regional and distant metastases. Efforts to increase the efficacy of radiation (RT) therapy in the treatment of TNBC have primarily focused on targeting DNA synthesis and DNA damage repair, including chemotherapies such as gemcitabine and cisplatin (3) or PARP1 inhibitors such as olaparib and veliparib (4,5). Although effective radiosensitization agents, these treatments are often associated with extensive normal tissue toxicities that have limited their clinical translatability (6).

In addition to increased DNA damage following RT, ionizing RT can lead to increased rates of apoptosis in tumor cells. Apoptosis is a highly regulated pathway of programmed cell death that is controlled by pro-apoptotic BH3-only proteins (Bid, Bim, Puma, Noxa), pro-apoptotic effector proteins (Bax, Bak, and Bok), and anti-apoptotic BH3 only proteins (Bcl-2 family proteins including Bcl-2, Bcl-xL, Mcl-1, Bcl-w) (7-13). Under normal physiological conditions, anti-apoptotic proteins are bound to effector proteins to inhibit apoptosis (8). Under conditions of cellular stress, the activation of the downstream effector proteins (often Bax/Bak) leads to dimerization and pore formation in the outer mitochondrial membrane, releasing SMAC and

cytochrome c; this leads to formation of the apoptosome and the irreversible caspase-mediated cleavage of proteins in the nucleus including PARP1 and, eventually, cell death (14-19).

Careful control of the balance between anti- and pro-apoptotic protein signaling cascades is mediated through cellular control of a number of signaling pathways – including the phosphatidyl inositol 3 kinase (PI3K) signaling pathway – which has been shown to directly modulate the expression of Bcl-2 family proteins such as Bcl-xL and Mcl-1 (20-23). In breast cancer, it is well known that activating mutations in *PIK3CA*, the gene encoding the catalytic subunit (p110α) of PI3K, occur in almost a quarter of hormone receptor positive (HR+) breast cancers and ~10% of TNBC (24). Paradoxically, despite worse outcomes for patients with HR+ *PIK3CA* mutant breast cancer, patients with *PIK3CA* mutant TNBC tend to have higher rates of overall survival compared to patients with subtype-matched tumors that express wild-type *PIK3CA* (24). Similar studies have also studied the effects of the tumor suppressor PTEN, that works in opposition to PI3K signaling in this context (25), where inactivating mutations and loss of PTEN expression lead to higher PI3K pathway activity. Thus, control of cellular apoptosis in breast cancer is partially dependent on the presence or absence of PI3K pathway mutations.

Apoptosis is not the primary mode in which RT induces cellular death in cancer cells (26), but the clinical development of targeted pharmacological inhibitors of anti-apoptotic proteins has made it increasingly possible to target apoptotic signaling in a variety of cancer types . Inhibition of anti-apoptotic proteins as a monotherapy, (specifically Bcl-2, Bcl-xL, and Mcl-1) is a successful cancer treatment strategy for acute myeloid leukemia (AML), chronic lymphocytic leukemia (CLL), and small lymphocytic lymphoma (27-30). As a result, efforts are underway to test the effects of inhibiting anti-apoptotic proteins in additional cancer types, particularly in combination with other small molecule treatments such as DNA damaging agents or compounds that target

PI3K/mTOR signaling (20,31-34). Despite this, few studies have focused on inhibition of anti-apoptotic proteins in combination with RT, and none have specifically examined Bcl-xL inhibition in combination with RT in the treatment of aggressive breast cancers (35). To that end, data from a screen performed in our lab to identify potential targets for radioresistant breast cancers nominated Bcl-2 family inhibition as a potential targeted approach to sensitize radioresistant breast cancers to RT (36). Thus, we hypothesized that the use of targeted inhibitors against Bcl-2 family proteins in TNBC would be a viable therapeutic strategy for patients with aggressive TNBC without PI3K pathway alterations for whom therapy intensification is needed.

Results

ABT-263, a nonspecific Bcl-2 family inhibitor, radiosensitizes *PIK3CA/PTEN* wild type triple negative breast cancers

First, we sought to assess the impact of pan Bcl-2 family inhibition on TNBC cell lines *in vitro* (**Figure 5.1A**). Cellular response to the Bcl-2 family pan inhibitor ABT-263 (37) varied across TNBC cell lines, with half-maximal inhibitory concentrations (IC_{50}s) less than 1μM in sensitive cell lines (red) and IC_{50}s greater than 5μM in resistant TNBC cell lines (blue). Consistent with prior studies (38-40), TNBC cell lines with wild-type *PIK3CA/PTEN* expression (MDA-MB-231, CAL-120) were sensitive to pan Bcl-2 inhibition, while *PIK3CA* mutant (CAL-51, SUM-159) and *PTEN* mutant (CAL-51, MDA-MB-468) cells were insensitive (**Figure 5.1B, Table 5.1-Table 5.2**). Thus, we hypothesized that cell lines with wild-type *PIK3CA/PTEN* would be radiosensitized by ABT-263, while those with mutations in the *PIK3CA/PTEN* pathway would not.

To assess the combined effects of radiation and pan Bcl-2 family inhibition, we performed clonogenic survival assays in *PIK3CA/PTEN* wild-type (MDA-MB-231, CAL-120) and mutant (CAL-51, MDA-MB-468, SUM-159) cell lines. *PIK3CA/PTEN* wild-type cells (**Table 5.1C-D**) were significantly radiosensitized by ABT-263 (MDA-MB-231 rER 500nM 1.52 ± 0.13; CAL-120 rER 500nM: 1.56 ± 0.20) even at concentrations 6-10 times lower than the IC_{50} value in each respective cell line. In both MDA-MB-231 and CAL-120 cells there was a significant decrease in surviving fraction of cells after 2 Gy RT (SF-2Gy) in cells treated with ABT-263 compared to vehicle-treated (DMSO) control cells. Conversely, in PTEN null TNBC cell lines, ABT-263 did not radiosensitize MDA-MB-468 (rER: 1.02 ± 0.05) or CAL-51 cells (rER: 1.07 ± 0.08) and failed to significantly change the SF-2Gy **(Figure 5.1E-F)**. Similar results were observed in the *PIK3CA* mutant cell line (SUM-159 rER 1μM: 0.96 ± 0.05; **Figure 5.1G**).

Pan Bcl-2 family inhibition potentiates radiation-induced apoptotic cell death in *PIK3CA/PTEN* wild type TNBC

Because Bcl-2 proteins are critical components of the cellular anti-apoptotic signaling cascade, we hypothesized that ABT-263-mediated radiosensitization of TNBC cell lines was due to an increase in apoptosis following the combined treatment. In our *PIK3CA/PTEN* wild-type TNBC models, ABT-263 + RT (4 Gy) led to a significant increase (doubling) in the number of apoptotic cells 48 hours after RT (absolute increase of 14.7% in MDA-MB-231 cells and 8.0% increase in CAL-120 cells compared to RT alone, **Figure 5.2A-B)**. In addition, ABT-263 pretreatment before RT (4 Gy) increased the formation of cleaved-PARP, a marker for late apoptosis, at 48 hours post RT compared to either RT or drug alone in both MDA-MB-231 and CAL-120 cells **(Figure 5.2A-B)**.

Alternatively, ABT-263 with RT (4 Gy) did not lead to a significant increase in apoptotic cells compared to RT alone in PTEN null cell lines **(Figure 5.2C-D)** or *PIK3CA* mutant cells **(Figure 5.2E)**. In all three cell lines (MDA-MB-468, CAL-51, SUM-159), ABT-263 + RT also failed to increase cleaved PARP formation, even demonstrating a slight decrease in cleaved PARP formation. Thus, combined inhibition of Bcl-2 and Bcl-xL using the nonspecific inhibitor ABT-263 led to increased apoptosis and radiosensitization in a *PIK3CA/PTEN* pathway dependent manner. Because *PIK3CA/PTEN* wild-type cell lines express higher levels of Bcl-2 and Bcl-xL and lower levels of Mcl-1 protein compared to *PIK3CA/PTEN* mutant TNBC cell lines (**Figure 5.2F**), we next sought to assess the contributions of individual Bcl-2 family proteins to the radiosensitization phenotype.

Specific inhibition of Bcl-xL, but not Bcl-2, radiosensitizes *PIK3CA/PTEN* wild-type TNBC

To determine the effect of inhibiting individual Bcl-2 protein family members on *PIK3CA/PTEN* wild-type TNBC cell lines, we used specific pharmacological inhibitors targeted against Bcl-2 family members: WEHI-539, a Bcl-xL specific inhibitor (and the orally bioavailable analog, A-1331852)(41); ABT-199 (navitoclax), a Bcl-2 specific inhibitor (42); and the Mcl-1 inhibitor S63845 (32). To assess Bcl-xL inhibitor-mediated effects on cell viability, we treated TNBC cell lines with 1nM-10μM WEHI-539 for 72 hours (**Figure 5.3A, Table 5.2**). Single agent effects of WEHI-539 on cell growth were dependent on *PIK3CA/PTEN* mutational status *in vitro*, with *PIK3CA/PTEN* mutant cell lines demonstrating resistance to Bcl-xL inhibition, which mirrored the lack of *in vitro* effects that were observed with the pan inhibitor ABT-263. Combined WEHI-539 and RT led to an increase in the number of apoptotic cells (**Figure 5.3B-C**) and cleaved PARP formation (**Figure 5.4A**) in both MDA-MB-231 and CAL-120 cells compared to 4 Gy RT alone (22.3% and 17.6% increases in the fraction of apoptotic cells, respectively).

Using clonogenic survival assays, we determined that the Bcl-xL inhibitor WEHI-539 led to clinically relevant levels of radiosensitization (rER > 1.2) in *PIK3CA/PTEN* intact TNBC (MDA-MB-231 and CAL-120, **Figure 5.3D-E)** that were comparable to the effects of combined ABT-263 pretreatment with RT (MDA-MB-231 rER 1μM: 1.31 ± 0.06; CAL-120 rER 1μM: 1.87 ± 0.38). Consequently, combined WEHI-539 treatment and RT led to a dose-dependent decrease in the SF-2Gy in both cell lines. To further confirm that Bcl-xL inhibition was responsible for radiosensitization of *PIK3CA/PTEN* wild-type TNBC cell lines, we repeated the clonogenic survival assays with A-1331852, an analog of WEHI-539 developed for *in vivo* use (41,43). As with WEHI-539, treatment with A-1331852 radiosensitized MDA-MB-231 and CAL-120 cells

(MDA-MB-231 rER 1μM: 1.32 ± 0.07; CAL-120 rER 1μM: 2.00 ± 0.47) and significantly increased cleaved PARP formation in combination treated groups **(Figure 5.4B-D)**.

Having established that Bcl-xL inhibition was sufficient to confer radiosensitivity to *PIK3CA/PTEN* wild-type TNBC models, we next sought to determine if Bcl-2 also contributed to this radiosensitization. Unlike ABT-263 and WEHI-539, which suppressed growth of *PIK3CA/PTEN* wild-type TNBC cell lines, the Bcl-2-specific inhibitor ABT-199 had no effect on TNBC cell line viability (regardless of *PIK3CA/PTEN* mutational status) at doses less than 5μM **(Figure 5.3F, Table 5.2)**. Not surprisingly, ABT-199 did not lead to increased apoptosis in MDA-MB-231 or CAL-120 cells (**Figure 5.3G-H**) nor did it lead to radiosensitization at concentrations up to 1μM (MDA-MB-231 rER: 0.98 ± 0.02; CAL-120 rER: 1.03 ± 0.07**, Figure 5.3I&J)**. Finally, the combination of ABT-199 and RT (4 Gy) did not increase cleaved PARP levels compared to either RT or drug alone **(Figure 5.4E)**.

Although ABT-263 is a less potent inhibitor of Mcl-1 compared to Bcl-2 or Bcl-xL, Mcl-1 has been suggested as a potential therapeutic target in TNBC in multiple studies (32,44); therefore, we sought to assess the effects of the Mcl-1 specific inhibitor S63845 (32) on radiosensitization in our *in vitro* models of TNBC. Pretreatment with S63845 did not significantly inhibit proliferation of TNBC cell lines (**Figure 5.5A, Table 5.2**), though modest effects were seen in *PIK3CA/PTEN* mutant cell lines at high concentrations, consistent with prior literature (32). S63845 failed to induce radiosensitization in *PIK3CA/PTEN* wild-type CAL-120 cells (**Figure 5.5B**, rER: 1.06 ± 0.08) or *PIK3CA* mutant SUM-159 cells (**Figure 5.5E**, rER: 0.95 ± 0.10), or *PIK3CA/PTEN* mutant CAL-51 cells (**Figure 5.5D**, rER: 1.07 ± 0.11), suggesting that Mcl-1 inhibition alone did not potentiate apoptosis in *PIK3CA/PTEN* wild-type or mutant TNBC cells.

Bcl-xL inhibition radiosensitizes *PIK3CA/PTEN* wild-type TNBC xenograft tumors

To examine the effects of Bcl-xL inhibitor-mediated radiosensitization *in vivo*, we generated MDA-MB-231 xenograft tumors by injecting cells into the mammary fat pads of female SCID CB-17 mice. Following the formation of established tumors (approximately 80mm^3) and randomization, mice were assigned to receive either 25 mg/kg of ABT-263 (pan Bcl-2 family inhibitor), 25 mg/kg of A-1331852 (Bcl-xL inhibitor), 9 fractions of 2 Gy RT, or a combination of either ABT-263 or A-1331852 with RT. In combination treated mice, RT treatment started 24 hours after the first drug treatment and drug was given for 10 days **(Figure 5.6A).** All treatment was discontinued after the ninth fraction of RT. Overall, pan Bcl-2 family inhibition with ABT-263 or specific Bcl-xL inhibition and RT significantly decreased tumor growth compared to drug or RT alone (**Figure 5.6B**) and significantly extended time to tumor tripling (**Figure 5.6C**).

In addition to a cell line-derived xenograft model, we tested the effects of Bcl-xL inhibition in a patient-derived xenograft (PDX) model of wild-type *PIK3CA/PTEN* TNBC using a similar treatment paradigm (**Figure 5.6D**). In this PDX model, combination treatment with A-1331852 and RT significantly decreased tumor growth (**Figure 5.6E**) and time to tumor tripling (**Figure 5.6F**) compared to either single treatment arm alone. Although the effects of ABT-263 were only additive with RT in cell line xenografts (FTV ratio < 1, **Table 5.3**), A-1331852 was synergistic with RT in both MDA-MB-231 and PDX4664 xenografts (FTV ratio > 1, **Table 5.3-Table 5.4**).

***PTEN* knockout leads to increased Mcl-1 expression and radioresistance**

To further understand how PI3K/PTEN signaling contributes to Bcl-xL inhibitor-mediated radiosensitization of TNBC, we next sought to understand the cellular changes induced by PI3K pathway mutations in these models. Using the Cancer Cell Line Encyclopedia, we analyzed expression of phosphorylated Akt (pAKT T308 and S473), a signaling mediator

downstream of activated PI3K, across breast cancer cell lines with either wild-type PI3K signaling or activating mutations in the PI3K pathway (**Figure 5.7A**). As expected, hyperactivation of PI3K signaling resulted in higher expression of pAkt, which we confirmed in our cell line models (**Figure 5.7B**). To understand the effects of PTEN loss in our models, we used CRISPR-Cas9 to generate isogenic models of MDA-MB-231 and CAL-120 with PTEN knockout (**Figure 5.7C**).

In these models, knockout of the *PTEN* tumor suppressor gene led to a baseline increase in pAkt (Ser473) and Mcl-1 expression in *PTEN* knockout cell lines compared to parental or Cas9 control cells. We assessed the effects of PTEN loss on Bcl-xL inhibitor-mediated radiosensitivity by repeating the clonogenic survival assays in *PTEN* knockout cells and Cas9-expressing CRISPR control TNBC cell lines. In MDA-MB-231 *PTEN* knockout cells, drug pretreatment failed to sensitize cells to RT when 1μM ABT-263 (rER: 0.98 ± 0.02), 1μM WEHI-539 (rER: 0.94 ± 0.02) or 1μM A-1331852 (rER: 1.07 ± 0.08) was given one-hour prior to RT (**Figure 5.7D**). Similar results were achieved with CAL-120 cells (1μM ABT-263 [rER: 0.98 ± 0.02], 1μM WEHI-539 [rER: 0.94 ± 0.02] or 1μM A-1331852 [rER: 1.07 ± 0.08]) (**Figure 5.7F**). The Bcl-2 specific inhibitor ABT-199, which did not lead to radiosensitization in *PTEN* wild-type parental cell lines, remained unable to induce radiosensitization in the *PTEN* knockout models (rER: 0.95-0.99).

Consistent with our previous results, isogenic control cell lines expressing the Cas9 protein with a control (*AAVS1)* gRNA were radiosensitized by pan Bcl-2 family inhibition (ABT-263) and Bcl-xL specific inhibition at magnitudes similar to the parental (non-CRISPR) cell lines (ABT-263 [rER: 1.30 – 1.72], WEHI-539 [rER: 1.31 – 1.38] or 1μM A-1331852 [rER: 1.49 – 1.75]) (**Figure 5.7E,G**), suggesting that the observed effect on radiosensitivity is

dependent on loss of PTEN. Mechanistically, PTEN knockout abolished Bcl-xL inhibitor-mediated induction of apoptosis following RT in MDA-MB-231 and CAL-120 cells (**Figure 5.7H,I**), but Cas9 control cells remained sensitive to the pro-apoptotic effects of pan Bcl-2 family inhibition (ABT-263) and Bcl-xL-specific inhibition (WEHI-539, and A-1331852).

Increased Akt signaling has been shown to lead to increased translation and expression of Mcl-1 (20). In our models, we hypothesized that higher expression of Akt/Mcl-1 in *PIK3CA/PTEN* mutant cell lines conferred radioresistance, and that we could induce radioresistance in *PIK3CA/PTEN* wild-type cells with transient Mcl-1 overexpression. In these models, transient Mcl-1 overexpression prevents WEHI-539-mediated radiosensitization of MDA-MB-231 (rER: 1.04 ± 0.01) and CAL-120 cells (rER: 1.02 ± 0.03; **Figure 5.8A-B,D**). Overexpression of Mcl-1 in MDA-MB-231 cells also led to a reduction in PARP1 cleavage following RT + WEHI-539 (**Figure 5.8C)**, suggesting that Mcl-1 expression induces radioresistance. Conversely, transient knockdown of *MCL1* in *PIK3CA/PTEN* mutant CAL-51 cells (rER: 2.35 ± 0.05) induced sensitivity to Bcl-xL inhibition and RT (**Figure 5.8D-E**). Furthermore, *MCL1* knockdown led to increased cleaved PARP formation (**Figure 5.8F**) and increased apoptosis (**Figure 5.8G-H**) with combined Bcl-xL inhibitor therapy and RT suggesting that Mcl-1 is a modulator of radioresistance in TNBC.

We also validated these changes in radiosensitivity through modulation of the upstream modulator, Akt, expression, in *PIK3CA/PTEN* mutant cell lines. Following *AKT1* knockdown by siRNA, Bcl-xL inhibition radiosensitized *PIK3CA* mutant CAL-51 cells (WEHI-539 1μM: rER: 1.46 ± 0.06) (**Figure 5.9A**). *AKT1* knockdown did not induce global sensitivity to Bcl-2 family inhibitors, as the Bcl-2 specific inhibitor ABT-199 remained unable to radiosensitize CAL-51 cells (rER 0.95 ± 0.07) despite *AKT1* knockdown (**Figure 5.9B**). Finally, although we previously

demonstrated that *PTEN* knockout abrogates Bcl-xL inhibitor-mediated radiosensitization in MDA-MB-231 cells, rescue experiments with the addition of *AKT1*-targeting siRNA partially restores radiosensitization (**Figure 5.9C-D**; rER 1.37 ± 0.03). Although these changes were more pronounced at higher RT doses (4-6 Gy compared to 2 Gy), these results further support the hypothesis that manipulation of the Akt/Mcl-1 signaling axis is sufficient to modulate Bcl-xL-inhibitor mediated radiosensitization in TNBC.

Mcl-1 signaling induces resistance to Bcl-xL inhibitor-mediated radiosensitization in TNBC through increased activation of Bak

To further elucidate the connection between increased Mcl-1 and increased apoptosis following treatment with Bcl-xL inhibition + RT, we assessed the expression of pro-apoptotic proteins such as Bcl-2 homologous antagonist killer (Bak) in TNBC cell lines. Bak protein was significantly elevated following treatment with WEHI-539 or WEHI-539 + RT in CAL-120 and MDA-MB-231 cells (**Figure 5.10A**). Induction of BAK did not occur in radioresistant *PTEN/PIK3CA* mutant CAL-51 or MDA-MB-468 cells (**Figure 5.10B**). When comparing isogenic models of *PTEN* loss in MDA-MB-231 cells, induction of Bak expression occurred in Cas9 control cells after treatment with WEHI-539 ± RT but failed to occur in MDA-MB-231 *PTEN* CRISPR (**Figure 5.10C**). Taken together, our results suggest that *PIK3CA/PTEN* wild-type TNBC cell lines can be radiosensitized through inhibition of Bcl-xL, but *PIK3CA/PTEN* mutant cell lines that overexpress Akt/Mcl-1 cannot properly induce Bak expression which may be responsible, at least in part, for apoptotic cell death in response to RT (**Figure 5.10D**).

Discussion

In this study, we describe the identification of a targeted approach that may be useful in increasing the efficacy of RT in aggressive, radioresistant, triple-negative breast cancers. First, we demonstrated that treating PIK3CA/PTEN wild type TNBC with either a pan Bcl-2 family inhibitor (ABT-263, Fig. 1) or specific inhibitors of Bcl-xL (WEHI-539, A-1331852, Fig. 3) – but not specific inhibitors of Bcl-2 or Mcl-1 – resulted in radiosensitization by potentiating RT-induced apoptotic cell death (Fig. 2 and 3). Pan-Bcl-2 family inhibition or Bcl-xL specific inhibition combined with RT *in vivo* led to significantly reduced tumor sizes and delayed tumor growth in cell line and patient derived xenograft TNBC models (Fig. 4). Finally, we show that in TNBC cell lines with activating PI3K pathway mutations (either PIK3CA mutations or PTEN loss), radioresistance occurs through increased basal levels of Akt and Mcl-1and cellular apoptosis that occurs in PIK3CA/PTEN wild type TNBC (Fig. 5 and 6). Together, our results provide preclinical data in support of Bcl-xL inhibition as a potential clinical strategy for radiosensitization of PIK3CA/PTEN wild type breast cancers.

Currently, the primary therapeutic modalities for TNBC are surgery, radiation therapy and cytotoxic chemotherapy – and in some cases the anti-PD-1 antibody pembrolizumab. Although we focused on the use of Bcl-xL inhibition in combination with RT, others have demonstrated parallel interactions *in vitro* between BH3 mimetics and chemotherapeutic agents. The antineoplastic agent docetaxel is synergistic with the Mcl-1 inhibitor S63845 in TNBC and HER2-amplified breast cancers (32), the first-generation pan Bcl-2 family inhibitor ABT-737 in ER+ breast cancer (40), and the Bcl-xL specific inhibitor A-1331852 in a wide range of solid tumor types (45). In addition, targeting Bcl-2 family proteins with BH3 mimetics such as ABT-737 and ABT-263 also sensitizes TNBC cells to other taxols including paclitaxel (46,47). In combination with anthracycline

chemotherapies, nuclear pAkt has been shown to predict the efficacy of PI3K and doxorubicin in breast and ovarian cancers. Furthermore, ABT-263 leads to selective cell death in *TP53* wild-type breast cancers after the induction of doxorubicin-induced senescence (48) and activating *PIK3CA* mutations confer resistance to chemotherapies in TNBC through increased Akt/mTOR signaling and a subsequent reduction in apoptosis (49). Radiation therapy, similar to systemic chemotherapy, can induce cytotoxic effects in tumor cells, but RT for the treatment of breast cancer can be administered locally with reduced risk to healthy organs and tissues; this suggests that our proposed combination therapy may be significantly less toxic than combination therapies using systemic chemotherapies.

Our data supports a growing body of literature that suggests that the role of each Bcl-2 family protein is determined in a context-dependent manner, leading to differential regulation of Bcl-xL, Mcl-1, and Bcl-2 expression across different cancer types. Our models support the current hypothesis that increased Akt signaling drives Mcl-1 expression (21,50-52) and that inhibition of PI3K/Akt signaling results in downregulation or degradation of Mcl-1 (22,23,53,54). It has also been shown that dual targeting of Bcl-xL and PI3K in *PIK3CA* mutant breast cancer models blocks tumor growth *in vivo* through modulation of mTOR-mediated Mcl-1 translation (20); this is consistent with our observation that blocking PI3K signaling (through genetic knockdown of *AKT1* or *MCL1*) renders *PIK3CA/PTEN* mutant TNBC models sensitive to Bcl-xL inhibitor-mediated radiosensitivity.

Despite many studies exploring Bcl-2 family proteins in breast cancer, most of the current literature has focused on the role of the anti-apoptotic protein Mcl-1 (32,44) in examining the efficacy of combination therapies using BH3 mimetics with other targeted agents such as NVP-BEZ235, everolimus (RAD001), and other pharmacological inhibitors that target mTOR or PI3K

signaling (23,32,39,55). Our studies extend this incomplete examination and describe a role for both Bcl-xL and Mcl-1 in mediating radiosensitivity in TNBC in a PI3K pathway-dependent manner. In addition, the synthetic vulnerability of *PTEN* loss and pharmacological Mcl-1 inhibition has been explored in the context of *PTEN*-deficient models of glioblastoma (67), but our study is the first to demonstrate that both *PIK3CA* mutations and *PTEN* loss in breast cancer cells can induce resistance to Bcl-xL inhibitor-mediated radiosensitivity. Although we focused on aggressive, radioresistant models of TNBC in this study, future studies in our laboratory are underway to determine the effects of Bcl-xL inhibition in other breast cancer subtypes. These ongoing studies will allow us to elucidate the potential for context-dependent differences in Bcl-2 family inhibitor-mediated radiosensitization across a more heterogenous population of breast cancer models and would build on recent literature demonstrating differences in sensitivity to Bcl-2 family inhibitors across different breast cancer subtypes (20,32,38,39). In addition, expanding these studies into additional breast cancer subtypes will allow us to explore the distinct functions of other Akt isoforms (56) in the context of Akt-mediated expression of Bak and Bcl-xL-mediated radiosensitization.

Taken together, our results suggest that Bcl-xL inhibition is a viable therapeutic strategy to increase the efficacy of radiation therapy when given as part of the standard of care for patients with TNBC in the absence of PI3K pathway activating mutations. ABT-199 (venetoclax) is FDA approved for the treatment of some hematologic malignancies, but the use of BH3 mimetics targeting Bcl-xL – such as A-1331852 – would need to undergo further safety and toxicity studies in combination with RT to identify and mitigate any potential overlapping toxicities such as acute decreases in platelet formation (27) or myelosuppression. Finally, there is a growing pipeline of novel BH3 mimetics (APG-2575, BM-1197, LOXO-388, and AZD0466, among others as well as

Bcl-xL PROTAC degraders (PZ703b) under preclinical and early clinical investigation (57) that, if given concurrently with ionizing radiation, have the potential to influence radiation sensitivity in a wide variety of tumor types.

Methods

Cell Culture

Frozen stocks of MDA-MB-231, CAL-120, MDA-MB-468, and CAL-51 TNBC cells were obtained from ATCC and grown in DMEM (Thermo Fisher 11965092) supplemented with 10% FBS (Atlanta Biologicals S11650H) and 1% penicillin/streptomycin (Thermo Fisher 15070063). SUM-159 cells were received courtesy of Steve Ethier from University of Michigan stocks and grown in Ham's F-12 media (Thermo Fisher 11765054) supplemented with 5% FBS, 5mL of 1M HEPES (Sigma H3375), 1μg/mL hydrocortisone (Sigma H4001), 1x antibiotic-antimycotic (Thermo Fisher 15240062) and 6μg/mL insulin (Sigma I9278). All cell lines were maintained in a humidified incubator (5% CO_2), tested for mycoplasma routinely (MycoAlert, Lonza LT07), and authenticated at the University of Michigan DNA sequencing core.

Gene Expression Knockout

Generation of CRISPR cell lines was performed using the lentiCRISPRv2 plasmid (Addgene #98291). Guides targeting *PTEN* were obtained from Integrated DNA Technologies and annealed at 95 degrees and cooled at a rate of 5º/minute. The lentiCRISPRv2 plasmid was digested with BsmB1, purified using the QIAquick Gel Extraction Kit (Qiagen #28706X4), and the guide sequences were annealed using T4 DNA Ligase (NEB M0202S). Transient transfection of HEK293T cells was used to generate lentivirus (1.5 μg PAX2 [Addgene #12260], 0.3μg MD2g [Addgene #12259], and 1.5 μg plasmid) in Opti-MEM media. Virus was collected in DMEM media containing 30% FBS for 48 hours then centrifuged and filtered (0.45-micron filter). Virus was added to exponentially growing cells for 48 hours with 0.8μg/mL polybrene after which point hygromycin was used for selection (500μg/mL). Pooled clones were used for all assays. CRISPR

control cells containing a control guide targeting *AAVS1* were also produced for use as Cas9 controls (5' CACCGGGGGCCACTAGGGACAGGAT 3').

For transient gene knockdown, si*MCL1* (#L-004501-00), si*AKT1* (#L-003000-00) and a control siRNA (#D-001810-10) were purchased from Dharmacon and used at a final concentration of 25nM. siRNA were transfected into cells using RNAiMAX (Thermo #13378030) in Opti-MEM (Invitrogen #31985-062) with antibiotic-free media. Transfected cells were replated 24 hours after transfection and treated with drug/radiation the following day (~48 hours post transfection). Lysates were harvested from cells 24-48 hours post-transfection (as indicated) to assess the efficiency of overexpression/knockdown at the protein level. Experimental conditions were similar with transient overexpression of *MCL1* (Origene RC200521) using 1µg plasmid DNA per well of a 6-well plate.

Drugs

ABT-263, ABT-199, WEHI-539, and A-1331852 were ordered from MedChemExpress (HY-10087, HY-15531, HY-15607, HY-19741) as 10mM solutions in DMSO.

Irradiation

Irradiation was performed using a Kimtron IC-225 at a dose rate of ~2 Gy/min at the University of Michigan Experimental Irradiation Core (225kVp). Dosimetry is performed semiannually using an ionization chamber connected to an electrometer system that is directly traceable to the National Institute of Standards and Technology (NIST) calibration. The beam was collimated with a 0.1 mm Cu added filter for cell line irradiation with a half-value-length of 0.51mm Cu. A Thoraeus

filter mm Cu filter (0.4 mm Sn + 0.25 mm Cu) and a half-value-length of 2.29 mm Cu was used for *in vivo* xenograft experiments.

Western Blot

Floating and adherent cells were collected and centrifuged to make cell pellets. Pellets were lysed with RIPA buffer (Thermo Fisher #89901) supplemented with cOmplete Mini protease and phosSTOP inhibitors (Sigma-Aldrich #PHOSS-RO, #CO-RO) and standardized using a BCA protein assay (Thermo Fisher #23225). Membranes were blocked in 5% milk and primary antibodies were diluted 1:1000 in 1% milk and used to probe for cleaved PARP (CST #5625), total PARP1 (CST #9542), Bcl-xL (CST #2762), Bcl-2 (CST #15071), Mcl-1 (CST #94296), pAKT (CST #4060, Ser473), total Akt (CST #9272), PTEN (CST #9559), p110α (CST #4249), Bak (CST #12105), β-Actin (CST #11262), and GAPDH (CST #2118). Secondary antibodies were HRP-conjugated for detection (CST #7074, #7076) and used at a 1:10,000 dilution.

IC_{50} of proliferation

Cells were plated in 96-well plates and allowed to adhere overnight. BH3 mimetics were added at various concentrations and, after 72 hours, AlamarBlue ($1/10^{th}$ volume; Thermo Fisher #DAL1025) was added. Absorbance was measured 3-4 hours after the addition of AlamarBlue with an excitation wavelength of 540 nm and an emission wavelength of 590 nm. Absorbance values were used to calculate normalized growth percentages compared to vehicle (DMSO) controls. A dose-response curve and half-maximal inhibitory concentrations (IC50s) were calculated in GraphPad Prism 8.0.

Clonogenic survival assays

Cells plated at single-cell density in 6 well plates were pretreated for one hour with inhibitor and plates were radiated at 0, 2, 4, or 6 Gy. Single cell colonies were allowed to grow for 1-3 during which time drug containing media was left on cells without replacement. Cells were fixed with 7:1 methanol and acetic acid and colonies (50+ cells) were visualized with 1% crystal violet staining. Linear-quadratic survival curves were fit to each experimental condition as described previously, (57) and radiation enhancement ratios were calculated as the ratio of the radiation-treated cells divided by the combination treated cells for each treatment group.

Annexin V Staining

The Annexin-V-FLUOS Staining Kit (Roche #11858777) was used to quantify apoptosis and necrosis by flow cytometry. Cells grown in 6-well plates were pretreated for one hour with Bcl-2 family inhibitors (ABT-263, ABT-199, WEHI-539, A-1331852) at the indicated concentrations and radiated at 4 Gy. Cells were collected after 48 hours, washed with PBS, and incubated in the dark in 200 µl of binding buffer containing 1 µl of Annexin V-FITC and 1 µl of PI for 30 minutes before detection using the BioRad Ze5 flow cytometer. Results were presented as the total percent of apoptotic cells, including both early apoptosis (Annexin V+/PI−) and late apoptosis (Annexin V+/PI+).

***In vivo* studies**

$2x10^6$ MDA-MB-231 cells or freshly passaged tumor fragments from patient derived xenografts (PDXs) were orthotopically implanted into the mammary fat pad of CB-17 SCID female mice.

Tumors were allowed to grow to ~80mm^3 and randomized before treatment began. For the MDA-MB-231 xenografts, ABT-263 or A-1331852 were given once a day for ten days at 25mg/kg and nine fractions of radiation were given, starting one day after the initiation of drug. For PDX4664 xenografts, drug was started one day prior to RT, given concurrently with six fractions of RT, and continued one day post-RT. Tumor size was measured approximately three times per week using a digital caliper. Tumor volume was calculated using the equation $V = (L * W2) * \pi/6$ (V=volume, L=length, W=width). Synergistic effects were calculated using the fraction tumor volume (FTV) method as previously described (58,59).

Study approval

The procedures listed above were approved by the Institutional Animal Care and Use Committee (IACUC) at the University of Michigan.

Statistics

Statistical analyses were performed using GraphPad Prism 8.0. One-way ANOVA with Dunnett's multiple comparisons test was used for clonogenic survival and Annexin V assays. One-way ANOVA with Dunnett's multiple comparisons test at the study endpoint and Log-rank (Mantel-Cox) test were used for *in vivo* analyses. (For simplicity, only the statistical comparisons for RT vs combination treatment with ABT-263 or A-1331852 are denoted on tumor growth curves). A p-value equal to or less than 0.05 was considered significant.

Acknowledgements

This work was supported by grants from the ASTRO-BCRF Career Development Award to End Cancer and the University of Michigan Rogel Cancer Center (N029402 and F049977 to C. Speers). This work was supported by multiple training grants and fellowships through the National Institute of Health including T32-CA140044 (BCC), T32-CA009676 (BCC), T32-GM007767 (AMP, KJ), F31-CA254138 (AMP), T-32 GM113900 (ARM), T32-GM007315 (ARM) and T32GM007863 (CAN). The SUM-159 cells were a gift from Stephen Ethier at the Medical University of South Carolina. In addition, AMP, BCC, and ARM are supported by Rackham Graduate School Research Grants. KJ is supported by the Rackham Merit Fellowship, and ARM is supported by the Rackham Predoctoral Fellowship. Finally, the authors would also like to thank the University of Michigan Flow Cytometry Core for assistance in flow cytometry data collection and analysis. This work was completed and submitted for publication with the following co-authors: Benjamin Chandler, Anna Michmerhuizen, Nicole Hirsh, Kari Wilder-Romans, Meilan Liu, Tanner Ward, Cassandra Ritter, Charles Nino, Kassidy Jungles, Lori J. Pierce, James Rae, and Corey Speers.

Figures

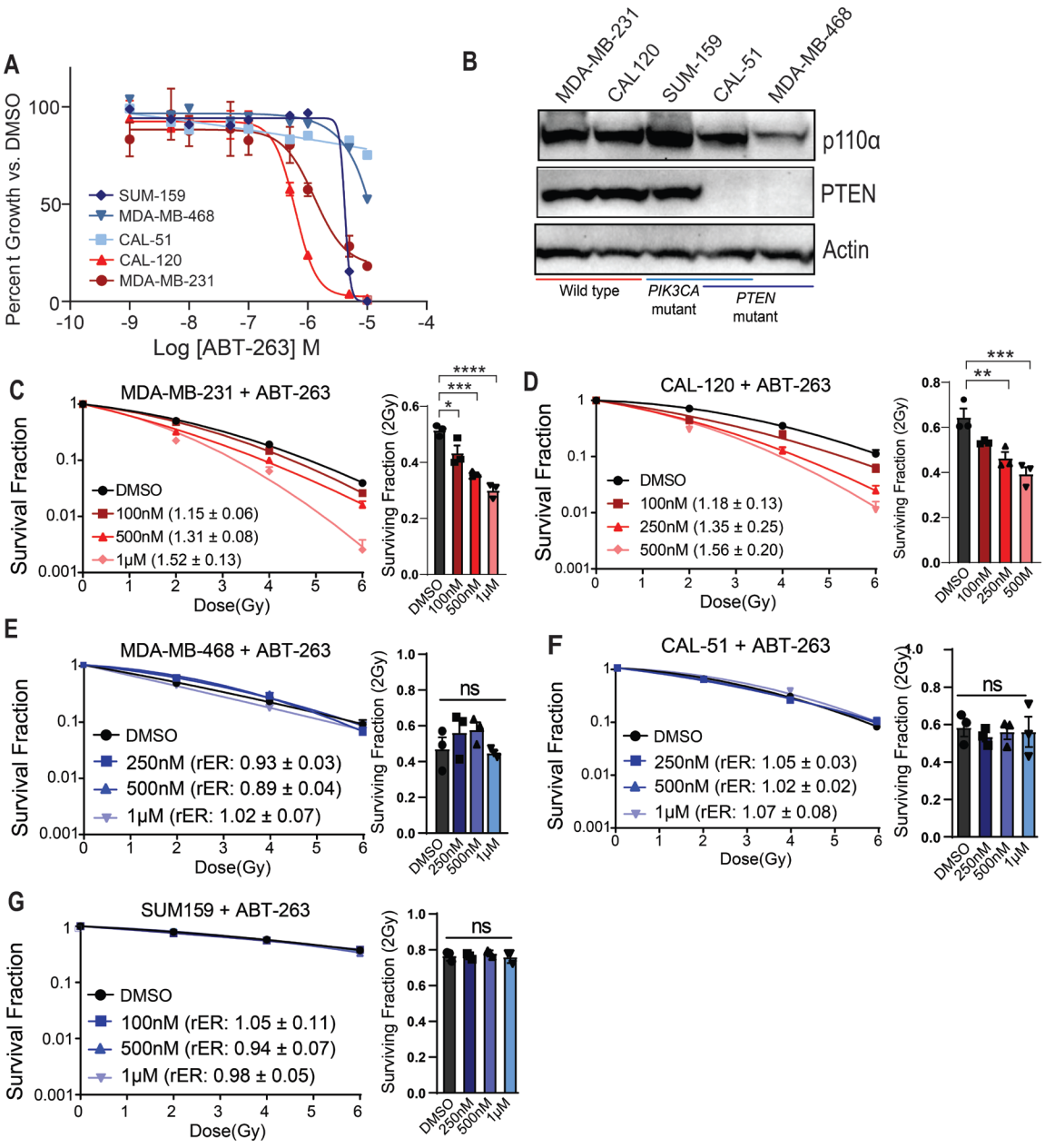

Figure 5.1: Pan Bcl-2 family inhibition radiosensitizes *PIK3CA/PTEN* wild-type TNBC.

Viability was assessed 72 hours after treatment with ABT-263 in TNBC cell lines (**A**). Expression of PTEN and p110α in TNBC cell lines was assessed by western blot (**B**). Clonogenic survival assays were used to calculate radiation enhancement ratios (rERs) in *PIK3CA/PTEN* wild-type TNBC (red, **C**,**D**) and *PIK3CA/PTEN* mutant TNBC (blue, **E-G**). All experiments represent the average of 3 independent replicates and one way ANOVA with Dunnett's post hoc test was used to compare the surviving fraction of cells at 2 Gy for each treatment condition. (ns = not significant, * = $p < 0.05$, ** = $p < 0.01$, *** = $p < 0.001$).

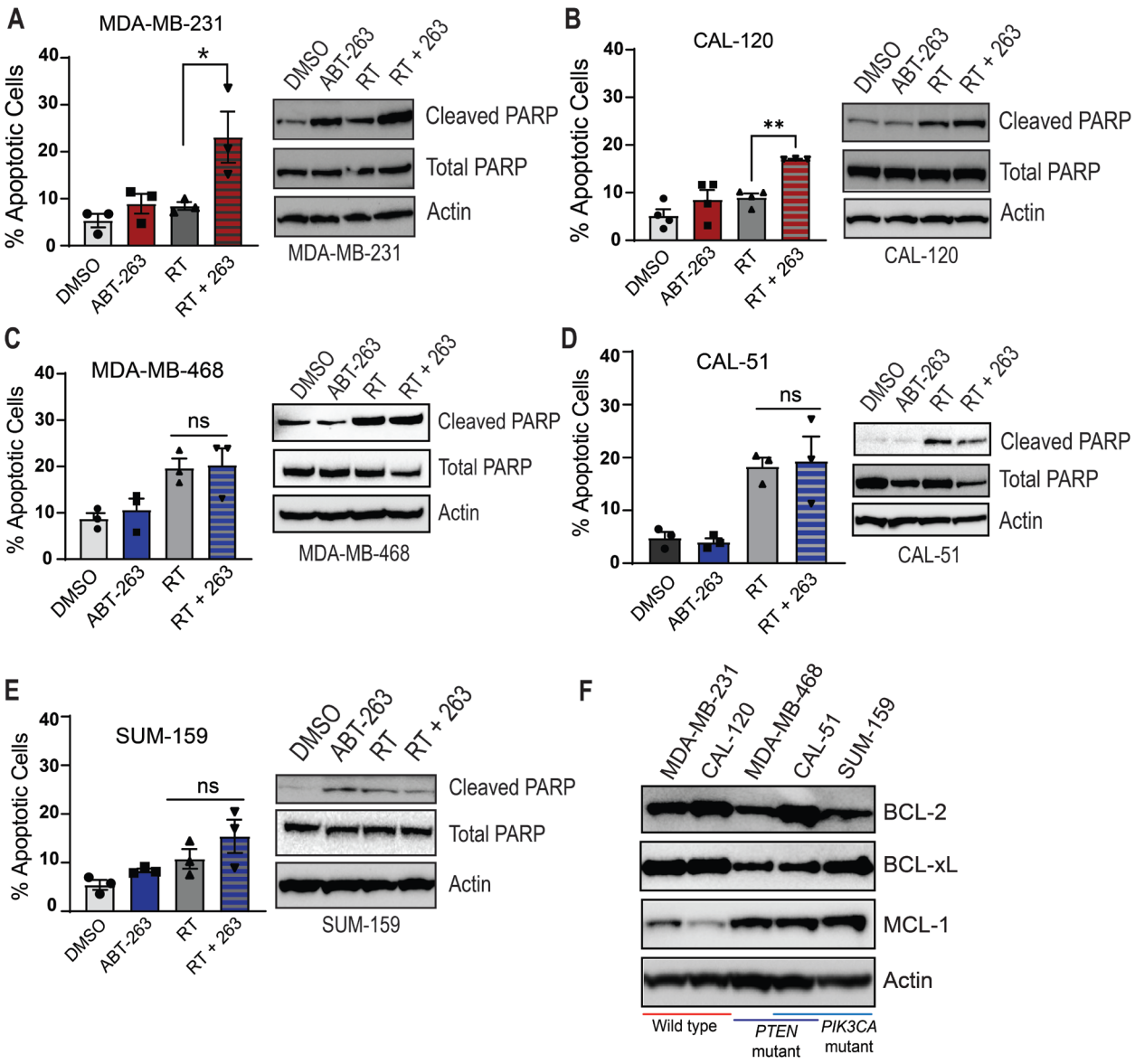

Figure 5.2: **Pan Bcl-2 inhibition leads to apoptosis in *PIK3CA/PTEN* wild-type TNBC.**

Apoptosis was assessed by annexin-V/PI flow cytometry in *PIK3CA/PTEN* wild-type TNBC (red, **A,B**) and *PIK3CA/PTEN* mutant TNBC (blue, **C-E**) 48 hours after RT treatment. Western blots were used to assess cleaved PARP formation 48 hours after combination treatment and the expression of Bcl-2 family proteins (Bcl-2, Bcl-xL, Mcl-1) in each of the TNBC cell lines at baseline (**F**). The concentration for the 1 hour ABT-263 pretreatment was 500nM in CAL-120 cells and 1μM in MDA-MB-231, MDA-MB-468, SUM-159, and CAL-51 cells. (ns = not significant, * = $p < 0.05$, ** = $p < 0.01$).

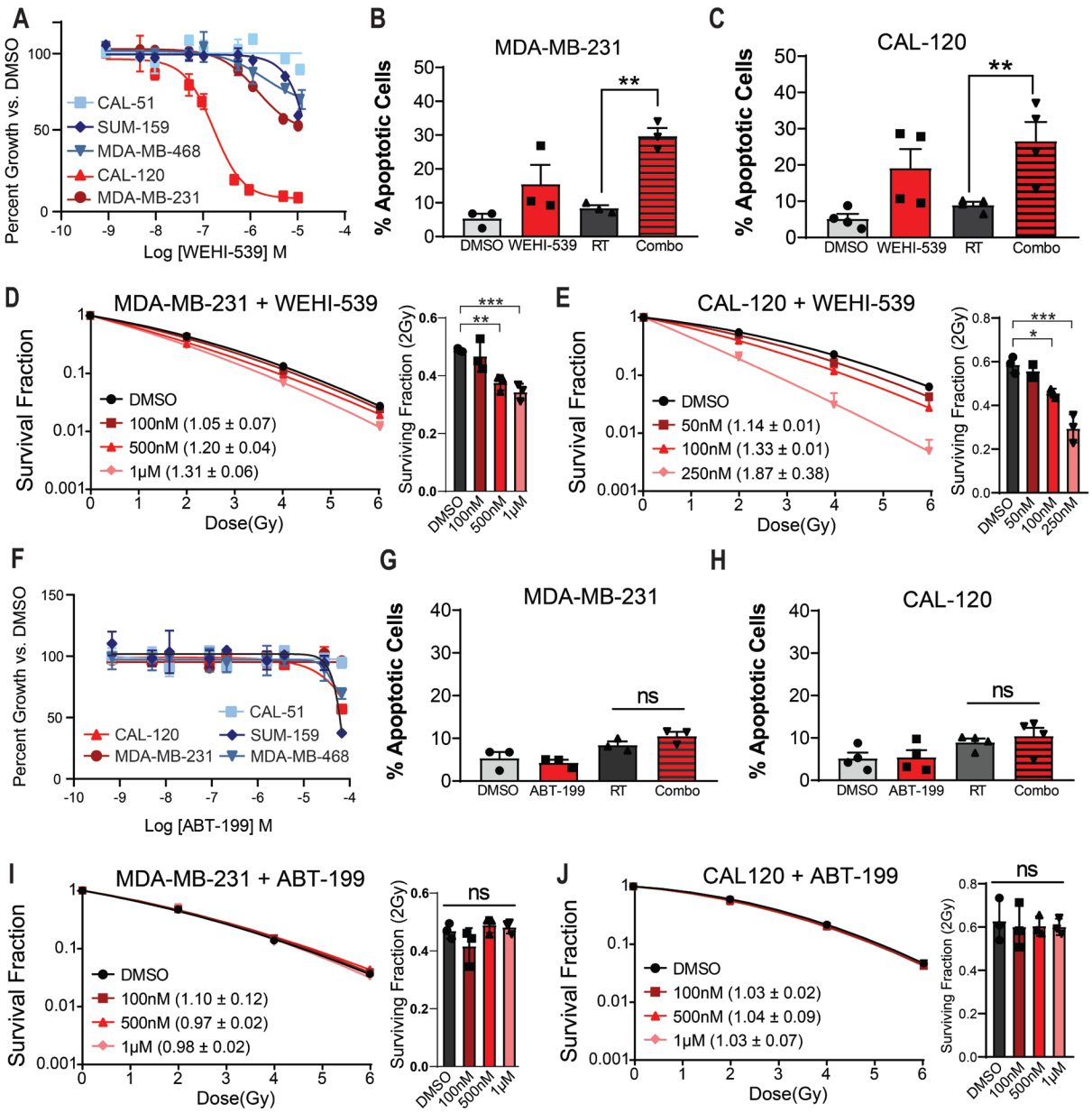

Figure 5.3: Bcl-xL, but not Bcl-2, is responsible for radiosensitivity in *PIK3CA/PTEN* wild-type TNBC.

Cellular viability was assessed in *PIK3CA/PTEN* wild-type (red) and mutant (blue) TNBC cell lines following 72-hour treatment with WEHI-539 (**A**) or ABT-199 (**F**). Annexin-V/PI flow cytometry was used to quantify the number of apoptotic cells following drug and/or RT treatment (**B,C,G,H**) and clonogenic survival assays were used to quantify the effects of combined RT + WEHI-539 (**D,E**¸1μM pretreatment for MDA-MB-231 and 250nM pretreatment for CAL-120) or ABT-199 (**I,J**, 1μM for both cell lines) in *PIK3CA/PTEN* wild-type TNBC. T-tests were used to compare RT and combination treated groups and a one-way ANOVA with Dunnett's post hoc test was used to compare SF 2 Gy values within each cell line (ns = not significant, * = $p < 0.05$, ** = $p < 0.01$, *** = $p < 0.001$).

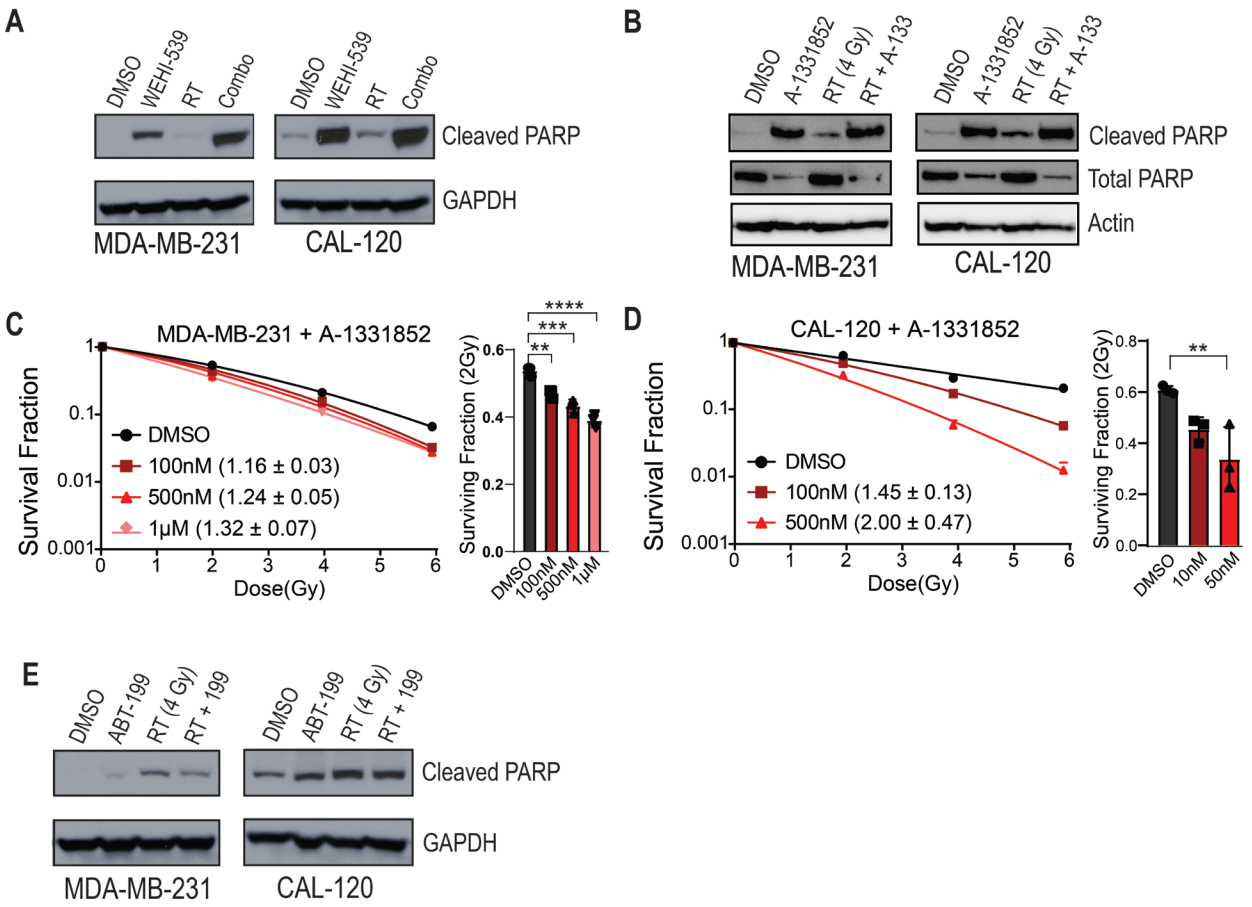

Figure 5.4: Bcl-xL inhibition induces apoptosis in *PIK3CA/PTEN* wild-type TNBC.

Apoptosis was assessed 48 hours after RT in MDA-MB-231 and CAL-120 cells pretreated for one-hour with WEHI-539 (1μM for MDA-MB-231 and 500nM for CAL-120), A-1331852 (1μM for MDA-MB-231 and 500nM for CAL-120), or 1μM ABT-199 prior to RT (**A,B,E**). Clonogenics (n=3) were used to assess A-1331852-mediated radiosensitivity and to assess the surviving fraction of cells at 2 Gy. (** = $p < 0.01$, *** = $p < 0.001$, **** $p < 0.0001$).

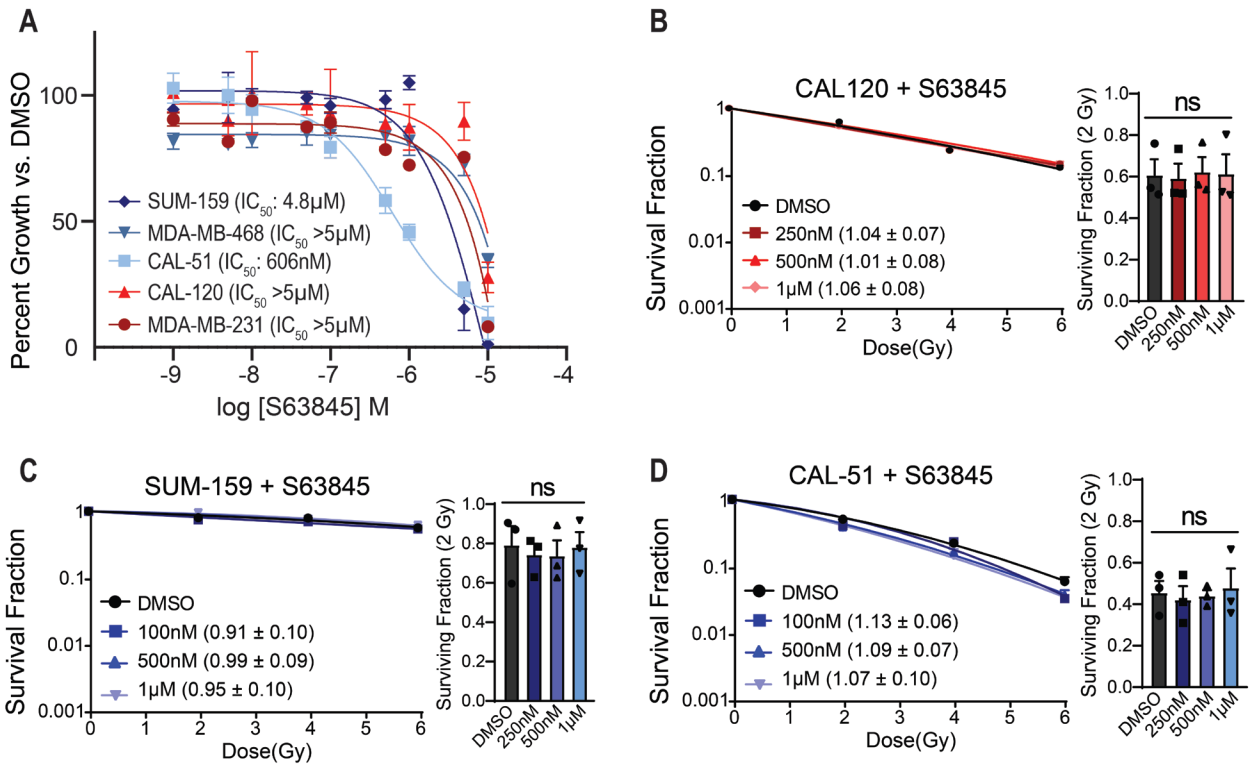

Figure 5.5: Mcl-1 inhibition does not radiosensitize TNBC cell lines regardless of *PIK3CA/PTEN* status.

Viability of TNBC cells was assessed 72 hours after treatment with the Mcl-1 inhibitor S63845 (**A**). Clonogenic survival assays were performed in *PIK3CA/PTEN* wild-type CAL-120 cells (**B**), and *PIK3CA* mutant SUM-159 cells (**C**), and *PIK3CA/PTEN* mutant CAL-51 cells (**C**) with S63845. (ns = not significant).

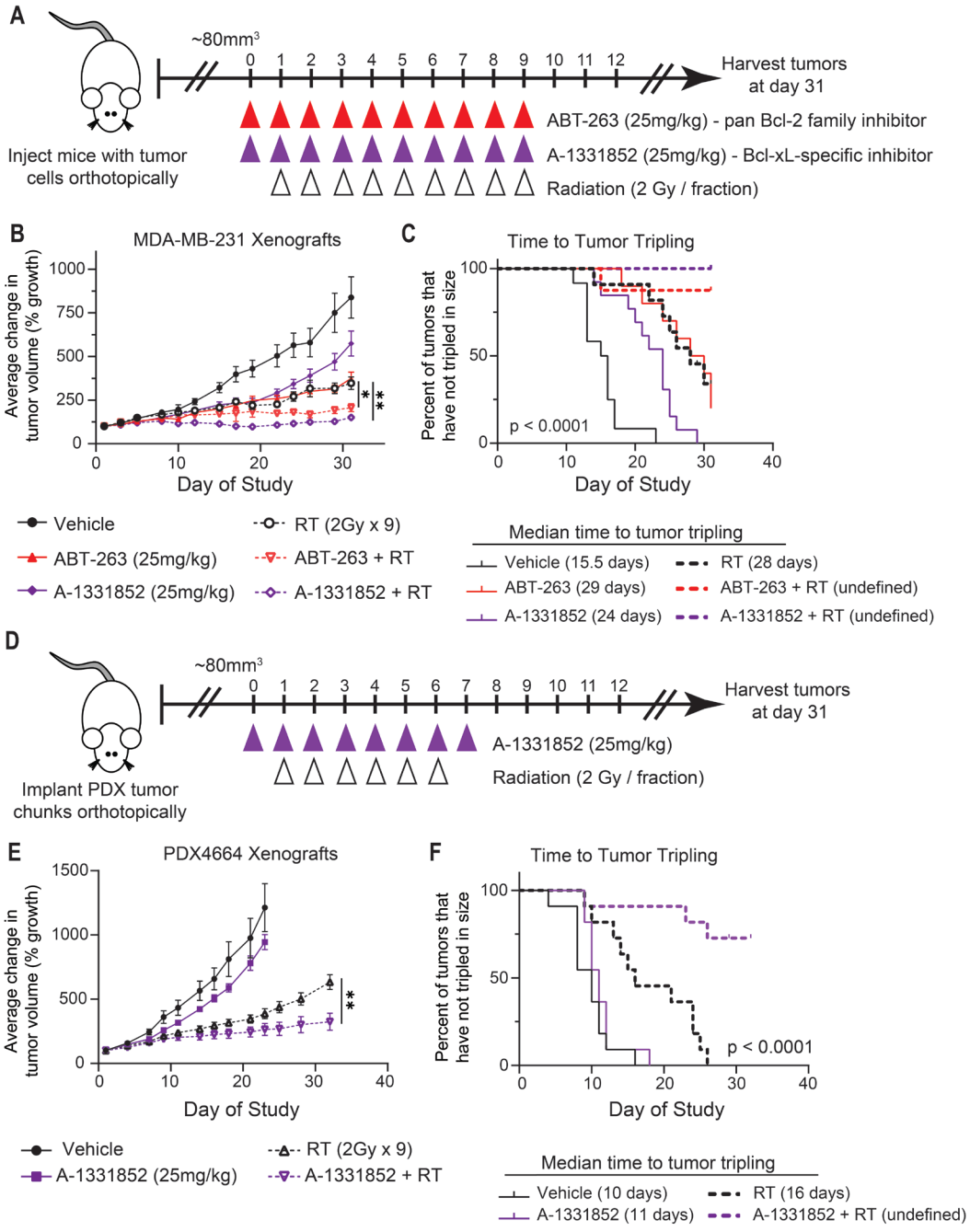

Figure 5.6: Pan Bcl-2 family inhibition or specific inhibition of Bcl-xL radiosensitizes *PIK3CA/PTEN* wild-type TNBC xenografts.

MDA-MB-231 xenograft tumors (**A**) were treated with 25mg/kg ABT-263 or 25mg/kg A-1331852 ± concurrent RT. Tumor volume was measured every 2-3 days (**B**) and used to calculate the median time to tumor tripling (**C**). A patient derived xenograft (PDX) model of TNBC was also used to assess effects of A-1331852 + RT (**D-F**). Tumor volume was compared using a one-way ANOVA at the study endpoint and Kaplan-Meier curves were compared using the log-rank (Mantel-Cox) test. (* = $p < 0.05$, ** = $p < 0.01$).

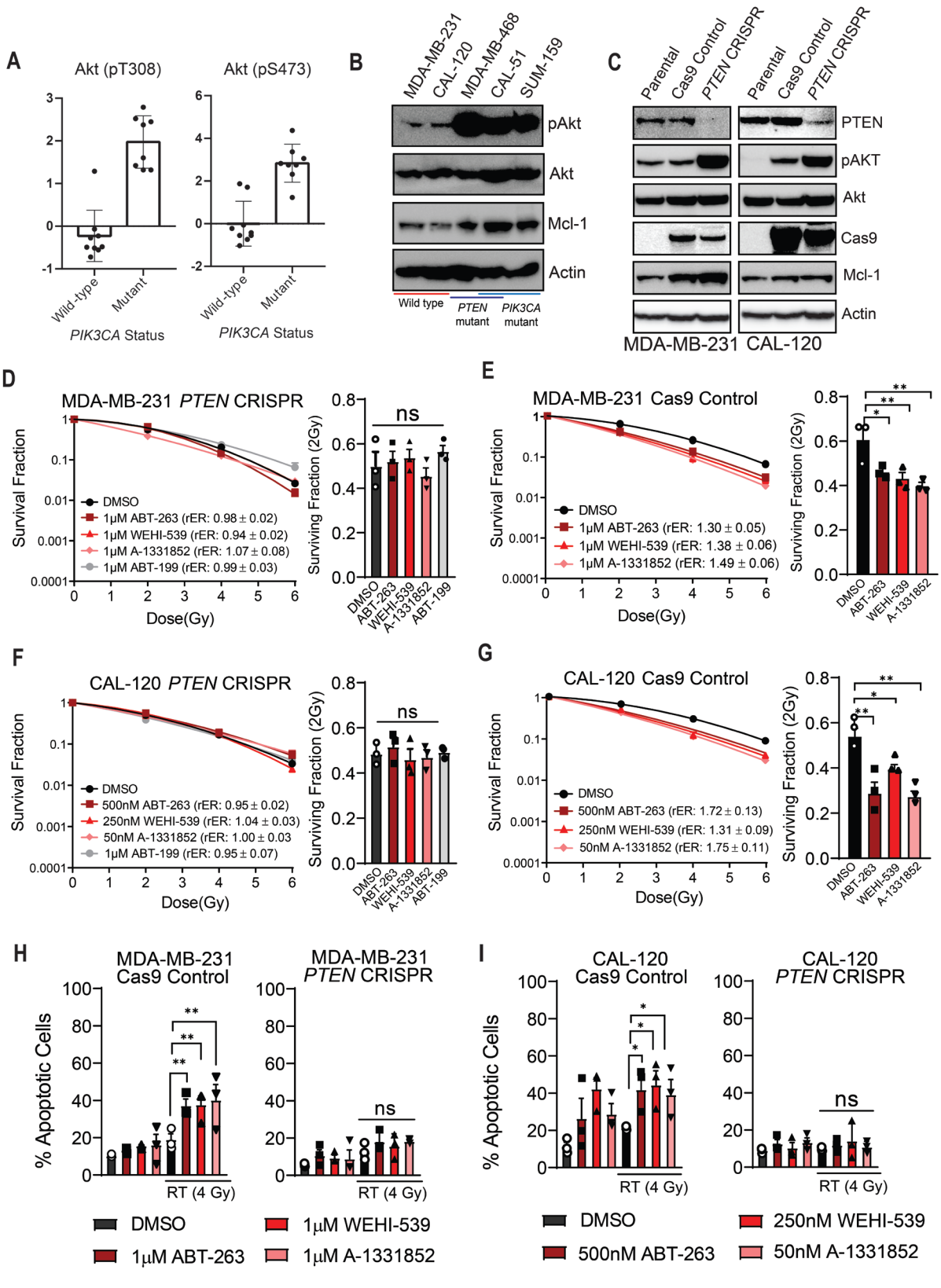
A
Akt (pT308)
Akt (pS473)
Wild-type
Mutant
PIK3CA Status
B
MDA-MB-231
CAL-120
MDA-MB-468
CAL-51
SUM-159
pAkt
Akt
Mcl-1
Actin
Wild type
PTEN mutant
PIK3CA mutant
C
Parental
Cas9 Control
PTEN CRISPR
PTEN
pAKT
Akt
Cas9
Mcl-1
Actin
MDA-MB-231
CAL-120
D
MDA-MB-231 PTEN CRISPR
Survival Fraction
Dose(Gy)
DMSO
1μM ABT-263 (rER: 0.98 ± 0.02)
1μM WEHI-539 (rER: 0.94 ± 0.02)
1μM A-1331852 (rER: 1.07 ± 0.08)
1μM ABT-199 (rER: 0.99 ± 0.03)
Surviving Fraction (2Gy)
ns
DMSO
ABT-263
WEHI-539
A-1331852
ABT-199
E
MDA-MB-231 Cas9 Control
DMSO
1μM ABT-263 (rER: 1.30 ± 0.05)
1μM WEHI-539 (rER: 1.38 ± 0.06)
1μM A-1331852 (rER: 1.49 ± 0.06)
F
CAL-120 PTEN CRISPR
DMSO
500nM ABT-263 (rER: 0.95 ± 0.02)
250nM WEHI-539 (rER: 1.04 ± 0.03)
50nM A-1331852 (rER: 1.00 ± 0.03
1μM ABT-199 (rER: 0.95 ± 0.07)
G
CAL-120 Cas9 Control
DMSO
500nM ABT-263 (rER: 1.72 ± 0.13)
250nM WEHI-539 (rER: 1.31 ± 0.09)
50nM A-1331852 (rER: 1.75 ± 0.11)
H
MDA-MB-231 Cas9 Control
MDA-MB-231 PTEN CRISPR
% Apoptotic Cells
RT (4 Gy)
DMSO
1μM ABT-263
1μM WEHI-539
1μM A-1331852
I
CAL-120 Cas9 Control
CAL-120 PTEN CRISPR
DMSO
500nM ABT-263
250nM WEHI-539
50nM A-1331852

Figure 5.7: *PTEN* loss leads to increased Akt/Mcl-1 expression and abolishes radiosensitization in TNBC cell lines.

CCLE data was used to plot pAkt expression based on *PIK3CA* mutation status in TNBC cell lines (A). Western blots were used to assess pAkt, Akt, and Mcl-1 expression at baseline (B) and following Cas9-mediated knockout of *PTEN* in MDA-MB-231 and CAL-120 cells (C). Clonogenic survival assays were performed in Cas9 control and *PTEN* CRISPR knockout cells to assess radiosensitivity with ABT-263, WEHI-539, A-1331852, and ABT-199 (D-G). Annexin V/PI-based flow cytometry was used to quantify apoptosis 48 hours after combination treatment in Cas9 control and *PTEN* knockout TNBC cell lines (H,I). (ns = not significant, * = $p < 0.05$, ** = $p < 0.01$, *** = $p < 0.001$).

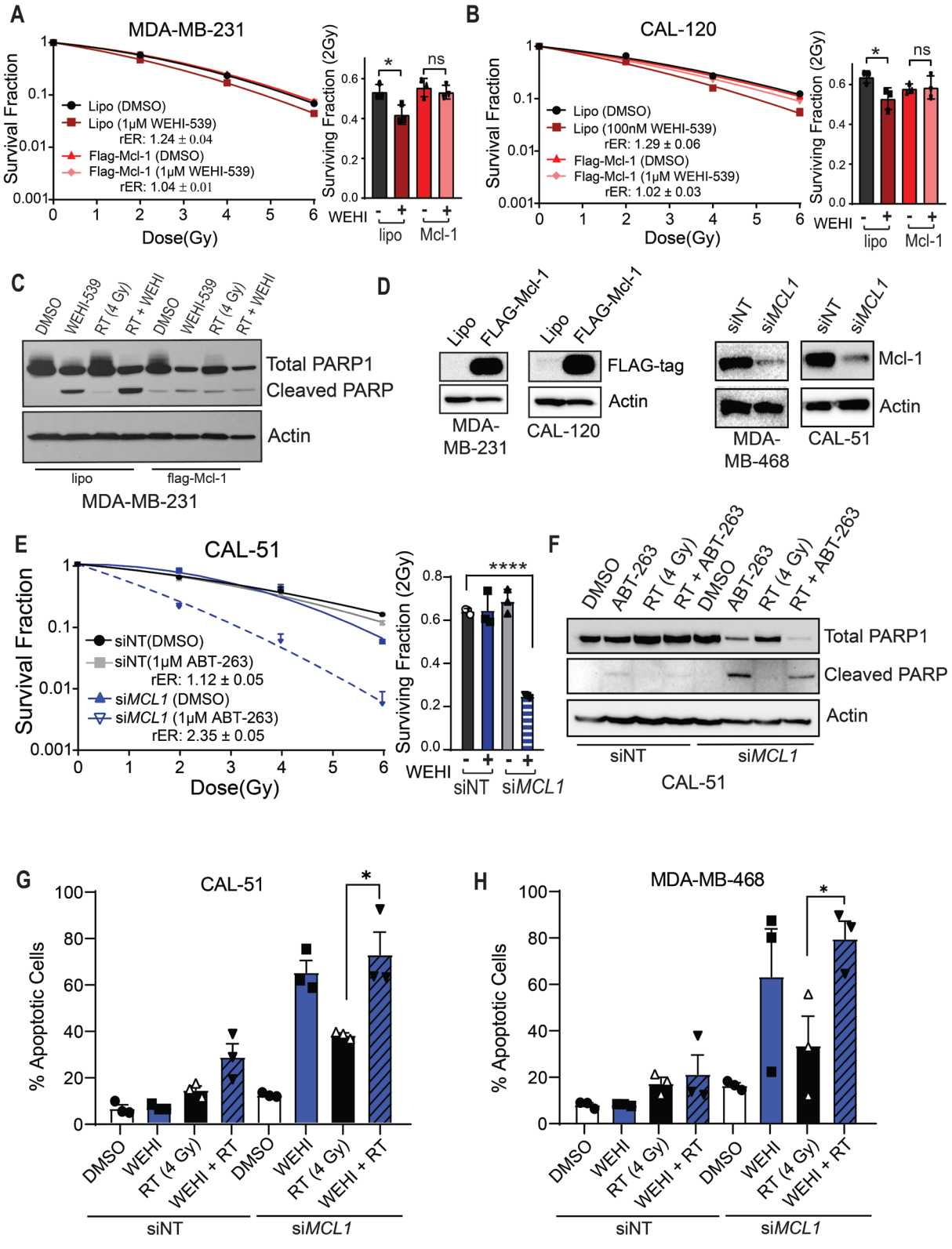
A
MDA-MB-231
Survival Fraction
Dose(Gy)
Lipo (DMSO)
Lipo (1μM WEHI-539)
rER: 1.24 ± 0.04
Flag-Mcl-1 (DMSO)
Flag-Mcl-1 (1μM WEHI-539)
rER: 1.04 ± 0.01
Surviving Fraction (2Gy)
WEHI
lipo
Mcl-1
B
CAL-120
Lipo (100nM WEHI-539)
rER: 1.29 ± 0.06
rER: 1.02 ± 0.03
C
DMSO
WEHI-539
RT (4 Gy)
RT + WEHI
Total PARP1
Cleaved PARP
Actin
lipo
flag-Mcl-1
MDA-MB-231
D
Lipo
FLAG-Mcl-1
FLAG-tag
Actin
MDA-MB-231
CAL-120
siNT
siMCL1
Mcl-1
MDA-MB-468
CAL-51
E
CAL-51
siNT(DMSO)
siNT(1μM ABT-263)
rER: 1.12 ± 0.05
siMCL1 (DMSO)
siMCL1 (1μM ABT-263)
rER: 2.35 ± 0.05
F
DMSO
ABT-263
RT (4 Gy)
RT + ABT-263
G
CAL-51
% Apoptotic Cells
WEHI
RT + RT
H
MDA-MB-468

Figure 5.8: Mcl-1 expression leads to radioresistance in TNBC cell lines.

Radiosensitization of cells with transient Mcl-1 overexpression was assessed in MDA-MB-231 (**A**) and CAL-120 cells (**B**). 24-hours post-transfection of FLAG-Mcl-1, cells were treated with WEHI-539 and/or RT (4 Gy) and harvested for western blot (**C**) at 48 hours post-RT. Radiosensitization was assessed when siMCL1 was used to transiently knockdown MCL1 expression in CAL-51 cells (**E**) and western blots were used to verify Mcl-1 protein expression 24 hours after transfection of siRNA or FLAG-Mcl-1 (**D**). Cells were treated with 1μM ABT-263 or 1μM WEHI-539 24 hours post-transfection (siMCL1) and harvested 48 hours post-RT for western blots or annexin V/PI-based flow cytometry (**F**,**G,H**) to assess apoptosis.

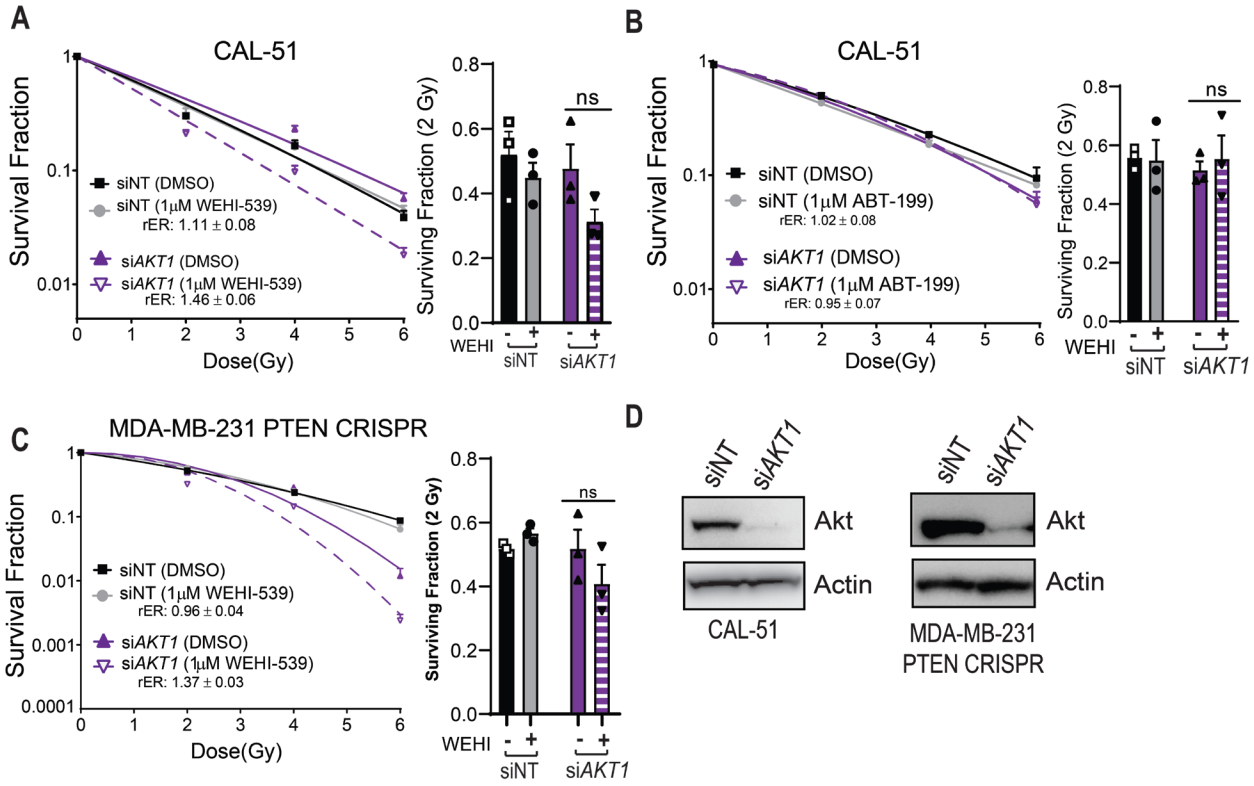

Figure 5.9: Akt is a modulator of Bcl-xL mediated radiosensitivity in TNBC cell lines.

Transient expression of si*AKT1* in CAL-51 (A,B) cells and MDA-MB-231 *PTEN* CRISPR (C) cells to perform clonogenic survival assays. Western blots were used to assess Akt expression following knockdown (24 hours post-transfection) (D). (ns = not significant, * = $p < 0.05$, ** = $p < 0.01$, *** = $p < 0.001$).

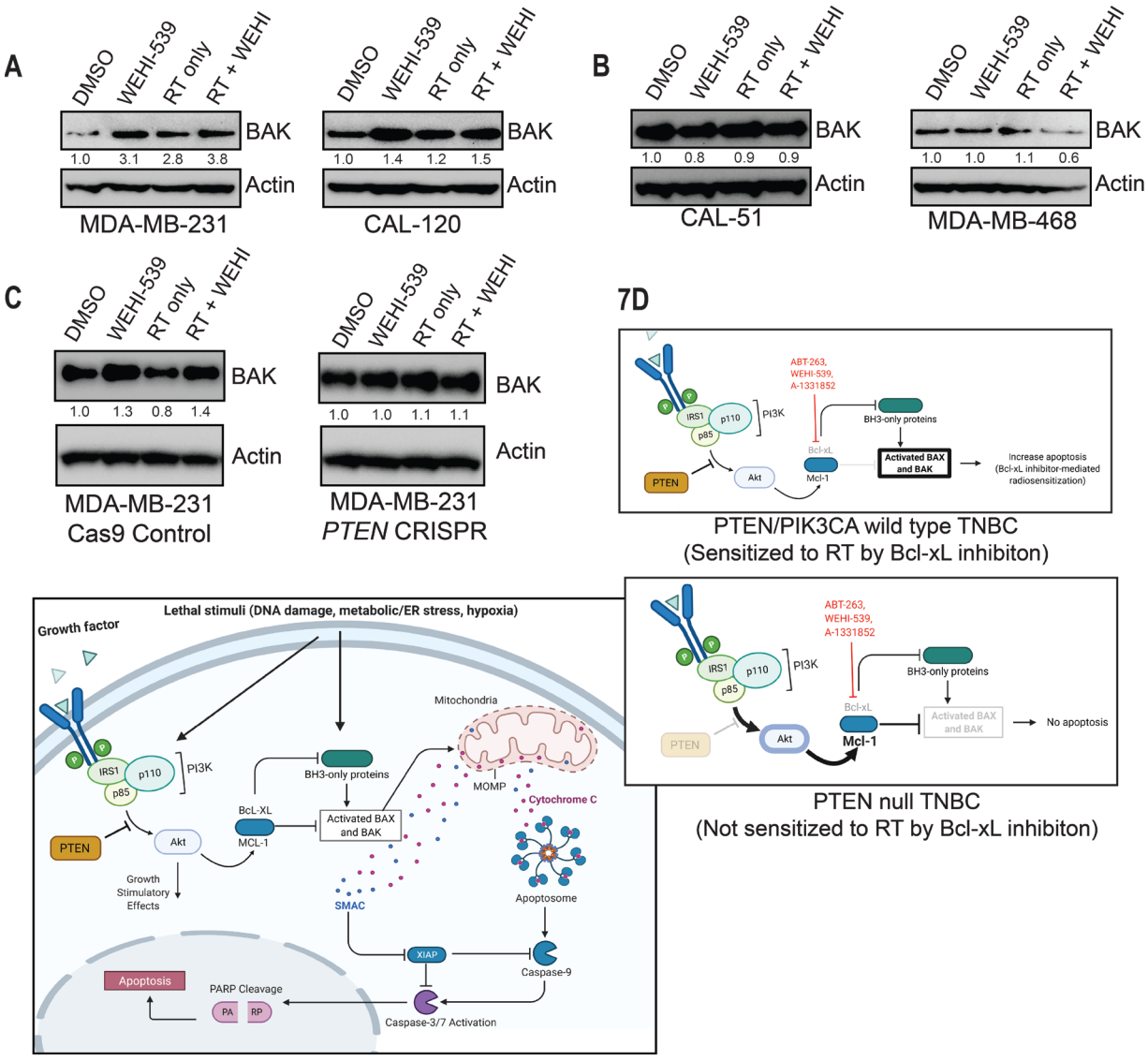

Figure 5.10: BAK mediates Bcl-xL inhibitor-mediated radiosensitivity in TNBC.

Expression of Bak was assessed 24 hours after RT (1 hour drug pretreatment before RT) in PIK3CA/PTEN wild-type (MDA-MB-231, CAL-120, MDA-MB-231 Cas9 control) and mutant (CAL-51, MDA-MB-468, MDA-MB-231 PTEN CRISPR) cell lines (**A-C**). In PIK3CA/PTEN wild-type cell lines, Bcl-xL inhibition leads to radiosensitization through suppression of Bcl-xL activity and increased Bak expression. In PIK3CA/PTEN mutant type cell lines, overactivation of AKT leads to increased Mcl-1 activation and minimal induction of Bak, preventing Bcl-xL inhibitor-mediated radiosensitization **(D)**.

	PIK3CA	*PTEN*
MDA-MB-231	wt	wt
CAL-120	wt	wt
CAL-51	missense mutation (E542K)	Frameshift (E288, TK321)
MDA-MB468	wt	Spice Site / Frameshift (A72fsX5)
SUM-159	missense mutation (H1047L)	wt

Table 5.1: Triple negative breast cancer cell line *PIK3CA/PTEN* mutational status

Cell Line	IC_{50} ABT-263	IC_{50} WEHI-539	IC_{50} ABT-199	IC_{50} S63845	IC_{50} A-1331852
MDA-MB-231	1.3μM	1.2μM	> 5 μM	> 5 μM	940nM
CAL-120	610nM	158nM	> 5 μM	> 5 μM	20.5nM
CAL-51	> 5 μM	> 5 μM	> 5 μM	606nM	-
MDA-MB-468	> 5 μM	> 5 μM	> 5 μM	> 5 μM	-
SUM-159	4.28μM	> 5 μM	> 5 μM	4.8μM	-

Table 5.2: IC_{50} values in TNBC cell lines with ABT-263, WEHI-539, and ABT-199.

MDA-MB-231 Fractional Tumor Volume (FTV) Calculations					
ABT-263			Combination		
Day	RT	ABT263	Expected	Observed	Ratio
8	0.914	0.801	0.732	0.761	**0.961**
12	0.770	0.716	0.551	0.702	**0.785**
19	0.553	0.581	0.321	0.407	**0.790**
29	0.428	0.485	0.208	0.269	**0.772**
Final	0.457	0.539	0.246	0.275	**0.895**

Table 5.3: Fractional tumor volume calculations for MDA-MB-231 xenografts treated with RT + ABT-263

MDA-MB-231 Fractional Tumor Volume (FTV) Calculations					
A-1331852			Combination		
Day	RT	A133	Expected	Observed	Ratio
8	0.914	0.809	0.739	0.720	**1.027**
12	0.770	0.780	0.600	0.497	**1.207**
19	0.553	0.607	0.336	0.232	**1.447**
26	0.428	0.612	0.262	0.211	**1.244**
Final	0.457	0.719	0.328	0.234	**1.405**

Table 5.4: Fractional tumor volume calculations for MDA-MB-231 xenografts treated with RT + A-1331852.

PDX-4664 Fractional Tumor Volume (FTV) Calculations					
A-1331852			Combination		
Day	RT	A133	Expected	Observed	Ratio
7	0.694	0.813	0.564	0.645	**0.874**
14	0.492	0.815	0.401	0.362	**1.109**
18	0.420	0.812	0.341	0.286	**1.190**
21	0.376	0.842	0.317	0.249	**1.276**
Final	0.539	0.813	0.438	0.268	**1.638**

Table 5.5: Fractional tumor volume calculations for PDX4664 xenografts treated with RT + A-1331852

References

1. Kyndi M, Sorensen FB, Knudsen H, Overgaard M, Nielsen HM, Overgaard J. Estrogen receptor, progesterone receptor, HER-2, and response to postmastectomy radiotherapy in high-risk breast cancer: the Danish Breast Cancer Cooperative Group. *J Clin Oncol* 2008;26(9):1419-26.
2. Skov K, MacPhail S. Interaction of platinum drugs with clinically relevant x-ray doses in mammalian cells: a comparison of cisplatin, carboplatin, iproplatin, and tetraplatin. *Int J Radiat Oncol Biol Phys*. 1991 Feb;20(2):221-5.
3. Pauwels B, Korst AEC, Lardon F, Vermorken JB. Combined Modality Therapy of Gemcitabine and Radiation. *The Oncologist* 2005;10(1):34-51.
4. de Haan R, van Werkhoven E, van den Heuvel MM, Peulen HMU, Sonke GS, Elkhuizen P, et al. Study protocols of three parallel phase 1 trials combining radical radiotherapy with the PARP inhibitor olaparib. *BMC Cancer* 2019;19(1):901.
5. Jagsi R, Griffith KA, Bellon JR, Woodward WA, Horton JK, Ho A, et al. Concurrent Veliparib With Chest Wall and Nodal Radiotherapy in Patients With Inflammatory or Locoregionally Recurrent Breast Cancer: The TBCRC 024 Phase I Multicenter Study. *J Clin Oncol* 2018;36(13):1317-22.
6. Ellis HM, Horvitz HR. Genetic control of programmed cell death in the nematode C. elegans. *Cell* 1986;44(6):817-29.
7. Oltval ZN, Milliman CL, Korsmeyer SJ. Bcl-2 heterodimerizes in vivo with a conserved homolog, Bax, that accelerates programed cell death. *Cell* 1993;74(4):609-19.
8. Kozopas KM, Yang T, Buchan HL, Zhou P, Craig RW. MCL1, a gene expressed in programmed myeloid cell differentiation, has sequence similarity to BCL2. *PNAS* 1993;90(8):3516.
9. O'Connor L, Strasser A, O'Reilly LA, Hausmann G, Adams JM, Cory S, et al. Bim: a novel member of the Bcl-2 family that promotes apoptosis. *EMBO J* 1998;17(2):384-95.
10. Vogler M. BCL2A1: the underdog in the BCL2 family. *Cell Death & Differentiation* 2012;19(1):67-74.
11. Montero J, Letai A. Why do BCL-2 inhibitors work and where should we use them in the clinic? *Cell Death & Differentiation* 2018;25(1):56-64.
12. Youle RJ, Strasser A. The BCL-2 protein family: opposing activities that mediate cell death. *Nature Reviews Molecular Cell Biology* 2008;9(1):47-59.
13. Yang J, Liu X, Bhalla K, Kim CN, Ibrado AM, Cai J, et al. Prevention of Apoptosis by Bcl-2: Release of Cytochrome c from Mitochondria Blocked. *Science* 1997;275(5303):1129.
14. Kluck RM, Bossy-Wetzel E, Green DR, Newmeyer DD. The Release of Cytochrome c from Mitochondria: A Primary Site for Bcl-2 Regulation of Apoptosis. *Science* 1997;275(5303):1132 doi 10.1126/science.275.5303.1132.
15. Chipuk JE, Green DR. Dissecting p53-dependent apoptosis. *Cell Death & Differentiation* 2006;13(6):994-1002.
16. Lanni JS, Lowe SW, Licitra EJ, Liu JO, Jacks T. p53-independent apoptosis induced by paclitaxel through an indirect mechanism. *PNAS* 1997;94(18):9679-83.

17. Wei MC, Lindsten T, Mootha VK, Weiler S, Gross A, Ashiya M, et al. tBID, a membrane-targeted death ligand, oligomerizes BAK to release cytochrome c. *Genes* Dev 2000;14(16):2060-71.
18. Gross A, Jockel J, Wei MC, Korsmeyer SJ. Enforced dimerization of BAX results in its translocation, mitochondrial dysfunction and apoptosis. *EMBO J* 1998;17(14):3878-85.
19. Souers AJ, Leverson JD, Boghaert ER, Ackler SL, Catron ND, Chen J, et al. ABT-199, a potent and selective BCL-2 inhibitor, achieves antitumor activity while sparing platelets. *Nature Medicine* 2013;19(2):202-8.
20. Oltersdorf T, Elmore SW, Shoemaker AR, Armstrong RC, Augeri DJ, Belli BA, et al. An inhibitor of Bcl-2 family proteins induces regression of solid tumours. *Nature* 2005;435(7042):677-81.
21. Park C-M, Bruncko M, Adickes J, Bauch J, Ding H, Kunzer A, et al. Discovery of an Orally Bioavailable Small Molecule Inhibitor of Prosurvival B-Cell Lymphoma 2 Proteins. *Journal of Medicinal Chemistry* 2008;51(21):6902-15.
22. Wilson WH, O'Connor OA, Czuczman MS, LaCasce AS, Gerecitano JF, Leonard JP, et al. Navitoclax, a targeted high-affinity inhibitor of BCL-2, in lymphoid malignancies: a phase 1 dose-escalation study of safety, pharmacokinetics, pharmacodynamics, and antitumour activity. *The Lancet Oncology* 2010;11(12):1149-59.
23. Gandhi L, Camidge DR, Ribeiro de Oliveira M, Bonomi P, Gandara D, Khaira D, et al. Phase I Study of Navitoclax (ABT-263), a Novel Bcl-2 Family Inhibitor, in Patients With Small-Cell Lung Cancer and Other Solid Tumors. *J Clin Oncol* 2011;29(7):909-16.
24. Merino D, Whittle JR, Vaillant F, Serrano A, Gong J-N, Giner G, et al. Synergistic action of the MCL-1 inhibitor S63845 with current therapies in preclinical models of triple-negative and HER2-amplified breast cancer. *Sci Trans Med* 2017;9(401):eaam7049.
25. Anderson GR, Wardell SE, Cakir M, Crawford L, Leeds JC, Nussbaum DP, et al. PIK3CA mutations enable targeting of a breast tumor dependency through mTOR-mediated MCL-1 translation. *Sci Trans Med* 2016;8(369):369ra175-369ra175.
26. Oakes SR, Vaillant F, Lim E, Lee L, Breslin K, Feleppa F, et al. Sensitization of BCL-2–expressing breast tumors to chemotherapy by the BH3 mimetic ABT-737. *PNAS* 2012;109(8):2766.
27. Vaillant F, Merino D, Lee L, Breslin K, Pal B, Ritchie Matthew E, et al. Targeting BCL-2 with the BH3 Mimetic ABT-199 in Estrogen Receptor-Positive Breast Cancer. *Cancer Cell* 2013;24(1):120-9.
28. Wu H, Schiff DS, Lin Y, Neboori HJR, Goyal S, Feng Z, et al. Ionizing radiation sensitizes breast cancer cells to Bcl-2 inhibitor, ABT-737, through regulating Mcl-1. *Radiat Res* 2014;182(6):618-25.
29. Longo PG, Laurenti L, Gobessi S, Sica S, Leone G, Efremov DG. The Akt/Mcl-1 pathway plays a prominent role in mediating antiapoptotic signals downstream of the B-cell receptor in chronic lymphocytic leukemia B cells. *Blood*. 2008 Jan 15;111(2):846-55.
30. Rahmani M, Aust MM, Attkisson E, Williams DC Jr, Ferreira-Gonzalez A, Grant S. Dual inhibition of Bcl-2 and Bcl-xL strikingly enhances PI3K inhibition-induced apoptosis in human myeloid leukemia cells through a GSK3- and Bim-dependent mechanism. *Cancer Res.* 2013 Feb 15;73(4):1340-51.

31. Jebahi A, Villedieu M, Pétigny-Lechartier C, Brotin E, Louis MH, Abeilard E, Giffard F, Guercio M, Briand M, Gauduchon P, Lheureux S, Poulain L. PI3K/mTOR dual inhibitor NVP-BEZ235 decreases Mcl-1 expression and sensitizes ovarian carcinoma cells to Bcl-xL-targeting strategies, provided that Bim expression is induced. *Cancer Lett*. 2014 Jun 28;348(1-2):38-49. doi: 10.1016/j.canlet.2014.03.001.
32. Mosele F, Stefanovska B, Lusque A, Tran Dien A, Garberis I, Droin N, et al. Outcome and molecular landscape of patients with PIK3CA-mutated metastatic breast cancer. *Ann Oncol.* 2020 Mar;31(3):377-386.
33. Luen SJ, Asher R, Lee CK, Savas P, Kammler R, Dell'Orto P, et al. Association of Somatic Driver Alterations With Prognosis in Postmenopausal, Hormone Receptor-Positive, HER2-Negative Early Breast Cancer: A Secondary Analysis of the BIG 1-98 Randomized Clinical Trial. *JAMA Oncol.* 2018 Oct 1;4(10):1335-1343.
34. Tse C, Shoemaker AR, Adickes J, Anderson MG, Chen J, Jin S, et al. ABT-263: A Potent and Orally Bioavailable Bcl-2 Family Inhibitor. *Cancer Research* 2008;68(9):3421.
35. Stratikopoulos EE, Kiess N, Szabolcs M, Pegno S, Kakit C, Wu X, et al. Mouse ER+/PIK3CA H1047R breast cancers caused by exogenous estrogen are heterogeneously dependent on estrogen and undergo BIM-dependent apoptosis with BH3 and PI3K agents. *Oncogene.* 2019 Jan;38(1):47-59.
36. Lee EY, Gong EY, Shin JS, Moon JH, Shim HJ, Kim SM, et al. Human breast cancer cells display different sensitivities to ABT-263 based on the level of survivin. *Toxicol In Vitro*. 2018 Feb;46:229-236.
37. Oakes SR, Vaillant F, Lim E, Lee L, Breslin K, Feleppa F, et al. Sensitization of BCL-2-expressing breast tumors to chemotherapy by the BH3 mimetic ABT-737. *PNAS*. 2012 Feb 21;109(8):2766-71.
38. Tao ZF, Hasvold L, Wang L, Wang X, Petros AM, Park CH, et al. Discovery of a Potent and Selective BCL-XL Inhibitor with in Vivo Activity. *ACS Med Chem Lett*. 2014 Aug 26;5(10):1088-93.
39. Lessene G, Czabotar PE, Sleebs BE, Zobel K, Lowes KN, Adams JM, et al. Structure-guided design of a selective BCL-xL inhibitor. *Nature Chemical Biology* 2013;9(6):390-7 doi 10.1038/nchembio.1246.
40. Leverson JD, Phillips DC, Mitten MJ, Boghaert ER, Diaz D, Tahir SK, et al. Exploiting selective BCL-2 family inhibitors to dissect cell survival dependencies and define improved strategies for cancer therapy. *Science Translational Medicine* 2015;7(279):279ra40.
41. Li H, Liu L, Chang H, Zou Z, Xing D. Downregulation of MCL-1 and upregulation of PUMA using mTOR inhibitors enhance antitumor efficacy of BH3 mimetics in triple-negative breast cancer. *Cell Death Dis*. 2018 Jan 26;9(2):137.
42. Leverson JD, Phillips DC, Mitten MJ, Boghaert ER, Diaz D, Tahir SK, et al. Exploiting selective BCL-2 family inhibitors to dissect cell survival dependencies and define improved strategies for cancer therapy. *Science Translational Medicine* 2015;7(279):279ra40.

43. Kasai S, Sasaki T, Watanabe A, Nishiya M, Yasuhira S, Shibazaki M, et al. Bcl-2/Bcl-xL inhibitor ABT-737 sensitizes pancreatic ductal adenocarcinoma to paclitaxel-induced cell death. *Oncol Lett.* 2017 Jul;14(1):903-908. doi: 10.3892/ol.2017.6211.
44. Panayotopoulou EG, Müller AK, Börries M, Busch H, Hu G, Lev S. Targeting of apoptotic pathways by SMAC or BH3 mimetics distinctly sensitizes paclitaxel-resistant triple negative breast cancer cells. *Oncotarget*. 2017 Jul 11;8(28):45088-45104.
45. Shahbandi A, Rao SG, Anderson AY, Frey WD, Olayiwola JO, Ungerleider NA, et al. BH3 mimetics selectively eliminate chemotherapy-induced senescent cells and improve response in TP53 wild-type breast cancer. *Cell Death & Differentiation* 2020;27(11):3097-116.
46. Hu H, Zhu J, Zhong Y, Geng R, Ji Y, Guan Q, et al. PIK3CA mutation confers resistance to chemotherapy in triple-negative breast cancer by inhibiting apoptosis and activating the PI3K/AKT/mTOR signaling pathway. *Ann Transl Med*. 2021 Mar;9(5):410.
47. Wang B, Ni Z, Dai X, Qin L, Li X, Xu L, et al. The Bcl-2/xL inhibitor ABT-263 increases the stability of Mcl-1 mRNA and protein in hepatocellular carcinoma cells. *Mol Cancer*. 2014 Apr 30;13:98.
48. Wang X, Chen W, Zeng W, Bai L, Tesfaigzi Y, Belinsky SA, et al. Akt-mediated eminent expression of c-FLIP and Mcl-1 confers acquired resistance to TRAIL-induced cytotoxicity to lung cancer cells. *Mol Cancer Ther*. 2008 May;7(5):1156-63.
49. Chen G, Park D, Magis AT, Behera M, Ramalingam SS, Owonikoko TK, et al. Mcl-1 Interacts with Akt to Promote Lung Cancer Progression. *Cancer Res*. 2019 Dec 15;79(24):6126-6138.
50. Thomas D, Powell JA, Vergez F, Segal DH, Nguyen NY, Baker A, et al. Targeting acute myeloid leukemia by dual inhibition of PI3K signaling and Cdk9-mediated Mcl-1 transcription. *Blood.* 2013 Aug 1;122(5):738-48.
51. Gómez Tejeda Zañudo J, Mao P, Alcon C, Kowalski K, Johnson GN, Xu G, et al. Cell Line-Specific Network Models of ER+ Breast Cancer Identify Potential PI3Kα Inhibitor Resistance Mechanisms and Drug Combinations. *Cancer Res*. 2021 Sep 1;81(17):4603-4617.
52. Williams MM, Elion DL, Rahman B, Hicks DJ, Sanchez V, Cook RS. Therapeutic inhibition of Mcl-1 blocks cell survival in estrogen receptor-positive breast cancers. *Oncotarget*. 2019 Oct 9;10(52):5389-5402.
53. Kline MP, Rajkumar SV, Timm MM, Kimlinger TK, Haug JL, Lust JA, et al. ABT-737, an inhibitor of Bcl-2 family proteins, is a potent inducer of apoptosis in multiple myeloma cells. *Leukemia* 2007;21(7):1549-60.
54. Li JY, Li YY, Jin W, Yang Q, Shao ZM, Tian XS. ABT-737 reverses the acquired radioresistance of breast cancer cells by targeting Bcl-2 and Bcl-xL. *J Exp Clin Cancer Res* 2012;31:102.
55. Hinz N, Jücker M. Distinct functions of AKT isoforms in breast cancer: a comprehensive review. *Cell Commun Signal*. 2019 Nov 21;17(1):154.
56. Billard C. Design of novel BH3 mimetics for the treatment of chronic lymphocytic leukemia. *Leukemia*. 2012 Sep;26(9):2032-8.

57. Gill S, Loprinzi C, Kennecke H, Grothey A, Nelson G, Woods R, et al. Prognostic web-based models for stage II and III colon cancer: A population and clinical trials-based validation of numeracy and adjuvant! online. *Cancer* 2011;117(18):4155-65 doi 10.1002/cncr.26003.
58. Yokoyama Y, Dhanabal M, Griffioen AW, Sukhatme VP, Ramakrishnan S. Synergy between Angiostatin and Endostatin: Inhibition of Ovarian Cancer Growth. *Cancer Research* 2000;60(8):2190.
59. Matar P, Rojo F, Cassia R, Moreno-Bueno G, Di Cosimo S, Tabernero J, et al. Combined Epidermal Growth Factor Receptor Targeting with the Tyrosine Kinase Inhibitor Gefitinib (ZD1839) and the Monoclonal Antibody Cetuximab (IMC-C225). *Clinical Cancer Research* 2004;10:6487-501.

Chapter 6 : Discussion

Summary

Radiation (RT) treatment is part of the standard of care for breast cancer patients and it is often used with other treatment strategies such as chemotherapy and surgery as part of a multimodal approach to treat patients with breast cancer (1). While radiation is an effective therapy that can be used for local disease control and the treatment of distant metastases, the benefits derived from adjuvant radiation therapy are not uniform across the different molecular and pathological subtypes of breast cancer (2). Although there are typically higher rates of locoregional recurrences in patients with inflammatory and/or triple negative breast cancer, disease control in women with multi-node positive breast cancers is suboptimal across all subtypes (1). To that end, our studies aimed to develop subtype-specific combination therapies that were effective in increasing the effectiveness of radiation therapy in *in vitro* and *in vivo* models of aggressive breast cancer.

First, in the context of inflammatory breast cancer (IBC), we demonstrated that inhibition of PARP1 with veliparib or olaparib (Lynparza) is selective and specific therapeutic approach to induce cell death through the potentiation of radiation-induced dsDNA breaks (**Chapter 2**) (3). Next, we demonstrated that specific inhibitors of cyclin-dependent kinase 4 and 6 including palbociclib (Ibrance), ribociclib (Kisqali), and abemaciclib (Verzenio) suppress homologous

recombination-mediated dsDNA repair and lead to radiosensitization of breast cancer cells when given in combination with RT (4). Although this strategy was initially proposed and validated in models of estrogen receptor positive (ER+) breast cancer (**Chapter 3**), our subsequent studies demonstrated that CDK4/6 inhibition + RT is an effective combination therapy in triple negative breast cancers that express the retinoblastoma (RB) tumor suppressor (**Chapter 4**). Finally, we showed that BH3 mimetics such as ABT-263 (Navitoclax) or Bcl-xL specific inhibitors (WEHI-539, A-1331852) – but not the Bcl-2 specific inhibitor ABT-199 (Venetoclax) – radiosensitized triple negative breast cancers in a manner dependent on upstream PI3K/PTEN signaling (**Chapter 5**). As a whole, this work demonstrates the efficacy and feasibility of subtype-specific approaches to radiosensitization for the treatment of breast cancer.

Future Directions

PARP Inhibition in Inflammatory Breast Cancer

One of the most important future directions is to characterize the mechanism of PARP1-mediated radiosensitization in inflammatory breast cancer. Although we demonstrated that RT + PARP1 inhibition potentiated dsDNA breaks, we have yet to elucidate the effects of this combination therapy on specific DNA repair pathways, including homologous recombination, non-homologous end joining, base excision repair, nucleotide excision repair, or mismatch exchange. The PARP1 protein has been shown to play an extensive role in these repair processes in other cancers, and targeting one or more of these pathways in addition to PARP1 may prevent or overcome clinical resistance to PARP1 inhibition. One recent example of this is the antibiotic novobiocin, which inhibits DNA polymerase theta (POLθ)-mediated DNA repair, which is synergistic with PARP1 inhibition in HR-deficient cancers, such as *BRCA2* mutated breast cancers (5).

Our studies predominately utilized veliparib and olaparib, but there are a number of new PARP1 inhibitors with the potential to induce radiosensitization of IBCs with reduced side effect profiles or more effective enzymatic inhibition of PARP1. Currently available PARP1 inhibitors can also be used as a pharmacophore to bind the PARP1 enzyme as part of novel PARP1 degraders, as is the case in novel compounds such as SK-575 or iRucaparib-AP6 (6-8). SK-575 leads to increased apoptosis, higher levels of DNA damage, and decreased cell migration in combination with temozolomide and cisplatin, and it is likely that novel PARP1 degraders would demonstrate similar levels of synergy in combination with radiation.

Differences in PARP trapping ability also induce different levels of immune system activation after PARP1 inhibition (9). Activation of the cGAS-STING pathway is well-

coordinated to levels of DNA damage and PARP1 trapping when comparing talazoparib, niraparib, rucaparib, olaparib, and veliparib (9). Interestingly, PROTAC-mediated degradation of PARP1 can block PARP1 catalytic activity without affecting PARP1 trapping (8,9) or immune system activation (9). Because we have yet to clarify which of the PARP1 inhibitor functions is essential for radiosensitization in models of TNBC and IBC, PARP1-targeted PROTACs represent an important future mechanistic direction of this work.

CDK4/6 Inhibition in ER+ and Triple Negative Breast Cancers

By extending our initial studies of CDK4/6 inhibition + RT from the context of ER+ to TNBC, we demonstrated that RB was an important biomarker for the efficacy of the combination therapy. Although we have not specifically tested this strategy in breast cancers that overexpress HER2, we hypothesize that HER2+ breast cancer cells lines that express RB will be radiosensitized by CDK4/6 inhibition and RT. In addition, this strategy may be beneficial in other histopathological classifications of breast cancer (lobular, inflammatory) that are RB intact. We demonstrated that manipulation of RB expression changes the overall efficiency of HR-mediated repair in breast cancer cell lines and that RB interacts with the HR mediator RAD51, but future studies should seek to specifically characterize this protein complex and identify additional protein mediators that participate in dsDNA repair in complex with the tumor suppressor RB. Alternatively, overexpression of phosphorylation-deficient RB protein or kinase dead (inactive) CDK4 or CDK6 could be used in our *in vitro* model systems to further refine our mechanistic understanding of CDK4/6 inhibitor-mediated radiosensitization.

Because CDK4/6 inhibitor-mediated radiosensitization occurs through suppression of homologous recombination, another important question to consider is how existing *BRCA1/2*

mutations may influence response to the proposed combination treatment. In these patients, pre-existing deficits in the homologous repair pathway may preclude response to combined CDK4/6 inhibition + RT and it may be more effective to pharmacologically target other DNA repair pathways such as NHEJ or single stranded DNA repair. In our study, we demonstrated that RAD51 and RB interact as part of a protein complex that is necessary for effective repair of dsDNA breaks through HR; future studies could address the role of BRCA1/2 in this repair complex and determine the effects of *BRCA1/2* mutations on the efficacy of CDK4/6 inhibitor-induced radiosensitization.

In the context of ER+ breast cancer, one important clinical question that remains is how to optimize the timing and sequence of CDK4/6 inhibition, anti-estrogen therapies, and RT. Although it has been debated in the past, recent evidence suggests that anti-ER therapies such as tamoxifen and fulvestrant can radiosensitize ER+ breast cancers through an increase in senescence a resulting decrease in the efficiency of non-homologous end joining-mediated DNA repair (10). The timing of the initiation of anti-estrogen therapy varies across different medical centers, and as CDK4/6 inhibitors make their way into the neoadjuvant/adjuvant setting, this will also be a necessary question to address. It is likely that these two strategies would have additive or synergistic effects when given together with RT in the clinic, but the benefits may be constrained by dose-limiting or overlapping toxicities with the triple combination. Furthermore, because there is recent evidence to suggest that CDK4/6 inhibition may be equally effective when started after fractionated radiation (11), there may be additional nuances in the timing of the combination therapy that require optimization in patients.

Finally, additional studies should be completed to assess the effects of CDK4/6 inhibition + RT in the presence of compounds targeting critical signaling pathways in breast cancer such as

PI3K or EGFR; although these therapies are administered less frequently than anti-estrogens in patients with ER+ disease, inhibition of PI3K or EGFR has also been shown to affect the radiation response in breast cancer (12-14). This is especially applicable for patients with ER+/HER2+ disease that receive anti-HER2 small molecule or monoclonal antibody therapies such as lapatinib and trastuzumab, respectively. Inhibition of HER2 suppresses HER2-stimulated growth pathways and can sensitize HER2+ breast cancer cells to RT; this may be potentiated by the addition of a CDK4/6 inhibitor if given concurrently with radiation. Altogether, we need to develop a more complete understanding of these potential drug-drug and drug-radiation interactions when it comes to developing the most effective, safe, and viable clinical path forward for patients with ER+ or ER+/HER2+ breast cancers. In the context of high-risk, early stage TNBC, the recent approval of pembrolizumab poses a similar clinical conundrum for implementation of CDK4/6 inhibition + RT. Radiation treatment induces a number of cellular changes even in the absence of additional small molecule modifiers, and recent evidence has even shown that low-dose, fractionated RT can promote tumoral T-cell infiltration and increase tumor immunogenicity (15) in cancer cells.

Similar to these radiation-mediated effects, CDK4/6 inhibitors cause increased antigen presentation and increased type III interferon production which stimulate the immune system and creates synergistic between CDK4/6 inhibitors and anti PD-1 or anti-CTLA4 therapies (16-20). Other groups have demonstrated that, in addition to the stimulation of effective T lymphocytes, CDK4/6 inhibition in immunocompetent models can alter the balance of T cell production by increasing the number of cytotoxic T cells relative to the number of immunosuppressive T cells in models of breast cancer (17,21). The expression of CDK6 is higher in Treg cells than other types of T cells, making this a selective strategy in which breast tumors can be primed for

immunotherapy (21,22). Our *in vivo* studies were done in immunocompromised mice, and in the future it will be important to evaluate the efficacy of this combination therapy in the context of an intact immune system – and in combination with anti PD-1 or CTLA4 therapies that modulate the immune system. Current clinical trials that seek to combine palbociclib (NCT02778685) or abemaciclib (NCT02779751) with pembrolizumab in metastatic, ER+ breast cancers have preliminary data to suggest that the combination therapy is generally well-tolerated (23), and future studies could evaluate this treatment strategy in ER+ or RB-intact TNBC in combination with RT to harness benefits of CDK4/6 inhibition on both radiosensitization and potentiation of the immune response.

Bcl-xL Inhibition in Triple Negative Breast Cancers

Our data demonstrated that pharmacologic inhibition of Bcl-xL was sufficient to radiosensitize triple negative breast cancers that express wild type *PIK3CA* and *PTEN*. In this context, AKT-dependent signaling through Mcl-1 and Bak is responsible for induction of apoptosis following radiation, and this can be modulated through knockdown or overexpression of Mcl-1. In the future, generating comprehensive transcriptomic and proteomic data from TNBC cell lines treated with Bcl-xL inhibition and RT would help to form a more complete mechanistic picture of this radiosensitization phenotype; extended profiling of *PIK3CA/PTEN* mutant cell lines also has the potential to identify additional critical signaling mediators that are responsible for radioresistance in this setting. Although more patients with ER+ breast cancer harbor activating *PIK3CA* mutations or inactivating *PTEN* mutations, future studies could test if Bcl-xL inhibition + RT could be a viable therapeutic strategy for the ER+ patients with wild type *PIK3CA/PTEN* expression.

Clinical Trial Design

PARP Inhibition + RT

Patients with IBC are treated according to the standard of care for the molecular composition of their tumor (anti ER/HER2 therapies). However, due to the biological heterogeneity of IBC, the current clinical trial landscape is diverse and covers a large number of biological signaling pathways (24,25). In addition to novel chemotherapy regimens, small molecules targeted against VEGFR/FGFR/PDGFRα/β (nintedanib and bevacizumab) or JAK1/2 (ruxolitinib) are currently under investigation for the treatment of IBC. In the metastatic setting, epigenetic modifiers (romidepsin), the viral oncolytic agent T-VEC, and immunomodulatory agents such as atezolizumab (PD-L1) and pembrolizumab (PD-1) are currently in phase II trials for patients with IBC.

In contrast to these treatment strategies, our proposed combination therapy of PARP1 inhibition in combination and radiation specifically aims to increase the efficacy of radiation therapy that patients receive as part of the standard of care. This is in alignment with other clinical studies that have shown benefit to higher doses of RT or radiation intensification for IBC patients compared to non-IBC patients (26,27). Aside from increasing RT dose, increasing the efficacy of RT can often be achieved by administering fractionated radiation in combination with small molecule/antibody therapies. To assess the safety and tolerability of this combination therapy, a 30-patient phase I study was conducted at the University of Michigan (TBCRC 024, NCT01477489) for patients with locally recurrent or inflammatory breast cancer. The PARP1 inhibitor veliparib was given at a dose of 50-200mg twice a day using a time-to-event continual reassessment method (TiTE-CRM) approach. 10Gy radiation was delivered in five fractions to the chest wall concurrent with administration of veliparib and used to assess safety and

tolerability of the combined therapy. Although short term toxicities were minimal, a significant number of patients developed severe acute toxicities.

Our phase II trial (SWOG 1706, NCT03598257, **Figure 6.1**) is currently the only open clinical trial studying a potential small molecule radiosensitizer specifically for patients with inflammatory breast cancer. This will be a ~300 patient phase II trial testing the efficacy of standard RT therapy against RT + the PARP1 inhibitor olaparib. Olaparib will be orally administered at 25mg BID concurrently with RT, with dosing started one day before RT and ended on the last day of RT. At the end of the trial, invasive disease-free survival will be compared between the two groups in addition to secondary objectives such as local recurrence-free survival, distant recurrence-free survival, and overall survival. Although this trial is still ongoing, it is one example of how targeted therapies can potentially be used in combination with radiation to improve rates of recurrence and overall survival in patients with inflammatory breast cancer.

CDK4/6 Inhibition + RT

Although we have compelling preclinical evidence to suggest that CDK4/6 inhibitors can be used to radiosensitize breast tumors, we ultimately sought to develop a clinical trial in which we could test our proposed combination therapy (CDK4/6 inhibition + RT) against the current standard (RT). Currently, CDK4/6 inhibitors are not generally administered concurrently with radiation; however, patients with metastatic breast cancer do receive RT for palliative pain relief, and there have been a number of case reports and retrospective clinical trials involving patients that received radiation while on a CDK4/6 inhibitor.

In these patients, the most common toxicities reported were neutropenias and GI disturbances, predominately in patients that received higher doses of radiation (>4 Gy / fraction). Of importance, no skin or normal tissue toxicities of Grade 3 or higher were reported in these studies and hematological toxicities were not significantly greater than those observed with CDK4/6 inhibitor monotherapy. Although our preclinical study suggests that patients who are in late-stage disease and resistant to CDK4/6 inhibition may not be the target population to benefit from our proposed combination therapy, these data still serve as evidence that CDK4/6 + RT is likely to be well-tolerated in patients.

In order to prospectively test the safety and efficacy of CDK4/6 inhibition + RT, we have proposed to test ribociclib administered concurrently with adjuvant radiation therapy for patients with hormone receptor positive (HR+) breast cancer (**Figure 6.2**). After a 30-patient phase I run in (**Figure 6.3**) to optimize dosing and monitor and dose-limiting toxicities, we have proposed a 300 patient, multi-center, randomized phase II clinical trial testing ribociclib and adjuvant RT (**Figure 6.4**). In addition to the presence of a HR+ breast tumor, patients must have multi-node (>3) positive disease or highly proliferative disease (grade 3) to be included in the study.

Ribociclib is not currently indicated for patients with HR+ breast cancer in the adjuvant setting, but this trial proposes a new indication wherein ribociclib would be combined with RT to treat early-stage disease. The overall treatment plan and medical toxicology assessment timeline for the study is outlined in **Figure *6.5***. Although the current trials are designed to recruit patients with hormone receptor positive breast cancer, the proposed studies could be extended in the future to patients with TNBC or other RB-intact breast cancers based on our additional preclinical data.

Final Remarks

In conclusion, our studies have demonstrated that targeted therapies can successfully be used to increase the efficacy of radiation therapy in a "precision medicine" type approach to treat aggressive breast cancers. By tailoring the treatment strategy to the molecular drivers and signaling pathways intrinsic to each subtype, we developed combination strategies using targeted agents against PARP1, CDK4/6, and Bcl-xL that have shown significant efficacy in preclinical models and have led to the development of multiple Phase I/II clinical trials across different breast cancer subtypes. While additional studies need to be performed to further characterize the proposed mechanisms of radiosensitization in our *in vitro* models, the most important future directions of this work are to validate these findings in a larger range of patient-derived xenograft models of breast cancer and to initiate early clinical trials to test the safety and efficacy of these combination therapies in patients with breast cancer that are at high risk for locoregional recurrence.

Figures

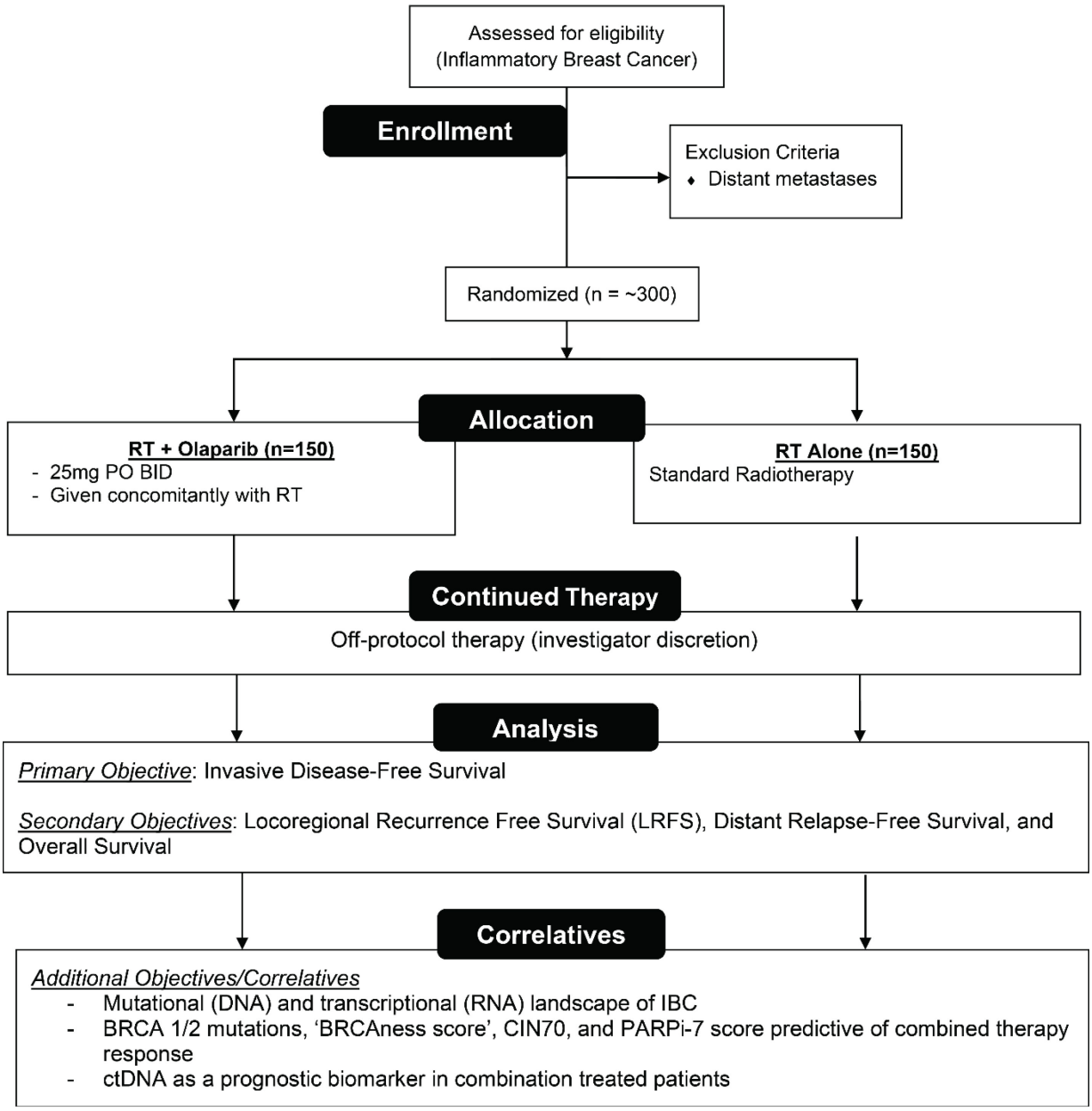

Figure 6.1: The phase II clinical trial "Radiation Therapy with or without Olaparib in Treating Patients with Inflammatory Breast Cancer" (NCT03598257).

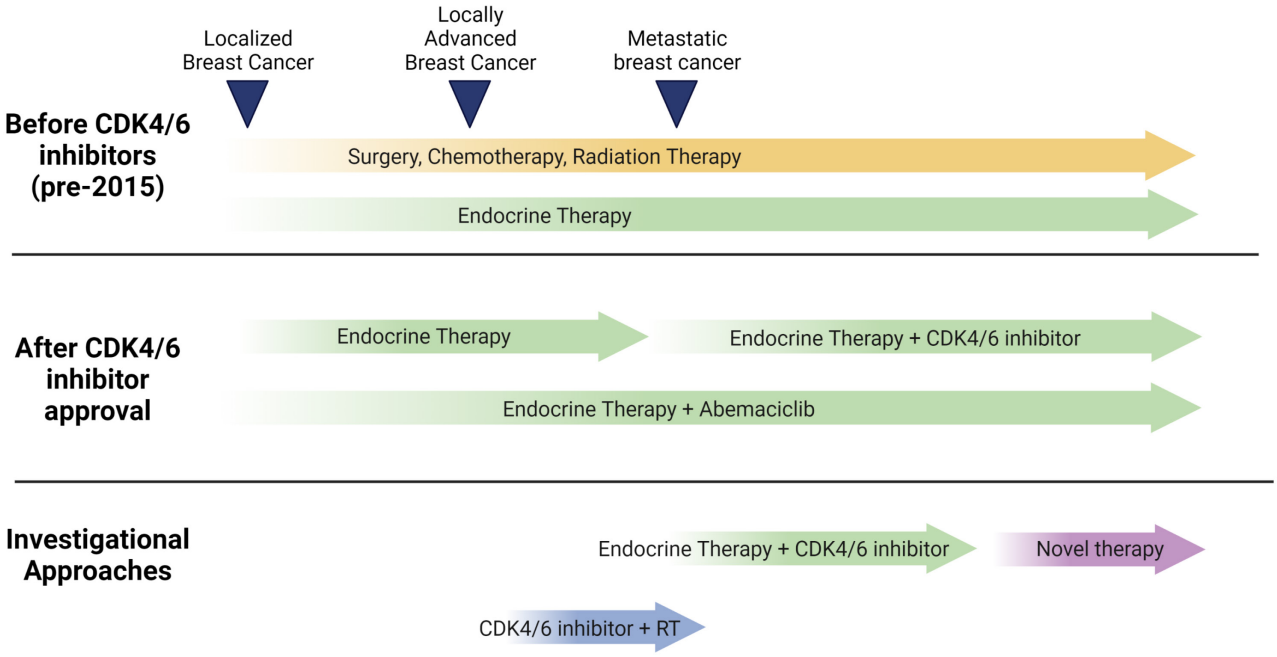

Figure 6.2: Treatment options for patients with ER+ breast cancer.

While all patients with ER+ disease receive endocrine therapy, CDK4/6 inhibitors are primarily restricted to the metastatic setting, with the exception of abemaciclib that can be used in the adjuvant setting. In contrast to current clinical trials that seek to nominate additional drugs that can be used in the event of disease progression on endocrine therapy and CDK4/6 inhibitor therapy, our proposed trial (with ribociclib + RT, denoted with the light blue arrow) would be used prior to the development of CDK4/6 inhibitor resistance.

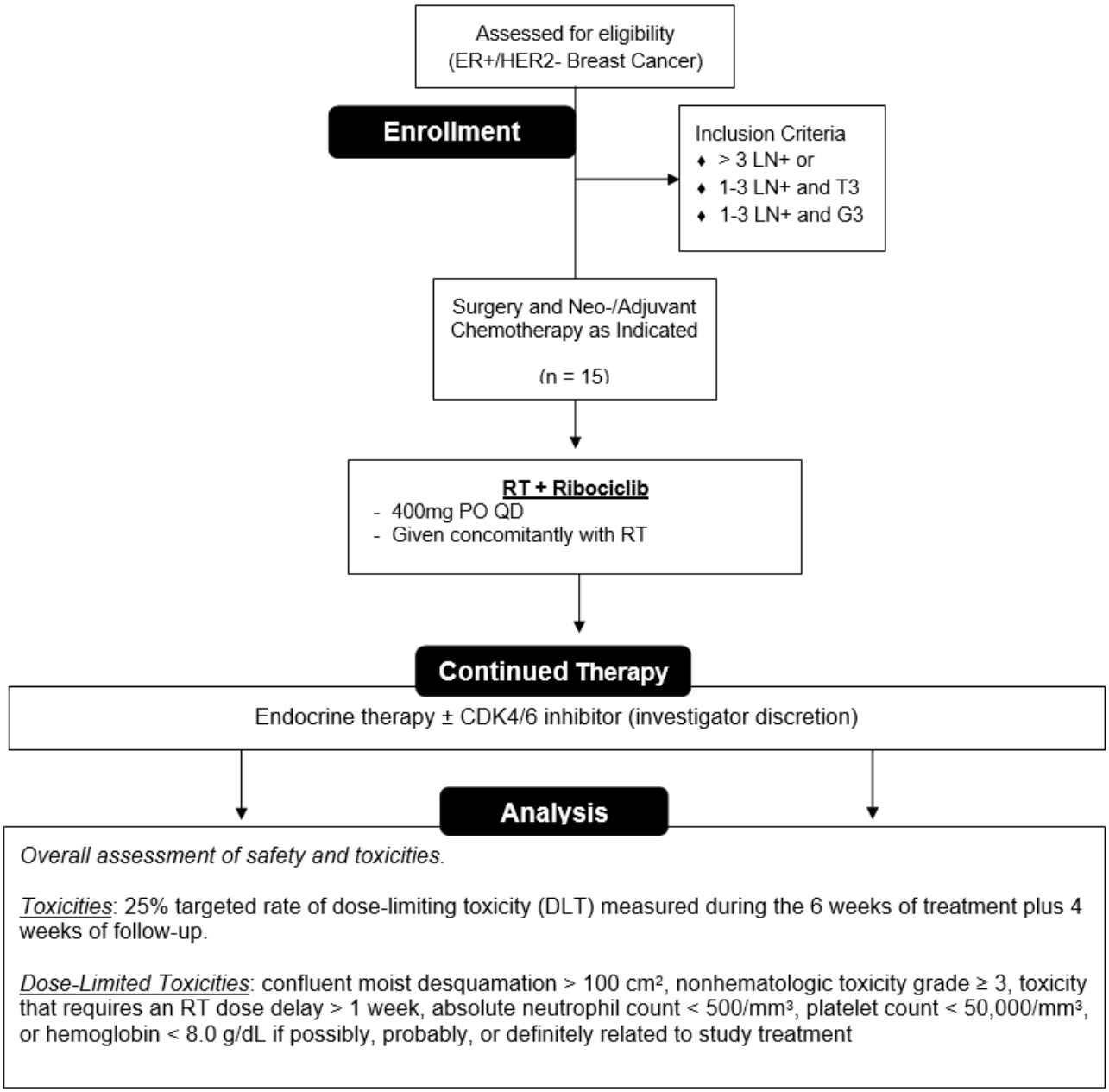

Figure 6.3: The proposed phase I run-in clinical trial to test the safety and tolerability of ribociclib + RT in patients with hormone receptor positive (HR+) breast cancer breast cancer.

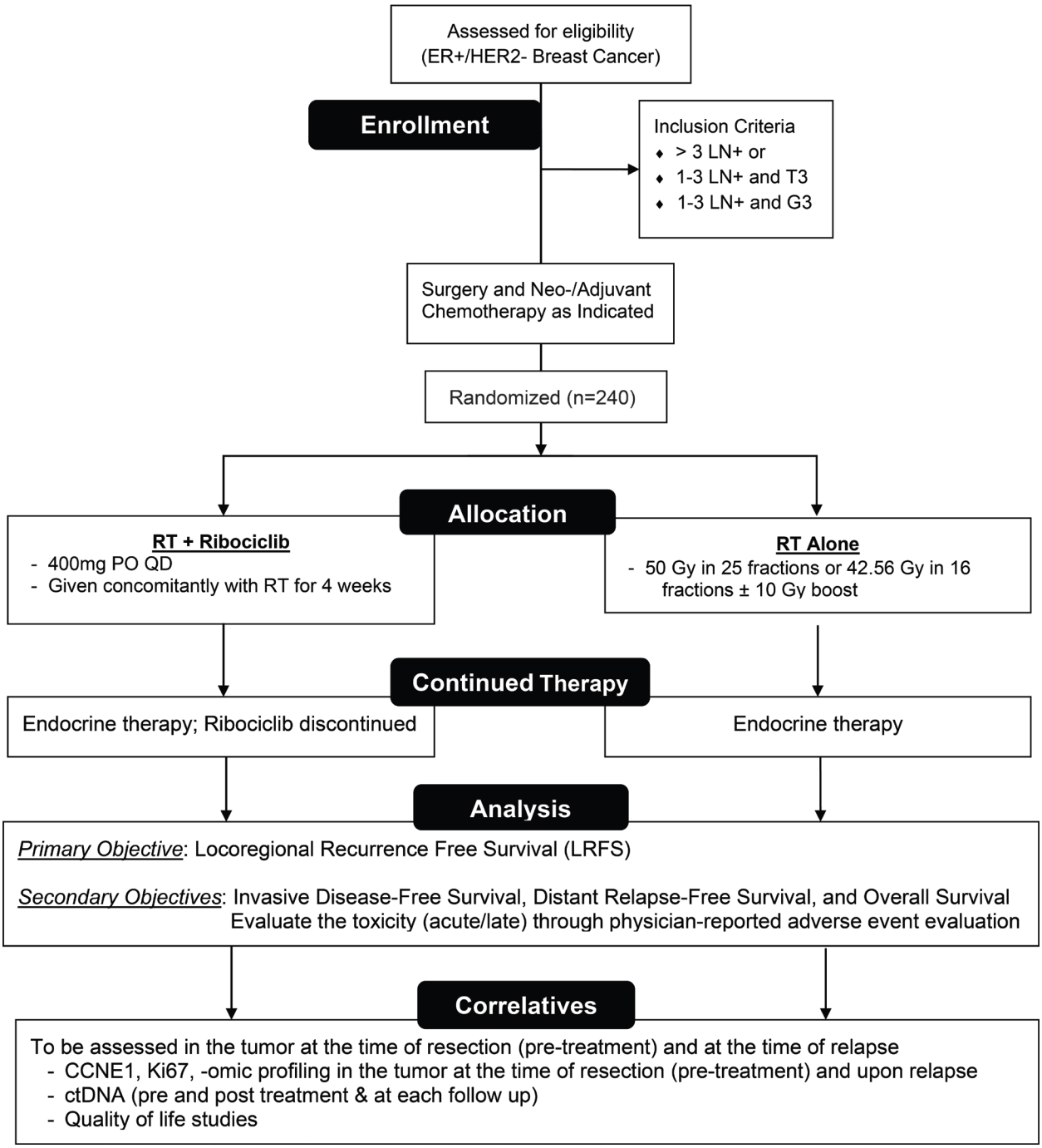

Figure 6.4: The proposed phase II trial for ribociclib + RT in patients with hormone receptor positive (HR+) breast cancer breast cancer.

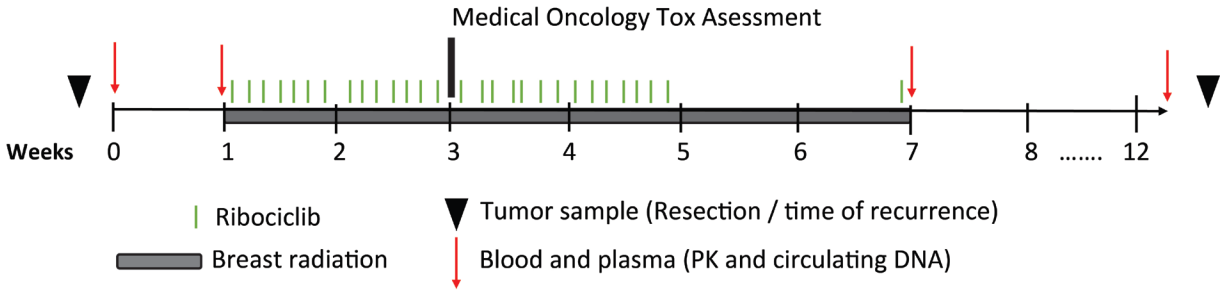

Figure 6.5: The treatment schematic for combined CDK4/6 inhibitor + RT therapy in patients with hormone receptor positive (HR+) breast cancer breast cancer.

References

1. Effect of radiotherapy after breast-conserving surgery on 10-year recurrence and 15-year breast cancer death: meta-analysis of individual patient data for 10 801 women in 17 randomised trials. *Lancet*. Volume 3782011. p 1707-16.
2. Kyndi M, Sorensen FB, Knudsen H, Overgaard M, Nielsen HM, Overgaard J. Estrogen receptor, progesterone receptor, HER-2, and response to postmastectomy radiotherapy in high-risk breast cancer: the Danish Breast Cancer Cooperative Group. *J Clin Oncol* 2008;26(9):1419-26 doi 10.1200/jco.2007.14.5565.
3. Michmerhuizen AR, Pesch AM, Moubadder L, Chandler BC, Wilder-Romans K, Cameron M, et al. PARP1 Inhibition Radiosensitizes Models of Inflammatory Breast Cancer to Ionizing Radiation. *Mol Cancer Ther* 2019 doi 10.1158/1535-7163.mct-19-0520.
4. Pesch AM, Hirsh NH, Chandler BC, Michmerhuizen AR, et al. Short-term CDK4/6 Inhibition Radiosensitizes Estrogen Receptor-Positive Breast Cancers. *Clin Cancer Res*. 2020 Dec 15;26(24):6568-6580.
5. Zhou J, Gelot C, Pantelidou C, Li A, Yücel H, Davis RE, Farkkila A, Kochupurakkal B, Syed A, Shapiro GI, Tainer JA, Blagg BSJ, Ceccaldi R, D'Andrea AD. A first-in-class Polymerase Theta Inhibitor selectively targets Homologous-Recombination-Deficient Tumors. *Nat Cancer*. 2021 Jun;2(6):598-610.
6. Cao C, Yang J, Chen Y, Zhou P, Wang Y, Du W, et al. Discovery of SK-575 as a Highly Potent and Efficacious Proteolysis-Targeting Chimera Degrader of PARP1 for Treating Cancers. *J Med Chem*. 2020 Oct 8;63(19):11012-11033.
7. Zhang Z, Chang X, Zhang C, Zeng S, Liang M, Ma Z, Wang Z, Huang W, Shen Z. Identification of probe-quality degraders for Poly(ADP-ribose) polymerase-1 (PARP-1). *J Enzyme Inhib Med Chem*. 2020 Dec;35(1):1606-1615.
8. Wang S, Han L, Han J, Li P, Ding Q, Zhang Q-J, et al. Uncoupling of PARP1 trapping and inhibition using selective PARP1 degradation. *Nature Chemical Biology* 2019;15(12):1223-31.
9. Kim C, Wang XD, Yu Y. PARP1 inhibitors trigger innate immunity via PARP1 trapping-induced DNA damage response. *Elife*. 2020 Aug 26;9:e60637.
10. Michmerhuizen AL, Lerner, LM. Pesch, AM, et al. Estrogen receptor inhibition mediates radiosensitization of ER-positive breast cancer models. *NPJ Breast Cancer*; 2022.
11. Petroni G, Buqué A, Yamazaki T, Bloy N, Liberto MD, Chen-Kiang S, Formenti SC, Galluzzi L. Radiotherapy Delivered before CDK4/6 Inhibitors Mediates Superior Therapeutic Effects in ER+ Breast Cancer. *Clin Cancer Res*. 2021 Apr 1;27(7):1855-1863.
12. Contessa JN, Abell A, Valerie K, Lin PS, Schmidt-Ullrich RK. ErbB receptor tyrosine kinase network inhibition radiosensitizes carcinoma cells. *Int J Radiat Oncol Biol Phys* 2006;65(3):851-8.
13. No M, Choi EJ, Kim IA. Targeting HER2 signaling pathway for radiosensitization: alternative strategy for therapeutic resistance. *Cancer Biol Ther* 2009;8(24):2351-61.
14. Sambade MJ, Kimple RJ, Camp JT, Peters E, Livasy CA, Sartor CI, et al. Lapatinib in combination with radiation diminishes tumor regrowth in HER2+ and basal-like/EGFR+ breast tumor xenografts. *Int J Radiat Oncol Biol Phys* 2010;77(2):575-81.

15. Herrera FG, Ronet C, Ochoa de Olza M, Barras D, et al. Low Dose Radiotherapy Reverses Tumor Immune Desertification and Resistance to Immunotherapy. *Cancer Discov*. 2021 Sep 3:candisc.0003.2021.
16. Kettner NM, Vijayaraghavan S, Durak MG, Bui T, Kohansal M, Ha MJ, et al. Combined Inhibition of STAT3 and DNA Repair in Palbociclib-Resistant ER-Positive Breast Cancer. *Clin Cancer Res* 2019;25(13):3996-4013.
17. Goel S, DeCristo MJ, Watt AC, BrinJones H, Sceneay J, Li BB, et al. CDK4/6 inhibition triggers anti-tumour immunity. *Nature* 2017;548(7668):471-5.
18. Chaikovsky AC, Sage J. Beyond the Cell Cycle: Enhancing the Immune Surveillance of Tumors Via CDK4/6 Inhibition. *Mol Cancer Res*. 2018 Oct;16(10):1454-1457.
19. Zhang J, Bu X, Wang H, Zhu Y, Geng Y, Nihira NT, et al. Cyclin D–CDK4 kinase destabilizes PD-L1 via cullin 3–SPOP to control cancer immune surveillance. *Nature* 2017;553(7686):91-5.
20. Teo ZL, Versaci S, Dushyanthen S, Caramia F, Savas P, Mintoff CP, Zethoven M, Virassamy B, Luen SJ, McArthur GA, Phillips WA, Darcy PK, Loi S. Combined CDK4/6 and PI3Kα Inhibition Is Synergistic and Immunogenic in Triple-Negative Breast Cancer. *Cancer Res*. 2017 Nov 15;77(22):6340-6352.
21. Deng J, Wang ES, Jenkins RW, et al. CDK4/6 Inhibition Augments Antitumor Immunity by Enhancing T-cell Activation. *Cancer Discov*. 2018 Feb;8(2):216-233.
22. De Simone M, Arrigoni A, Rossetti G, et al. Transcriptional Landscape of Human Tissue Lymphocytes Unveils Uniqueness of Tumor-Infiltrating T Regulatory Cells. *Immunity*. 2016 Nov 15;45(5):1135-1147.
23. Rugo HS, Delord JP, Im SA, et al. Safety and Antitumor Activity of Pembrolizumab in Patients with Estrogen Receptor-Positive/Human Epidermal Growth Factor Receptor 2-Negative Advanced Breast Cancer. *Clin Cancer Res*. 2018 Jun 15;24(12):2804-2811.
24. Menta A, Fouad TM, Lucci A, Le-Petross H, Stauder MC, Woodward WA, et al. Inflammatory Breast Cancer: What to Know About This Unique, Aggressive Breast Cancer. *Surgical Clinics* 2018;98(4):787-800.
25. Woodward WA, Cristofanilli M. Inflammatory breast cancer. *Semin Radiat Oncol*. 2009 Oct;19(4):256-65.
26. Scotti V, Desideri I, Meattini I, et al. Management of inflammatory breast cancer: focus on radiotherapy with an evidence-based approach. *Cancer Treat Rev*. 2013 Apr;39(2):119-24.
27. Woodward WA. Postmastectomy radiation therapy for inflammatory breast cancer: is more better? *Int J Radiat Oncol Biol Phys*. 2014 Aug 1;89(5):1004-1005.